January 1985

Identification and Modeling the Impact of Marine Shale Bedrock on Groundwater and Stream Salinity: Upper Colorado River Basin

Christopher J. Duffy

Jerome J. Jurinak

Sanjay Sangani

Ali Azimi

IDENTIFICATION AND MODELING THE IMPACT OF MARINE SHALE BEDROCK ON GROUNDWATER AND STREAM SALINITY: UPPER COLORADO RIVER BASIN

by

Christopher J. Duffy
Jerome J. Jurinak

and

Sanjay Sangani
Ali Azimi

"The research on which the report is based was financed in part by the United States Department of the Interior, Geological Survey, through the Utah Center for Water Resources Research."

HYDRAULICS AND HYDROLOGY SERIES
UWRL/H-85/01

FCCSET Category II-4
USDI, Contract No. 374702
Annual Cooperative Program
07/01/83 - 07/31/85

Utah Water Research Laboratory
Utah State University
Logan, Utah 84322

September 1985

TABLE OF CONTENTS

TABLE OF CONTENTS (Continued)

LIST OF FIGURES

LIST OF FIGURES (Continued)

LIST OF FIGURES (Continued)

LIST OF TABLES

LIST OF TABLES (Continued)

ABSTRACT

Recent studies have shown that groundwater is a major contributor to stream salinity in the Upper Colorado River Basin. The primary salt sources are the marine shales and shale residuum that underlie the soils of much of the basin. A field site in the Price River Basin, a tributary to the Green and Colorado Rivers, was selected to study the physical and chemical factors that control the interactions between groundwater and these shales. Preliminary data were available at the site as a result of a Bureau of Reclamation study conducted by CH2M Hill. On the basis of the CH2M Hill study and the additional data collected during this study groundwater flow paths, salt transport and weathering processes were identified. Results show that the groundwater evolves from a calcium-bicarbonate water to a sodium-sulfate water with depth and distance along the flow paths. Geochemical equilibrium modeling and mass balance computations were performed using the USGS models PHREEQE and BALANCE. A preliminary saturated-unsaturated two-dimensional flow model (UNSAT) was implemented along the identified groundwater flow path. Once a satisfactory flow calibration was achieved, a solute transport model was then implemented to examine the relative importance of advective, dispersive and diffusive mixing processes along the flow profile.

Preliminary management runs were made to study the effect of possible changes in land use practices. Results of these hypothetical cases suggest that water conservation methods (improved irrigation efficiency, canal lining and retiring irrigated land) will reduce return flow salt loads over the short run (about 50 years), when the transport of salts by displacement is most important. However, these salinity control alternatives are much less effective in the long range (> 50 years) because the diffuse salt loading from underlying marine shales is unaffected by groundwater flow rates in the alluvium. Although additional field data must be collected for verification the proposed model is a realistic first step towards a quantitative physically based approach to land use-salinity control issues.

CHAPTER I

INTRODUCTION

In the Upper Colorado River Basin, irrigated agriculture has been associated with increasing stream salinity and asked to implement control measures to reduce downstream adverse effects. A number of earlier studies at the Utah Water Research Laboratory (Riley et al. 1982, Bowles et al. 1982) found that only a small amount of the salt loading was coming from the land surface and the stream channels. Through a literature review and supplemental field studies, CH2M Hill (1983) estimated that as much as 90 percent of the stream salinity originates in groundwater flowing through salt bearing strata.

Strong economic and political factors are drawing increased attention to salinity control in the Colorado River Basin. A treaty with Mexico requires the United States to keep salinity levels within specified limits, and the cost of desalination to do so can be substantially reduced by lower salinity levels in the water entering the Lower Basin. This requirement and the economic losses to Lower Basin water users from higher salinity levels (Andersen and Kleinman 1978) are spawning a number of salinity control efforts in the Upper Basin, and these are largely centered on irrigation projects and agricultural water use. They vary greatly in cost effectiveness (Narayanan and Franklin 1982). In order to serve the Lower Basin water users with minimal disruption of Upper Basin agriculture and fossil fuel development, the salinity control projects must be based on quantitative relationships estimating salt loading rates as a function of controllable parameters in areas targeted for control measures.

Most researchers agree that the primary salt sources in the Upper Basin are the marine shales and shale residuum that underlie the soils of much of the basin, and that water is the primary agent leaching salts from these shales and transporting them to the streams. However, we lack the quantitative understanding of the physical factors controlling the movements and mixing of natural and irrigation waters through these formations and of the physical and chemical factors controlling the interactions between the moving waters and these shales required for an effective basinwide salinity control program. Depending on the local subsurface situation and on time-varying flow conditions, irrigation may either accelerate or retard the dissolution of salt from partially weathered strata. The mechanisms that control these processes are not sufficiently understood to establish relationships containing parameters that represent local field conditions for use in salinity control planning.

This report describes findings of a study undertaken to conceptualize the groundwater flow and salt transport processes at a selected field site in the Price River Basin, a subbasin of the Upper Colorado River. The purposes of this study are to identify the interaction and geochemical mixing processes associated with subsurface flow at the research site, and to develop and calibrate field scale models of these processes. The models are meant to

demonstrate an analytical approach to assessing subsurface salinity control measures. Development of the model begins by building understanding of the nature and extent of the subsurface salinity transport and geochemical mixing processes beneath irrigated lands within the Price River Basin. In this vein, a field data collection program was undertaken to supplement the CH2M Hill (1982, 1983) data base. The CH2M Hill study, in the view of the authors of this study, provided an important first step without which this research could not have been successful.

The main objectives of this research were:

1. To build a conceptual understanding of the flowpaths, mixing and salt transport processes resulting from shallow groundwater in contact with saline geologic strata in an irrigated setting.

2. To examine spatial and temporal geochemical salinity changes observed at an appropriate field site in the Price River Basin.

3. To implement flow and solute transport models of salt transport at a chosen site within the Price River subbasin.

4. To identify and estimate the important mass transport parameters of the system.

5. To use the physical models to assess the feasibility of controlling salt loading from agricultural and geologic salt sources of the site.

CHAPTER II

BACKGROUND INFORMATION

This chapter presents general information on the hydrology, climate and geology of the Price River subbasin. The selected study site in the Miller Creek drainage of the Price River drainage was selected because it exhibits hydrogeologic characteristics felt to be typical of many irrigated regions within the Upper Basin.

The Price River Basin Drainage Basin

A number of authors have contributed to our understanding of the hydrologic, geologic, climatic and geographic characteristics of the Price River Basin. The following descriptions are primarily based on reports by Mundorff (1972), Iorns et al. (1965), Laronne and Schumm (1977), a final report to the Bureau of Reclamation by CH2M Hill (1982), and the hydrologic inventory of the Utah Division of Water Resources (1975).

Setting

The Price River flows southeast from its headwaters in the Wasatch and Tavaputs plateaus into the Colorado River via the Green River (Figure II-1). The Price River Basin is located within the Carbon and Emery counties in east-central Utah (Figure II-2). The altitude range is approximately 6,000 feet, with the highest mountain peak in the Wasatch plateau estimated at 11,300 feet and the elevation at the confluence of the Price and Green Rivers at 4200 feet. The Price River Basin lies within three physiographic areas of the Colorado plateau--the Unita Basin, the High Plateaus, and the Canyonlands.

Hydrology

Figure II-3 provides contour maps of the mean annual water yield and precipitation for the Price River Basin. Runoff in the upper part of the basin (155 square miles of drainage area) is controlled by the 74,000 acre-foot Scofield Reservoir which stores a large part of the total subbasin water supply. The average annual discharge from this reservoir is approximately 45,100 acre-feet (62.3 cfs). Between Scofield and Heiner, the Price River drainage area increases by 300 square miles and reaches an average flow of 83,400 acre-feet (115 cfs). Over 80 percent of this annual flow volume occurs in April through August. The consumptive use is estimated at 15,900 acre-feet (22 cfs) annually in this upper subarea (CH2M Hill 1982). At Woodside, an average annual flow of 70,900 acre-feet (98 cfs) has been recorded. Between Heiner and Woodside, a yearly volume of approximately 44,800 acre-feet (62 cfs) enters as tributary inflow and/or irrigation return flow (CH2M Hill 1982). A complete hydrologic budget is difficult to determine due to uncertainty in estimation of consumptive use.

Figure II-1. Map of the Upper Colorado River Basin.

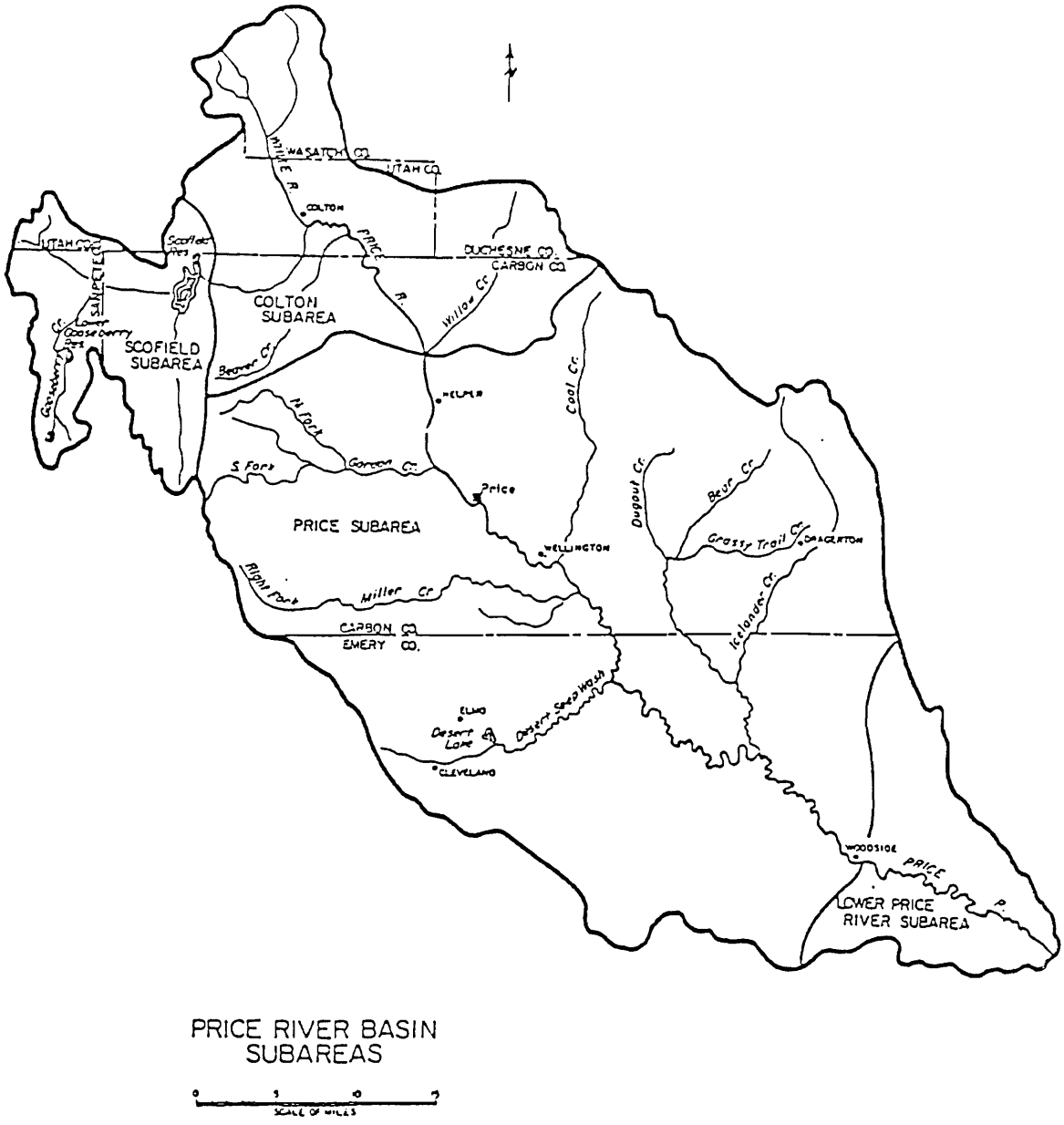

Figure II-2. Map of the Price River Basin. (Source: Utah Division of Water Resources, 1975).

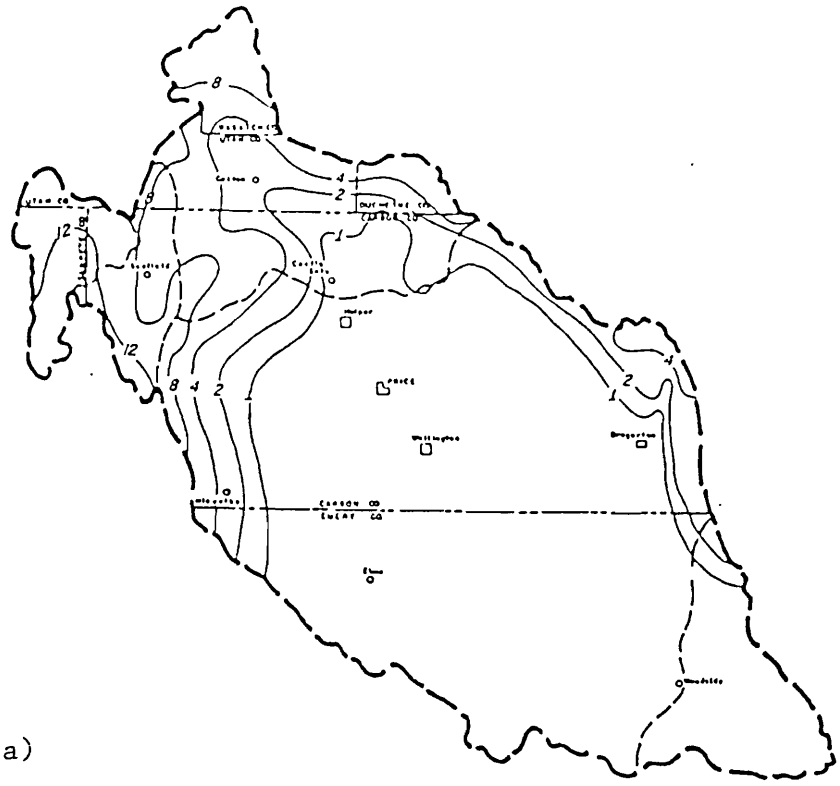

(a)

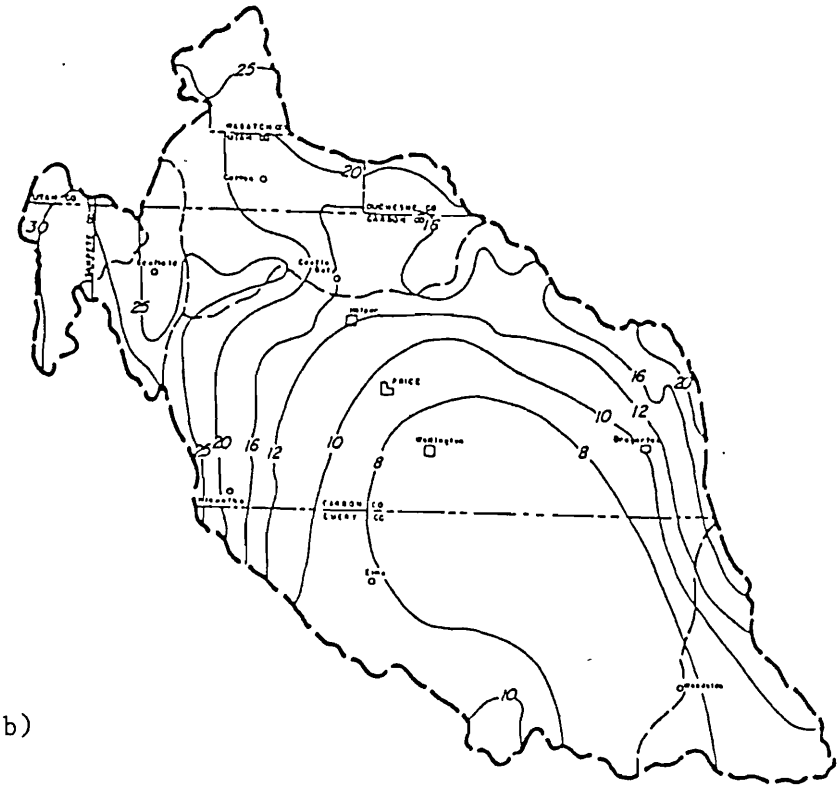

(b)

Figure II-3. (a) Mean annual water yield (in inches) for the Price River Basin, (b) Mean annual precipitation (in inches) for the Price River Basin. (Source: Utah Division of Water Resources 1975.)

Climate

The climate in the Price River Basin is generally classified as semiarid to arid. Average annual precipitation is less than 10 inches and ranges from 4 inches in the lower basin to greater than 25 inches in the high plateaus. Summer thunderstorm activity accounts for most of the precipitation in the area. Snowfall averages from 15 to 25 inches but increases to around 50 inches on the higher plateaus and exceeds 100 inches annually in the mountains. Temperatures in the basin range from a maximum of 100°F to a minimum of -42°F. Winds are generally light to moderate, with average speeds below 20 mph. Tornadoes are very rare, but strong winds may occur, particularly in mountain passes and canyons.

Hydrogeology and soils

The geology of the interior region of the Upper Colorado River Basin is chiefly comprised of flat to gently dipping mesozoic and paleozoic consolidated sediments of continental to marine origin. Most of the runoff originates as snowmelt in the adjacent mountains and high plateaus. The water is generally of good quality until it enters the interior low areas of the basin. There a thin veneer of soil and unconsolidated strata are found. The unconsolidated material consists of residuum and alluvium which are the products of erosion and weathering processes both locally and in the adjacent uplands. Underlying the thin veneer of unconsolidated material are various marine shale deposits. Hydrologically these rocks are often of low permeability and do not contribute significantly to streamflow, but do have a significant impact on the chemical quality of streamflow. The Price River drainage basin is one of the interior valleys underlain by a saline marine deposit known as the Mancos shale.

Five major soil group types have been identified within the Price River Basin. The soils vary between Aridisols, Badlands, Entisols, and Rocklands in the lower basin and Badlands, Mollisols, and Rocklands in the upper basin (CH2M Hill 1982). The soils have been grouped into four salinity classes as indicated in Table II-1. Soil salinity increases markedly for soils derived from the Mancos shale and for those which receive less than six inches of annual precipitation (U.S. Bureau of Land Management 1976, 1978).

Table II-1. Common agronomic soil salinity classification system.

Salinity Class	Electrical Conductivity at 25°C of Saturation Extract in mmhos/cm	
	Upper Soil Layer	Lower Soil Layer
Nonsaline	<4,000	<4,000
Slightly Saline	>4,000 above 8 inches	<4,000 to 16,000 below 16 inches
Moderately Saline	>4,000 - 16,000 above 20 inches	<16,000 below 20 inches
Strongly Saline	>16,000	>16,000

Source: U.S. Bureau of Reclamation (1975)

Related Research Issues

The literature review probed three major subject areas: 1) salinity and related problems in the Upper Colorado River Basin, 2) physical and chemical processes governing the groundwater quality, and 3) modeling approaches used to study these processes.

Salinity

Salinity is the most serious water quality problem in the Colorado River Basin and has been a subject of extensive research activities. Irrigation is the largest single user of water within the Upper Colorado River Basin, and various studies have shown that subsurface agricultural return flow can be a major source of salinity. However, the precise mechanisms controlling subsurface salt loading to streams are still largely conjecture. In Western Australia, Nulsen and Henschke (1981) have shown that reclamation of lands for agricultural development causes an increase in infiltration rates producing a local rise in the water table. This leads to deeper flow paths which intercept the unweathered saline rocks or sediments, ultimately producing additional salinity in adjacent streams.

Mundorff (1972) regards groundwater as a major source of salinity in the Price River. A recent study by CH2M Hill (1983) for the Bureau of Reclamation supports this conclusion and estimates that up to 90 percent of stream salinity may be through groundwater. The Mancos shale formation has been identified as a major contributor of salt to the Price River.

Extensive field and laboratory research has been carried out on the surficial salt loading mechanisms during overland flow and stream runoff (Rao et al. 1981, Nezafati et al. 1981, Riley et al. 1979). Jackson and Julander (1982) examined the erosion and dissolved solids production of upland Mancos shale and Mancos shale residuum. Ponce (1975), Riley et al. (1982), and Bowles et al. (1982) came to the common conclusions that surficial processes contribute only a small percentage of the total dissolved solids in drainage from the area.

Laronne and Schumm (1977) investigated geologic sources of soluble mineral content on nonirrigated lands and found that the thick alluvial deposits tend to have low salt contents near the surface and relatively higher salinity with depth, with a maximum salt content at the groundwater table. A report by Uintex Corporation (1982) for the Bureau of Land Management suggests that the salinity in the base flow of perennial streams in the Price River Basin is the result of weathering and dissolution processes. Both nonirrigated and irrigated lands contribute to stream salinity, but the study did not determine the relative amounts.

It is generally held that through improved irrigation water management, it is possible to reduce the salt load in irrigation return flow and thereby the concentration of dissolved solids in downstream reaches of a river system. El-Ashry (1980) suggested some management alternatives to salinity problems related to irrigation in the Colorado River Basin. Water losses and quantities of irrigation return flows can be reduced by improving on-farm irrigation efficiences and by partial or complete

lining of canals, laterals, and ditches. Andersen and Kleinman (1978) also examined various salinity management options for the Colorado River. Riley and Jurinak (1979) examined long-term salinity changes in streams related to irrigation management practices.

Hydrogeochemistry

Understanding the physical and chemical processes within the groundwater system is essential for successful hydrosalinity modeling and management. Transport of the solute via advection, dispersion, and diffusion processes have to be considered. Chemical reactions and mechanisms of precipitation and dissolution kinetics are equally important. Palciauskas and Domenico (1976) examined the approach to chemical equilibria in carbonate systems. From field and experimental data, the authors were able to verify the qualitative aspects of predicted concentration behavior. They concluded that the travel distance for subsurface water to attain saturation with respect to an individual mineral increases with increasing rates of dispersion and velocity of groundwater, and decreases with increasing rates of reaction (dissolution). The authors recognized the fact that the equilibrium approach is valid only in systems where reaction rates are relatively fast so that aqueous solutions rapidly approach chemical equilibrium with respect to one or a few solid mineral phases. If dispersion is large relative to the diffusion-controlled rate coefficient, the distance to saturation with respect to a mineral phase is increased, thus, weakening the equilibrium assumption. Saturation in carbonate systems is attained as a result of the interplay between dispersion, rates of reaction, and velocity of flow. For the diffusion process, the concentrations obtained when all the concentration gradients go to zero is a weighted average of the saturation concentrations of the individual minerals.

Rubin (1983) gave examples involving six broad reaction classes that show the profound effect chemistry may have on the mathematical formulation character of solute transport problem. He described two groups of reactions, the sufficiently fast reactions and the insufficently fast reactions. The local equilibrium assumption is valid, as previously stated by Palciauskas and Domenico (1976), only for sufficently fast reactions. Rubin listed four primary chemical factors that should be incorporated into the mathematical formulation of solute transport models as: 1) the general nature of chemical-relation equations (i.e. are they equilibrium or kinetic equations), 2) the presence or absence of solid phase concentration terms in the basic transport equations, 3) the importance of diffusion effects at the solid/liquid interface, and 4) the mobility of the solid/liquid interface.

Berner (1978) examined the rates, mechanisms, and the functional dependence of dissolution kinetics under earth surface conditions. He concluded that increased renewal of water or flushing, accelerates the dissolution of minerals in water-saturated rocks, soils, and sediments only up to a limiting flushing rate beyond which flushing has virtually no effect and dissolution is controlled solely by mineral reactivity. He suggested that current hydrodynamic models may not be based on correct assumptions on the processes controlling dissolution. These processes are categorized as surface reaction control and hydrodynamic control of the solution. He described several major dissolution processes which were

controlled by surface reaction and not by transport through solution nor by retarded diffusion through continuous coatings on mineral grains.

The examination of spatial and temporal hydrochemical variations is an extremely useful correlative and interpretative tool. Davison and Vonhoff (1978) looked at variations in the hydrostatic head distribution, responses to atmospheric barometric pressure changes, and distributions of chemical constituents and species in a semi-confined buried channel aquifer. They suggested chemical reactions that account for an apparent chemical evolution of prairie ground waters. The authors cite several other investigators who have reported significant temporal chemical variations in groundwater flow systems. These variations have been related to: 1) rapid groundwater transit after recharge in shallow aquifer systems (Jacobson 1973, Hoag 1975), 2) natural or artificial fluctuations of the zone of saturation into and out of weathering profiles (Bergstrom 1974), and 3) mixing of groundwaters of differing chemistries in highly pumped aquifers (Fritz et al. 1974).

Suarez (1983) presented the mechanisms of calcite supersaturation and precipitation kinetics to study whether $CaCO_3$ precipitation occurs in the lower Colorado River and whether it affects downstream water chemistry. He concluded that despite considerable supersaturation, $CaCO_3$ does not precipitate in measurable quantities. This reflects insufficient supersaturation for heterogenous nucleation and unavailability of suitable nuclei due to short residence times and high sediment loads.

Kemper et al. (1975) examined the dissolution of gypsum by flowing water in a laboratory column and suggested a kinetic dissolution rate expression controlled by the saturation concentration of gypsum and a first order rate constant. This same formulation was later recommended by Berner (1978). Jurinak et al. (1977) investigated the kinetics of salt release from a Mancos-shale derived soil. The salt release data plotted as a first-order reaction indicating dissolution as a simple diffusion controlled reaction. Evangelou et al. (1984) examined the role of the cation exchange complex in retention and release of soluble ions in Mancos shale. Through experimental investigations, the authors were able to identify the sources of dissolved ions from partially weathered and unweathered Mancos shale. They recognized that dispersed gypsum and alkaline earth carbonates provide soluble calcium to displace adsorbed sodium and magnesium that eventually add to the dissolved salt load in the Upper Colorado River.

Groundwater modeling

In the case of "transport affected chemistry," Rubin (1983) has pointed out that the groundwater and solute transport model should be directly coupled with the geochemical model. In multidimensional flow fields, the difficulty of solving the resulting highly nonlinear systems of equations often makes this general approach infeasible. An approximate alternative is to uncouple the flow and transport model from the geochemical model and examine each separately. The "uncoupled" approach was taken in the present research.

Flow and solute transport modeling. Konikow (1981) has examined the role of flow and solute transport models in the analysis of salinity problems

over large agricultural areas, and has suggested that modeling can be a valuable investigative tool for understanding processes and estimating parameters controlling the fate of salt movement in arid regions. In addition, the model approach provides a management tool for predicting responses and optimizing development and use of the resource.

Anderson (1979) analyzed the various approaches to modeling flow and solute transport and the difficulties associated with each. The author summarized a few of the limitations in current state-of-the-art groundwater modeling as: 1) lack of detailed field data, 2) need to theoretically define dispersivity, 3) need to establish a methodology for incorporating chemical reactions in existing solute transport models, 4) incorrect definitions of the properties of the medium, and 5) poor choice of boundary conditions.

Coupled flow and water quality models can be classified as distributed parameter models or lumped parameter models. Anderson (1979) found that lumped parameter models are easily calibrated and in some cases may be more appropriate than distributed parameter models which require a large data base. This is especially true where limited data are available and order-of-magnitude results are desired. Duffy (1984) described conceptual mechanisms of salt transport under irrigated lands using the lumped parameter approach. Gelhar et al. (1983) used two modeling approaches to simulate irrigation return flow water quality: 1) multiple-celled lumped parameter models, and 2) a profile finite element flow model coupled with the U.S. Bureau of Reclamation hydrosalinity model. The authors concluded that for the lumped parameter model the data requirements are less severe, parameter estimation is systematic, and the simple structure is easily modified to reflect site-specific conditions. They recommend that a systematic lumped parameter water and solute balance model be used initially to evaluate overall hydrologic conditions and provide regional, management-oriented predictions. Lumped parameter approaches have been used by other authors with apparent success (McLin 1981, Simonett 1981, Gelhar and Wilson 1974).

Geochemical modeling. Geochemical modeling of groundwater systems attempts to evaluate chemical reactions along ground-water flow paths. Plummer et al. (1983) discuss the philosophy and methodology of chemical reaction modeling which include calculations of 1) equilibrium speciation, 2) mass balance, and 3) reaction-path. Nordstrum et al. (1979) used several widely used geochemical models to summarize the inherent limitations to chemical modeling. The major sources of discrepancy result from differences in the thermodynamic data base, the number of complexes in each model, the form of the activity coefficent equation, the redox assumptions, the form of the alkalinity input and noncarbonate alkalinity correction, and the temperature and pressure corrections. The obstacles to development of geochemical models of groundwater systems are (Back and Cherry 1976):

1. The lack of adequate and valid geologic data.

2. The dearth of nonequivocal laboratory data on chemical mechanisms and kinetics of solution-precipitation reactions, and the role of trace elements and adsorption phenomena in these reactions.

3. The lack of information on the occurrence of bacteria, gases, organic compounds in groundwater and their behavior in the saturated zone.

4. The lack of a theoretical framework that can relate results of laboratory experiments to field conditions and the difficulty in transferring field experience and data to theoretical models.

CHAPTER III

FIELD INVESTIGATION AT MILLER CREEK SITE

This chapter outlines the field investigation at the Miller Creek site. Groundwater monitoring was carried out at existing wells from the CH2M Hill study (1982), and with additional wells installed during the present study.

Description of the Study Site

Early in the investigation a field reconaissance was carried out to select an appropriate field site for conducting a groundwater study. The Miller Creek subbasin site was selected based on such factors as accessibility, topography, and availability of data. Several monitoring wells had been installed by CH2M Hill (1982) on a hillslope with irrigated croplands on the upper parts and with irrigated pasture downslope. The wells are installed in clusters of three--shallow, intermediate, and deep. The first nest of wells (M-7) is located just south of Carbon Canal, the middle wells (M-9) are approximately half way along the transect, and the lower wells (M-10) are just north of Miller Creek. Figure III-1 is a schematic of the area showing the location of all wells used in the study. Well details and the chemistry data from the CH2M Hill (1983) study are provided in Appendix A.

Field Data Collection

Measurements were taken at monthly intervals from April 1984 to October 1984. The kinds of information gathered include:

1. Groundwater quality data from observation wells.

2. Surface water quality data from the Carbon Canal and from stations on the Miller Creek (upstream and downstream).

3. Water levels in the observation wells and streamflow measurements on Miller Creek at both water quality sampling locations.

Additional wells were installed to define the complex bedrock topography. From these wells it was determined that groundwater flow follows a depression in the bedrock topography, and that well 10 was located on a bedrock high adjacent to and above the groundwater flow path. Soil samples were taken along the transect to a depth of 5 feet. The soil sampling locations are shown in Figure III-2 on a transect along wells 7, 9, and 12. A topographic survey was carried out along the transect to determine the relative elevations of the wells.

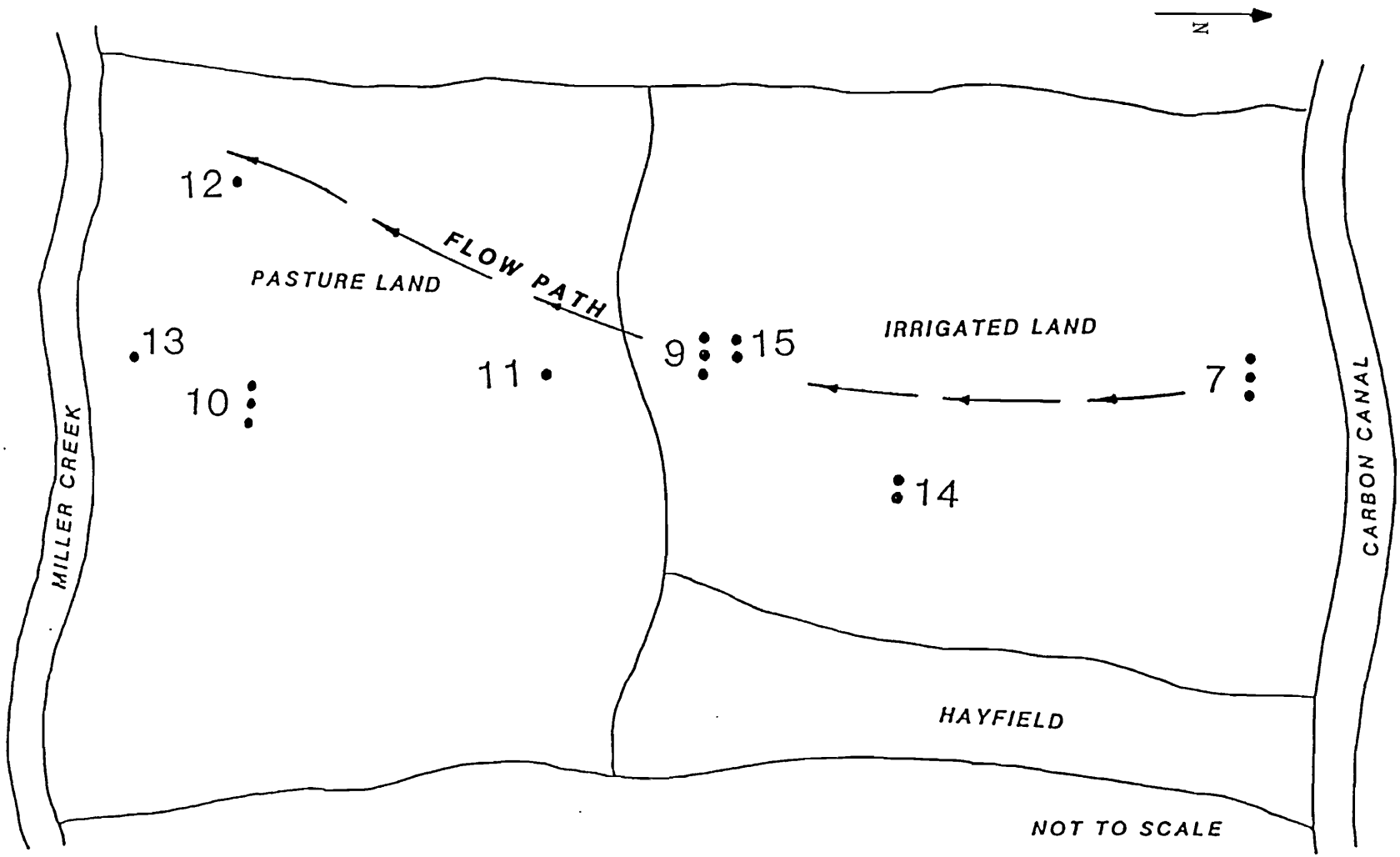

Figure III-1. Schematic of the study site showing location of newly installed wells.

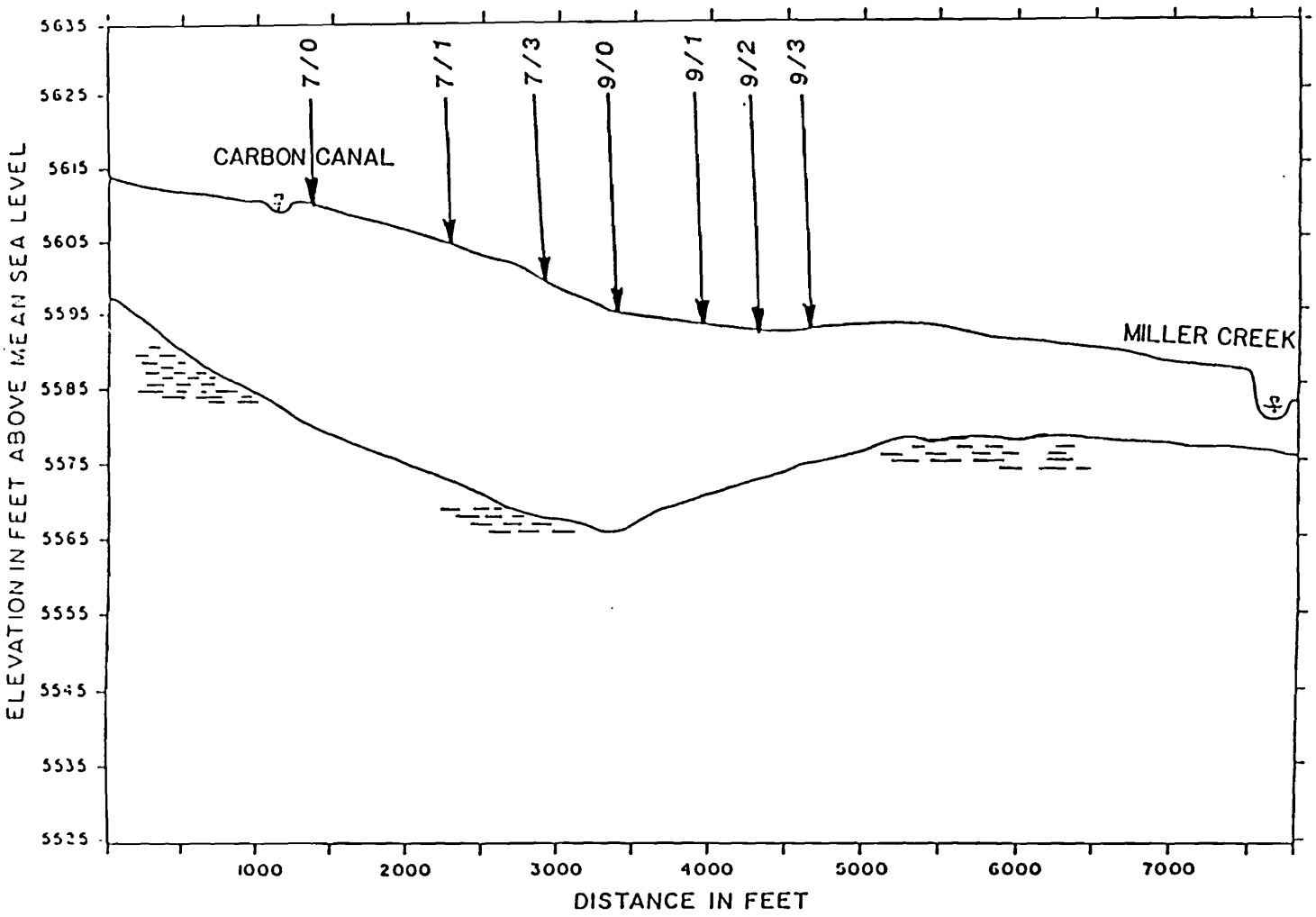

Figure III-2. Soil sampling locations on a transect along wells 7, 9, and 12. A zero marked after the slash indicates a sample taken at the well site and the other numbers represent locations downslope from the well in approximately 500-foot increments.

Methods and Procedures

Sampling

Both groundwater and surface water samples were collected in small (100 ml) and large (500 ml) plastic bottles. The samples were withdrawn from the wells using a bailer, and in the case of small diameter wells (1/2-inch), using a Jack-Rabbit™ pump. The pH and electrical conductivity (EC) of all the samples were measured immediately upon collection using a specific ion meter and a salinity bridge, respectively. The EC meter was calibrated using a standard solution of known electrical conductivity and the measurements were corrected to 25°C. Field measurements of total alkalinity were made within 6 hours of sampling using standard titrimetric methods. The smaller bottle samples were filtered immediately and acidified using a few drops of 50% HNO_3 (nitric acid) to preserve the metals. The samples were stored in ice at temperatures of $\simeq 2$°C and transported to the laboratory for further chemical tests. The larger bottle samples were filtered upon arrival at the laboratory. Water level measurements were taken at each well using a steel tape graduated to the nearest tenth of an inch. Flow gaging measurements were taken at the Miller Creek locations (approximately 1 mile in each direction from the transect).

Well installation

As previously mentioned, analysis of the CH2M Hill (1983) field data indicated a need to install additional wells to better describe the subsurface flow in the area and the relation of groundwater flow to changes in bedrock topography. The wells were numbered in increasing numbers after 10, the last well installed at the site by CH2M Hill (1983). Piezometer pounding equipment was used to install 1/2-inch diameter galvanized iron pipes to a depth of 9 feet at all the selected locations which were then replaced in most cases with 1/2-inch PVC tubing. Additional piezometers (wells) at a depth of 18 feet were installed at locations 14 and 15. To develop the wells, distilled water was poured into the pipes until full and air at a pressure of 150 psi was blown from the top of the well to evacuate this water. This method was repeated several times and then the well was bailed until the water quality stabilized. Sampling began on the month after the groundwater quality had stabilized.

Laboratory analysis

The pH of each sample in the unfiltered large bottles (500 ml) was determined upon arrival at the laboratory. Samples were analyzed by the soil, plant and water analysis laboratory at Utah State University. Laboratory procedures outlined in Agricultural Handbook No. 60 (U.S. Department of Agriculture 1954) were followed in determination of constituent concentrations in the water samples. The unfiltered samples were filtered and analyzed for the major anions (Cl^-, SO_4^{2-}, CO_3^{2-}, and HCO_3^-) using colorimetric, turbidimetric, and titrimetric methods. The filtered and acidified samples in the small bottles (100 ml) were analyzed for the major cations (Ca^{2+}, Na^+, Mg^{2+}, and K^+) using atomic absorption (AA) techniques. The AA determinations had detection limits up to one-tenth of one part per million (ppm). Samples analyzed for Na^+ and K^+ had to undergo emission spectroscopy prior to using AA techniques. Results of the laboratory analysis are summarized in Appendix B. A cation-anion balance check for equivalence was performed on the results and showed a maximum error of 10 percent.

CHAPTER IV

INTERPRETATION OF FIELD DATA

This chapter summarizes the hydrogeochemical analysis of data collected in the Miller Creek subbasin site. Trends and correlations of the chemical data are established in relation to the hydrologic system.

Summary of Data Collected

As described in Chapter III, data were collected regularly from existing and newly installed wells during the period of April to November 1984, and added to the existing data base (CH2M Hill 1983). Table IV-1 summarizes the average concentration of each of the chemical constituents (Ca^{2+}, Mg^{2+}, K^{+}, Na^{+}, HCO_3^{-}, CO_3^{2-}, Cl^{-}, and SO_4^{2-}), alkalinity (ALK), electrical conductivity (EC), temperature (TEMP), and pH for each well. Similarly, Table IV-2 summarizes the data for surface water quality in the Carbon Canal and the Miller Creek subbasin stations. The entire set of water quality and soil chemistry data is listed in Appendix B.

Hydrogeologic Analysis

Bedrock geology at the field site plays an important part in controlling both groundwater flow and water quality. This section summarizes our present understanding of the groundwater flow system from interpretation of well drilling and water level informationat the site. Trends and correlations are also established in the groundwater quality data.

Groundwater flow field

Irrigated agriculture has resulted in an extensive shallow groundwater system. The groundwater within the underlying Mancos shale is too meager to consider it as a significant aquifer. The Mancos shale is generally of low permeability, although groundwater recharge can occur through joints, fractures, and open bedding planes (Johnson and Schumm 1982). Inflow to the groundwater system is due to canal seepage, deep percolation of irrigation water, regional groundwater inflow (assumed but not proven to be minor at the Miller Creek site) and precipitation. Groundwater outflows are due to crop and phreatophyte consumption, discharge to surface water and regional groundwater outflow.

An analysis of the depth to bedrock from lithologic logs at the Miller Creek site suggests that the bedrock topography is a primary factor controlling the existence of a saturated zone and flow of groundwater. Saturated groundwater flow is essentially following the dip and irregularities in the bedrock surface. Thus, accurate mapping of the bedrock surface is of paramount importance in establishing the groundwater flow field. This objective has not been fully accomplished during this study, however, the additional wells installed did allow an estimate of the direction of groundwater flow. Using the available water level and bedrock elevation information the

Table IV-1. Average groundwater quality data.

Well ID	Concentration in mg/l								ALK mg/l as $CaCO_3$	EC µmhos/cm^2 @ 25°C	pH
	Ca	Mg	K	Na	HCO_3	CO_3	Cl	SO_4			
7I	123.2	30.5	3.9	23.4	280.7	9.0	16.2	76.8	241.5	587	7.7
7D	436.9	138.6	11.7	80.5	299.0	0.0	21.3	1,489.0	246.8	2,263	7.3
9S	77.0	31.4	7.8	32.2	313.6	0.0	18.4	49.2	256.8	542	7.6
9I	189.0	44.1	7.8	41.4	278.2	0.0	18.4	88.8	228.2	520	7.8
9D	76.2	1810.1	35.2	7395.4	567.4	36.0	1152.1	20,087	486.1	27,457	7.7
10I	424.8	352.5	19.6	443.7	390.5	0.0	124.1	2,916	320.0	4,479	7.4
10D	326.7	330.7	23.5	836.8	512.5	0.0	81.5	3,987	420.0	7,506	7.2
11I	421.8	104.5	-	52.2	189.7	0.0	13.8	1,248.8	155.5	2,310	7.2
12I	70.5	541.0	15.6	2806	382.6	0.0	189.0	7,370	313.5	11,422	8.0
13I	182.4	211.5	-	1381.6	573.5	0.0	113.4	6,186.4	467.8	11,620	7.1
14S	362.7	306.3	-	124.1	317.3	6.0	28.4	2,108.5	277.0	3,281	7.9
14D	315.8	313.6	-	533.3	146.4	0.0	141.8	3,338.1	120.5	5,419	7.8
15S	34.5	162.9	-	673.9	200.1	21.3	158.5	2,161.4	235.0	4,420	7.3

Table IV-2. Average surface water quality data.

ID	Concentration in mg/l								ALK mg/l as $CaCO_3$	EC µmhos/cm^2 @ 25°C	pH
	Ca	Mg	K	Na	HCO_3	CO_3	Cl	SO_4			
Carbon Canal	60.6	24.8	3.9	20.4	225.7	24.0	13.3	60.2	209.2	559	7.9
Miller Creek Upstream	180.4	150.7	11.7	213.8	250.2	0.0	88.6	1176.8	219.5	3031	8.1
Miller Creek Downstream	186.4	126.4	7.8	209.2	299.0	0.0	46.1	1109.5	245.6	2792	8.0

most probable flow path down this complex hillslope follows a line approximately defined by wells 7, 9, and 12. This line of wells delineates a continuous depression in the bedrock topography which follows the regional dip of the bedrock surface.

The available water level measurements over the saturated depth of the aquifer were used to map the hydraulic head contours in the vertical plane as illustrated in Figure IV-1. Vertical hydraulic gradients at well 7 aided in conceptualizing vertical flow near the upslope locations along the profile (7, 9 and 12). There were no vertical hydraulic gradients observed in the piezometer nests at the downslope wells indicating horizontal flow. This also indicates that little or no recharge occurs at the downslope part of the transect, a region characterized as lightly irrigated pasture land.

Water Quality Correlations

Well water levels and electrical conductivity (EC)

All the water level and EC data collected during the present study were plotted to establish a possible relation between EC and water table fluctuations (see Figures C-1 through C-6). Data collection began just before the irrigation season and continued until after the last irrigation. During the irrigation season deep percolation causes water levels to rise while conversely the EC goes down due to dilution. Correspondingly, when the irrigation season ends, water levels decline and the EC rises. CH2M Hill (1983) found similar trends in their data (Figures C-7 through C-9). The lower EC during the irrigation season can be attributed to dilution of the higher EC groundwater due to recharge from irrigation.

Major ions versus TDS

All the water chemistry data collected were analyzed and plotted to establish correlations between the major ions (Ca^{2+}, Na^{+}, Mg^{2+}, Cl^{-}, SO_4^{2-}, HCO_3^{-}) and the total dissolved solids (TDS). The percentage of the total milliequivalents per liter (meq/l) of each ion was plotted against TDS. These plots (Figures IV-2 through IV-4 show strong correlations for Ca^{2+}, Na^{+}, SO_4^{2-} and HCO_3^{-} ions. With increasing TDS, the relative concentrations of sodium and sulfate increase and those of calcium and bicarbonate decrease. The relative concentration (percentage) of Mg^{2+} and Cl^{-} appear to remain fairly constant with increasing TDS.

The above correlations provide a basis for understanding the chemical processes occurring. In general, dissolution of gypsum is the primary source of SO_4^{2-} concentrations which is the major anion at higher TDS. Na-Ca exchange reactions account for the inverse relationship of increasing sodium and decreasing calcium at higher TDS. These processes will be examined in more detail when the geochemical evolution along a flow path is investigated as described in a later section.

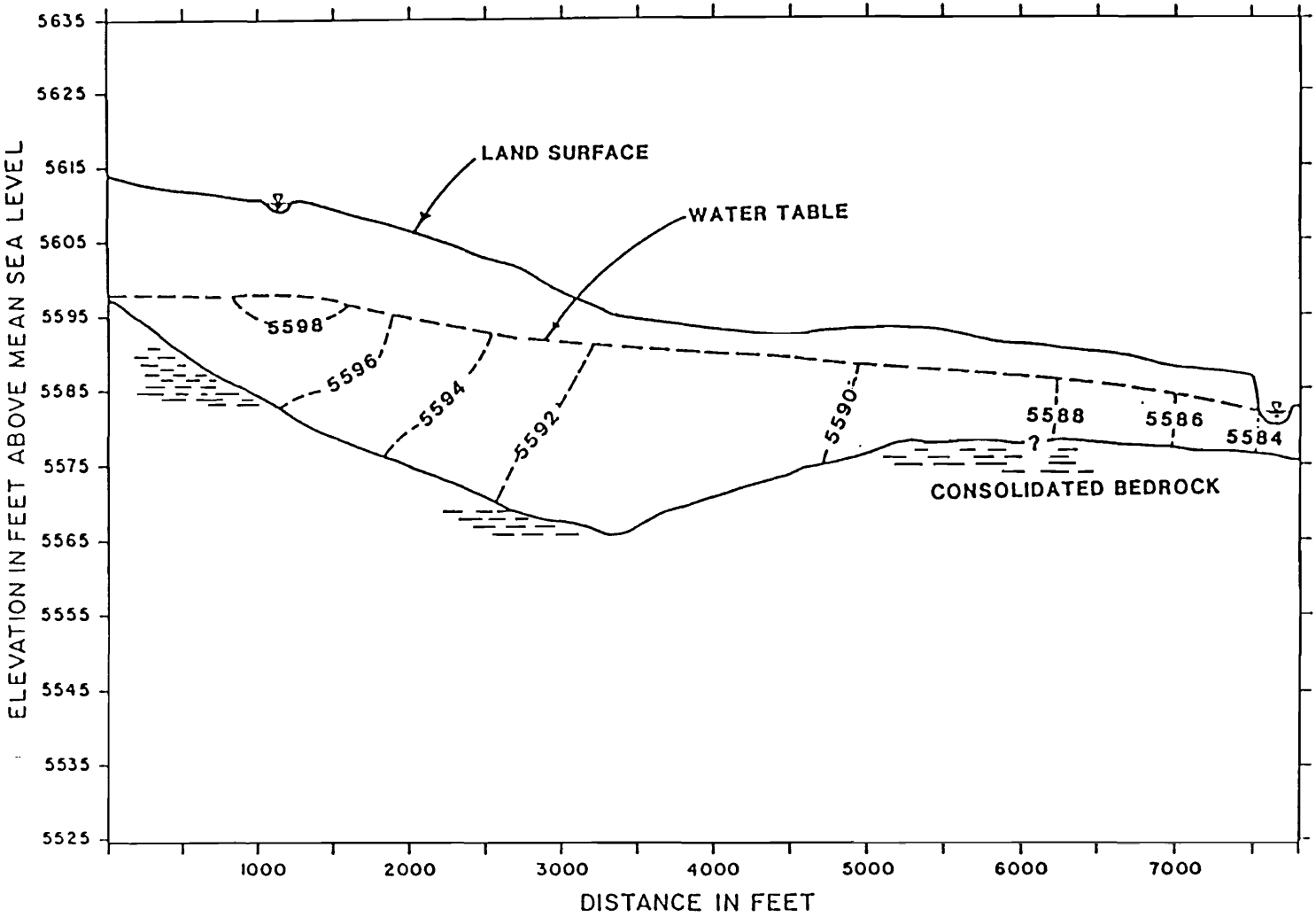

Figure IV-1. Hydraulic head contour map on a transect along wells 7, 9, and 12.

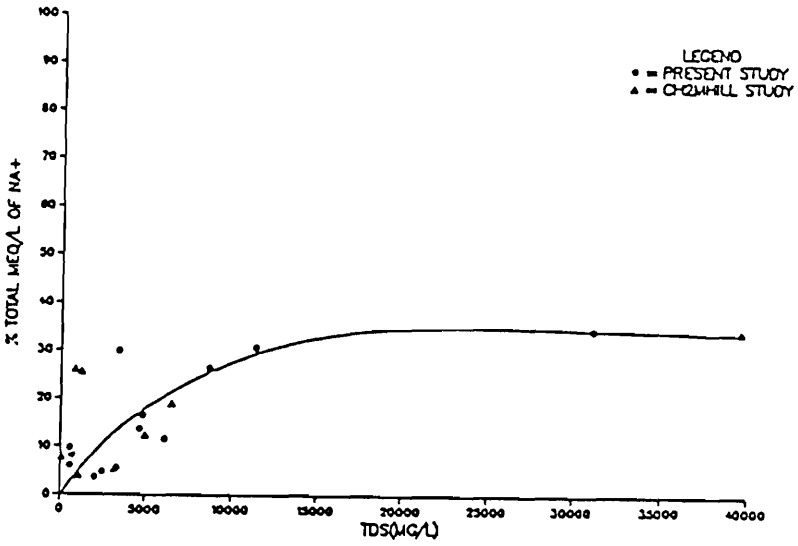

(a)

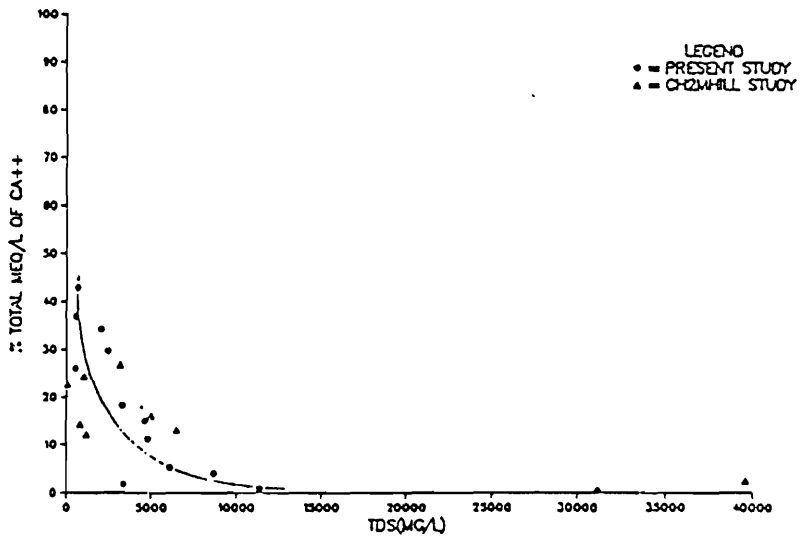

(b)

Figure IV-2. (a) Percentage of Na^{+} versus TDS, (b) Percentage of Ca^{2+} versus TDS.

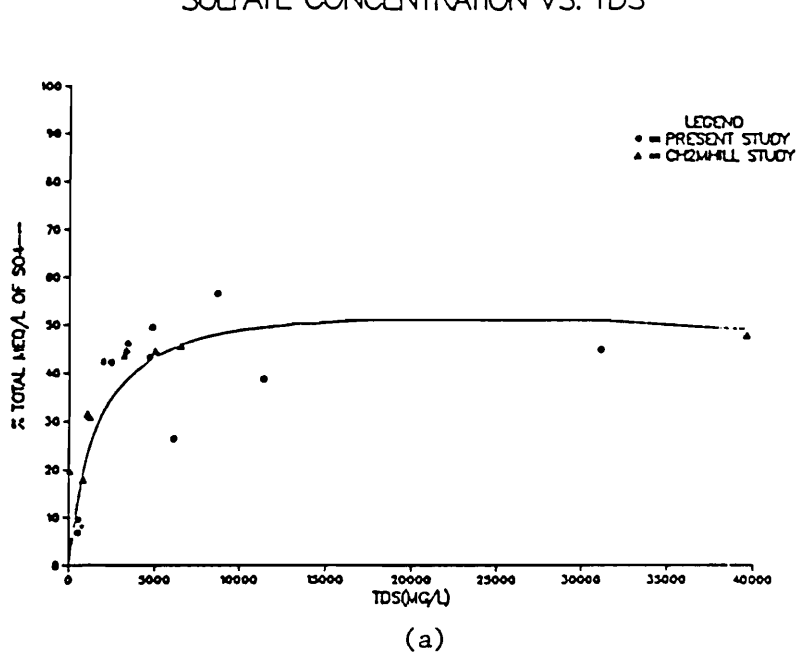

Figure IV-3. (a) Percentage of SO_4^{2-} versus TDS, (b) Percentage of HCO_3^- versus TDS.

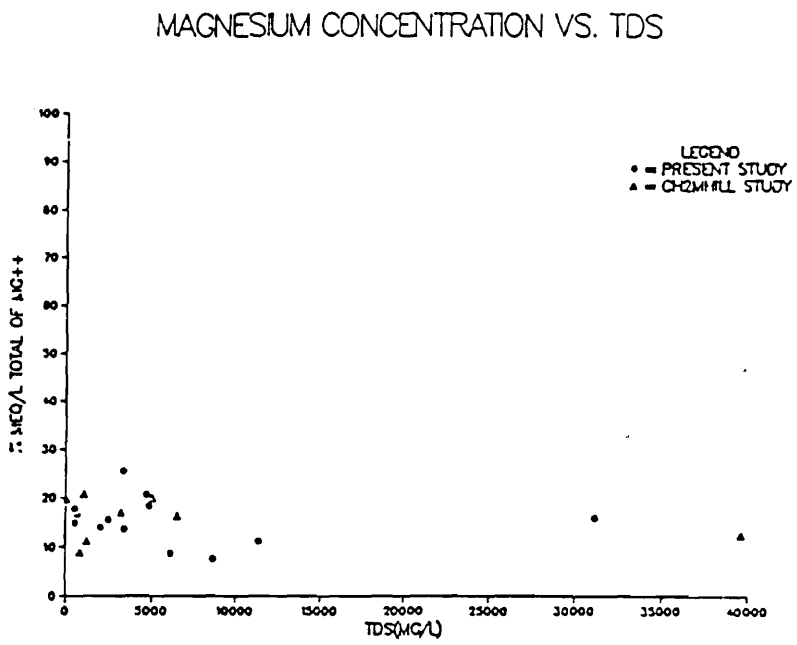

(a)

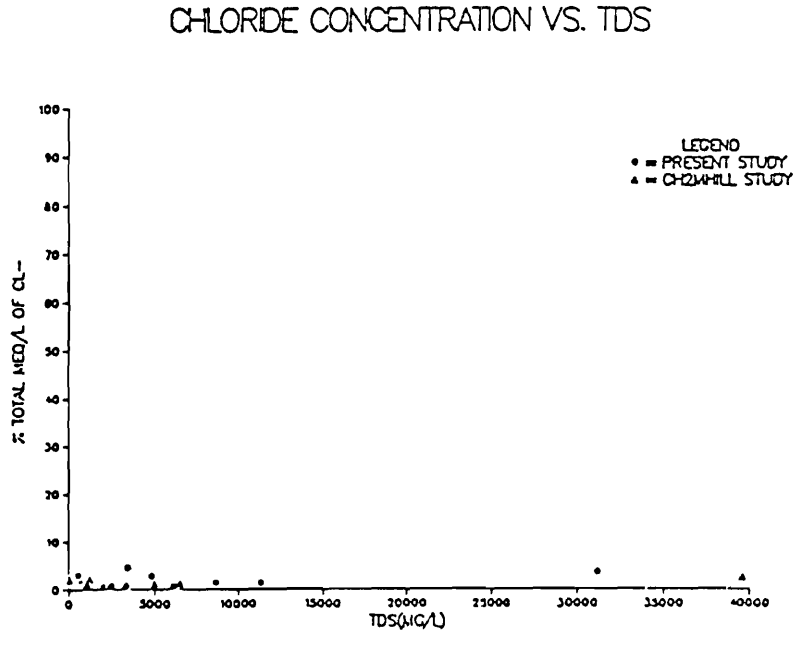

(b)

Figure IV-4. (a) Percentage of Mg^{2+} versus TDS, (b) Percentage of Cl^- versus TDS.

Geochemical Analysis

The analysis performed herein examines the chemical characteristics of the groundwater system from all the chemistry data gathered to date. Surface water quality data is used to identify the salt loads, and groundwater and soil quality data is used to identify the chemical evolution along the groundwater flow path. All the chemistry data is presented graphically on trilinear diagrams.

Temporal analysis of upstream and downstream water quality

CH2M Hill (1982, 1983) had gathered surface water quality data at two sites on Miller Creek. The sites are located above the Carbon Canal and at the mouth of the Miller Creek, respectively. To identify the mass loading due to the irrigation return flow, temporal data for flow, TDS and some major ions (Ca^{2+}, Na^{+}, Cl^{-}, SO_4^{2-}) were plotted for the period May 1981 through April 1982 (Figures IV-5 through IV-7). The mass flux rate (QC) was also plotted for the TDS and SO_4 (Figure IV-8). From these plots, the following interpretations can be made:

1. Flow in the Miller Creek above the Carbon Canal has a small seasonal component. The flow at the mouth is at its highest during early summer (May to June 1981) due to high spring runoffs from snowmelt. A net groundwater contribution is indicated by a higher flow at the downstream location than at the upstream location.

2. The total dissolved solids at the downstream site (at mouth of Miller Creek) shows an increasing trend. The effect of the solute response time is shown by an increase in TDS levels at the downstream site after the irrigation season. All the major ions (Ca^{2+}, Na^{+}, Cl^{-}, and SO_4^{2-}) exhibit similar behavior.

3. The mass flux rate for TDS and SO_4^{2-} at the downstream site is higher than at the upstream site during the spring and summer months (May through July). During the winter months the mass flux rate at both sites are fairly equal and start increasing at both sites soon after the winter season is over. It is evident that the increasing mass flux downstream is a result of irrigation return flow.

Chemical evolution along profile

The flow profile was examined to delineate zones of dominant chemistry and to examine changes in sodium adsorption ratios (SAR) along the flow path (7-9-12). Earlier it was postulated that the system is dominated by four representative ions Ca^{2+}, Na^{+}, SO_4^{2-}, and HCO_3^{-}. Average concentrations (in meq/l) of these four major ions were used to identify zones of dominant water type from measurements taken at each well. Figure IV-9 summarizes the results graphically. A similar analysis was performed for the soil chemistry (Figure IV-10). The inset to Figure IV-10 shows the soil sampling locations along the profile. The chemical zonation suggests:

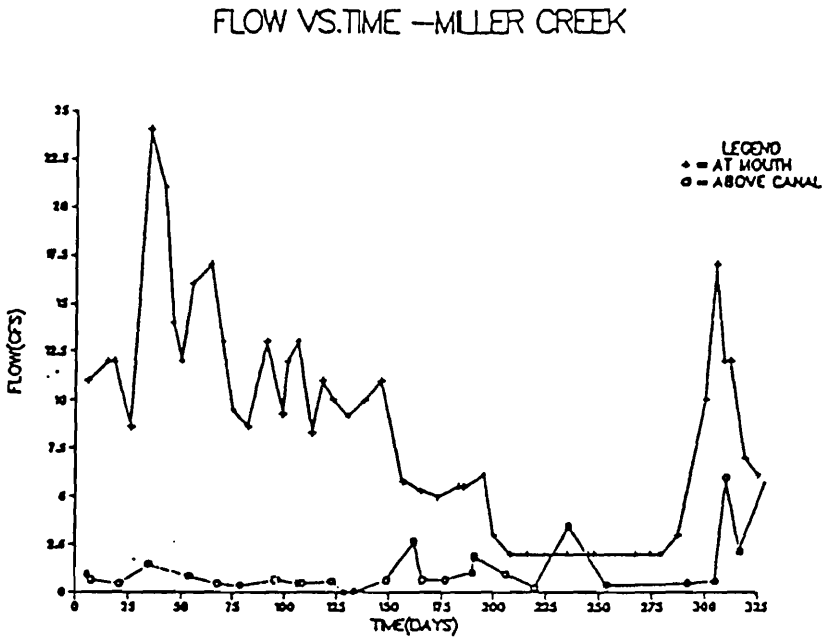

(a)

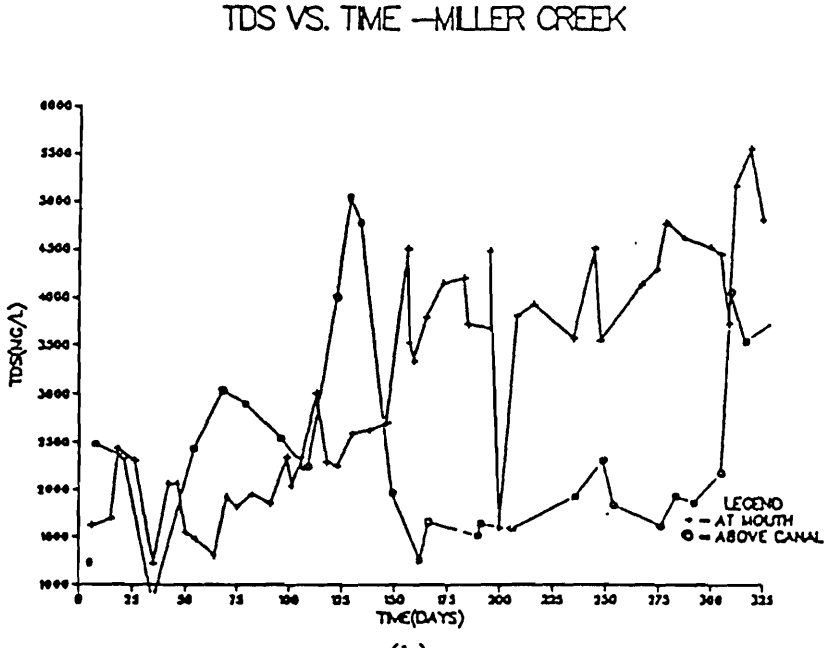

(b)

Figure IV-5. (a) Flow versus time at Miller Creek locations, (b) TDS versus time at Miller Creek locations. For the period May 1981-April 1982 (Source: CH2M Hill 1983).

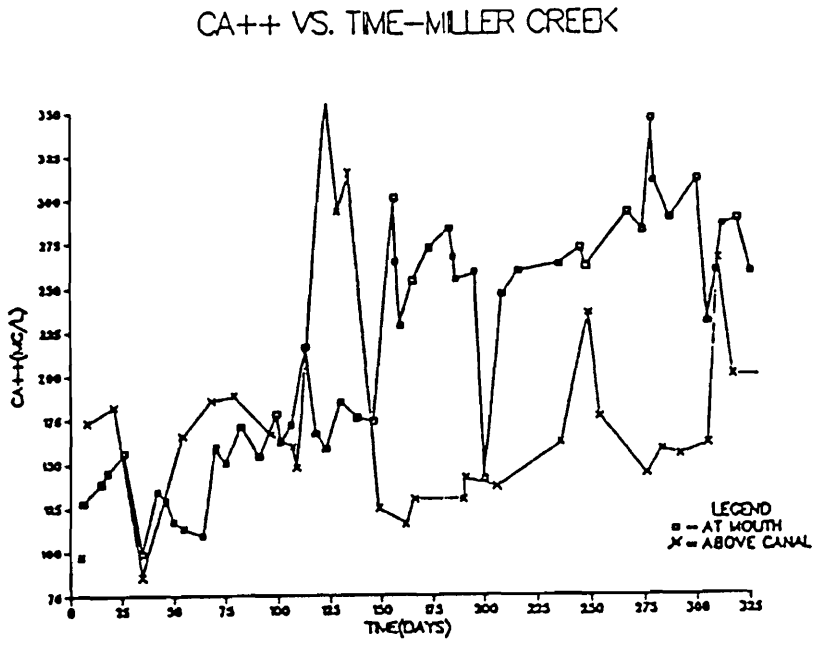

(a)

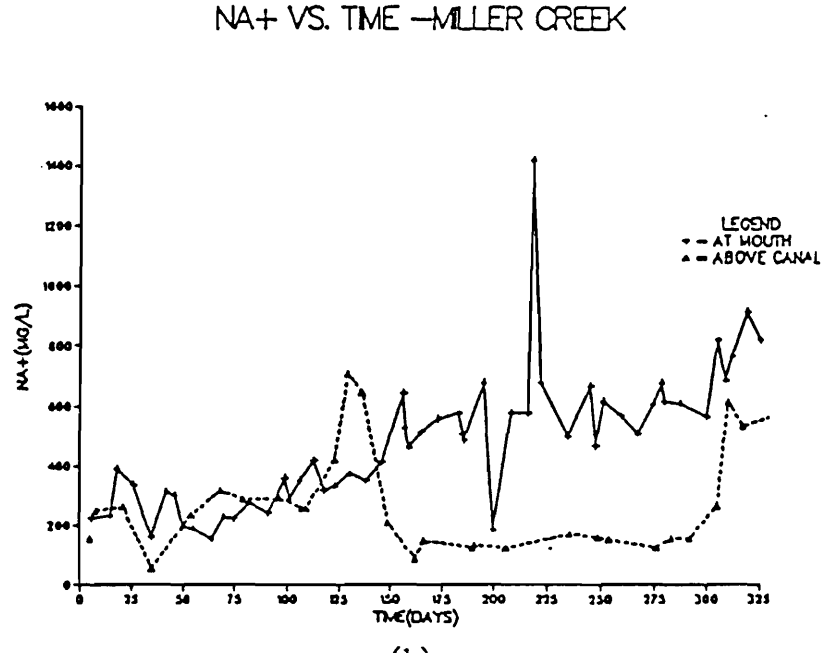

(b)

Figure IV-6. (a) Ca^{2+} versus time at Miller Creek locations, (b) Na^{+} versus time at Miller Creek locations. For the period May 1981-April 1982 (Source: CH2M Hill 1983).

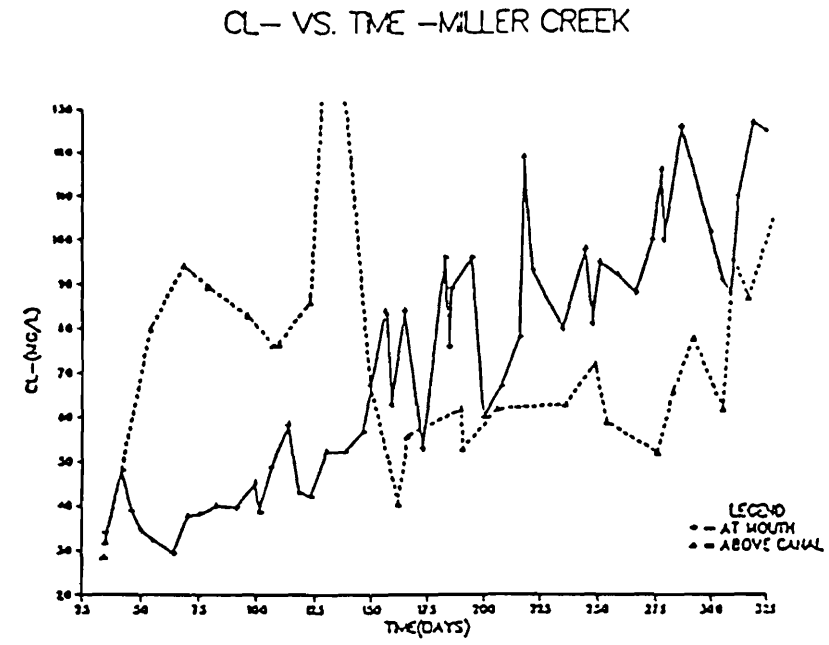

(a)

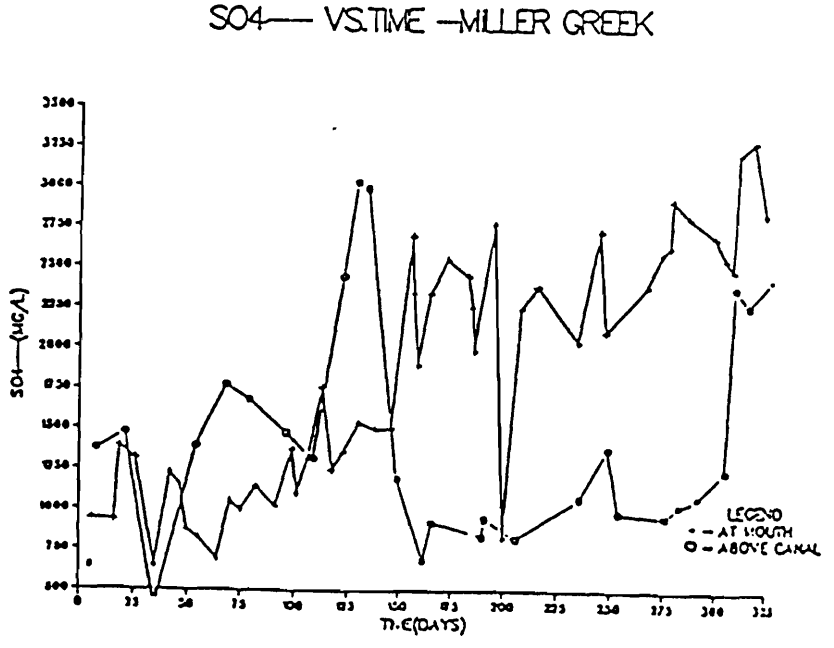

(b)

Figure IV-7. (a) Cl^- versus time at Miller Creek locations, (b) SO_4^{2-} versus time at Miller Creek locations. For the period May 1981-April 1982 (Source: CH2M Hill 1983).

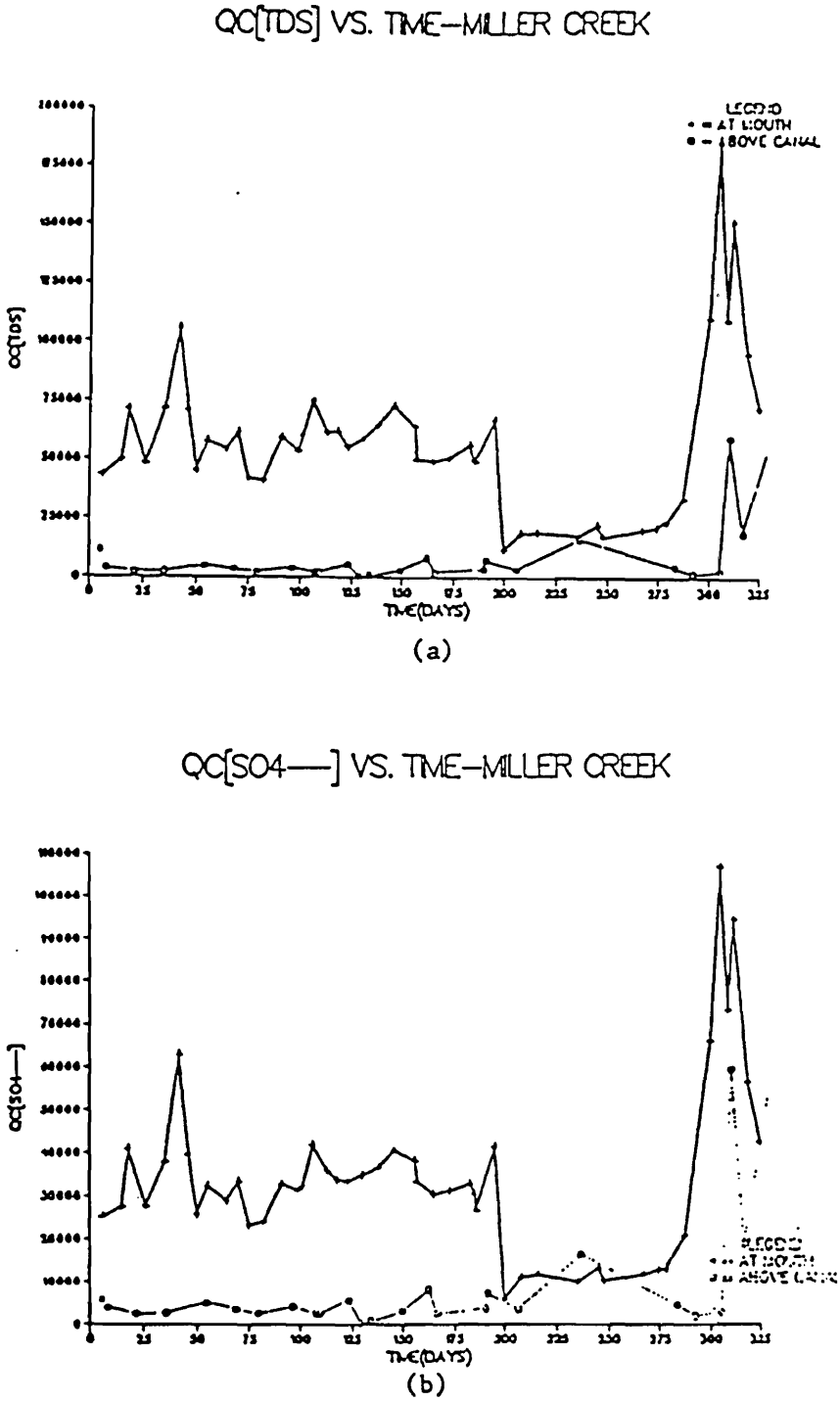

Figure IV-8. (a) Mass flux (TDS) versus time at Miller Creek locations, (b) Mass flux (SO_4^{2-}) versus time at Miller Creek locations. For the period May 1981-April 1982 (Source CH2M Hill 1983).

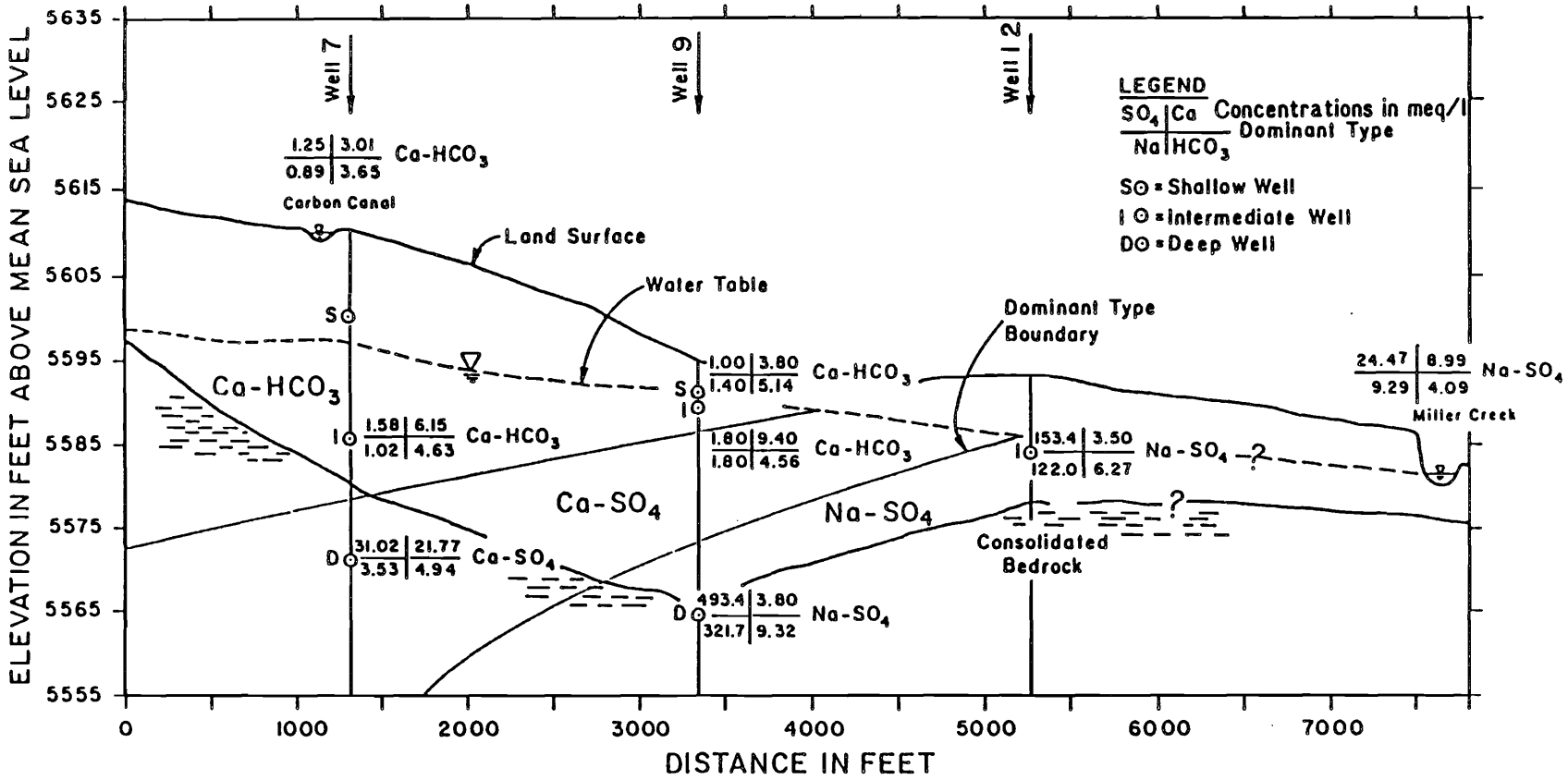

Figure IV-9. Chemical zonation of groundwater along profile.

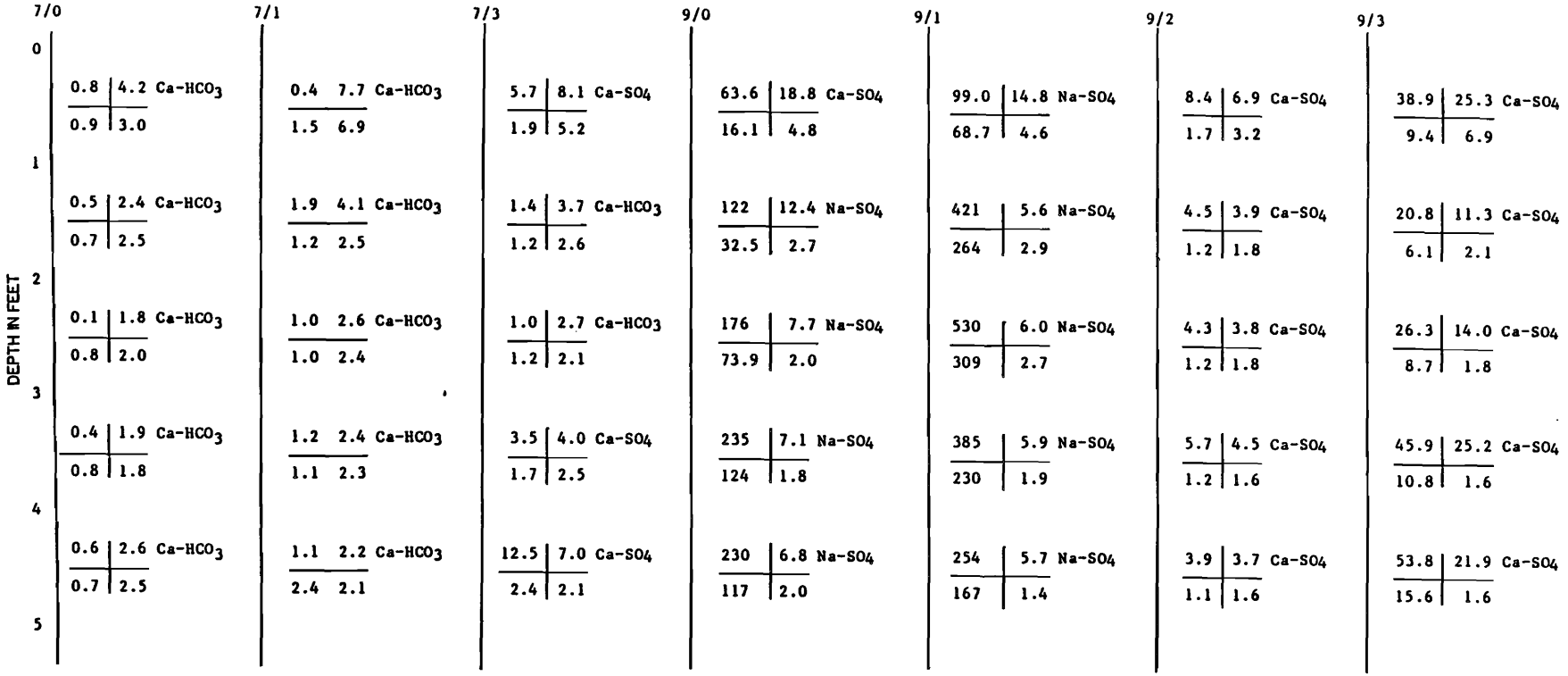

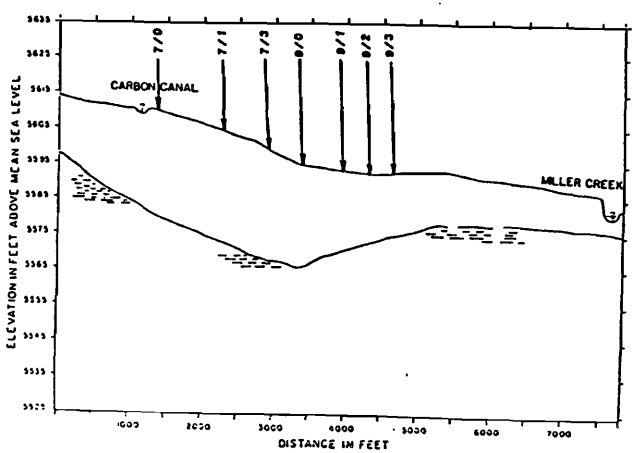

LEGEND

SO4 | Ca — Dominant Type
Na | HCO3
concentration in meq/l

Figure IV-10. Chemical zonation of soils (up to 5 feet depth) along profile.

1. There is a trend from a bicarbonate dominated water to a sulfate dominated water with depth and distance along the profile.

2. Sodium increases with depth and distance from the Carbon Canal. Since sulfate also increases and calcium does not, the exchange of calcium ions for sodium ions is postulated.

Sodium adsorption ratios (SAR) were computed using soil and water quality data from the present study (see Appendix D). Results of the SAR computations are provided in Table IV-3. The SAR values lead to the following conclusions.

1. The sodic hazard increases from the Carbon Canal towards the Miller Creek (increasing values of SAR).

2. Increasing SAR with depth at well 7 indicates little or no interaction with sodium-Mancos shale. This suggests that the shale could be weathered and the sodium leached out.

3. A region of Mancos shale of high exchangeable sodium percentage (ESP) probably exists around the deep well at 9 supported by an extremely high value of SAR at 9D.

4. The high SAR value at well 12 indicates either a contact with high ESP shale (unweathered) or just dilution and mixing of water from the upslope well (9).

Table IV-3. Results of SAR computations for soil and water chemistry.

Location	SAR = $Na/\sqrt{(Ca + Mg)/2}$
Groundwater	
7I	0.48
7D	0.86
9S	0.78
9I	0.71
9D	36.8
12I	24.9
Surface Water	
Carbon Canal	0.57
Miller Creek Upstream	2.84
Miller Creek Downstream	2.89
Soil	
7/0	0.55
7/1	0.67
7/3	0.80
9/0	10.93
9/1	30.08
9/2	0.69
9/3	2.57

CHAPTER V

GEOCHEMICAL MODELING

This chapter describes the development of a conceptual groundwater geochemical model based on field data from Chapter IV. Equilibrium speciation calculations were performed using the USGS geochemical model PHREEQE. Results of the equilibrium speciation calculations were then used in the USGS mass balance model BALANCE.

Conceptual Model

The purpose of this study was to identify the important mineral dissociation and ion-exchange reactions that control groundwater composition. Whittig et al. (1982) investigated the mineralogy of the Mancos shale. Their analysis indicated that only three detectable free minerals are present in unweathered and partially weathered shales: gypsum ($CaSO_4 \cdot 2H_2O$), calcite ($CaCO_3$), and dolomite ($MgCa(CO_3)_2$). The dissociation reactions for these minerals are presented with their respective solubility products (K_{sp}), enthalpies of formation (ΔH_f°) (Lindsay 1979) and free energies of formation (ΔG_f°) (Weast 1970, Lindsay 1979).

Gypsum

$$CaSO_4 \cdot 2H_2O \rightleftarrows Ca^{2+} + SO_4^{2-} + 2H_2O$$

$K_{sp} = 10^{-4.64}$; $\Delta H_f^\circ = -483.22$ Kcal/mole;

$\Delta G_f^\circ = -430.17$ Kcal/mole

Calcite

$$CaCO_3 \rightleftarrows Ca^{2+} + CO_3^{2-}$$

$K_{sp} = 10^{-8.42}$; $\Delta H_f^\circ = -288.77$ Kcal/mole;

$\Delta G_f^\circ = -270.18$ Kcal/mole

Dolomite

$$MgCa(CO_3)_2 \rightleftarrows Ca^{2+} + Mg^{2+} + 2CO_3^{2-}$$

$K_{sp} = 10^{-17.0}$; $\Delta H_f^\circ = -556.85$ Kcal/mole;

$\Delta G_f^\circ = -518.82$ Kcal/mole

Previously, it was speculated that ion-exchange involving Na-Ca exchange influenced the composition of the groundwater. To quantify this statement and include magnesium (Mg^{2+}) as a possible counter ion in exchange reactions,

the following exchange reactions and selectivity coefficients (K_s) were used in the conceptual model.

Na-Ca Exchange

$$1/2\ Ca^{2+} + X_{Na} \rightleftarrows Na^{+} + X_{Ca}$$

$$K_s = \frac{(Na)X_{Ca}}{(Ca)^{1/2}\ X_{Na}} = 5.8$$

Na-Mg Exchange

$$1/2\ Mg^{2+} + X_{Na} \rightleftarrows Na^{+} + X_{Mg}$$

$$K_s = \frac{(Na)X_{Mg}}{(Mg)^{1/2}\ X_{Na}} = 3.4$$

Ca-Mg Exchange

$$Mg^{2+} + X_{Ca} \rightleftarrows Ca^{2+} + X_{Mg}$$

$$K_s = \frac{(Ca)X_{Mg}}{(Mg)X_{Ca}} = 0.83$$

where X_i represents one/100 g of exchanageable ith ion and (i) signifies activities of the ith ion in the solution phase. The K_s values presented are mean values calculated from exchanageable ion data obtained under saturated moisture conditions using soils obtained from Huntington Creek subbasin within the Price River drainage. Details of the methodology can be found in Robins (1979).

Equilibrium Modeling Using PHREEQE

The USGS chemical equilibrium model, PHREEQE (Parkhurst et al. 1980) was used to represent chemical changes occurring in the groundwater by equilibrating the groundwater at each sampling well to the mineral phases assumed present in the soil. This permits the computation of the Saturation Indices (S.I.'s) of appropriate minerals and estimates ionic composition not directly determined analytically. The analytical concentrations, thus calculated, were used in mass balance computations. Amounts of precipitation or dissolution of the mineral phases (Δ-phases) are also determined as the groundwater is equilibrated with the appropriate mineral phase. This calculation identifies the potential for precipitation or dissolution of a particular mineral phase at any well location.

Statement of the problem

The conceptual model was applied to five equilibrium cases of increasing complexity involving mineral phase and ion exchange reactivity.

Case 1. Calcite and gypsum equilibrium without cation exchange.

Case 2. Calcite and gypsum equilibrium with Na-Ca exchange reaction.

Case 3. Introduction of dolomite as an additional mineral variable in cases 1 and 2.

Case 4. Calcite and gypsum equilibrium with dolomite added in increments of 0.0025 to 0.025 moles with Na-Ca and Na-Mg exchange reactions.

Case 5. Gypsum equilibrium with calcite added in increments from 0.0002 to 0.002 moles with Na-Ca and Ca-Mg exchange reactions.

Input data, limitations, and assumptions

The following input data is required according to the format specified in the PHREEQE manual (Parkhurst et al. 1980):

1. Concentrations of the constituents in each reaction.

2. Properties of the solution water such as temperature, pH and total alkalinity.

3. Mineral phases which the solution is to be equilibrated with, including properties of the mineral phase dissociation reactions such as: equilibrium constants (log K), enthalpies (ΔH_f°), operational valence and stoichiometric coefficients.

4. Cation exchange reactions taking place, if any, and their respective selectivity coefficients (K_s).

Numerical and conceptual limitations to the PHREEQE program are described in detail in the operating manual, and thus no attempt will be made here to duplicate this information. The input data for each well site is given in Table V-1.

Interpretation of the results

The relative locations of the observation wells for which the geochemical equilibrium simulations were calculated by PHREEQE are shown in Figure V-1. The saturation index (Log(Ion Activity Product/Ksp)) of each solution computed using PHREEQE are given in Table V-2. The saturation indices (S.I.'s) indicate that the groundwater is consistently undersaturated (negative values) with respect to gypsum; and thus if gypsum is present, dissolution will occur. The saturation indices also indicate that the groundwater is supersaturated with respect to calcite and dolomite (positive values) and the precipitation of these minerals is expected. Supersaturation with respect to calcite in the soil solution and surface water is a commonly observed phenomenon (Suarez 1983).

The results for cases 1 through 4 and case 5 are summarized in Tables V-3 and V-4, respectively. Visible trends on the effect of depth are indicated by the Δ-phases at several wells. Introduction of Na-Ca exchange reaction leads to more gypsum being dissolved at all wells, and less calcite

Table V-1. Input data summary for use in PHREEQE.

Well Ident.	Concentrations in mg/l					Alkalinity mg/l as $CaCO_3$	pH	Temp °C
	Ca 4	Na 6	Mg 5	Cl 14	SO_4 16			
7I	79.5	24.2	32.4	15.0	90.0	267.3	7.4	21.8
7D	447.1	87.4	151.0	20.3	1530.0	257.9	7.0	21.5
14S	376.8	115.0	327.0	29.4	2151.8	268.0	9.1	18.0
14D	330.7	478.4	345.3	133.7	3122.0	185.5	8.9	15.0
9S	77.0	32.2	31.4	18.4	49.2	251.7	7.6	25.0
9I	189.0	41.4	44.1	18.4	88.8	255.8	7.6	28.0
9D	80.0	7740.0	1798.0	1090.0	24,080	507.5	7.0	19.9
12I	70.5	2806.0	541.0	189.0	7370.0	313.5	7.9	29.0
13I	190.4	1462.7	257.8	102.1	5648.4	500.0	7.1	24.0
10I	424.4	443.9	352.9	123.1	2916.0	343.2	7.1	26.5
10D	358.3	850.0	321.5	78.5	3953.0	448.3	6.8	22.0

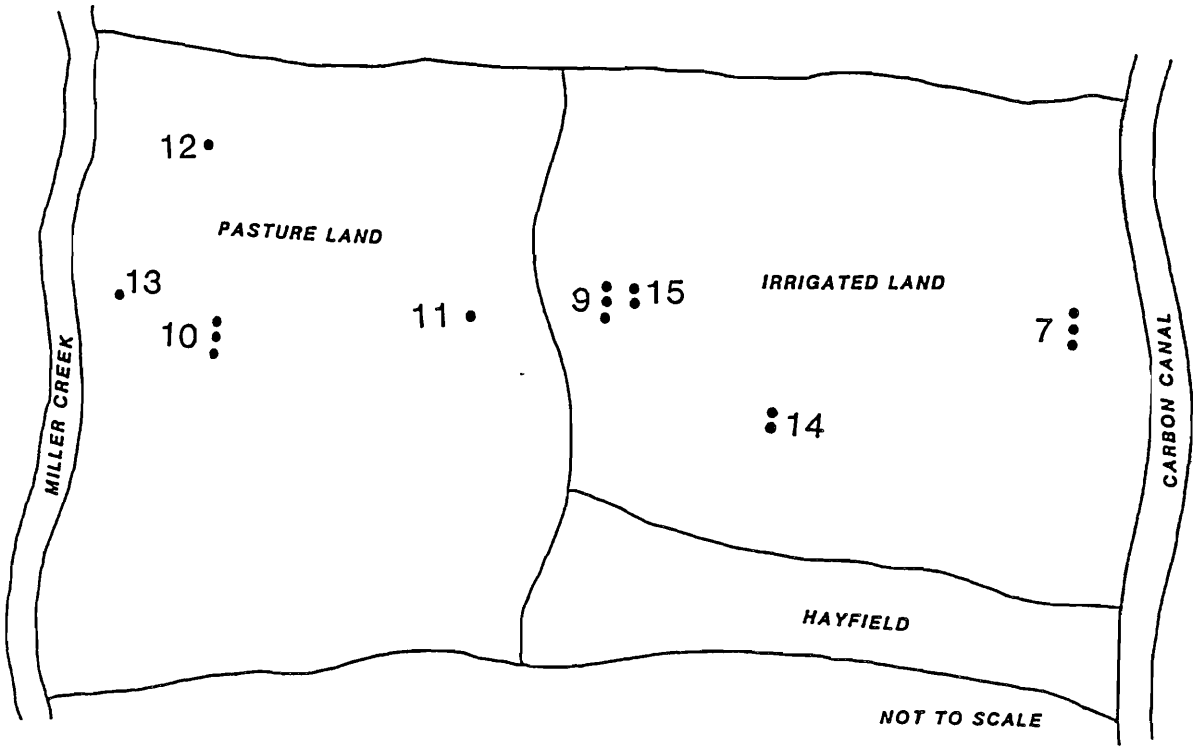

Figure V-1. Relative location of observation wells used in geochemical simulations.

Table V-2. Saturation index values computed using PHREEQE.

Well ID	Mineral Phase		
	Calcite	Gypsum	Dolom.
7I	0.244	-1.639	0.361
7D	0.251	-0.151	0.311
14S	1.939	-0.175	4.067
14D	1.505	-0.142	3.242
9S	0.266	-1.891	0.434
9I	0.837	-1.394	1.356
9D	-0.810	-0.558	0.029
12I	0.158	-0.755	1.560
13I	-0.002	-0.308	0.446
10I	0.380	-0.090	1.010
10D	-0.008	-0.090	0.233

Table V-3. Results on Δ-phases (in moles) for cases 1 through 4 from PHREEQE simulations.

Well	Phases	Gypsum and Calcite		Dolomite Gypsum and Calcite Equilibrium						
		Without Exchange	With Na-Ca Exchange	Without Exchange	With Na-Ca Exchange	With Na-Ca, Na-Mg exchange Dolomite added in increments				
						0.0025 moles	0.0075 moles	0.0125 moles	0.020 moles	0.025 moles
		Case 1	Case 2	Case 3		Case 4				
7I	Gypsum	1.49 x 10-2	1.32 x 10-1	2.33 x 10-2	1.37 x 10-1	1.30 x 10-1	1.30 x 10-1	1.30 x 10-1	1.30 x 10-1	1.30 x 10-1
	Calcite	-1.66 x 10-3	-3.80 x 10-5	-2.19 x 10-2	-1.09 x 10-2	-3.28 x 10-3	-1.33 x 10-2	-2.33 x 10-2	-3.83 x 10-2	-4.83 x 10-2
	Dolomite			1.02 x 10-2	5.43 x 10-3					
7D	Gypsum	3.10 x 10-3	1.19 x 10-1	8.84 x 10-3	1.21 x 10-1	1.23 x 10-1	1.23 x 10-1	1.23 x 10-1	1.23 x 10-1	1.23 x 10-1
	Calcite	-1.43 x 10-3	8.97 x 10-5	-1.18 x 10-2	-1.06 x 10-3	-3.41 x 10-3	-1.34 x 10-2	-2.34 x 10-2	-3.84 x 10-2	-4.84 x 10-2
	Dolomite			5.24 x 10-3	5.76 x 10-4					
9S	Gypsum	1.50 x 10-2	1.49 x 10-1	2.33 x 10-2	1.54 x 10-1	1.53 x 10-1	1.53 x 10-1	1.53 x 10-1	1.53 x 10-1	1.53 x 10-1
	Calcite	-1.63 x 10-3	3.21 x 10-5	-2.11 x 10-2	-1.00 x 10-2	-3.26 x 10-3	-1.33 x 10-2	-2.33 x 10-2	-3.83 x 10-2	-4.83 x 10-2
	Dolomite			9.82 x 10-3	5.03 x 10-3					
9I	Gypsum	1.37 x 10-2	1.64 x 10-1	2.15 x 10-2	1.69 x 10-1	1.76 x 10-1	1.76 x 10-1	1.76 x 10-1	1.76 x 10-1	1.76 x 10-1
	Calcite	-1.72 x 10-3	-1.03 x 10-4	-2.08 x 10-2	-8.53 x 10-3	-3.23 x 10-3	-1.32 x 10-2	-2.32 x 10-2	-3.82 x 10-2	-4.82 x 10-2
	Dolomite			9.64 x 10-3	4.22 x 10-3					
9D	Gypsum	6.40 x 10-3	-6.43 x 10-2	-6.26 x 10-2	-1.21 x 10-1	-1.23 x 10-1	-1.23 x 10-1	-1.23 x 10-1	-1.23 x 10-1	-1.23 x 10-1
	Calcite	-1.57 x 10-3	-1.95 x 10-3	1.38 x 10-1	1.37 x 10-1	-5.83 x 10-3	-1.58 x 10-2	-2.58 x 10-2	-4.08 x 10-2	-5.08 x 10-2
	Dolomite			-7.03 x 10-2	-6.97 x 10-2					
12I	Gypsum	7.79 x 10-3	1.38 x 10-3	7.65 x 10-3	1.40 x 10-1	1.31 x 10-1	1.31 x 10-1	1.31 x 10-1	1.31 x 10-1	1.31 x 10-1
	Calcite	-1.18 x 10-3	-8.61 x 10-4	3.08 x 10-2	3.35 x 10-2	-4.25 x 10-3	-1.43 x 10-2	-2.43 x 10-2	-3.93 x 10-2	-4.93 x 10-2
	Dolomite			-1.16 x 10-2	-1.70 x 10-2					
10I	Gypsum	2.17 x 10-3	1.05 x 10-1	-6.68 x 10-4	1.32 x 10-1	1.46 x 10-1	1.46 x 10-1	1.46 x 10-1	1.46 x 10-1	1.23 x 10-1
	Calcite	-2.10 x 10-3	-1.76 x 10-3	7.51 x 10-3	1.59 x 10-2	-3.64 x 10-3	-1.36 x 10-2	-2.36 x 10-2	-3.86 x 10-2	-4.86 x 10-2
	Dolomite			-4.87 x 10-3	-8.43 x 10-3					
10D	Gypsum	3.43 x 10-3	1.53 x 10-1	7.78 x 10-5	1.02 x 10-1	1.05 x 10-1	1.05 x 10-1	1.05 x 10-1	1.05 x 10-1	1.05 x 10-1
	Calcite	-2.77 x 10-3	-3.71 x 10-4	6.02 x 10-3	1.15 x 10-2	-3.91 x 10-3	-1.39 x 10-2	-2.39 x 10-2	-3.89 x 10-2	-4.89 x 10-2
	Dolomite			-4.46 x 10-3	-6.65 x 10-3					
13I	Gypsum	7.29 x 10-3	1.05 x 10-1	4.51 x 10-3	1.03 x 10-1	1.07 x 10-1	1.07 x 10-1	1.07 x 10-1	1.07 x 10-1	1.07 x 10-1
	Calcite	-3.08 x 10-3	-2.29 x 10-3	3.38 x 10-3	6.60 x 10-3	-4.12 x 10-3	-1.41 x 10-2	-2.41 x 10-2	-3.91 x 10-2	-4.91 x 10-2
	Dolomite			-3.26 x 10-3	-4.46 x 10-3					
14S	Gypsum	2.64 x 10-3	1.01 x 10-1	3.39 x 10-3	9.84 x 10-2	9.60 x 10-2	9.60 x 10-2	9.60 x 10-2	9.60 x 10-2	9.60 x 10-2
	Calcite	-1.22 x 10-3	1.39 x 10-4	1.54 x 10-3	1.21 x 10-2	-3.61 x 10-3	-1.36 x 10-2	-2.36 x 10-2	-3.86 x 10-2	-4.86 x 10-2
	Dolomite			-1.42 x 10-3	-6.02 x 10-3					
14D	Gypsum	1.64 x 10-3	8.07 x 10-2	4.83 x 10-4	7.77 x 10-2	7.36 x 10-2	7.36 x 10-2	7.36 x 10-2	7.36 x 10-2	7.36 x 10-2
	Calcite	-5.22 x 10-5	1.07 x 10-3	5.34 x 10-3	1.32 x 10-2	-3.88 x 10-2	-1.39 x 10-2	-2.39 x 10-2	-3.89 x 10-2	-4.89 x 10-2
	Dolomite			-2.76 x 10-3	-6.09 x 10-3					

Table V-4. Results on Δ-phases (in moles) for case 5 from PHREEQE simulation.

Well	Phases	Gypsum Equilibrium and Calcite Added in Increments Na-Ca and Ca-Mg Exchange					
		0.0002 moles	0.0006 moles	0.001 moles	0.0014 moles	0.0018 moles	0.002 moles
7I	Gypsum	1.22×10^{-1}	1.22×10^{-1}	1.22×10^{-1}	1.22×10^{-1}	1.21×10^{-1}	1.21×10^{-1}
7	Gypsum	1.16×10^{-1}	1.16×10^{-1}	1.16×10^{-1}	1.15×10^{-1}	1.15×10^{-1}	1.15×10^{-1}
14I	Gypsum	9.14×10^{-2}	9.12×10^{-2}	9.09×10^{-2}	9.07×10^{-2}	9.04×10^{-2}	9.03×10^{-2}
13I	Gypsum	7.03×10^{-2}	7.01×10^{-2}	6.98×10^{-2}	6.96×10^{-2}	6.94×10^{-2}	6.92×10^{-2}
9S	Gypsum	1.41×10^{-1}	1.41×10^{-1}	1.41×10^{-1}	1.41×10^{-1}	1.41×10^{-1}	1.40×10^{-1}
9I	Gypsum	1.64×10^{-1}	1.61×10^{-1}	1.61×10^{-1}	1.60×10^{-1}	1.60×10^{-1}	1.60×10^{-1}
9	Gypsum	-1.30×10^{-1}	-1.30×10^{-1}	-1.30×10^{-1}	-1.30×10^{-1}	-1.31×10^{-1}	-1.31×10^{-1}
11I	Gypsum	9.61×10^{-2}	9.58×10^{-2}	9.56×10^{-2}	9.55×10^{-2}	9.54×10^{-2}	9.54×10^{-2}
12I	Gypsum	9.77×10^{-2}	9.75×10^{-2}	9.73×10^{-2}	9.70×10^{-2}	9.68×10^{-2}	9.66×10^{-2}
10I	Gypsum	1.34×10^{-1}	1.33×10^{-1}	1.33×10^{-1}	1.33×10^{-1}	1.33×10^{-1}	1.33×10^{-1}
10	Gypsum	9.82×10^{-2}	9.79×10^{-2}	9.77×10^{-2}	9.74×10^{-2}	9.72×10^{-2}	9.71×10^{-2}

precipitated. The saturation indices indicate that groundwater from wells in the deeper portion of the aquifer or in the downgradient part of the aquifer were closer to gypsum saturation than shallower wells.

The elimination of dolomite and introduction of the Ca-Mg exchange reaction (case 5) aids in interpreting the effect of distance of travel downslope on groundwater composition. Because the molar solubility of calcite and dolomite with respect to calcium ions is approximately the same, calcium ions were considered to come from calcite.

The primary goal of the geochemical equilibrium modeling was to determine whether application of the model to analytical data obtained from solutions (samples) taken at various depths and distances along groundwater flow paths can adequately simulate the geochemical makeup of the waters in this system. In natural systems true equilibrium rarely exists for all reactions of interest. However, the application of "local equilibrium" and geochemical "steady-state" concepts appear to have utility in data interpretation. The analytical concentrations of the minerals determined in the speciation calculations were used in mass-balance calculations described in the following section.

Geochemical Evolution Using BALANCE

The USGS mass balance computer program, BALANCE (Parkhurst et al. 1982) was utilized to examine the geochemical evolution along the flow path, and to evaluate observed chemical changes using the mass balance approach. The results provide an estimate of the mass transfer (amounts of phases entering or leaving the aqueous phase) necessary to account for the observed changes in composition between two solutions located along the flow path.

Statement of the problem

This aspect of the study was undertaken to get an overall representation of the geochemical change as water travels along a flow path. Geochemical speciation calculations presented earlier aided in identifying the important reactions occurring in the conceptual model. Consequently, the two mineral phases chosen were calcite ($CaCO_3$) and gypsum ($CaSO_4.2H_2O$). Carbon dioxide (CO_2) gas was introduced assuming a P_{CO_2} of 10^{-2} atmospheres to provide a mineral source or sink for carbon. The reactions of the carbonate system were not fully developed because the primary source of salinity is considered to be solubilized gypsum in the underlying Mancos shale as affected by Na-Ca exchange on the clay surface. Although calcite can provide calcium ions for the exchange reaction, the excess of calcium from relatively soluble gypsum decreases the solubility of calcite and swamps out the impact of calcite as a source of salinity in a Mancos shale system.

Input data, limitations, and assumptions

To use BALANCE, only the total concentrations of each element present in the initial and final solutions were required. These data were generated from thermodynamic data using PHREEQE. It was assumed that the chemistry at the intermediate depth is representative of a completely mixed solution at each well location. Mass balance computations were performed along the

previously defined flow path through wells 7-9-12 (see Chapter IV). BALANCE requires the geochemistry of two points along the flowpath to be known, therefore the simulations were performed from points 7 to 9 and from 9 to 12. Figure V-2 illustrates the flow path problem. A summary of the observed analytical data for the three wells along the flow path are given in Table V-5.

The calculations are performed based on an observed net change in total concentrations of dominant elements in solution such that the masses of chemical elements are balanced in chemical reactions. Because BALANCE is not constrained by thermodynamic criteria it is possible that it could predict that thermodynamically invalid reactions may occur. To check the thermodynamic validity of the reaction models, it is therefore necessary to find a reaction-path simulation that reproduces the composition of the final water. The methods for identifying such a reaction-path are presented by Plummer et al. (1982).

Interpretation of the results

The results of the flow path mixing problem are given in Table V-6. Within the upslope portion of the system between wells 7 and 9, we see that as groundwater migrates downslope a small amount of gypsum precipitates while significant amounts of calcite are found to dissolve. The water type in this zone is primarily a $Ca\text{-}HCO_3$ type similar to excess irrigation water or Carbon canal water. It is reasonable to conclude that subsurface displacement and weathering of gypsum by groundwater in the alluvium and the underlying shale is largely complete, with only small amounts of gypsum remaining.

In the downslope portion of the system between wells 9 and 12 the mass balance indicates that extensive gypsum dissolution is occurring and calcite may be precipitating. Within the mixing zone the dominant water type evolves from a $Ca\text{-}SO_4$ to $Na\text{-}SO_4$ type. Although these results are preliminary with additional work pesently underway to better understand the role of Mg and P_{CO_2} in this process, we can conclude from these results that there is more potential for gypsum dissolution in the downslope portion of the hillslope where the displacement of dissolved salts from the alluvium and the weathering of bedrock is continuing. This conclusion is also supported by SAR calculations performed along the flow path as described earlier in Chapter IV.

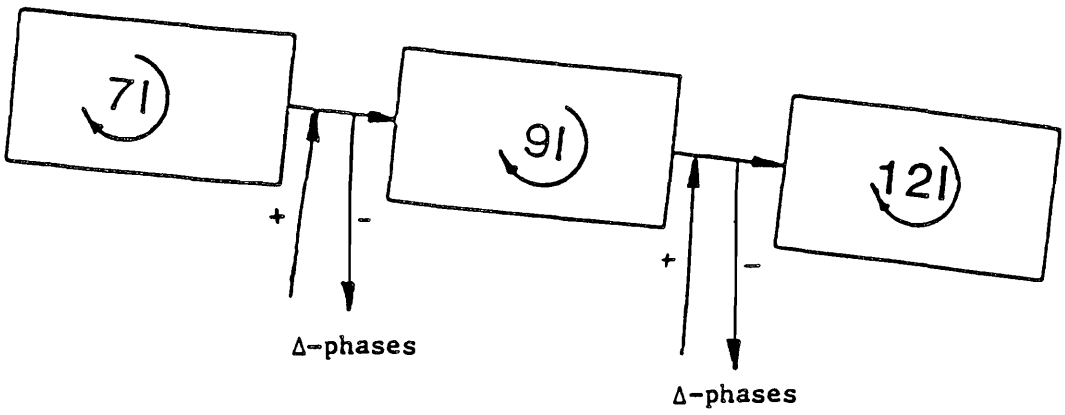

+ = dissolution
- = precipitation

Figure V-2. Illustration of the flow path problem.

Table V-5. Analytical data for the flow path problem.

Element	Total Concentration (mmol/kg H_2O)			
	Flow path 7 to 9		Flow path 9 to 12	
	Final Water Well 9I	Initial Water Well 7I	Final Water Well 12I	Initial Water Well 9I
Ca	4.72	1.98	10.5	4.72
Na	1.8	1.06	2.27	1.8
S	0.92	0.94	13.0	0.92
C	5.3	5.71	3.53	5.3

Table V-6. Results of the flow path problem.

Phases	Δ - Phases* (mmols/kg H_2O)	
	7I to 9I	9I to 12I
Gypsum	-0.02	12.08
Calcite	3.13	-6.07

*- = precipitation; + = dissolution

CHAPTER VI

MODELING FLOW AND SOLUTE TRANSPORT

In this section, mathematical models of groundwater flow and solute transport are used first to identify the important mechanisms controlling the migration of salinity in subsurface return flow and secondly, to estimate the impact of irrigation practices used on alluvial soils overlying Mancos shale on downstream salinity. The models can be characterized as distributed parameter, physical models. The Galerkin finite element method is used in conjunction with a triangular element discretization scheme to investigate flow and solute transport involving two spatial dimensions in the vertical plane. The parameters of the flow and solute transport models are adjusted by trial and error or independent field information to estimate the impacts of water infiltrating from canals and irrigated fields and its salt content on the amounts, timing, and chemical composition of the groundwater. The following is a description of how a conceptual model is calibrated to identify the contributing processes and mechanisms under field conditions at the Miller Creek subbasin.

Flow Modeling

An iterative Galerkin-type finite element method was used to solve the equation of seepage in saturated-unsaturated porous media under steady state conditions. To determine the free surface in an unconfined aquifer, steady state percolation of water from canals and irrigation is treated as a prescribed flux boundary condition at the land surface. The position of the water table (ψ = 0 (reference pressure) on the free surface profile) is determined for various volumes of canal seepage and deep percolation of irrigation water. Based on initial estimates of the hydraulic conductivity from field investigations, a trial and error procedure is then performed by adjusting the hydraulic conductivity and recharge rates until the simulated water table matches the measured one.

According to Neuman (1973), the flow of water in a slightly compressible unsaturated or partly saturated soil can be represented as:

$$L(\psi) = \frac{\partial}{\partial X_i}\left[K^r(\psi)\, K^s_{ij}\, \frac{\partial \psi}{\partial X_j} + K^r(\psi)\, K^s_{ij}\right] - \left[C(\psi) + \beta S_s\right] \frac{\partial \psi}{\partial t} + S = 0 \quad (1)$$

where L is a quasi-linear differential operator defined for the flow region, X_i (i = 1,2,3) are the spatial coordinates in three dimensions, K^r is the relative hydraulic conductivity, ψ is the pressure head, K^s_{ij} is a two-dimensional hydraulic conductivity tensor at saturation (j = 1,2,3), $C(\partial\theta/\partial\psi)$ defines the specific moisture capacity, θ is the moisture content, S_s is the specific storage, β is 1 in the saturated zone and 0 in the unsaturated zone, t is time, and S is the volume rate of water withdrawn per unit time per unit bulk volume of the soil. The unsaturated properties of the aquifer incorporated in the model are expressed by the relationships (Van Genuchten 1980) $\theta = S_e(\theta_s - \theta_r) + \theta_r$, and $K^r = S_e^{1/2}\left[1-(1-S_e^{1+1/\lambda})^{\lambda/\lambda+1}\right]^2$, in the first

equation s and r indicate saturated and residual values of the soil water content, and S_e is the effective saturation given by

$$Se = \left[\frac{1}{1 + (\psi/\psi_b)^{1+\lambda}} \right]^{\lambda/\lambda+1}$$

where ψ_b is the bubbling pressure (L), and λ is the pore size distribution index.

For the purpose of applying the finite element method to the Miller Creek subbasin transect along wells 7, 9, and 12, the transect was subdivided into a network of triangular elements. The soil thickness of the upper half of the transect from the canal to 2750 ft from the left boundary is uniform over the depth of the alluvium. Downslope from this point, the thickness of the soil-alluvium profile reduces to about 12 ft and remains constant for the rest of the distance to Miller Creek. A schematic of this cross-section with locations of the canal and alluvium-shale layers is illustrated on Figure VI-1a. The superimposed triangular finite element network is shown on Figure VI-1b.

The hydraulic properties of the soil vary with both distance and depth, and data on aquifer properties were obtained from field testing performed in the CH2M Hill (1983) study. These values were used as initial estimates for the unsaturated-saturated flow model, which was then run repeatedly with different sets of hydraulic conductivities until the model produced a free water surface similar to that plotted from available water level data. Deep percolation rates and canal seepage rates were taken from the CH2M Hill (1983) report. Based on this trial and error approach, the transect was divided into three zones with different hydraulic conductivities. Within each zone, all the elements were assigned similar hydraulic properties.

Geologic logs taken from well nest locations M-7, M-9, and M-10 by CH2M Hill (1983) indicate that soils along the transect are mostly classified as sandy loam, loam, and silt loam according to USDA soil texture classification method. The following parameters are used in each soil zone for total porosity, bubbling pressure, residual water content, and pore size distribution indexes given by Rawls et al. (1982).

Soil Zone	Texture Class	Total Porosity	Residual Saturation	Bubbling Pressure (ft)	Pore Size Distribution Index
1	Sandy Loam	0.401	0.030	-1.20	0.310
2	Clay	0.100	0.090	-2.81	0.165
3	Loam	0.401	0.030	-1.20	0.310

The alluvium and shale layers are assumed to be anisotropic with a K_x/K_z = 10, a typical value for fine grained sediments. The top alluvium layer in zones 1 and 3 are calibrated for a saturated hydraulic conductivity (K_x) of 54 ft/day and 114 ft/day, respectively. And the bottom shale layer was assigned a saturated hydraulic conductivity of 0.0283 ft/day in the x direction.

LEGEND

q_c = rate of canal seepage
C_c = salinity of canal seepage
q_i = rate of applied irrigation
C_i = concentration of applied irrigation
q_{et} = rate of evapotranspiration
q_o = rate of deep percolation
C_o = salinity of the deep percolation water

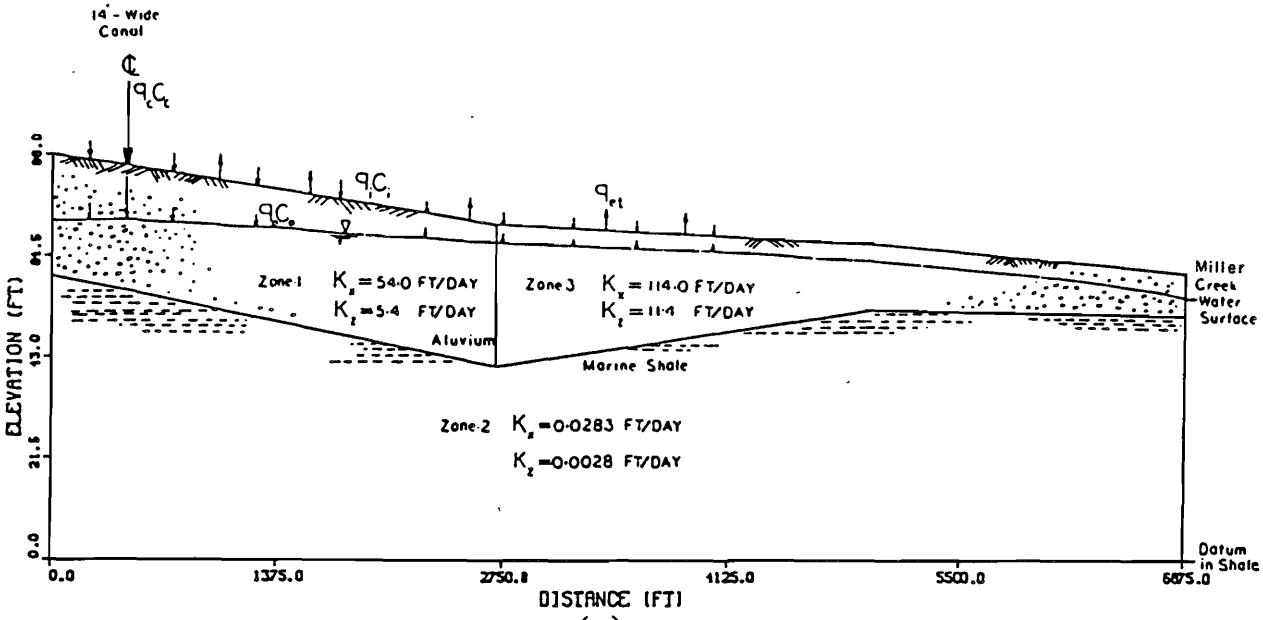

(a)

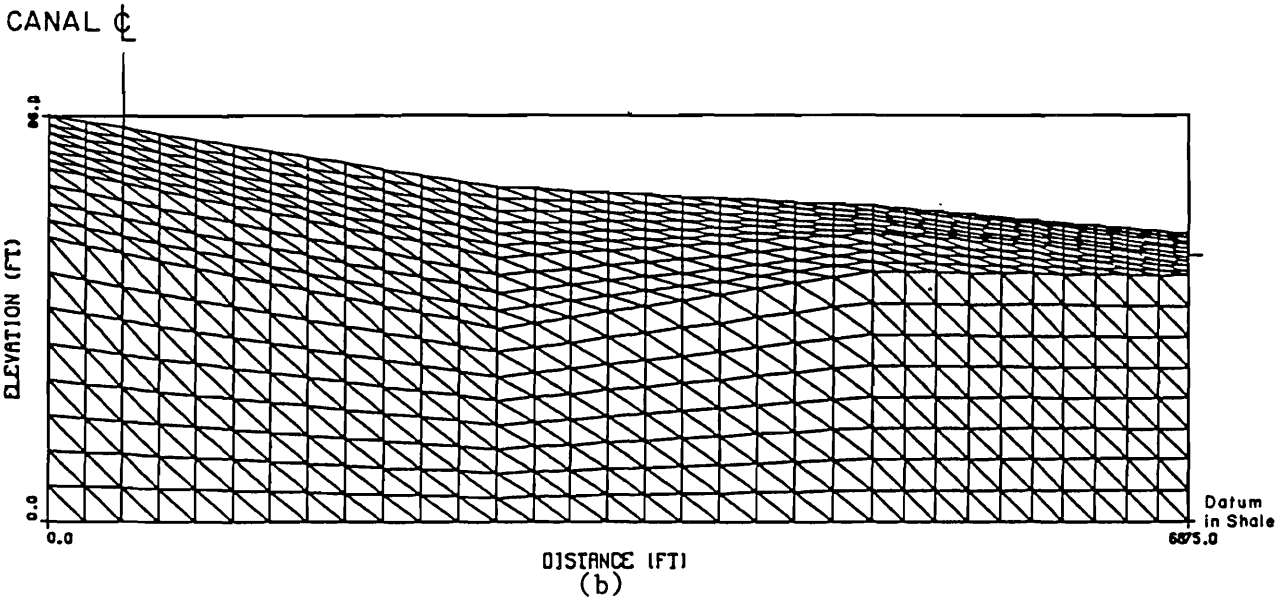

(b)

Figure VI-1. (a) Cross section of Miller Creek subbasin flow path with various zones of hydraulic conductivities. (b) Miller Creek stream-aquifer system with superimposed triangular finite element network.

Available canal seepage rate data from CH2M Hill (1983) seepage tests performed on the canal section at the study site were used as a prescribed flux boundary condition on canal location node. The spatial distribution of applied irrigation deep percolation and canal seepage is shown on Figure VI-2a. The leaching fraction LF = D_d/D_i, where D_d is the depth of deep percolation and D_i is the depth of irrigation water, is assumed to be 0.5 in the irrigated land. This value is typical of those encountered in the CH2M Hill (1983) study for irrigated lands. The downslope part of the transect which previously was classified as pastureland is less frequently irrigated, has a lower value of deep percolation rate with an LF estimated to be 0.25. The calibrated water table profile which closely matches the available water level data under present irrigation system is shown in Figure VI-2b. Construction of the flow net in Chapter IV demonstrates that groundwater flow is largely horizontal from recharge to discharge area. And because of the low permeability of the bedrock an active shallow groundwater flow is produced in the alluvium. The anisotropic flow net was constructed by first using the ratio $X = \sqrt{K_z/K_x}\, x$ to transform the x-axis into an equivalent isotropic system and drawing the flow lines orthogonal to equipotential lines and then inverting the scale and transforming to obtain the anisotropic flow net.

The calibrated model was then used to produce free surface profiles under three hypothetical management schemes: 1) lining the canal section, 2) increasing irrigation efficiency, and 3) retiring of agricultural land from irrigation. The spatial distributions of the applied fluxes for these management schemes is shown on Figures VI-3a through VI-3c. Figure VI-4a shows the relative positions of the free surface or water table profile for current irrigation practices, and the three management runs, assuming steady state conditions. For each case the groundwater velocity field was evaluated and subsequently used in the solute transport analysis to be discussed next.

Solute Transport Modeling

Solute transport is generally viewed as the net effect of two processes, advection and hydrodynamic dispersion. Advection is attributed to transport by flowing groundwater. Dispersion is caused by mechanical mixing and molecular diffusion at the interface between two fluids of different composition during fluid advection. Molecular diffusion takes place because of random molecular motion, from regions of lower to higher concentrations. Mechanical dispersion occurs at a microscopic scale and is a result of three processes. The first process occurs within the pores and at solid-solution interface where solute molecules travel at different velocities at different points due to variations in roughness of pore surfaces. The second process is caused by variations in pore geometries which causes differences in bulk fluid velocities. And the third spreading process is caused by the branching, interfingering and tortuosity of porous medium. In problems involving transport of nonreactive contaminants in groundwater, the most frequently used model is the solution of the advection-dispersion equation. This approach is employed in the solute transport analysis of this study to solve for concentration of $SO_4^=$ ion in space and time by spatial averaging of the microscopic changes to express the processes of advection, dispersion, and diffusion at the macroscopic scale.

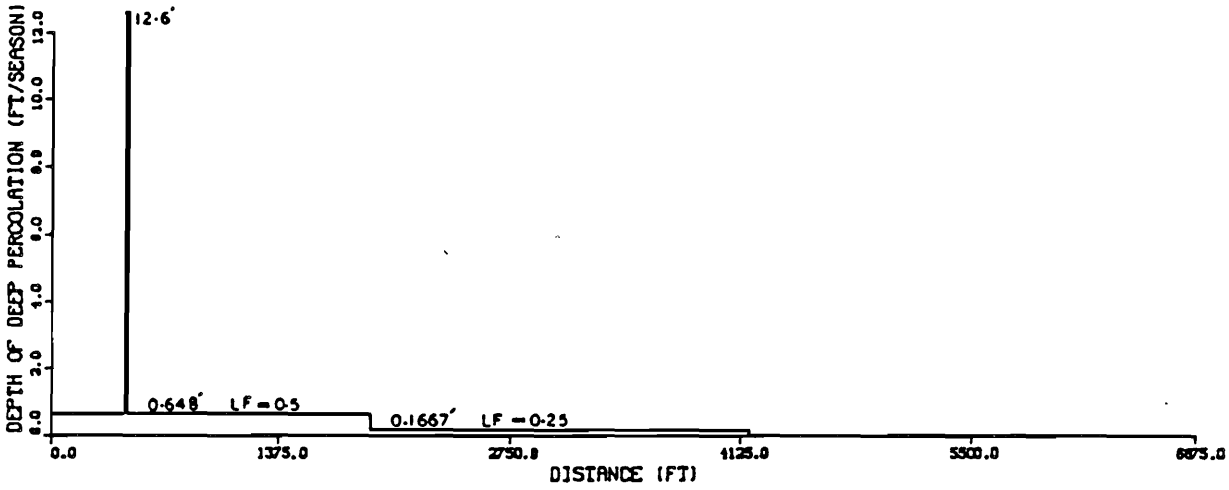

(a)

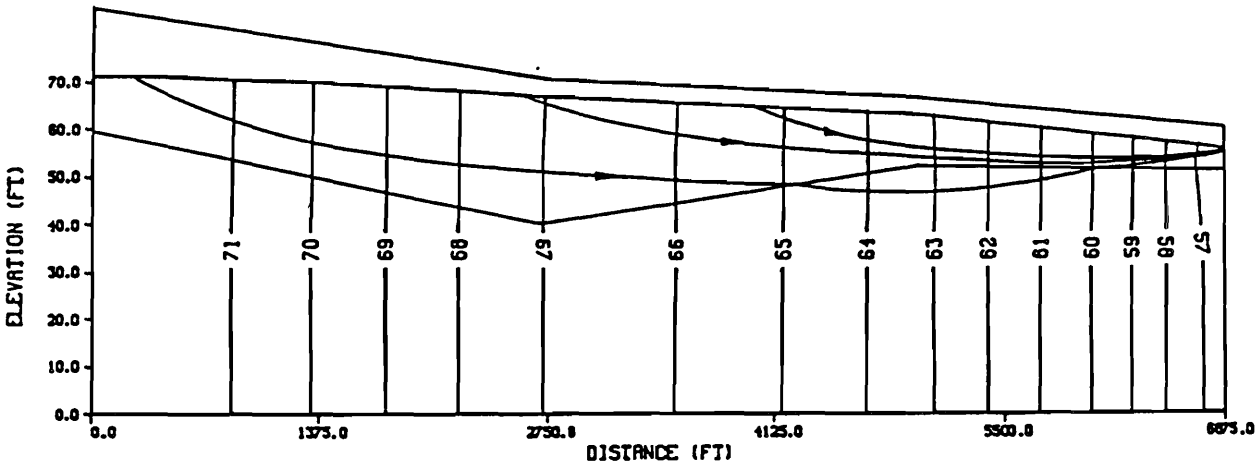

(b)

Figure VI-2. (a) Spatial distribution of applied irrigation deep percolation and canal seepage under current irrigation practices. (b) Illustration of the shallow groundwater flow net in a 2-D vertical cross section through the heterogeneous anisotrophic system.

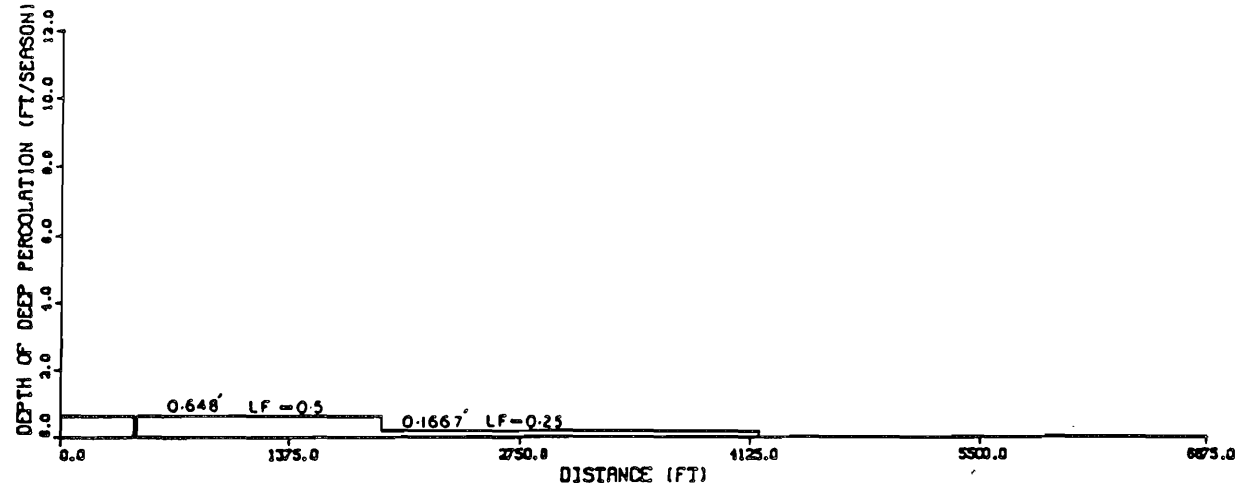

(a)

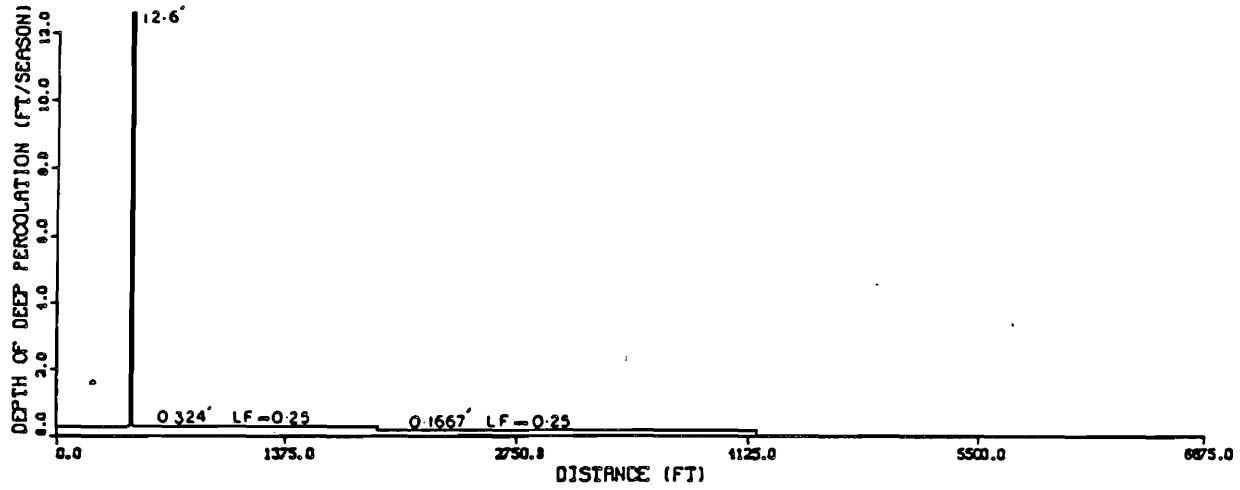

(b)

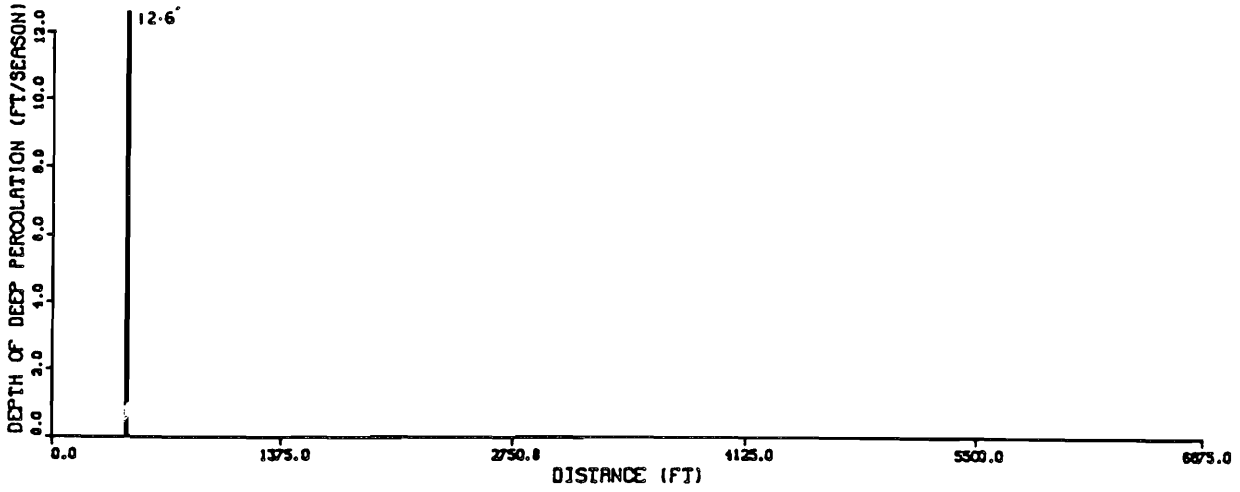

(c)

Figure VI-3. Spatial distribution of applied irrigation deep percolation for (a) lined canal section, (b) 50 percent reduction in deep percolation of irrigated land and (c) retired irrigated land.

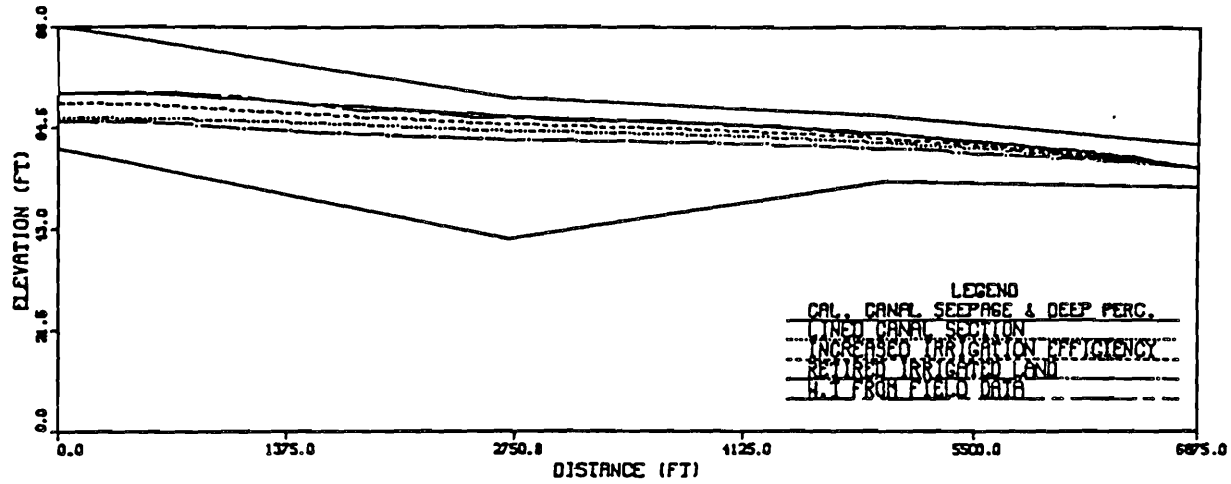

(a)

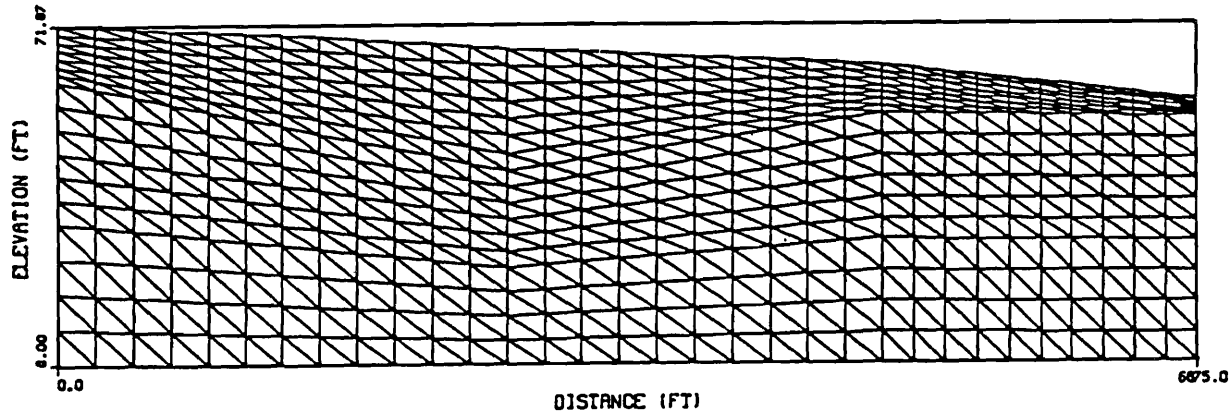

(b)

Figure VI-4. (a) Illustration of positions of p = 0 free water surface under various management runs. (b) A typical superimposed finite element network over the saturated soil profile.

The steady-state velocity field for saturated groundwater flow can be determined from a relationship given by Bear (1979), derived from Darcy's equation and the equation of continuity for two-dimensional flow in a vertical cross section:

$$\frac{\partial}{\partial x}\left(K_{xx}\frac{\partial h}{\partial x}\right) + \frac{\partial}{\partial y}\left(K_{yy}\frac{\partial h}{\partial y}\right) + \frac{\partial}{\partial x}\left(K_{xy}\frac{\partial h}{\partial y}\right) + \frac{\partial}{\partial y}\left(K_{yx}\frac{\partial h}{\partial x}\right) + q = 0 \qquad (2)$$

where h is hydraulic head, K_{xx}, K_{yy}, K_{xy}, and K_{yx} are the hydraulic conductivity tensors, and q is a source or sink term. For the special cases when the principal directions of anisotropy coincide with the x and y coordinate axes, Darcy velocity components are determined from

$$V_x = -\left(K_{xx}\frac{\partial h}{\partial x} + K_{xy}\frac{\partial h}{\partial y}\right) \qquad (3)$$

$$V_y = -\left(K_{yx}\frac{\partial h}{\partial x} + K_{yy}\frac{\partial h}{\partial y}\right) \qquad (4)$$

Advection is movement carried by the average linear groundwater velocity ($\bar{V} = V/\phi$ with V being Darcy velocity and ϕ the porosity).

The two-dimensional form for advection-dispersion, in a saturated flow for the solute species c(x,y,t) is (Bear 1979)

$$\frac{\partial}{\partial x}\left(D_{xx}\frac{\partial c}{\partial x}\right) + \frac{\partial}{\partial y}\left(D_{yy}\frac{\partial c}{\partial y}\right) + \frac{\partial}{\partial x}\left(D_{xy}\frac{\partial c}{\partial y}\right) + \frac{\partial}{\partial y}\left(D_{yx}\frac{\partial c}{\partial x}\right) - V_x\frac{\partial c}{\partial x} - V_y\frac{c}{\partial y}$$

$$= \phi R\frac{\partial c}{\partial t} + q(C - C_o) \qquad (5)$$

where C is the solute concentration (M/L^3); C_o is the solute concentration in the injected fluid (M/L^3); q is the source or sink term (a volume of water withdrawn per unit volume of aquifer per unit time or 1/T); D_{xx}, D_{yy}, D_{xy}, and D_{yx} are the components of the apparent hydrodynamic dispersion tensor (L^2/t); V_x and V_y are the Darcy velocity components (L/t); ϕ is the porosity; and R is a dimensionless retardation coefficient (R=1 for conservative solute species). The components of the apparent hydrodynamic dispersion tensor are given by:

$$D_{xx} = \frac{(\alpha_L - \alpha_t)V_x^2}{|V|} + \alpha_\ell |V| + D^*$$

$$D_{xx} = \frac{(\alpha_L - \alpha_t)V_x^2}{|V|} + \alpha_\ell |V| + D^*$$

$$D_{xy} = D_{yx} = (\alpha_L - \alpha_t)\frac{V_x V_y}{|V|}$$

where α_ℓ and α_t are the longitudinal and the transverse dispersivities (L), D* is the apparent molecular diffusion coefficient (L^2T^{-1}), and $|V| = (V_x^2 + V_y^2)^{1/2}$ is the magnitude of the Darcy Velocity vector (LT^{-1}).

The simulated water table profiles obtained from solution of unsaturated-saturated flow model (Equation 1) are used in determining the steady state velocity field of the saturated groundwater flow system. A finite element grid is superimposed over the saturated domain, and velocity vectors in x and y directions are determined for each element. The superimposed finite element network is illustrated on Figure IV-4b. Nodes corresponding to the irrigated section of the transect are treated as prescribed flux boundary conditions with a similar spatial distribution as determined from the unsaturated-saturated flow model at the free surface ($\psi = 0$). Nodes coinciding with Miller Creek are treated as constant pressure head boundaries. After determining the velocity field of the flow system from (Equation 2) the solute transport analysis is performed by using the velocity field as an input to obtain the spatial and temporal variations of the $SO_4^=$ concentration.

Because of geochemical characteristics of $SO_4^=$ ion, it is treated as a conservative solute specie in conceptual modeling of salinity transport from Mancos shale and overlying alluvium. This is a necessary simplification of the real system since the transport model does not include chemical reactions. The first run was made to simulate the historical changes in concentration of $SO_4^=$ ion under past and present conditions. According to the CH2M Hill study, in about the year 1920, Carbon Canal in the upper portion of the transect first began operation and delivered water for irrigation to adjacent lands. This time is used as a starting point in the simulation of historical $SO_4^=$ outflow concentration. An initial $SO_4^=$ concentration $C(x,z,t=0)$ of 24,000 mg/l is assigned over the entire grid points. This value is estimated from $SO_4^=$ concentrations of unweathered bedrock, and overlying residuum from bedrock is assumed to have the same initial concentration. The canal seepage concentration of C_c = 60 mg/l from surface water concentration data is used in the injected fluid at canal location node. The deep percolation concentration of irrigated land (C_o) is computed from relationship $LF = D_d/D_i = C_i,SO_4^=/C_d,SO_4^=$ which is 120 mg/l for a LF of 0.5. Using the same relationship, deep percolation concentration for the pastureland (which is irrigated less frequently) is 240 mg/l for a LF of 0.25. The canal seepage and deep percolation $SO_4^=$ mass flux are continuously introduced into the steady-state flow system and observed changes in concentration are recorded for each time step. Figure VI-5 shows the simulated historical and future outflow $SO_4^=$ concentration under present irrigation practices. It is important to note here that the simulated return flow is entirely dependent on the assumptions we have made concerning hydraulic parameters and geometry of the system. It should be viewed as a "conceptual" model to be used to guide interpretations of the system, and not as a tool for prediction. The data base is just not adequate for the latter.

Figure VI-6a illustrates the estimated spatial distribution of $SO_4^=$ concentration in year 1984. Figures VI-6b and VI-6c show the changes in concentrations in the soil water over simulation periods of 50 and 200 years in the future. As the saline groundwater in the alluvium is displaced by less concentrated canal seepage and deep percolation, a gradual freshening

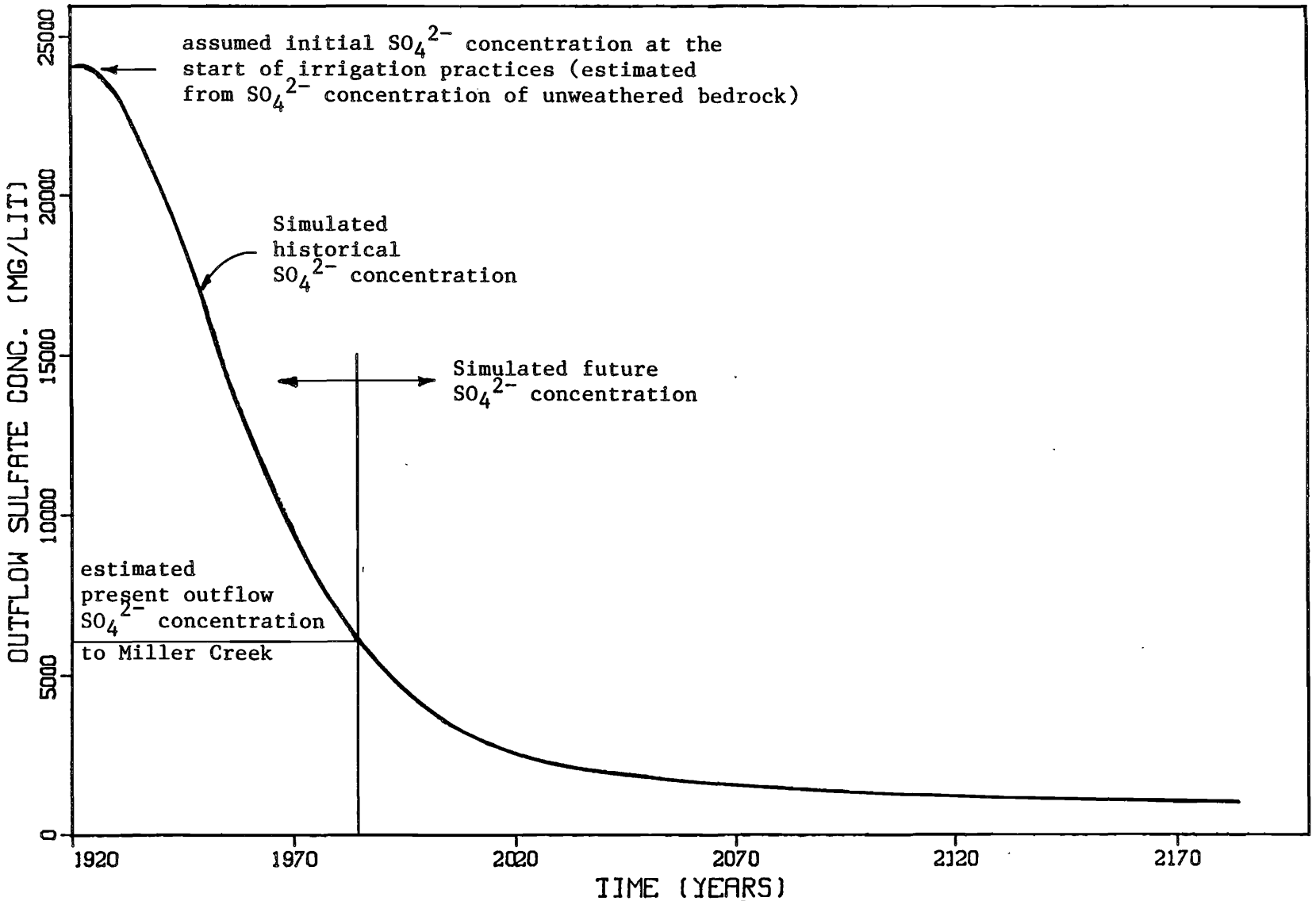

Figure VI-5. Simulated historical and future outflow SO_4^{2-} concentration under current irrigation practices.

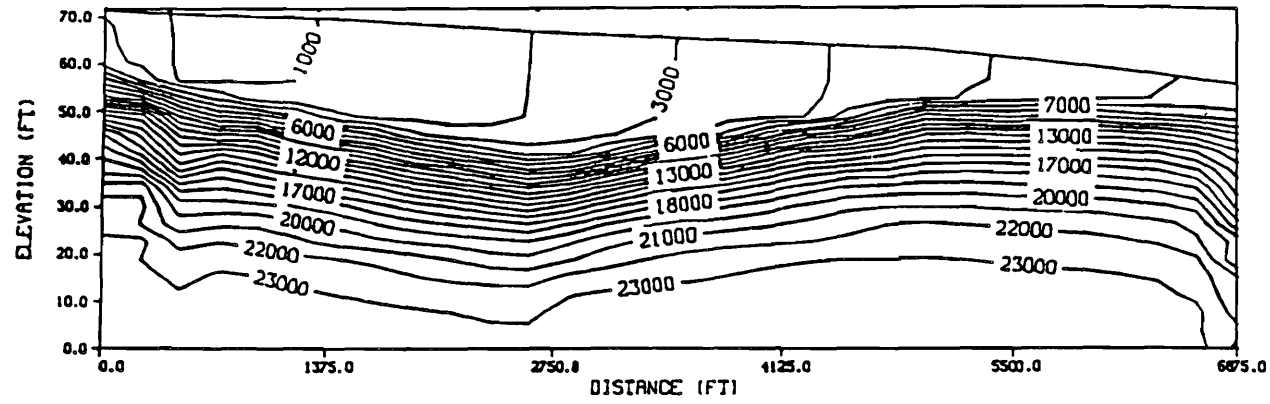

(a)

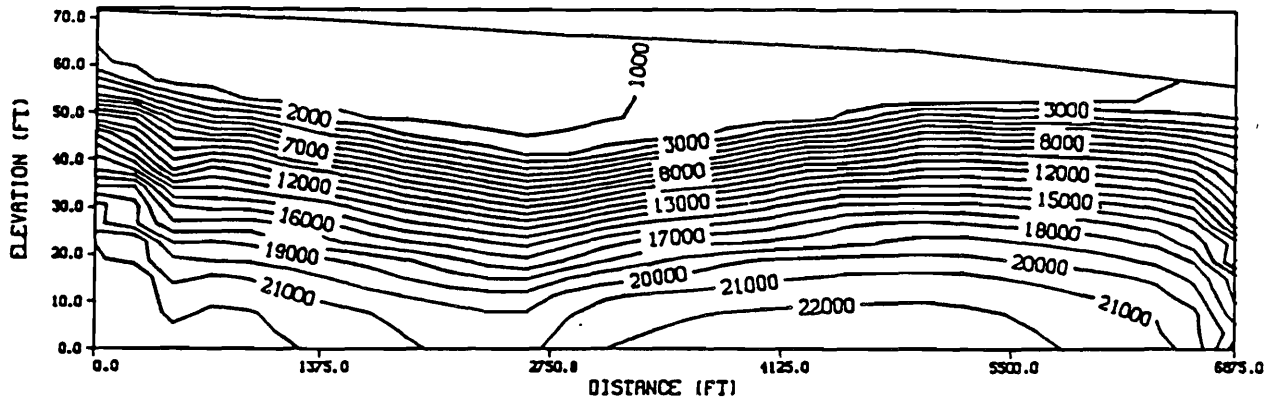

(b)

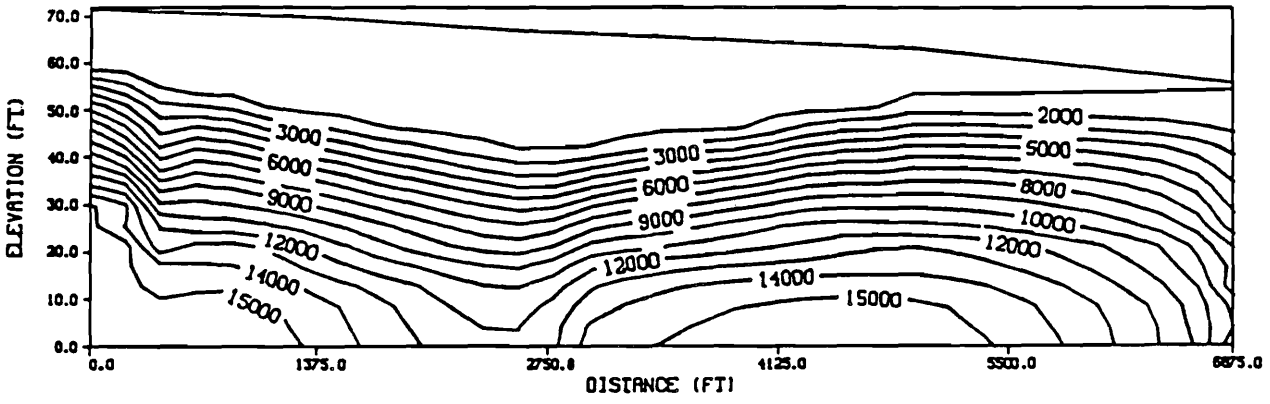

(c)

Figure VI-6. Simulated contours of equal concentration under current irrigation practices for (a) year 1984, (b) year 2034, and (c) year 2184.

of the aquifer takes place, this causes increased solute concentration gradients at the alluvium-shale interface. During the early years of irrigation, advection of solutes in the more permeable alluvium is the dominant transport process. As the groundwater with solute concentration of 24,000 mg/l is gradually displaced by canal seepage and deep percolation of irrigation water, the dilution of the water in the shallow alluvium aquifer increases the concentration gradients at the alluvium interface and salts from the consolidated marine shale diffuse upwards. As shown by contours of equal concentration, vertical gradients are steeper in the earlier years with a decrease in concentration gradients occurring later as canal seepage and deep percolation of irrigation water is continued and $SO_4^=$ ions diffuse from consolidated bedrock. The above analysis provides a quantitative demonstration of how the upward diffusion from consolidated bedrock contributes significant salinity to groundwater and streams even though very little water moves through this formation. In the next stage of the study, various irrigation management factors are examined to appraise alternatives for control of salt transport at the Miller Creek site.

Simulated steady state water table profiles under the three management alternatives previously described are used to compute $SO_4^=$ concentrations for each management scenario. The estimated spatial distribution of $SO_4^=$ concentration in year 1984 is used as an initial condition along with the steady state velocity field determined from Equations 1 and 2. Each management alternative is simulated for a period of 200 years, and outflow concentrations are recorded at each time step. Figure VI-7 illustrates the changes in outflow $SO_4^=$ concentration for each management alternative for the period 1984-2184.

A comparison of these results suggests that retiring the irrigated land will have the highest outflow concentrations in the future followed by lining canals, increasing irrigation efficiency, and continuation of present practices showing the lowest concentration. However, plotting the outflow mass flux of $SO_4^=$ vs time we see this trend reverses (Figure VI-8) with the retired irrigation land providing the least mass flow for the period 1984-2030, with continuation of present practices demonstrating the poorest performance. It is also interesting to note that irregardless of the management scheme instituted, after about 50 years all the mass flux outflow simulations become nearly the same. Our interpretation of this feature of the simulations is that over time upward diffusion from bedrock becomes the rate limiting step controlling salinization. As would be expected from these analyses, the rate of $SO_4^=$ loading is directly proportional to the rate of flow in the shallow groundwater. More efficient irrigation and/or canal lining produces higher concentrations but lower salt loads to Miller Creek, at least during the next 50 or so years of irrigation when the system reaches a kind of steady-state.

Integration of the $SO_4^=$ mass flux curve over time illustrates the cumulative $SO_4^=$ load for each hypothetical management scheme. This plot is shown on Figure VI-9. A comparison of total $SO_4^=$ loading in the next 200 years indicates that retiring the irrigated land would be the most effective management practice through the year 2040 (see Figure VI-8). After this period little difference exists among the proposed schemes. For the Miller Creek site, a 50 percent reduction in deep percolation through

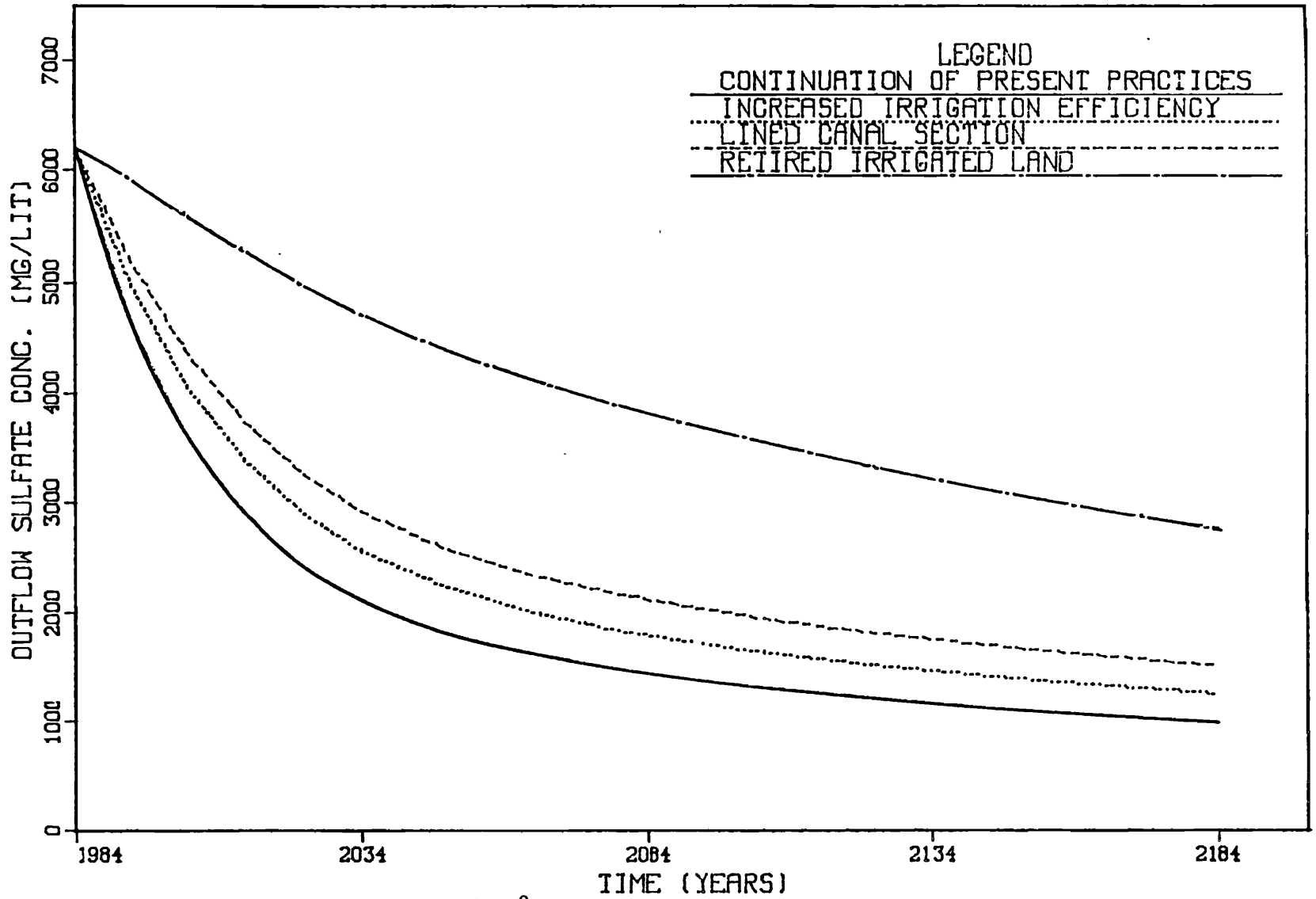

Figure VI-7. Simulated future outflow SO_4^{2-} concentrations for various management schemes.

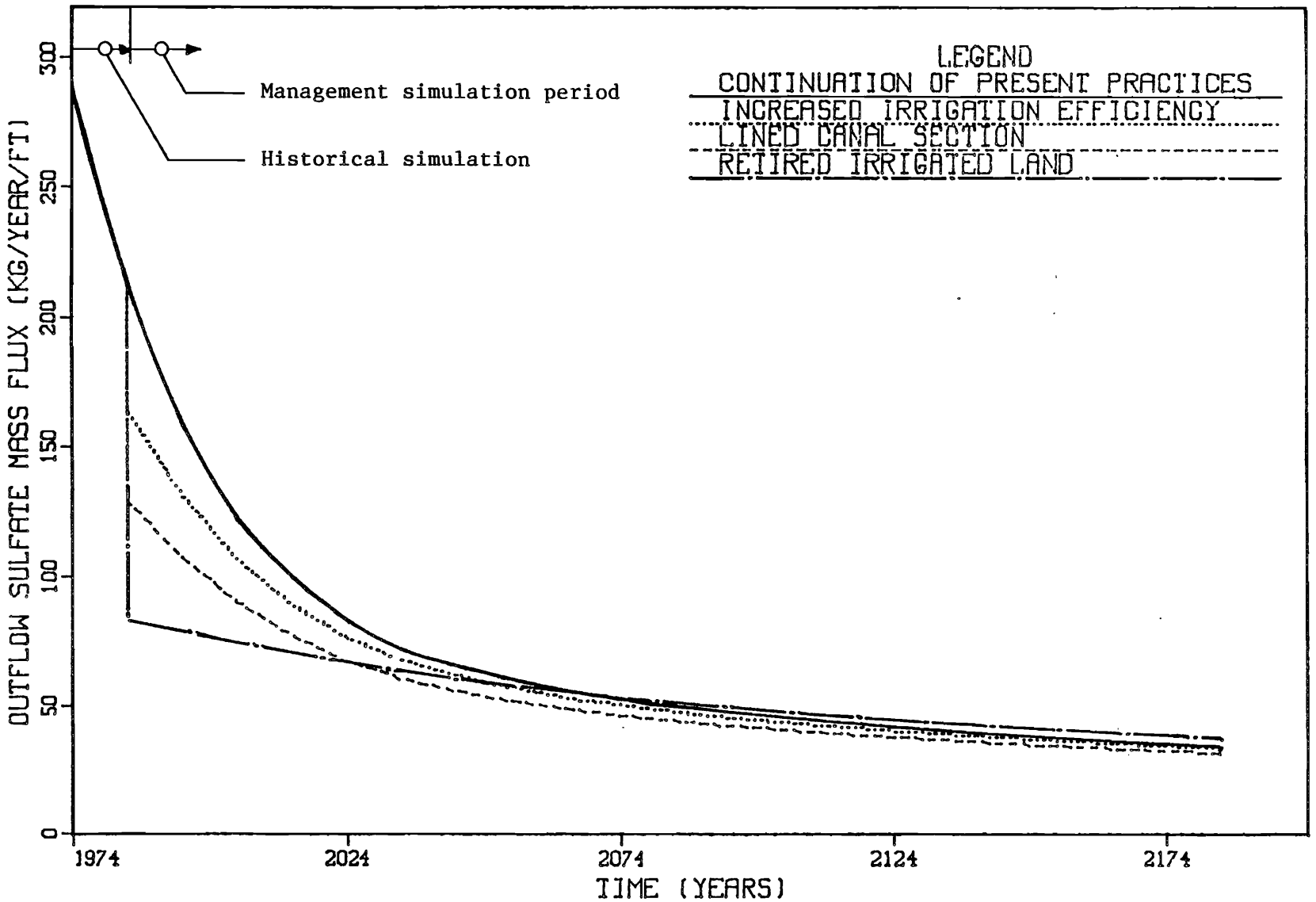

Figure VI-8. Simulated future outflow SO_4^{2-} mass flux for various management schemes.

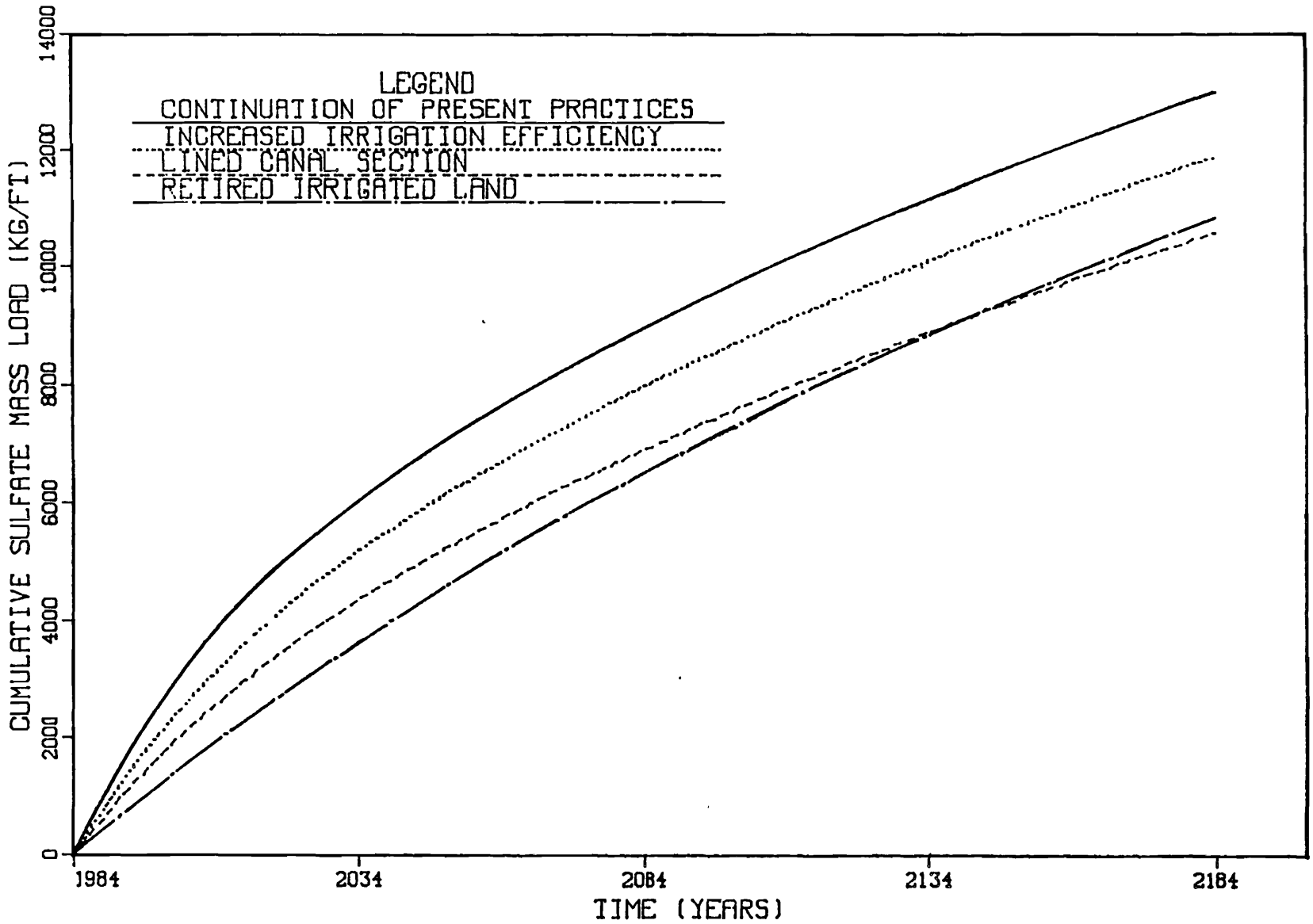

Figure VI-9. Cumulative distribution of SO_4^{2-} mass loading for various management schemes.

increased irrigation efficiency has the least effect for reducing $SO_4^=$ net loadings to Miller Creek.

The spatial distribution of $SO_4^=$ concentration in the year 2034 for the four management schemes is shown on Figures VI-10a through VI-11b. These results reinforce the importance of diffusion from low permeability bedrock after 2034. First, the concentration gradients for all management scenarios are in a vertically upwards direction within the bedrock, indicating that the flux of $SO_4^=$ is across the bedrock contact into the alluvium-residuum layer even though hydraulic gradients are in the horizontal direction (Figure VI-2(b). Secondly, the spatial distribution of concentration contours for all the management runs are not very much different after 50 years. It seems that the release of $SO_4^=$ from bedrock is not controlled by advection or displacement within the bedrock but rather is controlled by the concentration contrast between bedrock and the alluvium. The most likely process which would produce this concentration gradient is diffusion. However, the critical assumption made here is that the bedrock is of low permeability. As long as this is true diffusion is the most viable mechanism for producing salt from bedrock.

The results of these preliminary simulations suggest that efficient farm delivery systems and on farm water management practices will reduce the production of sulfate salts for the next 50 or so years of operation. However, the effectiveness of these practices becomes much less after about 50 years, when the slow release of salts from bedrock via chemical diffusion seem to predominate. The present study has dealt with physical processes of salt loading only, and implementation of management alternatives or combinations of them will require an economic evaluation of benefits and costs. We emphasize that the present conceptual model study is preliminary, since it is based on limited field data. Additional field data will be necessary before model verification is possible.

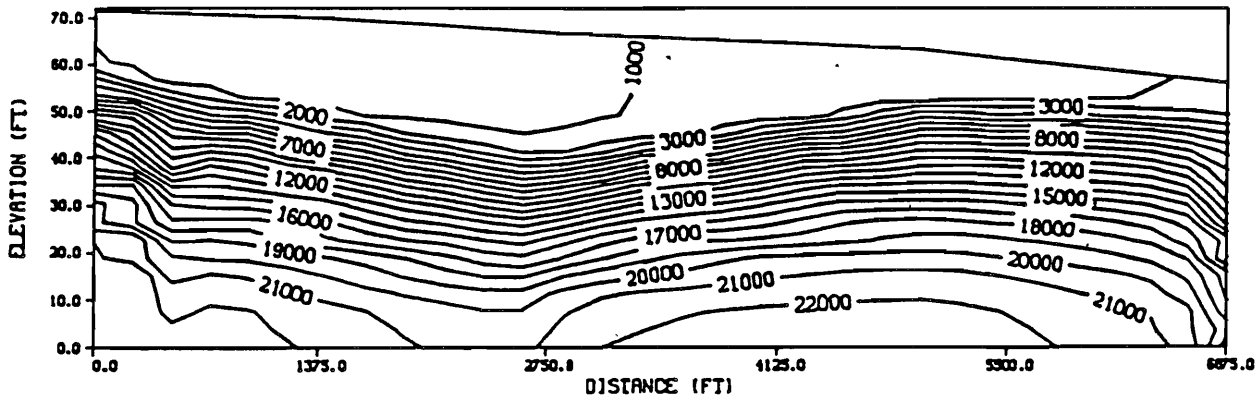

(a)

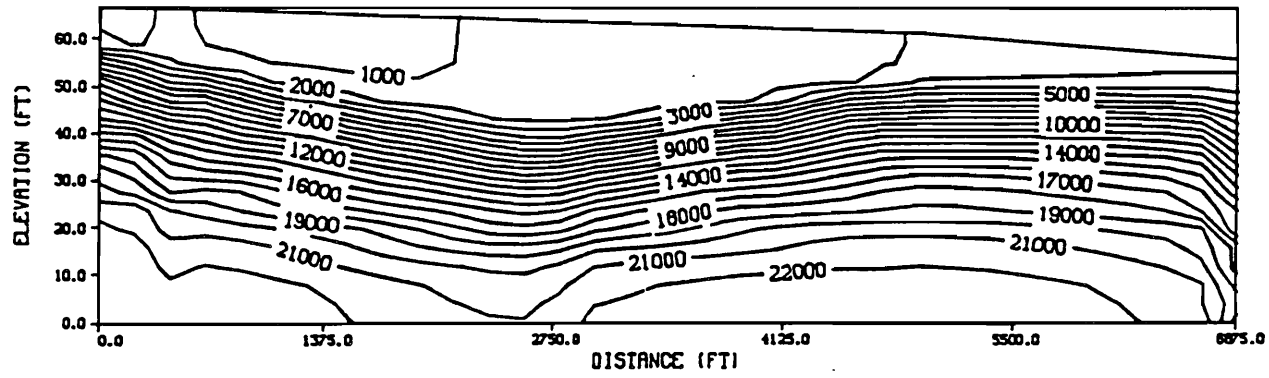

(b)

Figure VI-10. Simulated contours of equal concentration in year 2034 for (a) continuation of current irrigation practices in future and (b) lined canal section.

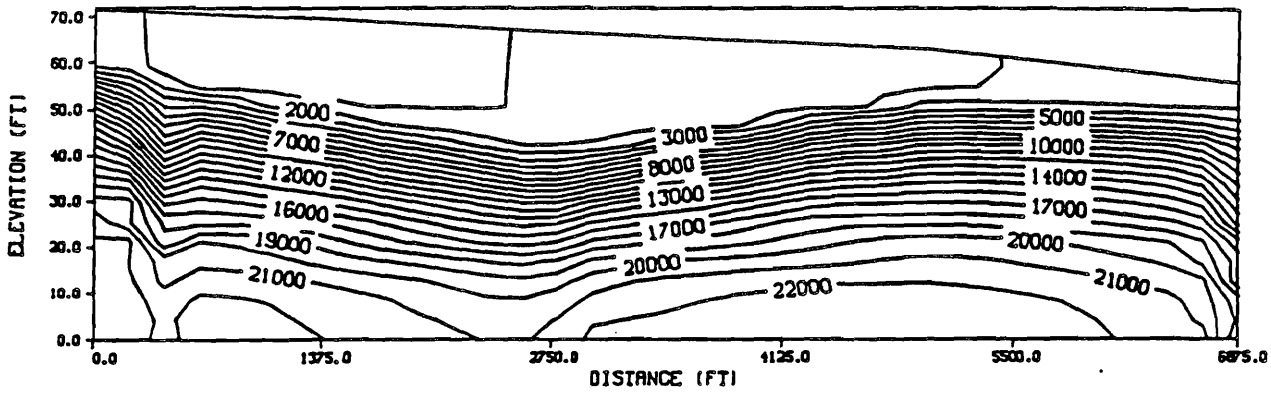

(a)

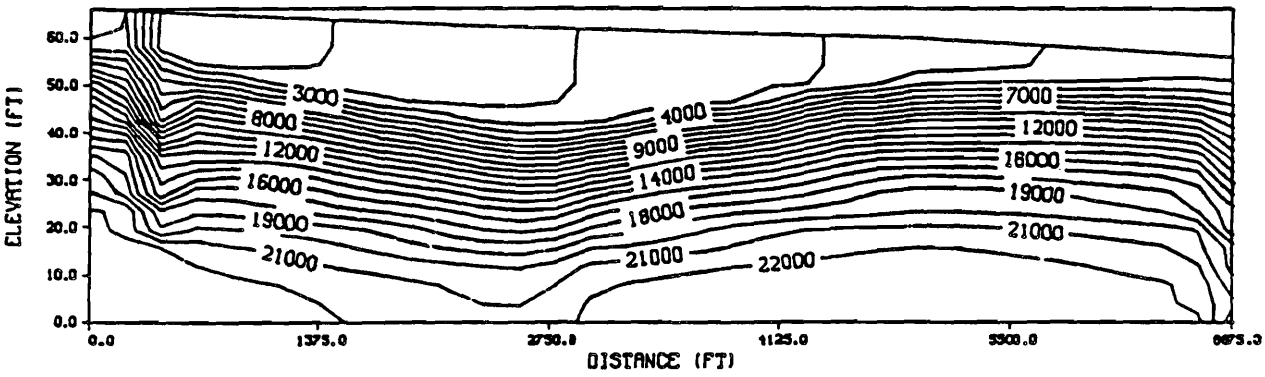

(b)

Figure VI-11. Simulated contours of equal concentration in year 2034 for (a) applied irrigation efficiency and (b) retired irrigated land.

CHAPTER VII

LIMITATIONS, CONCLUSIONS, AND RECOMMENDATIONS

All the significant findings of this study are summarized in this chapter. Limitations of the study are stated and recommendations are made for continued research into subsurface aspects of the salt loading processes in the Upper Colorado River Basin.

Limitations

The main limitation of this study is the sparse data on which the study was based. Inherent limitations to geochemical modeling have been stated earlier in Chapter V. Specific limitations relevant to this study are:

1. Bedrock topography and its relation to the landforms of the Colorado Plateau is extremely important to the hydrology and salt loading processes at the Miller Creek field site. The hydraulic, geochemical, and topographic properties of bedrock (Mancos shales) were not known in sufficient detail to accurately define the system for the present study. Additional field work is planned to supplement the existing data base reported in this study to better define the system and verify the proposed models (provided adequate funding is found).

2. Geochemical modeling was performed under the assumption of local chemical equilibrium without incorporating chemical kinetics within the groundwater system. The equilibrium constants used in geochemical modeling were current values documented in the literature. These values may change as more experimental investigations are performed to determine more precise values.

3. The flow and solute transport models applied to the Miller Creek site can only be viewed as conceptual and should not be considered as predictions of actual field behavior. Actual field conditions are highly heterogeneous with respect to both flow and solute properties. The simulations provided in this study provide a conceptual model on which to design and implement future studies to verify the proposed transport processes. Some specific limitations of the flow and solute transport are:

a) The hydraulic conductivity and porosity of bedrock and the alluvial material remain largely unknown. In-situ field tests need to be performed at a large number of sites to better determine their spatial distribution at the site, including unsaturated conductivity relations and moisture characteristic curves. As the weathering process proceeds through time, the porosity and permeability may change as dissolution processes increase the interconnected void space. This may be especially important to the rate of bedrock weathering.

b) The flow model was assumed to be steady in this study. Transient effects of seasonal application of irrigation water and canal leakages need to be incorporated in future work.

c) The diffusion and dispersion coefficients were estimated from the literature for application in the model. Field scale tests need to be designed for estimating these values. As has been shown in the literature (Freeze and Cherry 1979) laboratory experiments do not provide useful estimates of transport parameters due to scale effects.

Conclusions

An important general finding of this study was that identification of flow paths in the groundwater system enhances the consistent development of geochemical, flow and solute transport models. Without a reasonable idea of the nature of groundwater flow produced by excess irrgation and canal leakage it is impossible to estimate the extent and timing of subsurface salt loading to streams at the field site. At least to some degree this may be true throughout the Colorado Basin. Specific conclusions of this study were:

1. The chemical transition occurring along the flow path was determined to be a calcium-bicarbonate water becoming a sodium-sulfate water as it traveled from the Carbon Canal towards Miller Creek. Evidence to support this finding was obtained from geochemical analysis at observation wells over the groundwater profile, and correlation plots of TDS versus the dominant ions (Ca^{2+}, Na^{+}, SO_4^{2-} and HCO_3^{-}).

2. The geochemical modeling results suggest that the mineral phases of gypsum and calcite are the most important in determining the composition of the groundwater. Preliminary results indicate the presence of dolomite to be insignificant in determining groundwater composition and was eliminated from further analysis. However, additional work is necessary to evaluate the role of Mg^{2+} on the ion process. The saturation indices showed the potential for gypsum dissolution because the system was consistently undersaturated with gypsum. The Miller Creek field site is at an intermediate stage with respect to the weathering of gypsum salts in the groundwater, with little Ca^{2+}, SO_4^{2-}, Na^{+} evident in the upstream segment of the flow system and relatively large quantities of gypsum available in the downstream section.

3. Gypsum dissolution and Na-Ca exchange are felt to be the predominant reactions occuring within the groundwater system.

4. The low hydraulic conductivity of the Mancos shale at the field site would seem to rule out the displacement of sulfate salts from bedrock by advection and/or dispersion. The predominant transport process of $SO_4^{=}$ from bedrock appears to be a slow, vertically upwards release of sulfate salts via diffusion.

5. Four hypothetical management simulations were made for the period 1984 to 2184. Some tentative results are: At the Miller Creek site a management approach of retiring all irrigated lands (while canal seepage continues because of down-valley irrigation) produces the greatest reduction

in SO_4^{2-} mass flux during the next 50 years. Lining the irrigation canal provides the next greatest load reduction, followed by increasing irrigation efficiency. However, after the initial 50 year period, the mass flux of SO_4^{2-} salts is largely unaffected by any of the management simulations examined. An explanation of this apparent insensitivity of long term salt loading is that after the initial flushing of the alluvium (i.e., the next 50 years), the salt loading process is primarily controlled by a slow vertical diffusion of SO_4^{2-} salts from bedrock. Although the hypothetical management results provided in this study are preliminary, and based on limited field data, a general conclusion that can be made is that any water conservation practice will probably reduce the net salt-loading in return flow to streams over the short run ($\sim$40-50 years). Since during this period displacement of groundwater salinity in the upper alluvium and soil is the dominant transport mechanism for return flow. However, the long range (> 50 years) effectiveness of water conservation practices on salinity control, appear to be much less promising. Since during this time frame vertical diffusive transport from unweathered bedrock is largely unaffected by the rate of flow through the upper alluvial aquifer. Thus reducing subsurface return flow has minimal impact on the release of salts from low permeability bedrock.

Recommendations

The basic framework has been set in this study to do field scale modeling of the groundwater system to estimate the impact of irrigation and canals on stream quality. Towards this aim, the following recommendations are made:

1. In order to quantify salt loading to streams it will be necessary to better understand the subsurface hydrologic system, and the relation of this system to landform characteristics (bedrock topography, hydraulic properties, and geochemical properties of soil, alluvium and bedrock). Additional sampling and verification of the models developed in this study will go a long way towards resolving these issues.

2. Bedrock topography needs to be accurately mapped and related to groundwater flow paths.

3. The geochemical model using the concept of local equilibrium should be coupled with flow and transport processes.

4. Field scale estimates of hydraulic conductivity of Mancos shale need to be obtained through pump tests or obtaining core samples.

5. Application of the modeling approach developed here to other subbasins is presently in the planning stage.

SELECTED BIBLIOGRAPHY

Andersen, Jay C., and Alan P. Kleinman. 1978. Salinity management options for the Colorado River. Report P-78-003. Utah Water Research Laboratory, Utah State University, Logan, Utah.

Anderson, Mary P. 1979. Using models to simulate the movement of contaminants through groundwater flow systems. CRC Critical Reviews in Environmental Control 9:97-156.

Back, W., and J. A. Cherry. 1976. Chemical aspects of present and future hydrogeologic problems. In Z. A. Saleem (Ed.). Advances in groundwater hydrology. American Water Research Association, Minneapolis, Minnesota. 153 p.

Bear, J. 1979. Hydraulics and groundwater. McGraw-Hill, New York, New York.

Bergstrom, J. 1974. Seasonal variations and distribution of dissolved iron in an aquifer. Nordic Hydrology 5:1-31.

Berner, Robert A. 1978. Rate control of mineral dissolution under earth surface conditions. American Journal of Science 278:1235-1252.

Bowles, David S., Hooshang Nezafati, Bhasker Rao K., J. Paul Riley, and R. J. Wagenet. 1982. Salt loading from efflorescence and suspended sediments in the Price River Basin. Report UWRL/P-82/05. Utah Water Research Laboratory, Utah State University, Logan, Utah.

CH2M Hill. 1982. Salinity investigation of the Price-San Rafael Rivers Unit. Problem identification and quantification report to the U.S. Bureau of Reclamation-Colorado River Water Quality Improvement Program. Volumes I, II, and III.

CH2M Hill. 1983. Salinity investigation of the Price-San Rafael Rivers Unit. Verification Activities Report to the U.S. Bureau of Reclamation-Colorado River Water Quality Improvement Program. Volumes I and II.

Cordova, Robert M. 1964. Hydrogeologic reconnaissance of part of the headwaters area of the Price River, Utah. Utah Geological and Mineralogical Survey Water Resources Bulletin 4. Salt Lake City, Utah. 26 p.

Davison, C. C., and J. A. Vonhoff. 1978. Spatial and temporal hydrochemical variations in a semiconfined buried channel aquifer: Esterhazy, Saskatchewan, Canada. Groundwater 10:5.

Duffy, Christopher J. 1982. Stochastic modeling of spatial and temporal water quality variations in groundwater. PhD Dissertation. New Mexico Institute of Mining and Technology, Socorro, New Mexico.

Duffy, Christopher J. 1984. Conceptual models of geologic and agricultural salt loads in streams of the Upper Colorado River Basin. International Symposium on the State-of-the-art Control of Salinity, Ann Arbor Press, Ann Arbor, Michigan.

Duffy, C. J., L. W. Gelhar, and P. J. Wierenga. 1984. Stochastic models in agricultural watersheds. J. Hydrology 69:145-162.

El-Ashry, Mohamed T. 1980. Groundwater salinity problems related to irrigation in the Colorado River Basin. Groundwater 18:1.

Evangelou, V. P., L. D. Whittig, and K. K. Tanji. 1984. Dissolved mineral salts derived from Mancos shale. Journal of Environmental Quality 13:1.

Freeze, R. A., and J. A. Cherry. 1979. Groundwater. Prentice Hall, Englewood Cliffs, New Jersey. 604 p.

Fritz, P., R. J. Drimmie, and F. W. Render. 1974. Stable isotope contents of a major prairie aquifer in central Manitoba, Canada. Reprint from Isotope Techniques in Groundwater Hydrology, IAEA-SM-182/22, pp. 379-398.

Gelhar, L. W., P. J. Wierenga, K. R. Rehfeldt, C. J. Duffy, M. J. Simonett, T. C. Yeh, and W. R. Strong. 1983. Irrigation return flow water quality monitoring, modeling and variability in the Middle Rio Grande Valley, New Mexico. Project Summary. U.S. Environmental Protection Agency, Ada, Oklahoma.

Gelhar, L. W., and J. L. Wilson. 1974. Groundwater quality modeling. Ground Water 12:6.

Gifford, G. F., R. H. Hawkins, J. J. Jurinak, S. L. Ponce, and J. P. Riley. 1975. Effects of land processes on diffuse sources of salinity in the Upper Colorado River Basin. Report to the Bureau of Land Management and U.S. Bureau of Reclamation, USDI. Research Memorandum 3A.

Hoag, R. B. 1975. Periodic variations of dissolved constituents of Eustis mine area, Sherbrook, Quebec. PhD Dissertation. McGill University, Quebec, Canada.

Iorns, W. V., C. H. Hembree, and G. L. Oakland. 1965. Water resources of the Upper Colorado River Basin. U.S. Geological Survey Professional Paper 441. 370 p.

Jackson, W. L., and R. P. Julander. 1982. Runoff and water quality from three soil landform units on Mancos Shale. Water Res. Bul. 18(6):995-1001.

Jacobson, R. L. 1973. Controls on the quality of some carbonate groundwaters, dissociation constants of calcite and $CaHCO_3^+$ from 0°C to 50°C. PhD Dissertation, Pennsylvania State University, University Park, Pennsylvania.

Johnson, A. K., and S. A. Schumm. 1982. Geomorphic and lithologic controls of diffuse-source salinity, Grand Valley, Western Colorado. Colorado Water Resources Research Institute, Colorado State University, Fort Collins, Colorado.

Jurinak, J. J., J. C. Whitmore, and R. J. Wagenet. 1977. Kinetics of salt release from a saline soil. Soil Science Society of America Proceedings, Vol. 41.

Jury, W. A. 1975. Solute travel-time estimates for tile - drained fields: II. Application to experimental studies. Soil Science Society of America Proceedings, Vol. 39.

Kemper, W. D., John Olsen, and C. J. deMooy. 1975. Dissolution rate of gypsum in flowing water. Soil Science Society of America Proceedings 39:458-463.

Konikow, L. F., and J. D. Bredehoeft. 1974. Modeling flow and chemical quality changes in an irrigated stream-aquifer system. Water Resources Research 10:546.

Laronne, J. B., and S. A. Schumm. 1977. Evaluation of the storage of diffuse sources of salinity in the Upper Colorado River Basin. Completion Report Series No. 79. Environmental Resources Center, Colorado State University, Fort Collins, Colorado.

Lindsay, W. L. 1979. Chemical equilibria in soils. John Wiley and Sons, New York, New York. 449 p.

McLin, S. G. 1981. Validity of the generalized lumped parameter hydrosalinity model in predicting irrigation return flow. PhD Dissertation. New Mexico Institute of Mining and Technology, Socorro, New Mexico.

Mercer, J. W. and C. R. Faust. 1981. Groundwater modeling. GeoTrans, Inc., Herndon, Virgina. Copyrighted by National Water Well Association.

Mundorff, J. C. 1972. Reconnaissance of chemical quality of surface water and fluvial sediment in the Price River Basin, Utah. State of Utah, Department of Natural Resources Tech. Publ. No. 39, Salt Lake City, Utah. 55 p.

Narayanan, Rangesan, and Douglas R. Franklin. 1982. An evaluation of water conservation techniques in the Upper Colorado River Basin. Report UWRL/P-82/07. Utah Water Research Laboratory, Utah State University, Logan, Utah.

Narayanan, Rangesan, Sumol Padungchai, and A. Bruce Bishop. 1979. An economic evaluation of the salinity impacts from energy development: The case of the Upper Colorado River Basin. Report UWRL/P-79/07. Utah Water Research Laboratory, Utah State University, Logan, Utah.

Neuman, S. P., R. A. Feddes, and E. Bresler. 1975. Finite element analysis of two dimensional flow in soils considering water uptake by roots. Soil Science Society of America Journal 39:224-230.

Nezafati, Hooshang, David S. Bowles, and J. Paul Riley. 1981. Salt-release from suspended sediments in the Colorado River Basin. Water Forum '81, ASCE, San Francisco, California. pp. 1327-1334.

Nordstrum, D. K., L. N. Plummer, T. M. L. Wigley, T. J. Wolery, J. W. Ball, E. A. Jenne, R. L. Bassett, D. A. Crerar, T. M. Florence, B. Fritz, M. Hoffman, G. R. Holdren, Jr., G. M. Lafon, S. V. Mattigod, R. E. McDuff, F. Morel, M. M. Reddy, G. Sposito, and J. Thrailkill. 1979. A comparison of computerized chemical models for equilibrium calulations in aqueous systems. In E. A. Jenne (Ed.). Chemical modeling in aqueous systems. ACS Symposium Series 93, pp. 857-892.

Nulsen, R. A., and C. J. Henschke. 1981. Groundwater systems associated with secondary salinity in western Australia. Agricultural Water Management 4:173-186.

Orlob, G. T., and P. C. Woods. 1967. Water quality management in irrigation systems. Journal of the Irrigation and Drainage Division, ASCE, 93(IR2):49-66.

Palciauskas, V. V., and P. A. Domenico. 1976. Solution chemistry mass transfer and the approach to chemical equilibrium in porous carbonate rocks and sediments. Geological Society of America Bulletin 87:207-214.

Parkhurst, David L., L. Niel Plummer, and Donald C. Thorstenson. 1982. BALANCE--A computer program for calculating mass transfer for geochemical reactions in ground water. U.S. Geological Survey Water-Resources Investigations 82-14. 29 p.

Parkhurst, David L., Donald C. Thorstenson, and L. Niel Plummer. 1980. PHREEQE--A computer program for geochemical calculations. U.S. Geological Survey Water-Resources Investigations 80-96. 216 p.

Piper, A. M. 1944. A graphic procedure in the geochemical interpretation of water analysis. American Geophysical Union Transactions 25:914-923.

Plummer, L. Niel, David L. Parkhurst, and Donald C. Thorstenson. 1983. Development of reaction models for ground-water systems. Geochimica et Cosmochimica Acta 47:665-686.

Ponce, S. L., II. 1975. Examination of a non-point source loading function for the Mancos Shale wildlands of the Price River Basin. Unpublished PhD Dissertation. Utah State University, Logan, Utah. 177 p.

Rao, Bhasker K., David S. Bowles, and R. Jeff Wagenet. 1981. Preliminary identification of salt efflorescence: a nonpoint source of salinity. Water Forum '81, ASCE, San Francisco, California. pp. 1335-1339.

Rawls, W. J. D. L. Brakensiek, and K. E. Saxton. 1982. Estimation of soils water properties. Transactions of the ASAE, pp. 1316-1320.

Riley, J. P. and J. J. Jurinak. 1979. Irrigation management for river salinity control. Journal of the Irrigation and Drainage Division, ASCE, 105(IR4).

Riley, J. P., D. S. Bowles, D. G. Chadwick, and W. J. Grenney. 1979. Preliminary identification of Price River Basin salt pick-up and transport processes. Water Res. Bul. 15(4):984-995.

Riley, J. Paul, Eugene K. Israelsen, William N. McNeill, and Brian Peckins. 1982. Potential of water and salt yields from surface runoff on public lands in the Price River Basin. Report UWRL/P-82/01. Utah Water Research Laboratory, Utah State University, Logan, Utah. 84 p.

Robins, Charles W. 1979. A salt transport and storage model for calcareous soils that may contain gypsum. PhD Dissertation. Soil Science Department, Utah State University, Logan, Utah. 104 p.

Rubin, Jacob. 1983. Transport of reacting solutes in porous media: relation between mathematical nature of problem formulation and chemical nature of reactions. Water Resources Research 19:5:1231-1252.

Simonett, M. J. 1981. Irrigation return flow modeling at San Acacia, New Mexico. Unpublished MS Thesis. New Mexico Institute of Mining and Technology, Socorro, New Mexico. 112 p.

Suarez, D. L. 1983. Calcite supersatuation and precipitation kinetics in the Lower Colorado River, All-American Canal and East Highline Canal. Water Resources Research 19(3):653-661.

Uintex Corporation. 1982. Runoff and water quality of selected perennial streams in the Price River Basin, Utah. Prepared for USDI/BLM, Special Studies Division, Denver Federal Center, Denver, Colorado.

U.S. Bureau of Land Management. 1976. The feasibility of salinity control from national resources lands in the Upper Colorado River Basin. Denver Service Center, Division of Standards and Technology, Watershed Staff, Colorado River Salinity Team, Denver, Colorado.

U.S. Bureau of Land Management. 1978. The effects of surface disturbance (primarily livestock use) on the salinity of public lands in the Upper Colorado River Basin (1977 Statis. Report). Denver, Colorado.

U.S. Bureau of Land Management. 1980. Control of salinity from point sources yielding groundwater discharge and from diffuse surface runoff in the Upper Colorado River Basin. Denver, Colorado.

U.S. Bureau of Reclamation. 1975. Salinity and sediment study, Upper Colorado River Basin, Utah, Colorado, and Wyoming. Salt Lake City, Utah.

U.S. Department of Agriculture. 1954. Diagnosis and improvement of saline and alkali soils. Agricultural Handbook No. 60. L. A. Richards (Ed). Soil and Water Conservation Research Branch, Agricultural Research Service, Washington, D.C.

U.S. Department of the Interior. 1983. Status report: Colorado River water quality improvement program. Bureau of Reclamation, Colorado River Water Quality Office, Denver, Colorado. 154 p.

U.S. Geological Survey. 1984. Hydrology of Area 56, Northern Great Plains and Rocky Mountain coal provinces, Utah. USGS Water Resources Investigations, Open-File Report 83-88, Salt Lake City, Utah.

Utah Division of Water Resources. 1975. Hydrologic inventory of the Price River Basin. Utah State Department of Natural Resources, Salt Lake City, Utah. 63 p.

Van Genuchten, M. Th. 1980. A closed-form equation for predicting the hydraulic conductivity of unsaturated soils. Soil Science Society of America Journal 44:892-898.

Wang, H. F., and M. P. Anderson. 1982. Introduction to groundwater modeling. Freeman Press, San Francisco, California.

Weast, Robert C. (Ed.). 1970. Handbook of chemistry and physics. 51st Edition. The Chemical Rubber Co., Cleveland, Ohio.

Whittig, L. D., A. E. Deyo, and K. K. Tanji. 1982. Evaporite mineral species in Mancos shale and salt efflorescence, Upper Colorado River Basin. Soil Science Society of America Journal 46:645-651.

APPENDICES

Appendix A

CH2M Hill Data

Table A-1. Groundwater quality data (in mg/l) from CH2M Hill (1983) study.

Monitoring Well	Ca	Mg	K	Na	HCO_3	CO_3	Cl	SO_4	TDS	EC @ 25°C (micromhos)	ALK	Hard-ness	pH
M7-D (MA1CUW/D)													
4/20/82	471.0	214.0	13.1	123.0	293.0	0.1	1.0*	2016	3362	3515	240.0	2057.0	6.9
5/24/82	540.0	186.0	13.1	111.0	289.0	0.1	21.0	2080	3415	3167	237.0	2114.0	7.5
7/09/82	482.0	186.0	11.6	125.0	329.0	0.1	21.0	2058	3242	3205	270.0	1969.0	7.4
8/16/82	548.0	184.0	12.9	118.0	540.0	0.1	43.1	1820	3206	3041	443.0	2125.0	7.0
9/28/82	448.0	507.0	10.6	88.0	365.0	0.1	28.8	3125	4524	2873*	299.0	3208.0	7.2
11/10/82	486.0	218.0	14.0	111.0	291.0	0.1	17.0	2080	3136	3181	238.0	2114.0	7.4
1/26/83	506.0	174.0	11.0	100.0	273.0	0.1	26.0	1740	2969	2933	224.0	1981.0	7.6
M7-I (MA1CUM/I)													
4/20/82	88.0	27.0	2.9	28.4	289.0	0.1	1.0*	129	487	727	237.0	330.0	7.1
5/24/82	94.0	35.0	2.1	30.1	292.0	0.1	13.0	169	521	755	239.0	378.0	7.6
7/09/82	108.0	84.0	2.3	29.0	215.0	0.1	16.0	473	874	793	176.0	618.0	8.2
8/16/82	99.0	34.0	3.5	42.0	329.0	0.1	10.6	176	556	808	270.0	387.0	7.3
9/28/82	80.0	65.0	2.5	42.0	481.0	0.1	16.2	98	509	696	394.0	469.0	7.6
11/10/82	60.0	40.0	2.1	35.0	336.0	0.1	8.0	120	466	745	275.0	534.0	7.8
1/26/83	91.0	34.0	2.4	32.0	326.0	0.1	14.0	126	416	670	267.0	366.0	8.0
M7-S (MA1CUE/S)													
7/09/82	225.0	118.0	3.7	29.0	284.0	0.1	12.0	890	1605	1757	223.0	1050.0	7.5
8/16/82	90.0	43.0	4.2	32.0	420.0	0.1	13.7	94	545	759	344.0	401.0	7.5
M9-D (MA2IMN/D)													
4/20/82	471.0	1599.0	35.7	5180.0	530.0	0.1	1099.0	17300	33735	30550	434.0	7756.0	7.5
5/24/82	422.0	1970.0	41.1	7070.0	563.0	0.1	1150.0	21200	40734	30580	462.0	9165.0	7.6
7/09/82	857.0	1703.0	32.1	7780.0	584.0	0.1	1096.0	24170	39813	32254	478.0	9151.0	7.5
8/17/82	423.0	1966.0	37.4	8790.0	610.0	0.1	.0*	28880	39993	30814	500.0	9148.0	7.1
9/28/82	1252.0*	1345.0	29.7	7910.0	6780.0*	0.1	1275.0	23928	40667	30351	5558.0*	8662.0	7.4
11/17/82	421.0	2126.0	47.0	9570.0	559.0	0.1	656.0	26880	41969	31761	458.0	9800.0	7.5
1/26/83	514.0	289.0	40.0	11090.0	573.0	0.1	103.0	25280	40356	32309	469.0	2475.0	7.8

Table A-1. Continued.

Monitoring Well	Ca	Mg	K	Na	HCO_3	CO_3	Cl	SO_4	TDS	EC @ 25°C (micromhos)	ALK	Hard-ness	pH
M9-I (MA2IMM/I)													
5/24/82	94.0	52.0	7.7	227.0	423.0	0.1	29.0	575	1214	1679	347.0	450.0	7.7
M9-S (MA2IMS/S)													
5/24/82	81.0	31.0	10.0	168.0	543.0	0.1	1.1*	240	843	1229	445.0	328.0	7.9
M10-D (MA3ILW/D)													
4/20/82	413.0	512.0	20.4	798.0	469.0	0.1	4.6*	4150	7585	7395	384.0	3142.0	7.5
5/24/82	525.0	333.0	24.4	788.0	555.0	0.1	1.9*	3786	6671	6246	455.0	2681.0	7.4
7/09/82	527.0	271.0	21.6	655.0	464.0	0.1	50.0	3568	5833	5166	380.0	2433.0	7.2
8/17/82	471.0	367.0	23.4	772.0	520.0	0.1	72.6	3890	6269	5832	426.0	3687.0	7.0
9/28/82	457.0	278.0	20.8	736.0	1031.0*	0.1	91.2	4375	6495	6155	845.0*	2286.0	7.0
11/17/82	461.0	369.0	31.0	883.0	477.0	0.1	73.0	3950	6450	6116	391.0	2673.0	7.3
1/26/83	455.0	372.0	23.0	871.0	467.0	0.1	91.0	3900	6272	6111	383.0	2668.0	7.7
M10-I (MA3ILM/I)													
7/09/82	501.0	357.0	19.4	398.0	429.0	0.1	76.0	3300	5317	4977	351.0	2472.0	7.1
8/17/82	481.0	346.0	21.5	437.0	578.0	0.1	54.9	3245	5155	484*	474.0	2627.0	7.0
9/28/82	444.0	380.0	17.6	383.0	652.0	0.1	66.9	3075	4483	4686	535.0	2672.0	7.1
11/17/82	495.0	357.0	24.0	483.0	367.0	0.1	59.0	3140	5092	4815	301.0	2707.0	7.1

*Indicates sample may contain errors.

Table A-2. Monitoring well information matrix (CH2M Hill 1983).*

Well Information								Soils					Water Levels					Chemical											
																				Cations				Anions			
Well Number	Location	Elevation Above Mean Sea Level	Depth Drilled (ft)	Distance from Canal (ft)	Distance to Surface Drainage (ft)	Depth to Bedrock (ft)	Well Depth - Deep, Intermediate, Shallow (ft)	Texture	Source Residual - Transported	Soil Salinity Type	Irrigated	Amount of Water Applied in Acre-Feet	Vertical Gradients	Change in Water Levels (ft)	Artesian	Depth to Groundwater Minimum (ft)	Depth to Groundwater Maximum (ft)	Average Total Dissolved Solids mg/l	Change in Total Dissolved Solids mg/l	Calcium mg/l	Magnesium mg/l	Potassium mg/l	Sodium (Na) mg/l	Bicarbonate (HCO_3) mg/l	Carbonate (CO_3) mg/l	Chloride (CL) mg/l	Sulfate (SO_4) mg/l
M-7D	15-10-9dc	5,611.0	39.0	100	6,100	30.0	D	SH	R	SS	Y	0.62	D	9.9	N	16.4	26.3	3,407	1,555	497	238	12	111	340	0.1	26	2,131
M-7I	15-10-9cd	5,610.8	24.0	100	6,100	30.0	I	AL	R	SS	Y	0.62	D	13.0	N	7.8	20.8	547	458	89	46	3	34	324	0.1	13	184
M-7S	15-10-9dc	5,611.0	10.0	100	6,100	30.0	S	SL	R	SS	Y	0.62	D	>2.9	N	7.1	--	1,075	1,060	158	81	4	31	352	0.1	13	492
M9D	15-10-16ab	5,577.8	30.0	1,700	4,600	27.0	D	SH	R	SS	Y	0.62	D	3.8	N	5.2	10.9	39,609	6,234	518	1,571	38	8,199	570	0.1	897	23,948
M9I	15-10-16ab	5,577.5	5.0	1,700	4,600	27.0	I	AL	R	SS	Y	0.62	D	>2.3	N	2.7	--	1,214	--	94	52	8	227	423	0.1	29	575
M9S	15-10-16ab	5,577.4	3.0	1,700	4,600	27.0	S	AL	R	SS	Y	0.62	--	>0.24	N	2.8	--	843	--	81	31	10	168	543	0.1	0	240
M10D	15-10-16ad	5,547.5	10.0	3,650	2,600	10.0	D	SH	R	SS	N	0.62	E	2.1	N	5.1	7.2	6,510	1,752	473	357	24	786	492	0.1	76	3,946
M10I	15-10-16ad	5,547.5	7.0	3,650	2,600	10.0	I	SH	R	SS	N	0.62	E	>1.7	N	5.3	--	5,011	834	480	360	20	425	507	0.1	64	3,190
M10S	15-10-16ad	5,547.6	4.0	3,650	2,600	10.0	S	SH	R	SS	N	0.62	--	--	N	--	--	--	--	--	--	--	--	--	--	--	--

WELL INFORMATION
KEY TO TABLE A-2

Well Number

Location:
T__ S R__ E Sec.___

Elevation: Ground Level at Well

Total Well Depth: Feet Below Land Surface

Distance From Canal (ft)

Distance to Drain (ft)

Depth to Bedrock (ft)

Deep (D) Intermediate (I) Shallow (S)

Texture at Screen

SH Shale
SL Silt Loam
AL Sandy Loam

Source of Soil

R Residual
T Transported

Soil Type

SS Slightly Saline

Irrigated

Yes (Y)
No (N)

Amount of Water Applied (acre-feet)

Vertical Gradient

(U) Up
(D) Down
(X) Crosses
(E) Equal

Change in Water Levels (ft)

Artesian

Yes (Y)
No (N)

Minimum Depth to Water (ft)

Maximum Depth to Water (ft)

Average Total Dissolved Solids (mg/l)

Change in Total Dissolved Solids (mg/l)

Average Calcium Concentrations (mg/l)

Average Magnesium Concentrations (mg/l)

Average Potassium Concentrations (mg/l)

Average Sodium Concentrations (mg/l)

Average Bicarbonate Concentrations (mg/l)

Average Carbonate Concentrations (mg/l)

Average Chloride Concentrations (mg/l)

Average Sulfate Concentrations (mg/l)

Appendix B

Field Data from This Study

Table B-1. Groundwater quality data (in mg/l) from present study.

Monitoring Well	Concentration in ppm (= mg/l)								Alkalinity as mg/l $CaCO_3$		pH		EC µmhos/cm	Field Temperature
	Ca	Na	Mg	K	Cl	SO_4	HCO_3	CO_3	Lab	Field	Lab	Field	@ 25°C	°C
7I														
04/06/84	84.2	23.0	26.8	<4.0	13.6	75.8	284.3	0.0	233.0	235.0	7.9	-	375	12.1
05/12/84	92.2	27.6	49.9	3.9	14.2	96.1	322.1	0.0	264.2	293.3	7.7	7.2	876	27.0
06/14/84	248.0	25.3	30.9	<4.0	17.9	108.0	306.9	0.0	251.4	247.5	7.5	7.3	620	29.0
07/25/84	62.1	20.7	21.9	3.9	13.8	79.3	274.6	0.0	225.0	293.3	7.5	7.6	586	19.0
08/28/84	60.1	20.7	26.8	-	18.8	38.4	250.8	12.0	245.5	214.2	-	7.5	512	21.0
10/06/84	192.8	23.0	26.7	-	18.8	57.6	255.0	6.3	230.0	233.0	8.1	7.8	552	-
7D														
04/06/84	420.8	75.9	153.2	7.8	16.4	1,070.0	308.7	0.0	253.0	262.1	7.2	-	917	15.0
05/12/84	450.9	73.6	149.6	11.7	14.2	1,676.3	297.1	0.0	243.4	260.0	7.2	6.8	2,753	27.0
06/14/84	492.0	80.5	148.0	11.7	30.4	1,710.0	309.9	0.0	254.0	251.7	7.3	6.9	2,743	27.0
07/25/84	424.8	119.6	153.2	11.7	18.8	1,661.9	283.1	0.0	232.0	257.9	7.1	7.2	3,069	17.0
08/28/84	434.9	69.0	126.5	-	24.1	1,522.6	311.8	0.0	255.5	226.7	-	8.2	1,583	18.0
10/06/84	393.0	68.3	98.5	-	19.1	1,296.8	296.5	0.0	243.0	243.4	7.6	7.6	2,510	-
14S														
08/28/84	376.8	115.0	327.1	-	29.4	2,151.8	327.0	0.0	268.0	-	-	9.1	3,082	18.0
10/06/84	349.3	135.2	284.5	-	24.5	2,065.3	305.1	10.8	286.0	-	7.9	8.3	3,480	-
14D														
08/28/84	330.7	478.4	345.3	-	133.7	3,122.0	226.4	0.0	185.5	-	-	8.1	4,988	15.0
10/06/84	300.8	586.5	282.0	-	153.1	3,544.3	67.7	0.0	55.5	43.7	7.8	7.6	5,850	-
9S														
06/14/84	77.0	32.2	31.4	7.8	18.4	49.2	313.6	0.0	256.8	251.7	7.6	7.4	542	25.0
9I														
06/14/84	189.0	41.4	44.1	7.8	18.4	88.8	278.2	0.0	228.2	255.8	7.8	7.6	520	28.0

Table B-1. Continued.

Monitoring Well	Concentration in ppm (= mg/l)								Alkalinity as mg/l $CaCO_3$		pH		EC µmhos/cm @ 25°C	Field Temperature °C
	Ca	Na	Mg	K	Cl	SO_4	HCO_3	CO_3	Lab	Field	Lab	Field		
9D														
04/06/84	80.2	7498.0	1970.0	31.3	2460	24,800	601.6	0.0	493.0	488.8	7.8	-	11,288	10.0
05/12/84	78.2	7291.0	2031.0	35.2	106.4	24,160	573.5	0.0	470.1	499.2	7.7	7.2	29,251	24.0
06/14/84	80.8	7797.0	1950.0	31.3	1086.0	20,800	605.9	0.0	496.6	499.2	7.8	7.1	31,807	21.5
07/25/84	80.2	8372.0	1240.0	35.2	1092.2	23,295	594.9	0.0	487.5	542.9	7.6	6.8	30,026	24.0
08/28/84	60.1	6352.3	2349.2	-	1180.9	25,120	520.4	36.0	546.5	457.6	-	6.8	28,172	16.0
10/06/84	79.6	7084.0	1325.1	-	989.0	21,134	516.2	0.0	423.0	505.4	7.9	7.6	34,200	-
15S														
10/06/84	34.5	673.9	162.9	-	158.5	2,161.4	200.1	21.3	235.0	-	7.2	6.9	4,420	-
11I														
07/25/84	380.8	181.7	280.9	27.4	-	-	-	-	-	-	-	7.2	3,900	14.0
10/06/84	421.8	52.2	104.5	-	13.8	1,248.8	189.7	0.0	155.5	-	6.8	7.3	2,310	-
12I														
06/14/84	70.5	2806	541.0	15.6	189.0	7,370	382.6	0.0	313.5	-	8.0	7.9	11,422	29.0
07/25/84	56.1	2415	272.4	19.6	-	-	-	-	-	-	-	6.5	290	19.0
13I														
08/28/84	190.4	1462.7	257.2	-	102.1	5,648.4	610.1	0.0	500.0	588.6	-	7.1	12,240	24.0
10/06/84	172.9	1301.8	164.1	-	123.4	6,724.3	531.4	0.0	435.5	553.3	-	7.1	11,000	22.0
10I														
06/14/84	456	450.8	375.0	19.5	137.0	2,710	396.6	0.0	325.0	343.2	7.4	7.1	4,160	30.0
07/25/84	392.8	437.0	330.7	19.5	109.2	3,122	383.2	0.0	314.0	-	7.4	7.1	4,798	23.0
10D														
06/14/84	414	894.4	334.0	23.5	72.2	3,900	537.5	0.0	440.6	445.1	7.2	6.9	3,847	22.0
07/25/84	302.6	830.3	309.0	23.5	84.8	4,006	488.1	0.0	400.0	451.4	7.2	6.6	11,746	22.0
08/28/84	288.6	770.5	36.5	-	85.1	3,900	507.6	0.0	416.0	359.8	-	7.2	7,429	21.0
10/06/84	300.6	876.3	312.4	-	79.8	4,130.6	516.2	0.0	423.0	449.3	-	7.4	7,000	23.0

Table B-2. Surface water quality data (in mg/l) from present study.

Location	Concentration in ppm (= mg/l)								Alkalinity as mg/l $CaCO_3$		pH		EC µmhos/cm	Field Temperature
	Ca	Na	Mg	K	Cl	SO_4	HCO_3	CO_3	Lab	Field	Lab	Field	@ 25°C	°C
Carbon Canal														
04/06/84	60.8	-	27.2	136.9	8.9	49.1	236.7	0.0	194.0	241.3	8.4	-	200	8.3
05/12/84	-	-	-	-	10.6	43.2	317.3	0.0	260.0	247.5	8.0	7.85	532	24.0
06/14/84	71.1	13.8	19.0	<4.0	10.6	35.1	239.8	0.0	196.4	191.4	8.2	7.8	341	28.5
07/25/84	54.1	16.1	20.7	3.9	12.8	85.0	137.3	21.0	182.5	226.6	8.1	7.9	1072	14.0
08/28/84	56.1	27.6	30.4	-	19.9	67.2	167.8	27.0	227.5	218.4	-	8.1	609	18.0
10/06/84	60.7	24.2	26.7	-	17.0	81.7	237.4	0.0	194.5	187.2	7.9	7.85	600	-
Miller Creek Upstream														
04/06/84	188.4	225.3	138.6	7.8	173.0	994.0	312.4	0.0	256.0	270.4	8.41	-	1372	15.0
05/12/84	190.4	229.9	172.6	7.8	88.9	1032.5	253.8	0.0	208.0	233.0	8.2	7.8	2276	31.0
06/14/84	121.8	144.8	111.0	7.8	47.8	750.0	269.1	0.0	220.6	214.2	8.5	7.9	1743	26.0
07/25/84	234.5	303.6	153.2	15.6	80.5	1681.1	211.1	0.0	173.0	176.8	8.1	7.4	6984	15.0
08/28/84	196.4	241.5	199.4	-	90.4	1777.1	178.8	27.0	236.5	181.0	-	7.3	3713	18.0
10/06/84	147.7	136.6	128.9	281.6	54.9	816.5	272.1	0.0	223.0	239.2	8.1	7.6	2100	-
Miller Creek Downstream														
04/06/84	154.3	140.2	121.6	3.9	36.0	720.0	286.8	0.0	235.0	235.0	8.28	-	757	14.5
05/12/84	164.3	149.4	96.0	7.8	32.0	662.8	304.5	0.0	249.6	289.1	8.0	7.85	1374	30.0
06/14/84	130.0	137.9	100.0	3.9	35.0	706.0	288.0	0.0	236.0	233.0	8.4	7.9	1344	29.0
07/25/84	246.5	377.2	153.2	15.6	58.2	1767.5	291.6	0.0	239.0	247.5	7.8	7.2	7106	18.0
08/28/84	228.5	246.1	154.4	-	45.6	1633.0	317.9	0.0	260.5	257.9	-	7.2	3542	18.0
10/06/84	196.8	201.3	131.3	320.7	59.6	1152.7	309.4	0.0	253.5	255.8	8.0	7.7	2630	-

Table B-3. Groundwater quality data (in meq/l) from present study.

Monitoring Well	Concentration in meq/l							
	Ca	Na	Mg	K	Cl	SO_4	HCO_3	CO_3
7I								
04/06/84	4.2	1.0	2.2	<0.1	0.4	1.6	4.66	0.0
05/12/84	4.6	1.2	4.1	0.1	0.4	2.0	5.28	0.0
06/14/84	12.4	1.1	2.5	<0.1	0.5	2.2	5.03	0.0
07/25/84	3.1	0.9	1.8	0.1	0.39	1.65	4.5	0.0
08/28/84	3.0	0.9	2.2	-	0.53	0.8	4.11	0.4
10/06/84	9.62	1.00	2.2	-	0.53	1.2	4.18	0.21
7D								
04/06/84	21.0	3.3	12.6	0.2	0.5	22.3	5.06	0.0
05/12/84	22.5	3.2	12.3	0.3	0.4	34.9	4.87	0.0
06/14/84	24.6	3.5	12.2	0.3	0.9	35.6	5.08	0.0
07/25/84	21.2	5.2	12.6	0.3	0.53	34.6	4.64	0.0
08/28/84	21.7	3.0	10.4	-	0.68	31.7	5.11	0.0
10/06/84	19.61	2.97	8.1	-	0.54	27.0	4.86	0.0
14S								
08/28/84	18.8	5.0	26.9	-	0.83	44.8	5.36	0.0
10/06/84	17.43	5.88	23.4	-	0.69	43.0	5.00	0.36
14D								
08/28/84	16.5	20.8	28.4	-	3.77	65.0	3.71	0.0
10/06/84	15.01	25.5	23.2	-	4.32	74.0	1.11	0.0
9S								
06/14/84	3.8	1.4	2.58	0.2	0.5	1.0	5.14	0.0
9I								
06/14/84	9.4	1.8	3.63	0.2	0.5	1.8	4.56	0.0
9D								
04/06/84	4.0	326.0	162.0	0.8	69.4	516	9.86	0.0
05/12/84	3.9	317.0	167.0	0.9	3.0	503	9.40	0.0
06/14/84	4.0	339.0	160.4	0.8	30.6	42.3*	9.93	0.0
07/25/84	4.0	364.0	102.0	0.9	30.8	485	9.75	0.0
08/28/84	3.0	276.2	193.2	-	33.3	523	8.53	1.2
10/06/84	3.97	308.0	109.0	-	27.9	440	8.46	0.0
15S								
10/06/84	1.72	29.3	13.4	-	4.47	45.0	3.28	0.71
11I								
10/06/84	21.05	2.27	8.6	-	0.39	26.0	3.11	0.0

Table B-3. Continued.

Monitoring Well	Concentration in meq/l							
	Ca	Na	Mg	K	Cl	SO_4	HCO_3	CO_3
12I								
06/14/84	3.5	122	44.5	0.4	5.3	153.4	6.27	0.0
07/25/84	2.8	105	22.4	0.5	-	-	-	-
13I								
08/28/84	9.5	63.6	21.2	-	2.88	117.6	10.0	0.0
10/06/84	8.63	56.6	13.5	-	3.48	140.0	8.71	0.0
10I								
06/14/84	22.8	19.6	30.8	0.5	3.9	56.4	6.50	0.0
07/25/84	19.6	19.0	27.2	0.5	3.08	65.0	6.28	0.0
10D								
06/14/84	20.7	37.8	27.5	0.6	2.0	81.2	8.81	0.0
07/25/84	15.1	36.1	25.4	0.6	2.39	83.4	8.00	0.0
08/28/84	14.4	33.5	3.0*	-	2.40	81.2	8.32	0.0
10/06/84	15.00	38.1	25.7	-	2.25	86.0	8.46	0.0

*Indicates sample may contain errors.

Table B-4. Surface water quality data (in meq/l) from present study.

Location	Concentration in meq/l							
	Ca	Na	Mg	K	Cl	SO_4	HCO_3	CO_3
Carbon Canal								
04/06/84	3.0	115.0*	2.2	3.5	0.25	1.02	3.88	0.0
05/12/84	-	-	-	-	0.3	0.9	5.20	0.0
06/14/84	3.5	0.6	1.6	<0.1	0.3	0.7	3.93	0.0
07/25/84	2.7	0.7	1.7	0.1	0.36	1.77	2.25	0.7
08/28/84	2.8	1.2	2.5	-	0.56	1.4	2.75	0.9
10/06/84	3.03	1.05	2.2	-	0.48	1.7	3.89	0.0
Miller Creek Upstream								
04/06/84	9.4	9.8	11.4	0.2	4.9	20.7	5.12	0.0
05/12/84	9.5	10.0	14.2	0.2	2.5	21.5	4.16	0.0
06/14/84	6.1	6.3	9.1	0.2	1.3	15.6	4.41	0.0
07/25/84	11.7	13.2	12.6	0.4	2.27	35.0	3.46	0.0
08/28/84	9.8	10.5	16.5	-	2.55	37.0	2.93	0.9
10/06/84	7.37	5.94	10.6	7.2*	1.55	17.0	4.46	0.0
Miller Creek Downstream								
04/06/84	7.7	6.1	10.0	0.1	1.02	15.0	4.70	0.0
05/12/84	8.2	6.5	7.9	0.2	0.9	13.8	4.99	0.0
06/14/84	6.5	6.0	8.2	0.1	1.0	14.7	4.72	0.0
07/25/84	12.3	16.4	12.6	0.4	1.64	36.8	4.78	0.0
08/28/84	11.4	10.7	12.7	-	1.40	34.0	5.21	0.0
10/06/84	9.82	8.75	10.8	8.2*	1.68	24.0	5.07	0.0

*Indicates sample may contain errors.

Table B-5. Soil chemistry data (in meq/l) from present study.

USU Log #	Ident.	meq/l in Sat. Ext. Cl	HCO_3	SO_4	Ca	Mg	Na	K	pH	ECe*	CEC*
S4-1700	7/0 0-12	0.9	3.0	0.8	4.2	2.2	0.9	0.6	8.1	0.6	8.5
1701	" 12-24	<0.1	2.5	0.5	2.4	1.5	0.7	0.5	8.2	0.4	8.9
1702	" 24-36	<0.1	2.0	<0.1	1.8	1.3	0.8	0.5	8.4	0.3	8.2
1703	" 36-48	<0.1	1.8	0.4	1.9	1.2	0.8	<0.1	8.4	0.3	7.2
1704	" 48-60	<0.1	2.5	0.6	2.6	1.1	0.7	0.1	8.3	0.3	6.5
S4-1705	7/1 0-12	0.6	6.9	0.4	7.7	4.2	1.5	0.6	7.9	1.0	
1706	" 12-24	0.9	2.5	1.9	4.1	2.5	1.2	<0.1	8.3	0.6	
1707	" 24-36	0.2	2.4	1.0	2.6	1.7	1.0	<0.1	8.3	0.4	
1708	" 36-48	0.2	2.3	1.2	2.4	1.9	1.1	<0.1	8.4	0.4	
1709	" 48-60	0.2	2.3	1.1	2.2	2.0	1.1	<0.1	8.4	0.4	
S4-1710	7/3 0-12	0.6	5.2	5.7	8.1	4.5	1.9	0.3	8.1	1.1	
1711	" 12-24	0.6	2.6	1.4	3.7	1.9	1.2	<0.1	8.3	0.4	
1712	" 24-36	0.2	2.1	1.0	2.7	1.6	1.2	<0.1	8.4	0.4	
1713	" 36-48	0.3	2.5	3.5	4.0	2.9	1.7	<0.1	8.4	0.7	
1714	" 48-60	0.5	2.1	12.5	7.0	8.1	2.4	<0.1	8.3	1.4	
S4-1715	9/0 0-12	2.3	4.8	63.6	18.8	31.8	16.1	1.4	8.1	4.9	
1716	" 12-24	6.2	2.7	122	12.4	67.7	32.5	0.2	8.4	8.1	
1717	" 24-36	8.2	2.0	176	7.7	89.8	73.9	0.1	8.5	12	
1718	" 36-48	10.9	1.8	235	7.1	104	124	0.2	8.5	17	
1719	" 48-60	10.7	2.0	230	6.8	96.3	117	0.6	8.5	17	
S4-1720	9/1 0-12	2.4	4.6	99.0	14.8	20.3	68.7	1.3	8.2	8.0	
1721	" 12-24	12.5	2.9	421	5.6	91.1	264	1.1	8.5	31	
1722	" 24-36	15.5	2.7	530	6.0	154	309	0.9	8.4	33	
1723	" 36-48	13.2	1.9	385	5.9	111	230	0.8	8.4	26	
1724	" 48-60	7.8	1.4	254	5.7	62.5	167	0.6	8.4	19	

Table B-5. Continued.

USU Log #	Ident.	meq/l in Sat. Ext. Cl	HCO_3	SO_4	Ca	Mg	Na	K	pH	ECe*	CEC*
S4-1725	9/2 0-12	0.3	3.2	8.4	6.9	3.7	1.7	0.3	8.2	1.0	
1726	" 12-24	<0.1	1.8	4.5	3.9	2.0	1.2	0.2	8.3	0.6	
1727	" 24-36	0.2	1.8	4.3	3.8	1.8	1.2	0.2	8.3	0.5	
1728	" 36-48	0.2	1.6	5.7	4.5	2.1	1.2	0.2	8.3	0.6	
1729	" 48-60	0.2	1.6	3.9	3.7	1.8	1.1	0.2	8.3	0.5	
S4-1730	9/3 0-12	0.8	6.8	38.9	25.3	15.1	9.4	0.7	8.1	3.4	11.3
1731	" 12-24	0.4	2.1	20.8	11.3	8.5	6.1	0.5	8.2	1.9	8.9
1732	" 24-36	0.5	1.8	26.3	14.0	7.5	8.7	0.3	8.2	2.4	10.9
1733	" 36-48	0.4	1.6	45.9	25.2	11.7	10.8	0.2	8.1	3.6	12.6
1734	" 48-60	0.5	1.6	53.8	21.9	15.1	15.6	0.2	8.2	4.2	14.3

*ECe = Electrical conductivity of saturation extract measured in mmhos/cm.

CEC = Cation exchange capacity measured in meq/100 g.

Table B-6. Water levels and elevation of groundwater above mean sea level (MSL).

Monitoring Well	Water Level from Ground Surface (feet-inches)	Elevation of Groundwater (feet above MSL)
7I		
04/06/84	18-8	5592.0
05/12/84	17-5	5593.5
06/14/84	15-0	5596.0
07/25/84	15-4	5595.7
08/28/84	16-5	5594.5
10/06/84	17-0	5594.0
7D		
04/06/84	23-2	5587.9
05/12/84	23-8	5587.3
06/14/84	22-2	5588.9
07/25/84	22-6	5588.5
08/28/84	23-9	5587.3
10/06/84	21-3	5589.8
14S		
08/28/84	8-0	5578.0
10/06/84	4-9	5581.3
14D		
08/28/84	7-5	5578.5
10/06/84	4-5	5581.5
9I		
06/14/84	4-4	5592.0
9D		
04/06/84	9-5	5586.9
05/12/84	9-7	5586.8
06/14/84	9-3	5587.2
07/25/84	8-4	5588.1
08/28/84	9-2	5587.3
10/06/84	9-2	5587.3
15S		
10/06/84	6-4	5590.1
15D		
10/06/84	6-4	5590.1
11I		
07/25/84	9-8	5589.9
10/06/84	8-0	5591.6

Table B-6. Continued.

Monitoring Well	Water Level from Ground Surface (feet-inches)	Elevation of Groundwater (feet above MSL)
10I		
04/06/84	7-4	5578.6
06/14/84	6-8	5579.2
07/25/84	7-0	5578.9
10/06/84	7-1	5578.8
10D		
04/06/84	8-4	5577.6
05/12/84	7-8	5578.2
06/14/84	6-10	5579.0
07/25/84	7-1	5578.8
08/28/84	7-5	5578.5
10/06/84	7-5	5578.5

Appendix C

Correlation Plots of Well Water Levels Versus Electrical Conductivity

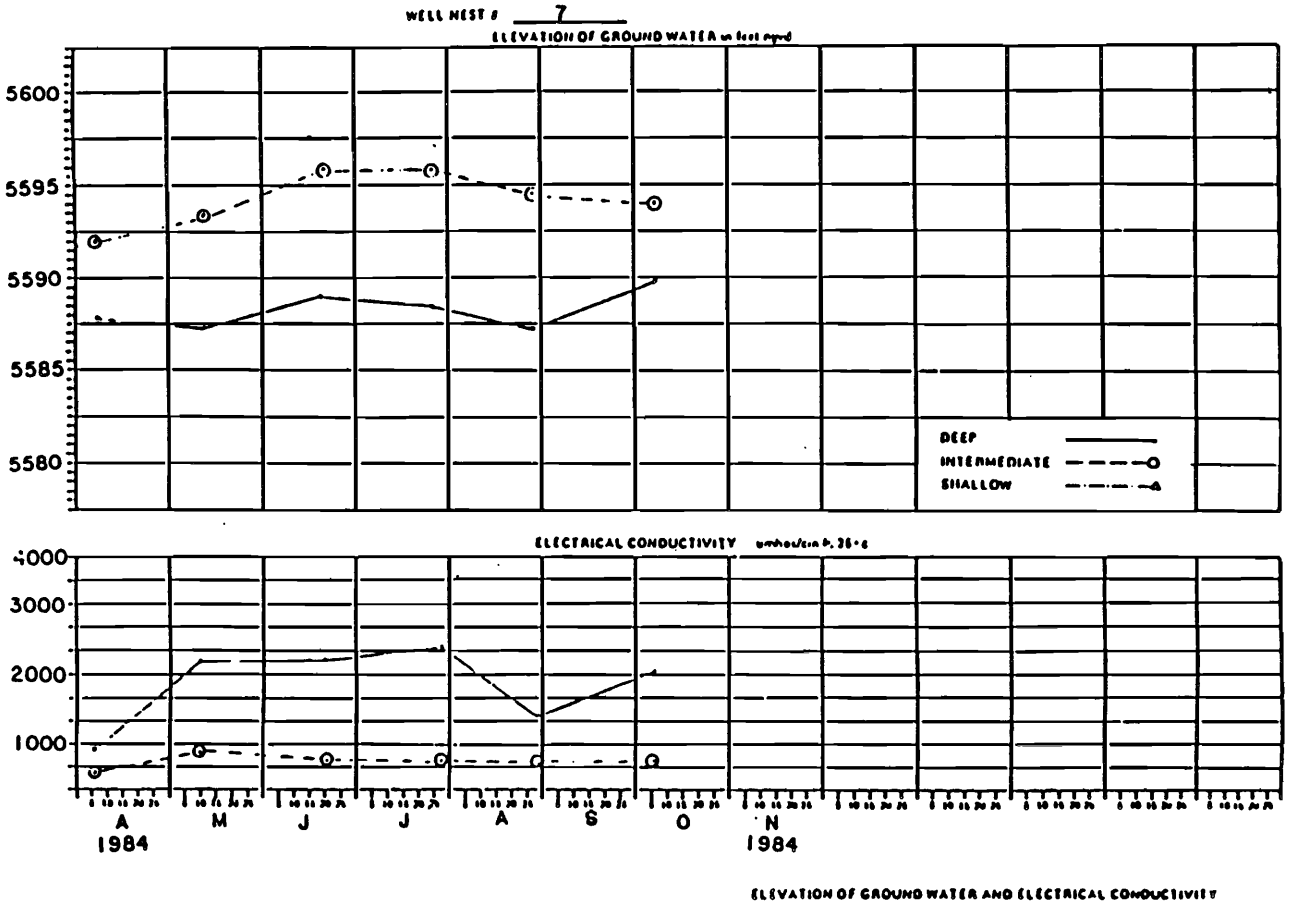

Figure C-1. Correlation of well water levels and EC-well 7.

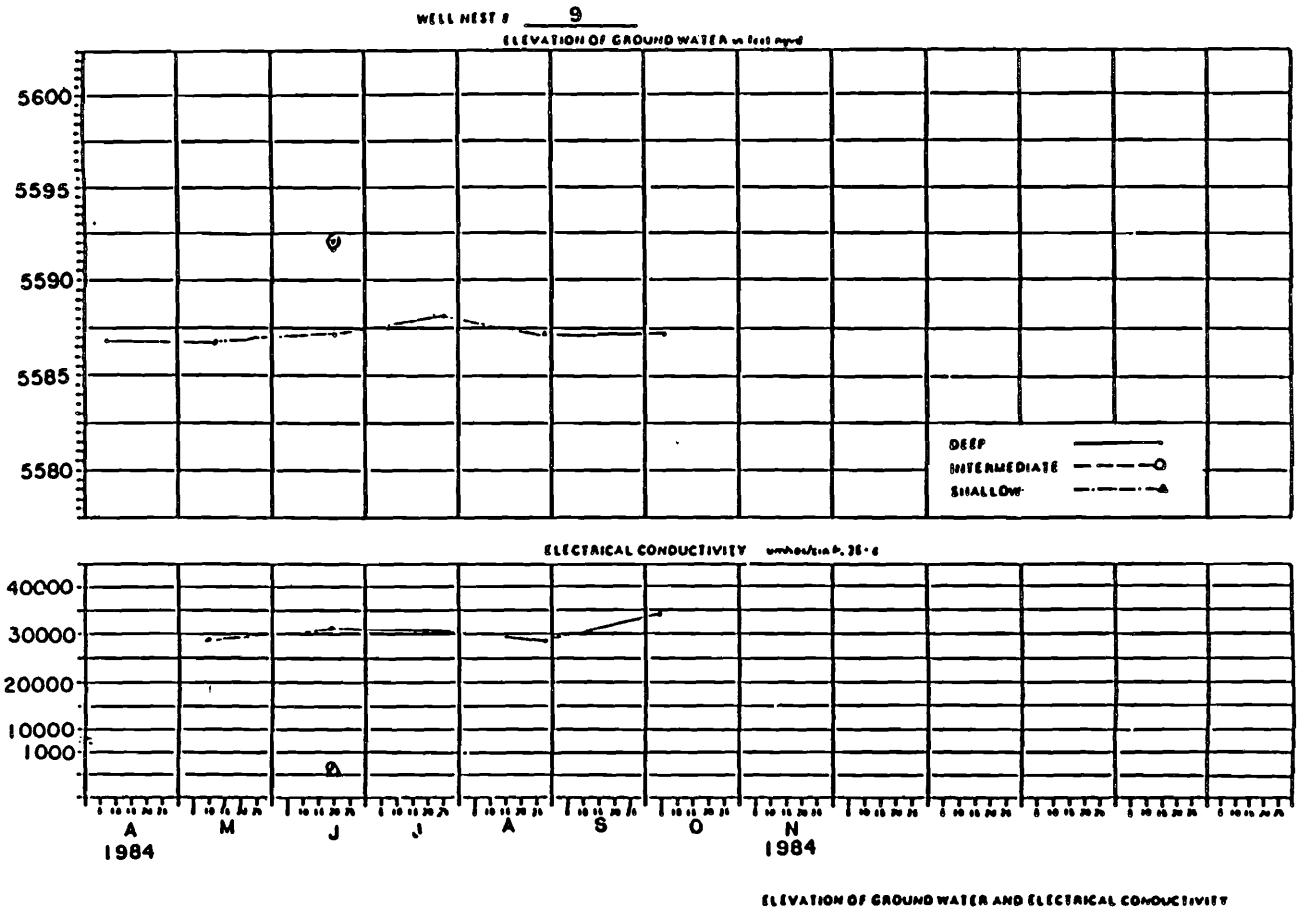

Figure C-2. Correlation of well water levels and EC-well 9.

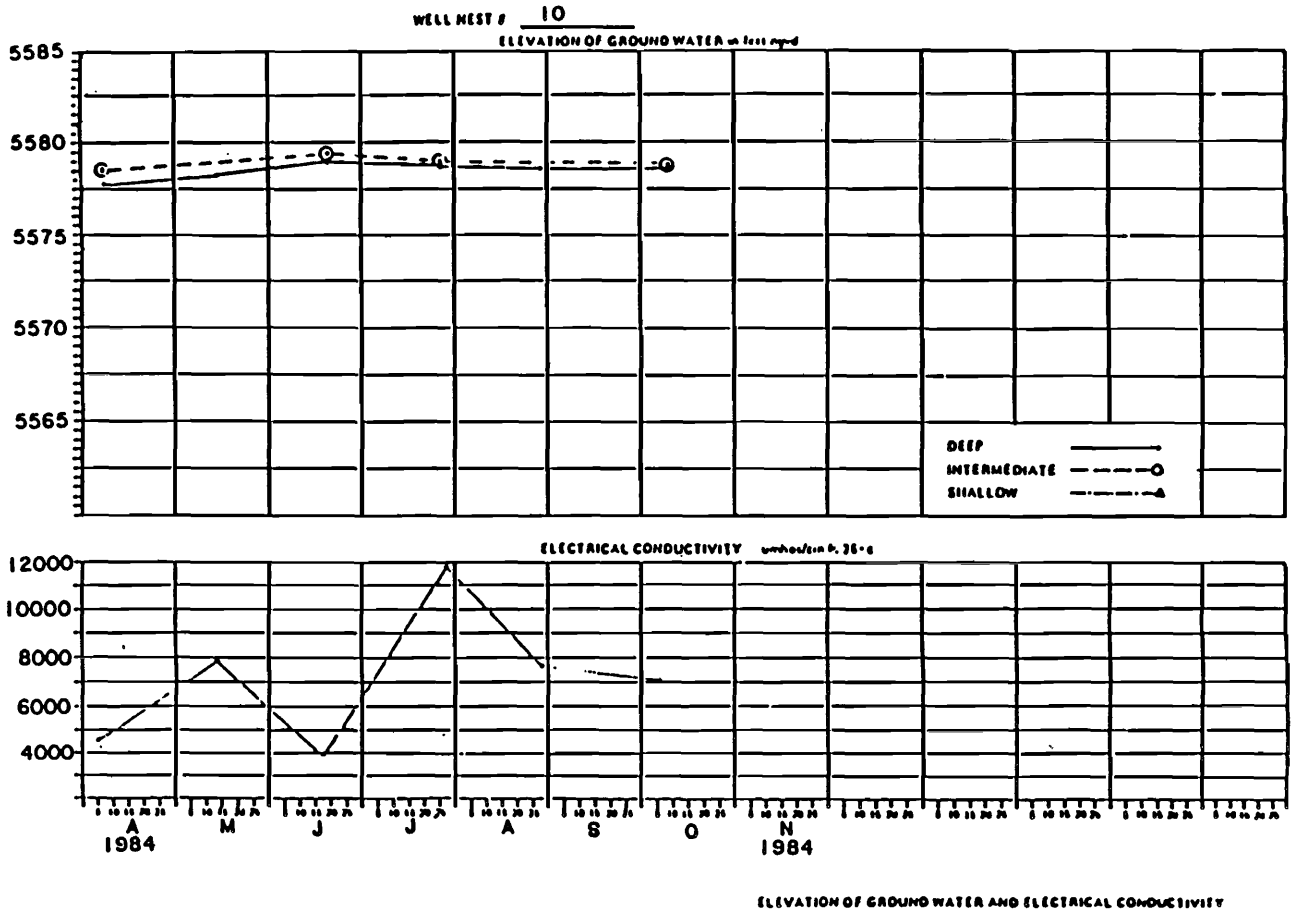

Figure C-3. Correlation of well water levels and EC-well 10.

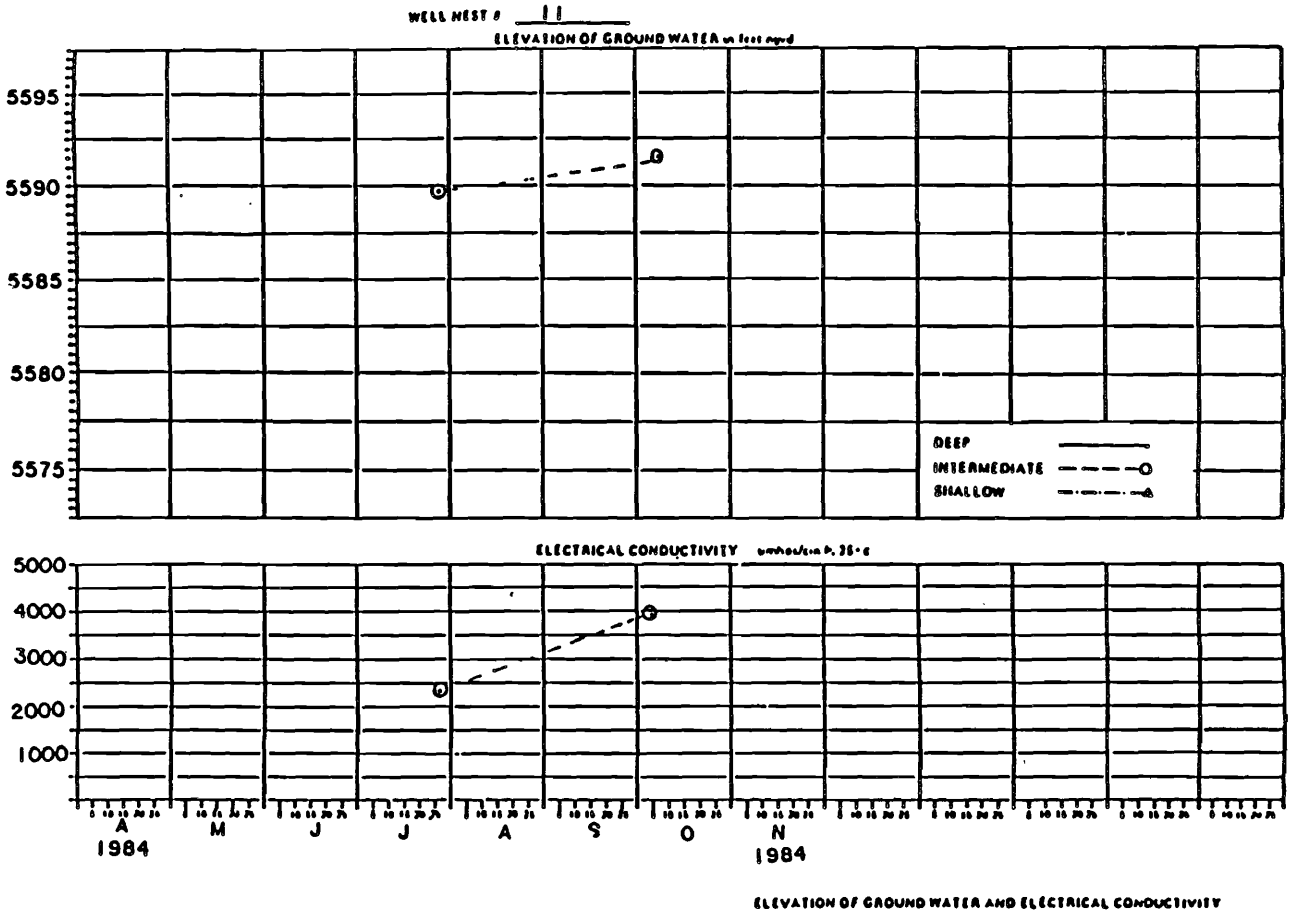

Figure C-4. Correlation of well water levels and EC-well 11.

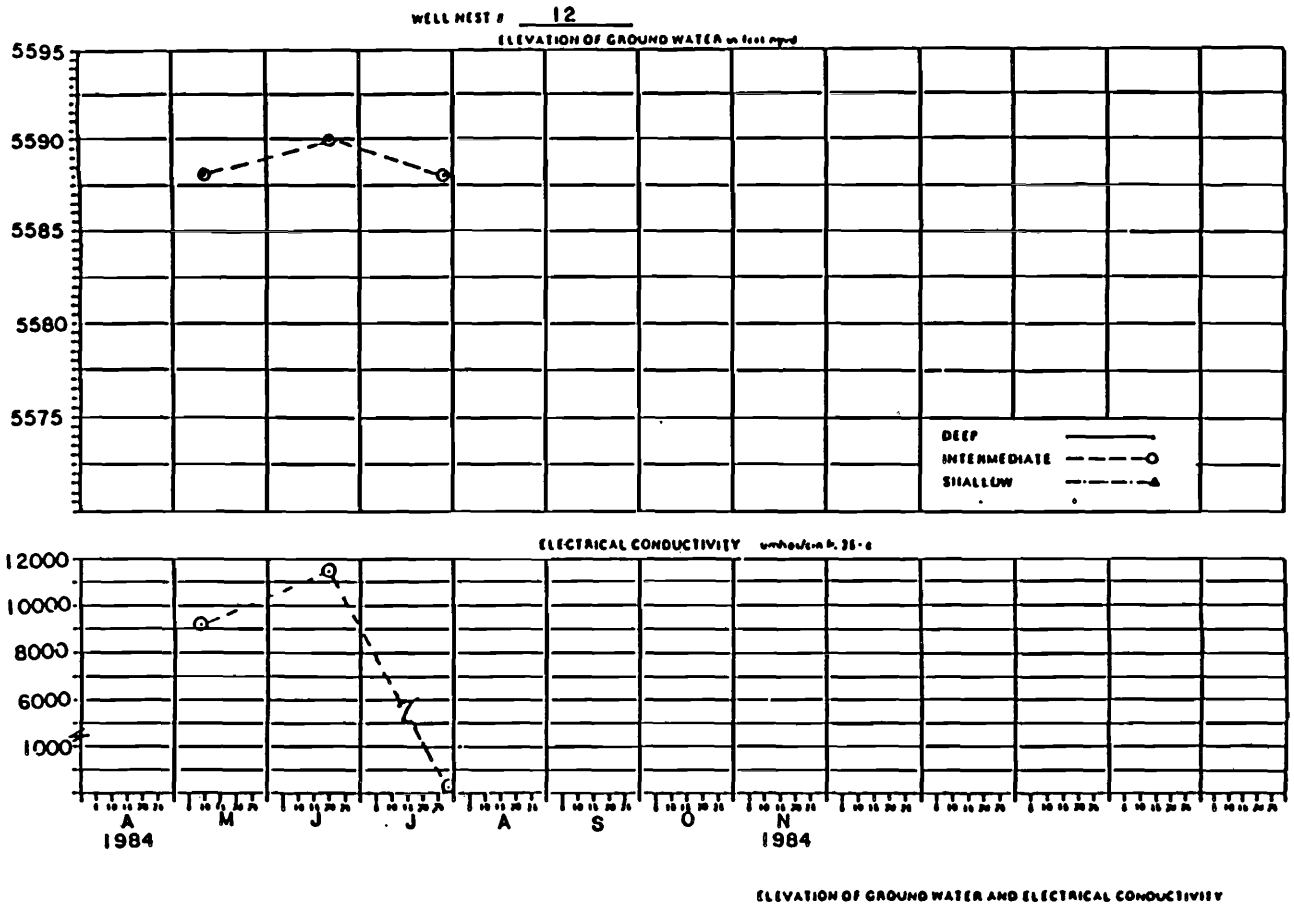

Figure C-5. Correlation of well water levels and EC-well 12.

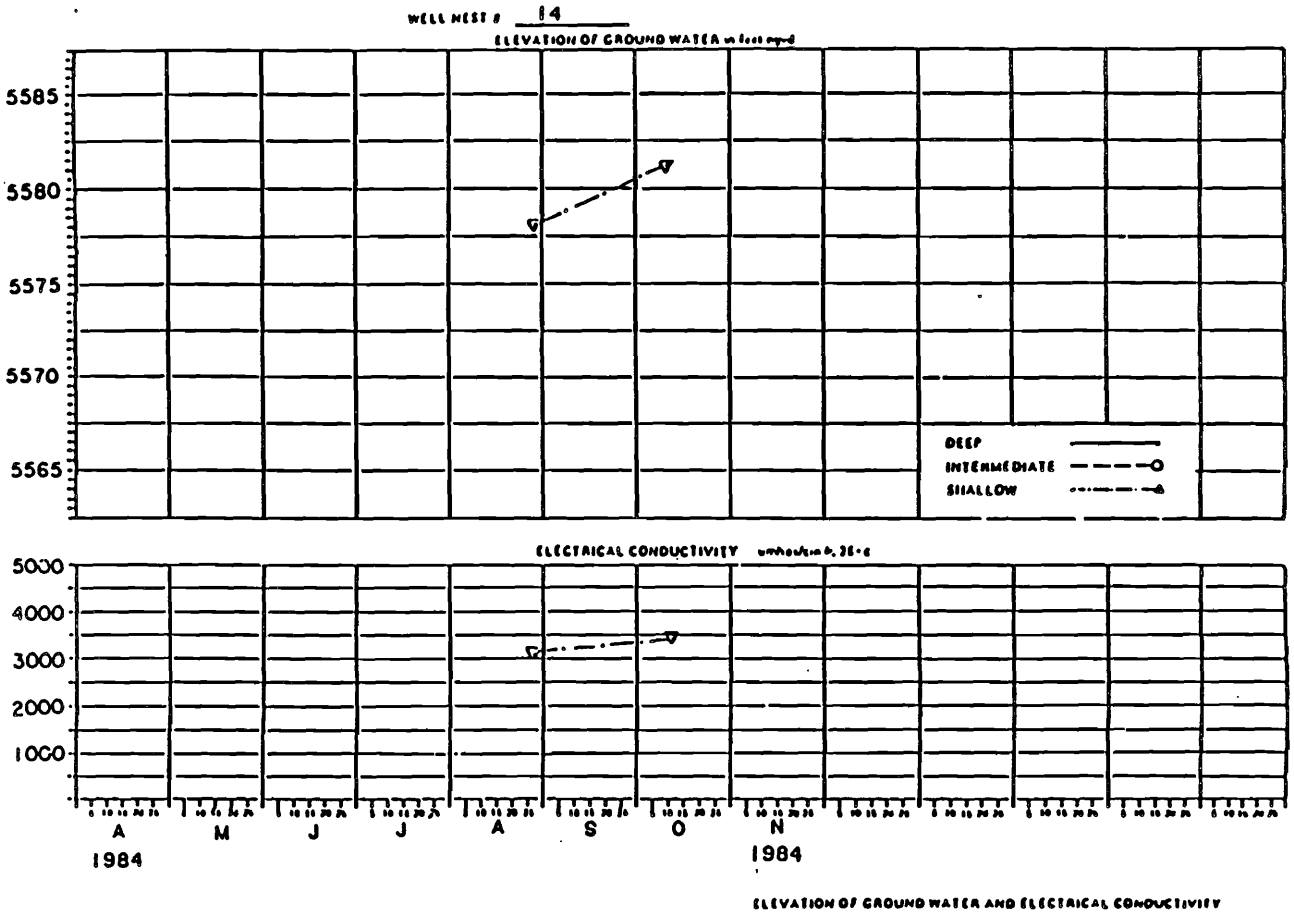

Figure C-6. Correlation of well water levels and EC-well 14.

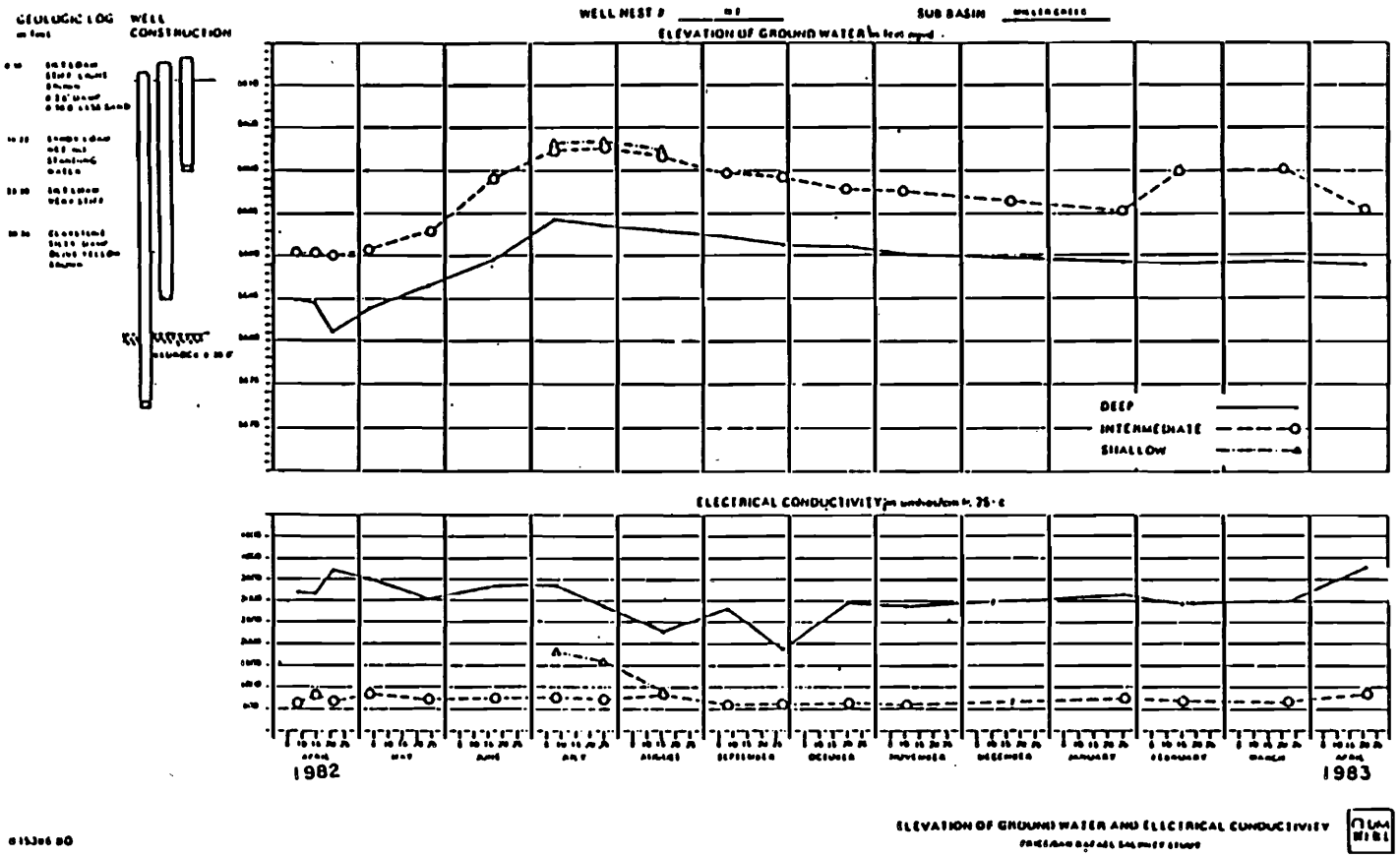

Figure C-7. Correlation of well water levels and EC-well 7 (CH2M Hill data).

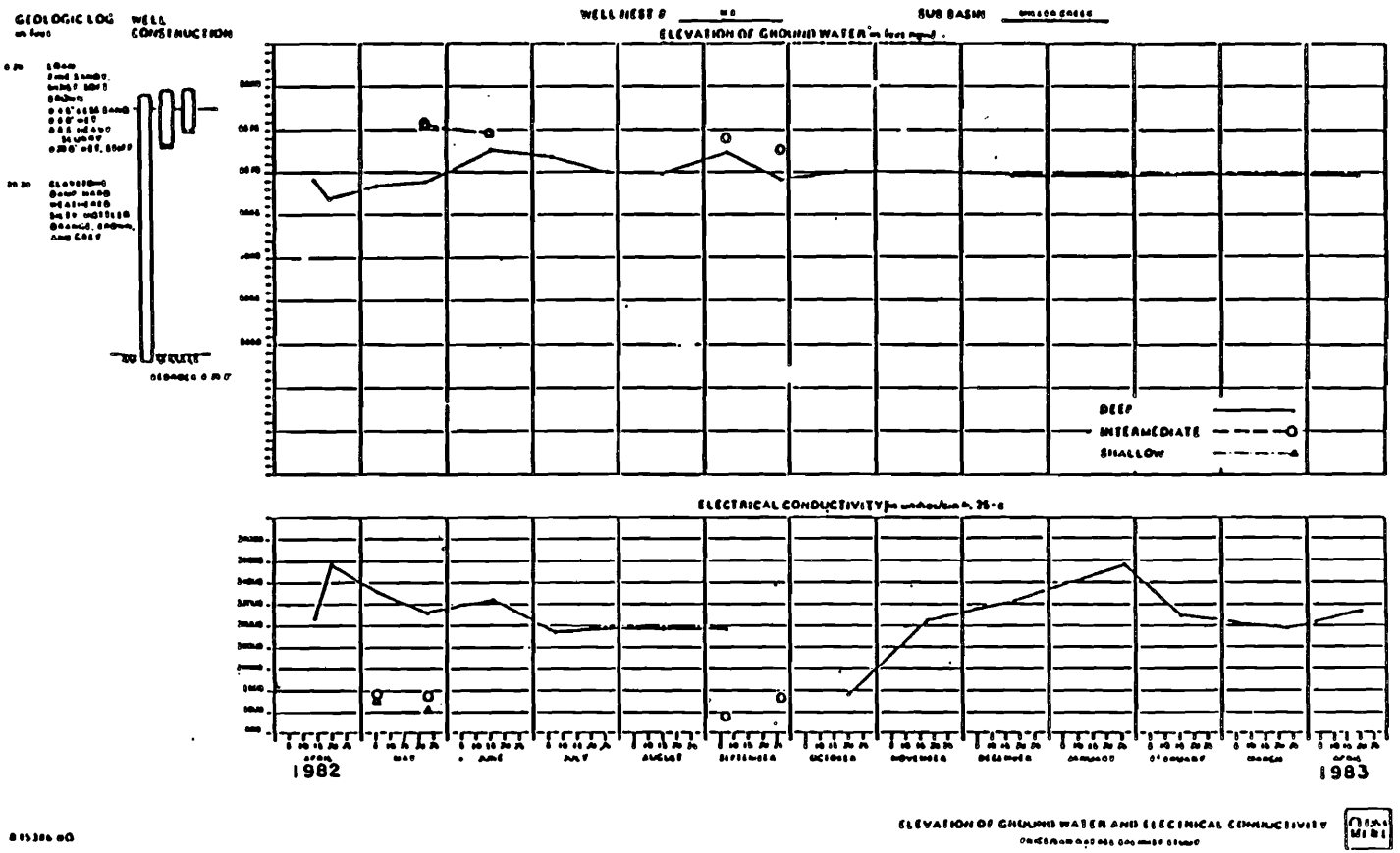

Figure C-8. Correlation of well water levels and EC-well 9 (CH2M Hill data).

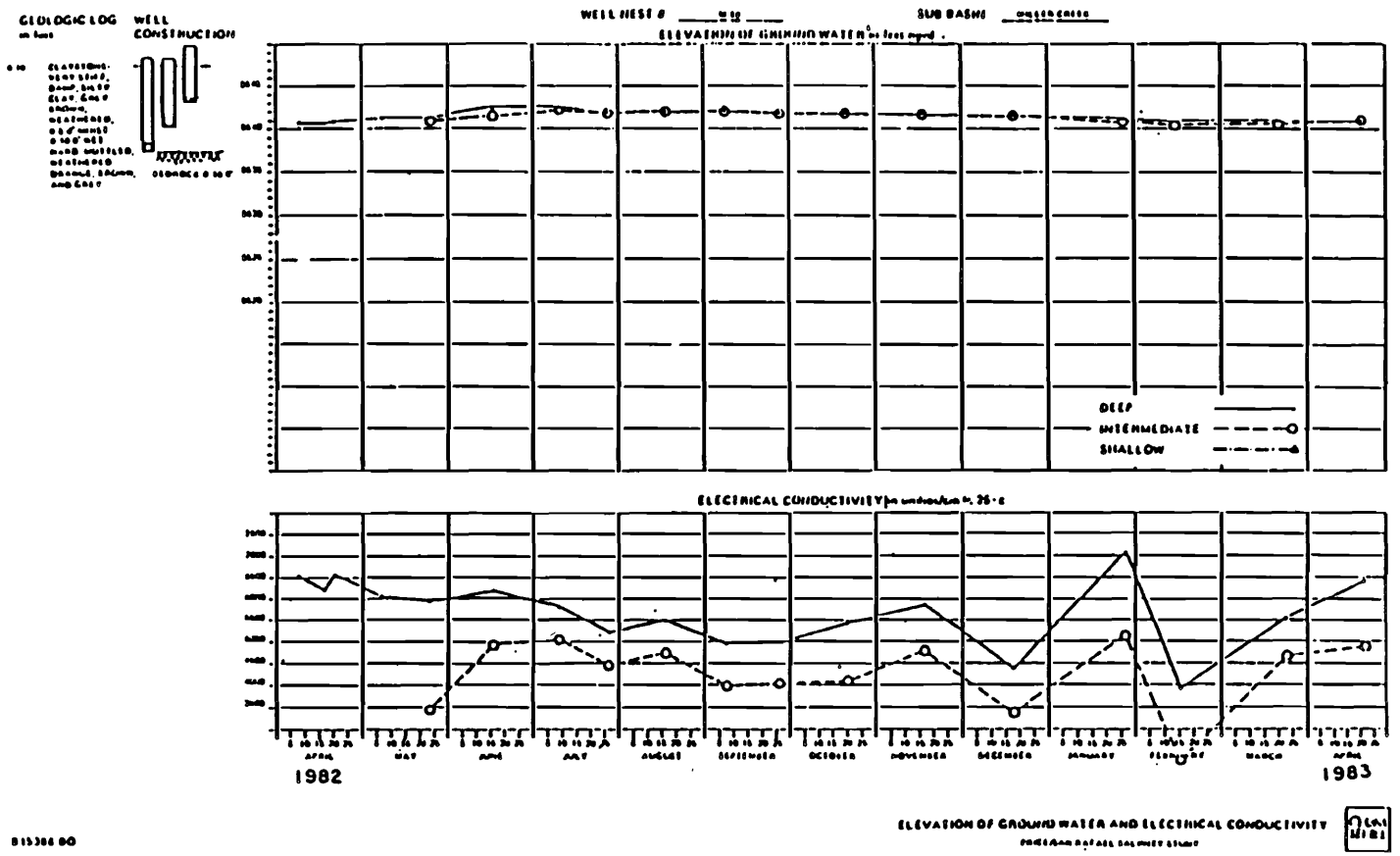

Figure C-9. Correlation of well water levels and EC-well 10 (CH2M Hill data).

Appendix D

Sodium Adsorption Ratio (SAR) Computations

Table D-1. SAR computations for soil chemistry.

Location (range of depth in feet)	Na (meq/l)	Ca (meq/l)	Mg (meq/l)	$\frac{Ca + Mg}{2}$ (meq/l)	$\frac{Na}{\sqrt{(Ca+Mg)/2}} = SAR$
7/0 (0-2)	0.8	3.3	1.75	2.53	0.50
7/1 (0-2)	1.35	5.9	3.35	4.63	0.63
7/3 (0-2)	1.55	5.9	3.2	4.55	0.73
9/2 (0-2)	1.45	5.4	2.85	4.13	0.71
9/3 (0-2)	7.75	18.3	11.8	15.05	2.00
9/0 (0-2)	24.3	15.6	49.75	32.68	4.25
9/1 (0-2)	166.4	10.2	55.7	32.95	28.99
7/0 (4-5)	0.7	2.6	1.1	1.85	0.51
7/1 (4-5)	1.1	2.2	2.0	2.1	0.76
7/3 (4-5)	2.4	7.0	8.1	7.55	0.87
9/2 (4-5)	1.1	3.7	1.8	2.75	0.66
9/3 (4-5)	15.6	21.9	15.1	18.5	3.63
9/0 (4-5)	117	6.8	96.3	51.55	16.30
9/1 (4-5)	167	5.7	62.5	34.1	28.60
7/0 (0-5)	0.78	2.58	1.46	2.02	0.55
7/1 (0-5)	1.18	3.80	2.46	3.13	0.67
7/3 (0-5)	1.68	5.10	3.80	4.45	0.80
9/2 (0-5)	1.28	4.56	2.28	3.42	0.69
9/3 (0-5)	10.12	19.54	11.58	15.56	2.57
9/0 (0-5)	72.7	10.56	77.92	44.24	10.93
9/1 (0-5)	207.74	7.6	87.78	47.69	30.08

Table D-2. SAR computations for water chemistry.

Location	Na (meq/l)	Ca	Mg	$\frac{Ca + Mg}{2}$	$\frac{Na}{\sqrt{(Ca+Mg)/2}}$ = SAR
7I	1.0	6.1	2.5	4.3	0.48
7D	3.5	21.8	11.4	16.6	0.86
9S	1.4	3.8	2.6	3.2	0.78
9I	1.8	9.4	3.6	6.5	0.71
9D	321.5	3.8	148.6	76.2	36.8
10I	19.3	21.2	28.95	25.1	3.85
10D	36.4	16.3	27.1	21.7	7.81
11I	2.3	21.0	8.6	14.8	0.60
12I	122.0	3.5	44.4	24.0	24.9
13I	60.1	9.1	17.4	13.3	16.5
14S	5.4	18.1	25.1	21.6	1.16
14D	23.2	15.8	25.7	20.8	5.09
15S	29.3	1.7	13.4	7.6	10.6
Carbon Canal	0.9	3.0	2.0	2.5	0.57
Miller Creek Upstream	9.3	9.0	12.4	10.7	2.84
Miller Creek Downstream	9.1	9.3	10.4	9.9	2.89

Appendix E

Computations for Trilinear Plots

Table E-1. Computations for trilinear plots of groundwater quality.*

Well ID	Concentration	Cations						Anions					
		Ca (1)	Na (2)	K (3)	Na + K (4)	Mg (5)	Total (1)+(4)+(5)	Cl (1)	SO_4 (2)	HCO_3 (3)	CO_3 (4)	$HCO_3 + CO_3$ (5)	Total (1)+(2)+(5)
7I	meq/l	6.15	1.02	0.1	1.12	2.50	9.77	0.46	1.58	4.63	0.10	4.73	6.77
	% of total	62.9	10.4	1.0	11.4	25.6	100.0	6.8	23.3	68.4	1.5	69.9	100.0
7D	meq/l	21.77	3.53	0.18	3.71	11.37	36.85	0.59	31.02	4.94	0.0	4.94	36.55
	% of total	59.1	9.6	0.5	10.1	30.9	100.0	1.6	84.9	13.5	0.0	13.5	100.0
14S	meq/l	18.12	5.44	0.0	5.44	25.15	48.71	0.76	43.90	5.18	0.18	5.36	50.02
	% of total	37.2	11.2	0.0	11.2	51.6	100.0	1.5	87.8	10.4	0.4	10.8	100.0
14D	meq/l	15.76	23.15	0.0	23.15	25.80	64.71	4.05	69.50	2.41	0.0	2.41	75.96
	% of total	24.4	35.8	0.0	35.8	39.9	100.0	5.3	91.5	3.2	0.0	3.2	100.0
9S	meq/l	3.80	1.40	0.2	1.60	2.58	7.98	0.5	1.0	5.14	0.0	5.14	6.64
	% of total	47.6	17.5	2.5	19.7	32.3	100.0	7.5	15.1	77.4	0.0	77.4	100.0
9I	meq/l	9.40	1.80	0.20	2.0	3.63	15.03	0.50	1.80	4.56	0.0	4.56	6.86
	% of total	62.5	12.0	1.3	13.3	24.2	100.0	7.3	26.2	66.5	0.0	66.5	100.0
9D	meq/l	3.81	321.7	0.85	322.55	148.93	475.29	32.5	493.4	9.32	0.24	9.56	535.46
	% of total	0.8	67.7	0.2	67.9	31.3	100.0	6.1	92.1	1.70	0.0	1.70	100.00
15S	meq/l	1.72	29.30	0.0	29.30	13.40	44.42	4.47	45.0	3.28	0.71	3.99	53.46
	% of total	3.9	66.0	0.0	66.0	30.2	100.0	8.4	84.2	6.1	1.3	7.4	100.0
11I	meq/l	21.05	2.27	0.0	2.27	8.60	31.92	0.39	45.0	3.28	0.71	3.99	49.38
	% of total	65.9	7.1	0.0	7.1	26.9	100.0	0.8	91.1	6.6	1.4	8.0	100.0
12I	meq/l	3.50	122.0	0.4	122.4	44.5	170.4	5.30	153.4	6.27	0.0	6.27	164.97
	% of total	2.1	71.6	0.2	71.8	26.1	100.0	3.2	93.0	3.8	0.0	3.8	100.0
13I	meq/l	9.07	60.10	0.0	60.10	17.35	86.52	3.18	128.8	9.36	0.0	9.36	141.34
	% of total	10.5	69.5	0.0	69.5	20.1	100.0	2.2	91.1	6.6	0.0	6.6	100.0
10I	meq/l	21.2	19.30	0.5	19.80	29.0	70.0	3.49	60.70	6.39	0.0	6.39	70.58
	% of total	30.3	27.6	0.7	28.3	41.4	100.0	4.9	86.0	9.1	0.0	9.1	100.0
10D	meq/l	16.30	36.38	0.6	36.98	26.20	79.48	2.26	82.95	8.40	0.0	8.40	93.61
	% of total	20.5	45.8	0.8	46.6	33.0	100.0	2.4	88.6	9.0	0.0	9.0	100.0

*Based on an average of time series data over a 6-month period.

Table E-2. Computations for trilinear plots of surface water quality.*

Location	Concentration	Cations						Anions					
		Ca (1)	Na (2)	K (3)	Na + K (4)	Mg (5)	Total (1)+(4)+(5)	Cl (1)	SO_4 (2)	HCO_3 (3)	CO_3 (4)	$HCO_3 + CO_3$ (5)	Total (1)+(2)+(5)
Carbon Canal	meq/l	3.01	0.89	0.95	1.84	2.04	6.89	0.38	1.25	3.65	0.27	3.92	5.55
	% of total	43.7	12.9	13.8	26.7	29.6	100.0	6.8	22.5	65.8	4.9	70.7	100.0
Miller Creek Upstream	meq/l	8.98	9.29	1.37	10.66	12.40	32.04	2.51	24.47	4.09	0.15	4.24	31.22
	% of total	28.0	29.0	4.3	33.3	38.7	100.0	8.0	78.4	13.1	0.5	13.6	100.0
Miller Creek Downstream	meq/l	9.32	9.08	1.50	10.58	10.37	30.27	1.27	23.05	4.91	0.0	4.91	29.23
	% of total	30.8	30.0	5.0	35.0	34.3	100.0	4.3	78.9	16.8	0.0	16.8	100.0

*Based on an average of time series data over a 6-month period.

Table E-3. Computations for trilinear plots of soil chemistry (0-5 ft).*

Section	Concentration	Cations						Anions					
		Ca (1)	Na (2)	K (3)	Na + K (4)	Mg (5)	Total (1)+(4)+(5)	Cl (1)	SO_4 (2)	HCO_3 (3)	CO_3 (4)	$HCO_3 + CO_3$ (5)	Total (1)+(2)+(5)
7/0	meq/l	2.58	0.78	0.34	1.12	1.46	5.16	0.2	0.46	2.36	-	2.36	3.02
	% of total	50.0	15.1	6.6	21.7	28.3	100.0	6.6	15.2	78.2	-	78.2	100.0
7/1	meq/l	3.8	1.18	0.15	1.33	2.46	7.59	0.42	1.12	3.28	-	3.28	4.82
	% of total	50.1	15.5	2.0	17.5	32.4	100.0	8.7	23.2	68.1	-	68.1	100.0
7/3	meq/l	5.10	1.68	0.1	1.78	3.8	10.68	0.44	4.82	2.90	-	2.90	8.16
	% of total	47.8	15.7	0.9	16.6	35.6	100.0	5.4	59.1	35.5	-	35.5	100.0
9/0	meq/l	10.56	72.7	0.5	73.2	77.92	161.68	7.66	165.32	2.66	-	2.66	175.64
	% of total	6.5	45.0	0.3	45.3	48.2	100.0	4.4	94.1	1.5	-	1.5	100.0
9/1	meq/l	7.6	207.7	0.94	208.64	87.8	304.04	10.28	337.8	2.7	-	2.7	350.78
	% of total	2.5	68.3	0.3	68.6	28.9	100.0	2.9	96.3	0.8	-	0.8	100.0
9/2	meq/l	4.56	1.28	0.22	1.50	2.28	8.34	0.2	5.36	2.0	-	2.0	7.56
	% of total	54.7	15.3	2.6	17.9	27.4	100.0	2.6	70.9	26.5	-	26.5	100.0
9/3	meq/l	19.54	10.12	0.38	10.50	11.58	41.62	0.52	37.14	2.78	-	2.78	40.44
	% of total	46.9	24.3	0.9	25.2	27.8	100.0	1.3	91.8	6.9	-	6.9	100.0

*Range of depth in the soil zone.

Table E-4. Computations for trilinear plots of soil chemistry (0-2 ft).*

Section	Concentration	Cations						Anions					
		Ca (1)	Na (2)	K (3)	Na + K (4)	Mg (5)	Total (1)+(4)+(5)	Cl (1)	SO_4 (2)	HCO_3 (3)	CO_3 (4)	$HCO_3 + CO_3$ (5)	Total (1)+(2)+(5)
7/0	meq/l	3.3	0.8	0.55	1.35	1.75	6.4	0.5	0.65	2.25	-	2.25	3.4
	% of total	51.6	12.5	8.6	21.1	27.3	100.0	14.7	19.1	66.2	-	66.2	100.0
7/1	meq/l	5.9	1.35	0.35	1.70	3.35	10.95	0.75	1.15	4.7	-	4.7	6.6
	% of total	53.9	12.3	3.2	15.5	30.6	100.0	11.4	17.4	71.2	-	71.2	100.0
7/3	meq/l	5.9	1.55	0.2	1.75	3.2	10.85	0.6	3.55	3.9	-	3.9	8.05
	% of total	54.4	14.3	1.8	16.1	29.5	100.0	7.5	44.1	48.4	-	48.4	100.0
9/0	meq/l	15.6	24.3	0.8	25.1	49.75	90.45	4.25	92.8	3.75	-	3.75	100.8
	% of total	17.2	26.9	0.9	27.8	55.0	100.0	4.2	92.1	3.7	-	3.7	100.0
9/1	meq/l	10.2	166.4	1.2	167.6	55.7	233.5	7.45	260.0	3.75	-	3.75	271.2
	% of total	4.4	71.3	0.5	71.8	23.9	100.0	2.7	95.9	1.4	-	1.4	100.0
9/2	meq/l	5.4	1.45	0.25	1.70	2.85	9.95	0.2	6.45	2.5	-	2.5	9.15
	% of total	54.3	14.6	2.5	17.1	28.6	100.0	2.2	70.5	27.3	-	27.3	100.0
9/3	meq/l	18.3	7.75	0.6	8.35	11.8	38.45	0.6	29.9	4.45	-	4.45	34.95
	% of total	47.6	20.2	1.6	21.8	30.7	100.0	1.7	85.6	12.7	-	12.7	100.0

*Range of depth in the soil zone.

Table E-5. Computations for trilinear plots of soil chemistry (4-5 ft).*

Section	Concentration	Cations						Anions					
		Ca (1)	Na (2)	K (3)	Na + K (4)	Mg (5)	Total (1)+(4)+(5)	Cl (1)	SO_4 (2)	HCO_3 (3)	CO_3 (4)	$HCO_3 + CO_3$ (5)	Total (1)+(2)+(5)
7/0	meq/l	2.6	0.7	0.1	0.8	1.1	4.5	<0.1	0.6	2.5	-	2.5	3.2
	% of total	57.8	15.6	2.2	17.8	24.4	100.0	3.1	18.8	78.1	-	78.1	100.0
7/1	meq/l	2.2	1.1	<0.1	1.2	2.0	5.4	0.2	1.1	2.3	-	2.3	3.6
	% of total	40.7	20.4	1.9	22.3	37.0	100.0	5.6	30.6	63.9	-	63.9	100.0
7/3	meq/l	7.0	2.4	<0.1	2.5	8.1	17.6	0.5	12.5	2.1	-	2.1	15.1
	% of total	39.8	13.6	0.6	14.2	46.0	100.0	3.3	82.8	13.9	-	13.9	100.0
9/0	meq/l	6.8	117.0	0.6	117.6	96.3	220.7	10.7	230.0	2.0	-	2.0	242.7
	% of total	3.1	53.0	0.3	53.3	43.6	100.0	4.4	94.8	0.8	-	0.8	100.0
9/1	meq/l	5.7	167.0	0.6	167.6	62.5	235.8	7.8	254.0	1.4	-	1.4	263.2
	% of total	2.4	70.8	0.3	71.1	26.5	100.0	3.0	96.5	0.5	-	0.5	100.0
9/2	meq/l	3.7	1.1	0.2	1.3	1.8	6.8	0.2	3.9	1.6	-	1.6	5.7
	% of total	54.4	16.2	2.9	19.1	26.5	100.0	3.5	68.4	28.1	-	28.1	100.0
9/3	meq/l	21.9	15.6	0.2	15.8	15.1	52.8	0.5	53.8	1.6	-	1.6	55.9
	% of total	41.5	29.5	0.4	29.9	28.6	100.0	0.9	96.2	2.9	-	2.9	100.0

*Range of depth in the soil zone.

Cost Minimization For Coal Conversion Pollution Control: A Mixed Integer Programming Model

Michael F. Torpy
A. Bruce Bishop
Rangesan Narayanan

The work reported by this project completion report was supported with funds provided by the Department of the Interior, Office of Water Research and Technology, under P.L. 88-379, Agreement Number 14-34-0001-7094, (A-032-Utah).

WATER RESOURCES PLANNING SERIES

Report P1

Utah Water Research Laboratory
College of Engineering
Utah State University
Logan, Utah 84322
March 1978

ABSTRACT

A mixed integer program was structured to identify the least cost combination of recycling and treatment alternatives that can be used to control the liquid, solid, and gas waste streams produced from a 750-megawatt coal fired steam electric power plant. The model compared methods of liquid stream recycle and waste discharge treatment to meet given air and water quality standards. The model was then used to study the effects on the optimal solution of changes in capital, operation and maintenance, and energy and water costs. In addition, the effects on optimum system design of changes in particulate and sulfur oxide emission standards and stream discharge standards were evaluated.

Nonlinear cost functions for system components were structured with binary integer variables to define the ordinate intercept and with continuous variables to define the slopes of total cost curve segments. The binary and continuous variables were associated with each other in pairs to approximate nonlinear total cost functions of alternative pollution control units.

The optimal plant design was sensitive to increases in capital, operation and maintenance, and energy costs as well as air emission standard changes. The model identified the optimal treatment unit alternatives and their sizes when segments of the total costs and environmental standards were changed. The optimal solutions always identified water recycle, rather than stream discharge, as the optimal production strategy.

ACKNOWLEDGMENTS

This is the final report of a project supported with funds provided by the Office of Water Research and Technology of the United States Department of the Interior as authorized under the Water Resources Research Act of 1964, Public Law 88-379. The work was accomplished by personnel of the Utah Water Research Laboratory, Utah State University. The authors wish to thank Drs. Trevor C. Hughes, Dennis B. George, William J. Grenney, and L. Douglas James for their technical and editorial assistance, Barbara South and Vicki Westover for typing the report, Susan Bissland and Art Rivers for drafting the figures; Donna Falkenborg for her editing contribution, and Ann Torpy for her typing assistance.

TABLE OF CONTENTS

TABLE OF CONTENTS (CONTINUED)

LIST OF TABLES

LIST OF TABLES (CONTINUED)

LIST OF FIGURES

LIST OF FIGURES (CONTINUED)

LIST OF FIGURES (CONTINUED)

INTRODUCTION

NATURE OF THE PROBLEM

The contribution of coal conversion to the nation's energy requirements has become increasingly significant as the reserves of other energy sources diminish and the cost of supplies increase. Various residuals are produced during coal conversion, and must be controlled to avoid environmental degradation. With the increasing use of coal conversion due to the relative abundance of coal, the problem of pollution control for coal conversion facilities becomes more important to a clean environment. Pollution control costs are a significant part of the total energy conversion costs and an evaluation of the pollution control alternatives may reduce the cost of protecting to environment and promote resource conservation.

The residuals generated during coal conversion are in the liquid, gas, and solid forms. Various pollution control technologies are available for controlling the residuals from coal conversion facilities to meet the federal and state discharge standards. The pollution control technologies require combinations of capital and other factors such as water, energy, and other operation-maintenance expenses to meet expected performance standards. When a firm's objective is to minimize its costs at given output levels and operate within residual discharge constraints, its choice among pollution control alternatives would be the combination of alternatives with the least cost to meet the discharge standards imposed by society. When the management personnel of a proposed coal conversion facility evaluate and compare the feasible pollution control alternatives available to adequately control residual emissions at the least costs, the task of rationally selecting the least cost control strategy becomes difficult because of the large number of alternative combinations. When the possibilities of changes in factor costs are considered along with changes in discharge and emission standards, the task of comparing and evaluating the residual control alternatives becomes even more complex.

OBJECTIVES OF THE RESEARCH

The objective of this research is to develop a mathematical model which can be used to select and evaluate the least cost pollution control technology that will allow coal conversion facilities to meet water, air quality, and solid waste discharge standards. The model is designed to provide a method for evaluating the economic impact to a firm when conditions for residual discharge standards and resource costs are changed.

SIGNIFICANCE OF THE STUDY

Several pollution control technologies are available for use when coal conversion processes require different combinations of capital and other inputs. The optimal combination of treatment processes depends on the relative costs of capital and operation and maintenance including energy and water costs. When the unit costs for the various inputs change, the least cost solution among the pollution control alternatives would be expected to shift to or from alternatives that use more capital. Likewise, when the cost of capital changes the optimal solution among the control alternatives may require more or less of the other inputs.

In arid areas of the Western States, the potential for coal development may be limited by available water supplies. When water resources are used most efficiently in the water limited areas, economic opportunities in the area can be greatest. Water has traditionally been used for steam cooling in steam electric power generation. As the price per unit of water increases, the choice of cooling towers would be expected to change from wet cooling towers which lose water through evaporation and blowdown, to hybrid (wet and dry) cooling towers or to dry type cooling towers.

Mixed integer linear programming can be used to consider the many possible treatment processes and to identify the least cost pollution control strategies for coal conversion processes. In addition, mixed integer programming can be used to evaluate the effects of factor cost changes and of changes in discharge standards on the optimal least-cost solution.

REVIEW OF LITERATURE

The demonstration of optimization methods applied to the selection of pollution control strategies for production facilities is relatively limited in the literature. Most mathematical programming applications related to industrial pollution control have been directed toward river and air basin management and have essentially ignored the problem of optimum control with individual facilities. In the application, optimum solutions were found for the problem of allocating treatment requirements along a stream or in a basin. The objective of the models was to find the minimum cost of treatment for all discharging activities to meet water or air quality standards within a basin. In most cases such as in the studies by Teller and Norsworthy (1970) and Kohn (1969) either the dissolved oxygen level in a water body or sulfur levels in an air basin were used as single discharge constraints. In comparison to basin optimization studies, however, relatively few authors have directed their attention to solving production system optimization problems.

DYNAMIC PROGRAMMING

A few models have been reported in the literature which were designed to identify the optimal pollution control facilities within a plant. Shih and Krishnan (1969) demonstrated the use of dynamic programming for optimizing the design of an industrial wastewater treatment plant. The optimum combinations and performances of various unit processes in a multi-state treatment plant were identified when the model was applied to pulp and paper plant data. Different treatment combinations were defined in the model and the dynamic programming solution identified the combination of treatment units which could be used in sequence to meet the ultimate design and discharge constraints. The criterion for discharge was the BOD level of the final effluent, and cost estimates in the model were based on the BOD removal.

Evenson, Orlob, and Monser (1969) demonstrated the use of dynamic programming to identify the optimum wastewater treatment design for a cannery wastewater. Like Shih and Krishnan's model, the pollution control performance was measured in terms of BOD removal. It was explained that practical application of dynamic programming was limited to two or three pollutant parameters, and when more than three parameters are used, the problem becomes inordinately complex.

GEOMETRIC PROGRAMMING

Ecker and McNamera (1971) used geometric programming to solve the same problem that Shih and Krishnan solved with dynamic programming. Geometric programming can be used to reduce a problem involving a function of any degree to a problem requiring a solution of linear equations. According to Ecker and McNamera, their geometric program is more attractive than the dynamic program because of its computational ease and sensitivity analysis for variations in effluent quality. Geometric programming in Ecker-McNamera required that the cost equations be in the form:

$$y = ax^b$$

in which

- y = total annual cost
- a = a fixed positive constant
- x = a fraction of 5-day BOD remaining on process completion
- b = a fixed negative exponent

The authors explained that unless the cost data are represented by equations of this type, then geometric programming cannot be used. In the models of Shih and Krishnan; Evenson, Orlob and Monser; and Ecker and McNamera; the problem of solid waste treatment and disposal was ignored as part of the integrated pollution control problem and therefore the models did not necessarily insure an optimal solution.

LINEAR PROGRAMMING

Linear programming applications to optimizing pollution control in production plants has received some attention from a few authors. Stone,

et al. (1975a) presented the results of an economic linear programming model designed to integrate the ethylene production plant design with pollution control facilities. The model was developed to evaluate the effect of water discharge standard changes and water price changes on: 1) the costs of producing ethylene, 2) the choice of feed stock, and 3) the marginal costs of treating some of the major pollutants.

Stone et al. (1975b) developed a linear programming model to identify the minimum cost of producing olefins and treating the wastewater effluents from the alternative production processes. The olefin model design was also based on the changing price of water and changing water discharge standards. Stone et al. (1975b, p. 23-24) explained that

> ...the costs of the treatment units used in the model are, in general, nonlinear functions of unit capacity, influent concentration, and sometimes effluent concentration. In most cases, cost estimates developed from literature sources expressing treatment costs in terms of flow volume and pollutant loads. Next, flow capacity requirements estimates for the model plant. Finally, a linear approximation to the nonlinear cost function is obtained by specifying a line (or plane) which is tangent or near tangent to the cost function at the point representing the capacity requirement.
>
> Normally, a linear model requires that the process cost equations have a zero intercept because of the impossibility of properly including fixed cost elements in the objective function.

The results of the model indicated that the incremental costs of equipping a modern ethylene plant to comply with any level of environmental regulation, including zero discharge would be relatively modest.

Singleton et al. (1975) designed an integrated power process model of water use and chlor-alkali production. The linear model was designed with objectives similar to those of the ethylene production plant model designed by Stone et al. (1975a). Calloway, Schwartz, and Thompson (1974) developed a linear model whose design was similar to those of Singleton et al. (1975), and Stone et al. (1975a, 1975b). The model was used to minimize the cost of producing ammonia. Calloway, Schwartz, and Thompson made no provisions in their model for stream mixing and assumed that the optimum solution could be identified without mixing effluent streams to meet quality standards. However, the assumption may not be valid.

Inoue et al. (1974) used linear programming to evaluate the effect of environmental emission policies and unit water cost changes on the cost of generating electric power. The pollution vector in the linear program was based on heat discharge. Choices for pollution control were once-through cooling, closed cycle wet tower cooling, open cycle wet cooling, and dry tower cooling.

NETWORK MODELING

Adams and Panagiotakopoulos (1977) described a network model which was designed to find the least cost treatment design for the example originally presented by Shih and Krishnan. According to the authors, the model could handle both convex and concave nonlinear cost functions of the non-increasing type. The model, it was reported, could be optimized by including multiple constant parameters such as BOD, SS, COD and nutrients. However, the publication did not demonstrate the use of the constraints in the example and demonstration of the technique in another publication (according to the authors) is still forthcoming. Although the model seems to have overcome many of the deficiencies of earlier models the possible economies of scale in large scale production plants were not considered. In addition, the model requires an exhaustive search to evaluate the alternatives and computational time may become prohibitively long when the model's complexity increases.

MIXED INTEGER PROGRAMMING

PROBLEM AND MODEL SPECIFICATION

To systematically analyze available pollution control alternatives for coal conversion facilities, a mixed interger integer model has been designed to provide a basis for evaluating and identifying the least cost pollution control system when costs of pollution control alternatives and environmental standards are changed. The flow diagram of Figure 1 illustrates the basic processes and flows required for structuring the mixed integer programming model. The model is designed to allow an effluent from a production unit or a treatment unit to receive partial or complete treatment. The effluents from a unit can be mixed with effluents from other units and recycled and/or discharged to the environment. Whether a stream is discharged or recycled, production quality and environmental discharge quality standards must be satisfied.

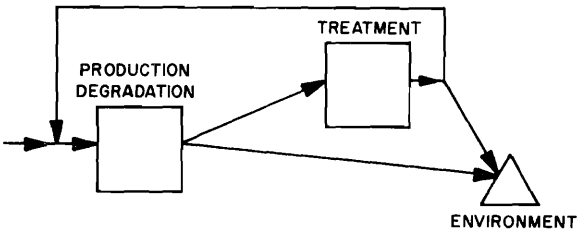

Figure 1. Flow pattern.

MODEL DESCRIPTION IN GENERAL TERMS

Objective function

The costs which appear in the model's objective function are the total costs of each treatment unit. However, some costs of the production facility such as some cooling costs, are unavoidable and are discounted in the objective function. Once-through cooling has been traditionally used as the method of choice for cooling when that alternative is acceptable. Therefore, the cooling costs identified in the objective function of the mixed integer programming model are those costs in addition to the costs that would be required for once-through cooling.

The total cost for each alternative treatment unit is the sum of capital and other input costs. The cost of using a treatment unit is often defined by a nonlinear cost function of the form:

$$y = ax^b$$

in which

- y = the total cost per unit of time
- a = a defined coefficient
- x = the flowrate
- b = a positive exponent with a value less than unity

The equation is nonlinear but can be approximated in a linear form.

When the approximate quantity of treatment is known, the nonlinear total cost equation can be accomodated in linear programming by defining an average cost for the flow range. Unless the flow range is relatively small, the average cost is only a gross approximation.

When the flow range is relatively large, a nonlinear cost curve can be approximated by the use of separable programming. In separable programming, the nonlinear total cost curve is replaced by a series of piecewise linear segments similar to that shown in Figure 2. However, each piecewise approximation requires a separate variable to be defined in the objective function and in the constraints. In using separable programming

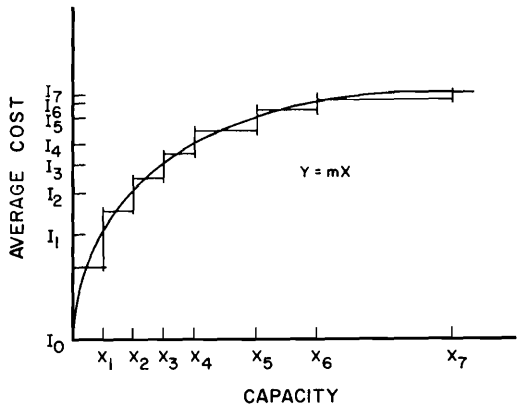

Figure 2. Stepwise linear cost approximations.

to describe a nonlinear cost function over a large flow range, the model becomes extremely complex unless restricted to a small number of treatment units.

The method of approximating nonlinear cost curves developed for this study is to define a set of linear equations that approximate a segment of a nonlinear cost curve. The linear approximation functions would have the mathematical form:

$$y = \beta + mx$$

in which

- y = the cost per unit of time
- β = the value at the y intercept when the linear approximation is plotted on an X-Y axis.
- m = the slope of the linear function and has the units of cost per flow.
- x = the flowrate

The cost equation for unit j may be hypothetically represented by the cost curves in Figure 3 to demonstrate the concept of approximating nonlinear cost curves by a set of linear functions.

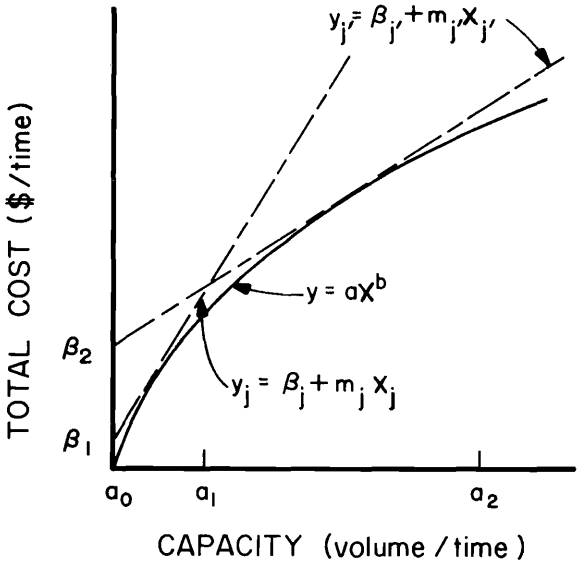

Figure 3. Nonlinear total cost function and linear approximations.

When the flowrate x is between a_0 and a_1 the linear equation $y_j = \beta_j + m_jX_j$ would apply for defining the cost of unit j. When the flowrate x is between a_1 and a_2, then the linear equation $y_j = \beta_j + m_jK_j$ would apply for defining the cost of unit j. To insure that β_j is equal to zero in the objective function when X_j is zero, and that β_j is equal to zero in the objective function when $X_{j'}$ is zero, binary integer variables are introduced in the objective function. If the binary variable I_j is associated with X_j, and the binary variable $I_{j'}$ is associated with $X_{j'}$, then the objective function would appear as:

$$\text{MIN} \ldots + \beta_j I_j + m_j X_j + \beta_{j'} I_{j'} + m_{j'} X_{j'} + \ldots$$

with the addition of the linear constraints:

$$1)\ X_j - a_0 I_j \geqslant 0$$
$$2)\ X_j - a_1 I_j \leqslant 0$$
$$3)\ X_{j'} - a_1 I_{j'} \geqslant 0$$
$$4)\ X_{j'} - a_2 I_{j'} \leqslant 0$$
$$5)\ I_j + I_{j'} \leqslant 1$$
$$6)\ I_j, I_{j'} = 0,1$$

The added constraints serve to insure that only X_j, or $X_{j'}$, can appear in the optimal solution.

Flow and quality equations

The model constraints represent the linear flow balance and linear influent quality constraints for the individual treatment and production units. The construction of the flow balance and quality constraints can be demonstrated by describing the simplified model presented in Figure 4.

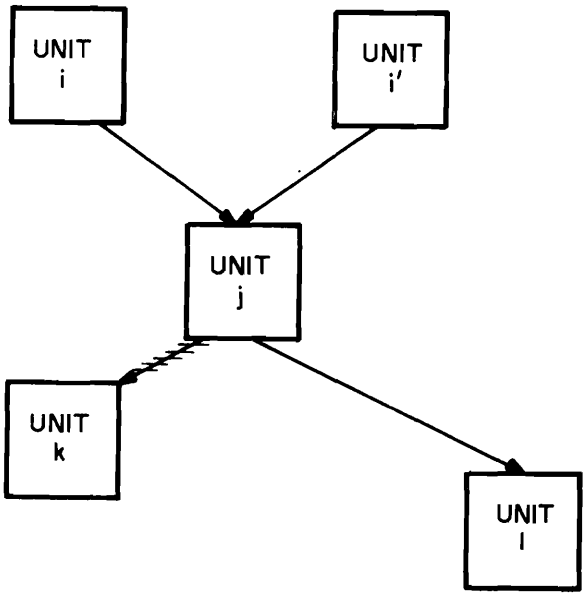

Figure 4. Generalized stream flow diagram.

When streams from units i and i' can be treated by unit j, the influent flow balance equation required for unit j can be expressed by:

$$X_j = Q_{i,j} + Q_{i',j} \ldots\ldots\ldots\ldots\ldots\ldots\ldots\ldots (1)$$

in which

X_j = flowrate through unit j
Q = influent and effluent flowrates

and:

the subscript of the X variable represents the unit destination of the stream

the i part of the subscript of the Q variables represents the origin of the streams

the j part of the subscript of the Q variables represents the destination of the streams

A treatment process usually produces both a high quality product stream and a concentrated brine stream. The brine stream vector from a unit is identified by hash marks in the stream flow diagram. The brine stream from unit j can be treated by unit k and the product stream flows to unit 1, so the effluent flow balance equation required for unit j can be expressed by:

$$Q_{jk} + Q_{jl} = X_j \quad \ldots\ldots (2)$$

By convention, the coefficients of the Q variables representing the influent streams are negative while the coefficients of the Q variables representing the effluent streams are positive in the linear flow equations. Equations 1 and 2 can, therefore, be expressed respectively as:

$$X_j - Q_{ij} - Q_{i'j} = 0 \quad \ldots\ldots (3)$$

and

$$Q_{jk} + Q_{jl} - X_j = 0 \quad \ldots\ldots (4)$$

When a stream is split at a unit, such as the effluent from unit j in Figure 4, the linear model requires a definition of the fraction of the influent stream which is converted to a product or a brine streem. With the unit j defined by the flow balance Equations 3 and 4 and the brine stream fraction of the influent is defined by Φ, then the linear equation:

$$Q_{jk} - \phi X_j = 0 \quad \ldots\ldots (5)$$

is used to explicitly define the brine stream fraction in the model. An alternate method to serve the same purpose would be to define the fraction that is the product stream as $1-\Phi$.

Quality constraints are used to define the upper concentration limits for the combined concentrations of the influent streams into a unit. When the concentration of a stream Q_i is Θ_i, the concentration of stream $Q_{i'}$ is $\Theta_{i'}$, and the upper concentration limit for unit j is Θ_j, then the equation

$$\Theta_i Q_{ij} + \Theta_{j'} Q_{ij'} - \Theta_j X_j \leqslant 0 \quad \ldots\ldots (6)$$

is used to define the upper allowable concentration of the combined streams entering unit j.

The values of the right hand side vector, other than the zero values, define production unit effluent flowrates and upper limits on the mass of a pollutant discharged from the facility.

MODEL STRUCTURE ILLUSTRATIONS

The construction of the model can be demonstrated by the use of a relatively simple example illustrated by Figure 5.

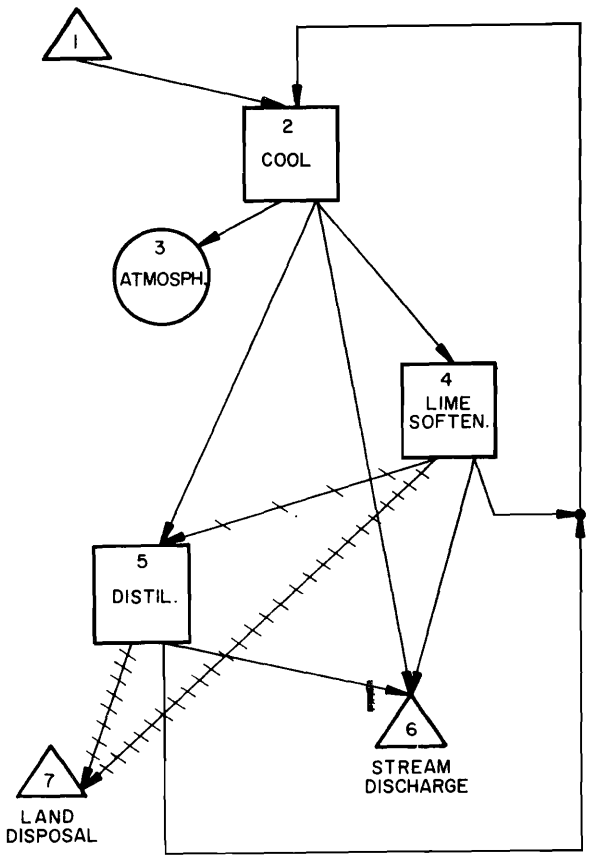

Figure 5. Simplified model flow diagram.

Flow balance equations

The flow equations for the example problem of Figure 5 are developed from the flow data for each of the processes as summarized in Table 1. The example consists of a cooling tower that loses 2.3 percent of its influent water to the atmosphere as effluent evaporation. The remainder of the cooling

Table 1. Flow data for simplified model.

	Quantity Influent	Product Fraction
STREAM		
COOL	46.6	
ATMOSPH.	0.023 X_2	
LIME SOFT		0.9
DISTILL.		0.95
STREAM DIS.		
LAND DISP.		

tower effluent can be treated with the lime softener unit, a distillation unit, and/or discharged to the stream. The alternative sources of the cooling tower influent are the stream, the lime softener product water and the distillation product water. The product effluent from the lime softener unit is defined as 90 percent of the influent water and the product effluent from the distillation unit is 95 percent of its influent water.

The concentrated or brine streams from the units are represented by arrows marked with slashes on the flow diagram. The brine effluent streams from the units are implicitly defined as the remaining fraction of the total effluent, since the product and brine effluents total 100 percent. The brine stream from the lime softener can be treated by the distillation unit and/or transferred to a land disposal sink. The brine produced from the distillation unit is transferred to the land disposal sink. For the simplified mode, Table 2 provides a summary of the required flow balance equations.

Table 2. Simplified model flow balance equations.

COOLQIN	X_2	$= 46.6$
COOLX	X_2	$= Q_{1,2}+Q_{4,2}+Q_{5,2}$
COOLQ	$Q_{2,3}+Q_{2,4}+Q_{2,5}+Q_{2,6}$	$= X_2$
EVPQ	$Q_{2,3}$	$= 0.023\ X_2$
LIMEX	X_4	$= Q_{2,4}$
LIMEQ	$Q_{4,2}+Q_{4,5}+Q_{4,6}+Q_{4,7}$	$= X_4$
LIMEPQ	$Q_{4,2}+Q_{4,6}$	$= 0.90\ X_4$
DISTILX	X_5	$= Q_{2,5}+Q_{4,5}$
DISTILQ	$Q_{5,2}+Q_{5,6}+Q_{5,7}$	$= X_5$
DISTILPQ	$Q_{5,2}+Q_{5,6}$	$= 0.95\ X_5$
LANDX	X_7	$= Q_{4,7}+Q_{5,7}$

The X variable for each unit is, in effect, a transhipment variable representing both the sum of the influent streams to the unit and the sum of the effluent streams from the unit. The only exception is when a unit is a final sink such as land disposal and for which only the influent streams are defined. The Q variables represent the influent and effluent streams of a unit. The influents to a unit are defined, by convention, on the right hand side of the flow balance equation and the effluents are defined on the left hand side of the flow balance equation. The flow balance equations are equality constraints and the variables are in units of thousand tons of water per day.

The Q variable subscripts indicate the direction of the stream flow. The first part of the subscript indicates the Q stream's origin and the second part of the subscript is the Q stream's destination. The single subscript on the X variable indicates the process unit for which the variable is defined. The constraint equations are defined as rows in the mixed integer programming model. Each row is distinguished by an abbreviation of the unit name for which the row is intended to define, then attaching a second abbreviation to distinguish each row from the other rows that define something about the unit.

A definition of the row names is provided in Table 3 for the example problem.

Table 3. Row name description.

	Row Name Description
COOLQIN	– explicit definition of influent water required for the cooling tower
COOLX	– the sources of cooling tower influent
COOLQ	– the cooling tower effluent streams
EVPQ	– explicit definition of evaporation part of cooling tower effluent
LIMEX	– sources of lime softener unit influent
LIMEQ	– lime softener unit effluent streams
LIMEPQ	– a definition of the portion of the lime softener unit influent which is the product effluent stream from that unit
DISTILX	– sources of distillation unit influent
DISTILQ	– distillation unit effluent streams
DISTILPQ	– a definition of the portion of distillation unit influent which is the product effluent stream from that unit
LANDX	– sources of land disposal unit influents

Flow quality equations

In addition to the flow balance equation, stream quality constraints are also required for the model. Table 4 is a summary of the stream quality data for the example which is incorporated into the upper concentration limits presented in Table 5.

Table 4. Simplified model stream quality data.

	Influent Quality Limit	Effluent Product Quality	Effluent Brine Quality
STREAM		1,200 ppm	
COOL	340 ppm		5,000 ppm
ATMOSPH.			
LIME SOFT	5,500 ppm	10 ppm	54,000 ppm
DISTILL.	55,000 ppm	11 ppm	
STREAM DIS.	500 ppm		
LAND DISP.			

ppm = parts per million of total dissolved solids.

Table 5. Simplified model quality constraints.

COOLUPQ	$1200\,Q_{1,2}+10Q_{4,2}+11\,Q_{5,2}$	$\leqslant 340\,X_2$
LIMEUPQ	$5000\,Q_{2,4}$	$\leqslant 5500\,X_2$
DISTLUPQ	$5000\,Q_{2,5}+54{,}000\,Q_{4,5}$	$\leqslant 55{,}000\,X_5$
STRMUPQ	$5000\,Q_{2,6}+10Q_{4,6}+11Q_{5,6}$	$\leqslant 500\,X_6$

For example, the constraint COOLUPQ defines the quality of the cooling tower influent streams. Accordingly, the constraint states that the quality of the combined influent streams must be less than or equal to 340 parts per million total dissolved solids (TDS). Likewise, the quality of the combined lime softener unit influent streams must be less than or equal to 5,000 ppm of TDS, the quality of the combined distillation unit influent streams must be less than or equal to 55,000 ppm of TDS, and the quality of the combined effluent streams that are discharged to the aqueous environment must be less than or equal to 500 ppm of TDS.

Objective function

Suppose that the total cost equation for a distillation unit can be represented as a nonlinear curve approximated by two linear equations presented in Figure 6.

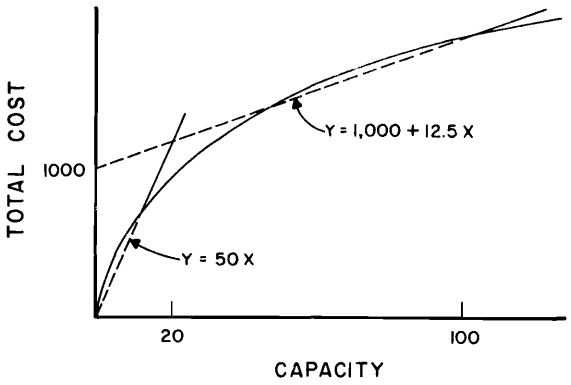

Figure 6. Total cost curve for distillation unit with two flow segments.

For purposes of the model, the distillation unit is divided into two segments, each considered a separate unit in the model. One distillation unit segment, designated as 5a, would have a flow capacity between 0 and 20 KTONs of water per day and the other segment, designated as 5b, would have a flow capacity between 20 and 100 KTONs of water per day. A flow diagram of the example with the segmented distillation units is presented in Figure 7.

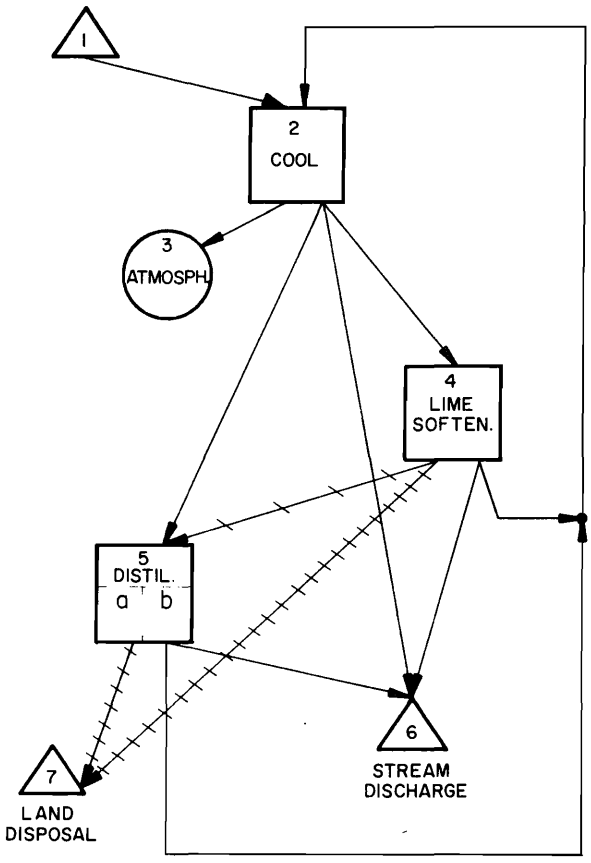

Figure 7. Simplified model with two distillation segments.

The data required for the objective function and constraints for the two distillation units are presented in Table 6. When a unit is segmented in the model the flow balance constraints required to describe the additional segments are constructed as if the segments were separate units.

Table 7 presents the objective function modified to include the extra distillation unit and the additional constraints required to insure that: 1) the binary variable Z_1 has a value of unity

Table 6. Data for two distillation segments

Linear Cost Function	Flow Limits	Binary Variable
$Y_{5a} = 50\ X_{5a}$	$0 \leqslant X_{5a} < 20$	Z_1
$Y_{5b} = 1{,}000 + 12.5\ X_{5b}$	$20 \leqslant X_{5b} < 100$	Z_2

Table 7. Objective function and exclusion constraints for a two segment distillation unit.

MINIMIZE ... + 50 X_{5a} + 1,000 Z_2 + 12.5 X_{5b} + ...

s.t	1. $X_{5a} - 20\ Z_1$	$\leqslant 0$
	2. $X_{5b} - 20\ Z_2$	$\geqslant 0$
	3. $X_{5b} - 100\ Z_2$	$\leqslant 0$
	4. $Z_1 + Z_2$	$\leqslant 1$
	5. Z_1, Z_2	$= 0,1$

only when the distillation unit influent flowrate is between 0 and 20 KTONs of water per day; 2) Z_2 has a value of unity only when the distillation unit influent flowrate is between 20 and 100 KTONs of water per day. Whenever the values of Z_1 and Z_2 are not unity, then they must be zero. With the constraints provided in Table 7, the model can identify either unit 5a or 5b, or neither of the units, in the optimal solution.

When a binary variable is equal to unity, the intercept and slope for the correct linear total cost approximation equations are calculated together. For example, if X_{5b} has a value other than zero, then Z_2 is equal to unity and the total cost equation for unit segment 5b is calculated. Otherwise X_{5b} is zero, Z_2 is constrained to a value of zero and a cost for unit segment 5b is not included in the objective function.

In addition to dividing a unit process for reasons of approximating a nonlinear total cost function, the unit is also divided because different total cost functions are appropriate for different influent stream qualities. For example, the total cost function that describes distillation unit with an influent quality of 10,000 ppm would probably be considerably less than the total cost function that describes a distillation unit with an influent quality of 54,000 ppm and producing the same product quality. Figures 8 and 9 are hypothetical total cost equations for distillation units with upper concentration limits on the influent quality of 10,000 and

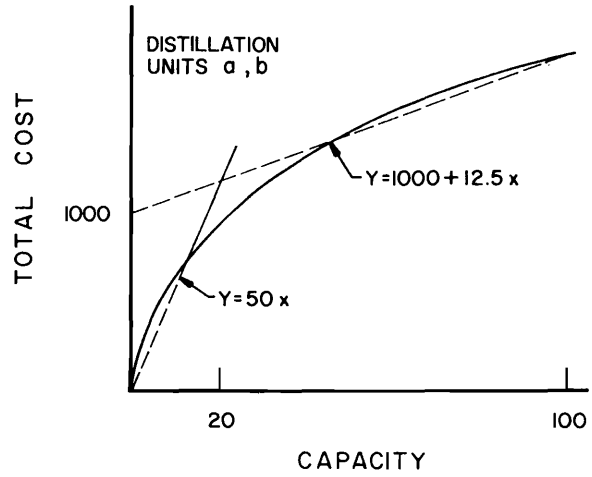

Figure 8. Total cost curve for distillation unit with upper influent quality capacity of 10,000 ppm.

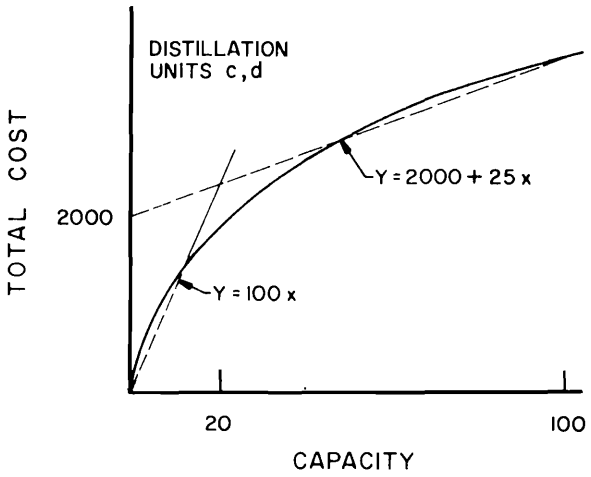

Figure 9. Total cost curve for distillation unit with upper influent quality capacity for 54,000 ppm.

54,000 ppm, respectively. By the use of linear approximations, the distillation units are divided into four segments. Each segment is treated as a separate unit in the model. Figure 10 is a presentation of the flow diagram of the simplified model when the distillation unit is segmented into four parts.

Table 8 is a summary of the data associated with each distillation unit segment that is used in the objective function and concentration limit constraints presented in Table 9.

The constraints in Table 9 insure that no more than one of the unit segments will be identified in

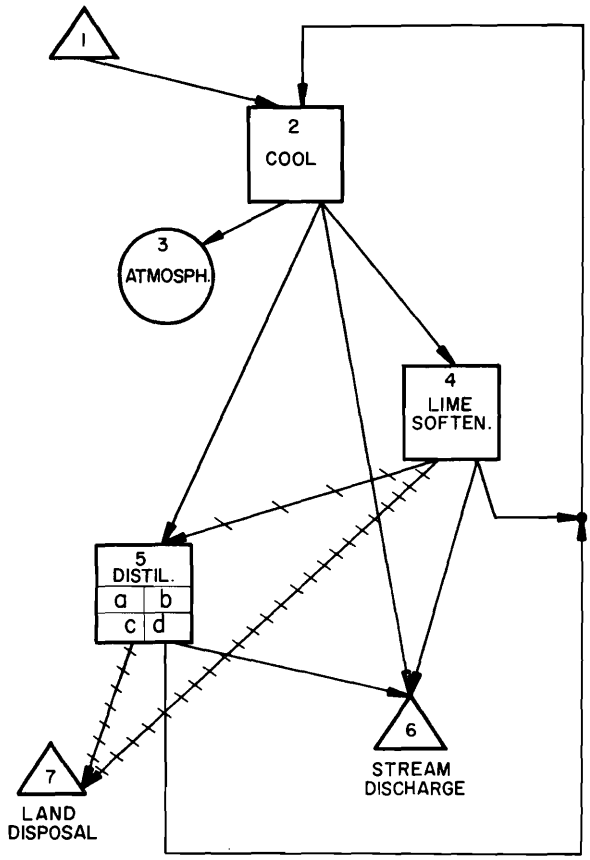

Figure 10. Simplified model with four distillation segments.

the optimal solution and that the binary variables associated with each segment are calculated correctly in the objective function with their paired X variable.

Table 8. Data for a four segment distillation unit.

Linear Cost Functions	Binary Variable	Upper Conc.
$Y_{5a} = 50\ X_{5a}$	Z_1	10,000
$Y_{5b} = 1{,}000 + 12.5\ X_{5b}$	Z_2	10,000
$Y_{5c} = 100\ X_{5c}$	Z_3	54,000
$Y_{5d} = 2{,}000 + 25.\ X_{5d}$	Z_4	54,000

Table 9. Objective function, upper limit quality constraints, and exclusion constraints for a four segment distillation unit.

MINIMIZE ... $+ 50\ X_{5a} + 1{,}000\ Z_2 + 12.5\ X_{5b}$

$+ 100\ X_{5c} + 2{,}000\ Z_4 + 25.\ X_{5d} + \ldots$

DSTLaUP	$5{,}000\ Q_{2,5a} + 54{,}000\ Q_{4,5a}$	$\leqslant 10{,}000\ X_{5a}$
DSTLbUP	$5{,}000\ Q_{2,5b} + 54{,}000\ Q_{4,5b}$	$\leqslant 10{,}000\ X_{5b}$
DSTLcUP	$5{,}000\ Q_{2,5c} + 54{,}000\ Q_{4,5c}$	$\leqslant 54{,}000\ X_{5c}$
DSTLdUP	$5{,}000\ Q_{2,5d} + 54{,}000\ Q_{4,5d}$	$\leqslant 54{,}000\ X_{5d}$
DSTEX	$Z_1 + Z_2 + Z_3 + Z_4$	$\leqslant 1$
DST0-1	Z_1, Z_2, Z_3, Z_4	$= 0,1$

EXAMPLE APPLICATION: PROCESS DESCRIPTION AND DATA DEVELOPMENT

The mixed integer program was developed to identify the pollution control and recycle opportunities and their associated costs for a 750 megawatt coal fired steam electric power generating facility, located in a setting resembling the environment in southern Utah. The production effluent streams that would be generated by the facility and that must be controlled are the cooling tower blowdown streams, sanitary and laboratory waste streams, boiler tube cleaning waste streams, pre-heater cleaning waste streams, coal pile runoff waste streams, and stack gas streams. The waste streams are controlled by federal and/or state legislation. Alternative treatment units have been evaluated and incorporated in the model for controlling water, air, and solid waste streams generated by the production facility.

Figure 11 provides a description of the production facility and indicates the locations in the facility where environmental controls are required. A system analysis of the production facility, and points of environmental control, includes the water, air, and solid streams.

MODEL DESIGN

Variables

The air, water, and solids streams from each production and treatment unit are distinguished from each other by the variable designations. Variables that represent liquid streams are identified in the model by the letter Q when the liquid stream is a flow from one unit to another and the letter X when the liquid stream is the sum of influent streams to a unit. Thus:

$$X_j = \sum_{i=1}^{n} Q_{ij}$$

in which

i = the origin unit of streams

j = the destination unit of streams

n = the total number of streams to unit j

The variables that represent gas streams in the model are identified by the letter A when the gas stream is a flow from one unit to another and the letter Q when the gas stream is the sum of the influent streams to a unit. Stated in equation form:

$$O_j = \sum_{i=1}^{n} A_{ij}$$

The variables that represent solid streams in the model are identified by the letter T. Accordingly:

$$T_i = \sum_{i=1}^{n} T_{ij}$$

The sulfur and particulates in the gas streams are distinguished from other solids in some parts of the model for convenience. The mass balance for the sulfur stream, represented by the letter S in the model is:

$$S_i = \sum_{i=1}^{n} S_{ij}$$

and the particulate stream represented by the letter P is:

$$P_i = \sum_{i=1}^{n} P_{ij}$$

Other variables that appear in the model are SL which is a definition of the energy in solid (coal) form, XT which is a definition of the combined solid and liquid streams in the disposal units, H, the height of the stack measured in feet, and XX, the sum of the water consumed that could otherwise be avoided if once-through cooling were used.

Each production and treatment unit is assigned a unit number. A variable is subscripted consistently and uniquely with three characters. Numerically, i and j subscripts are represented by up to three characters each. The first two characters of the subscript, the unit number, identify the unit which the variable describes, and the third character distinguishes segments of the unit. By the convention described, the i subscript and j subscript each require three characters.

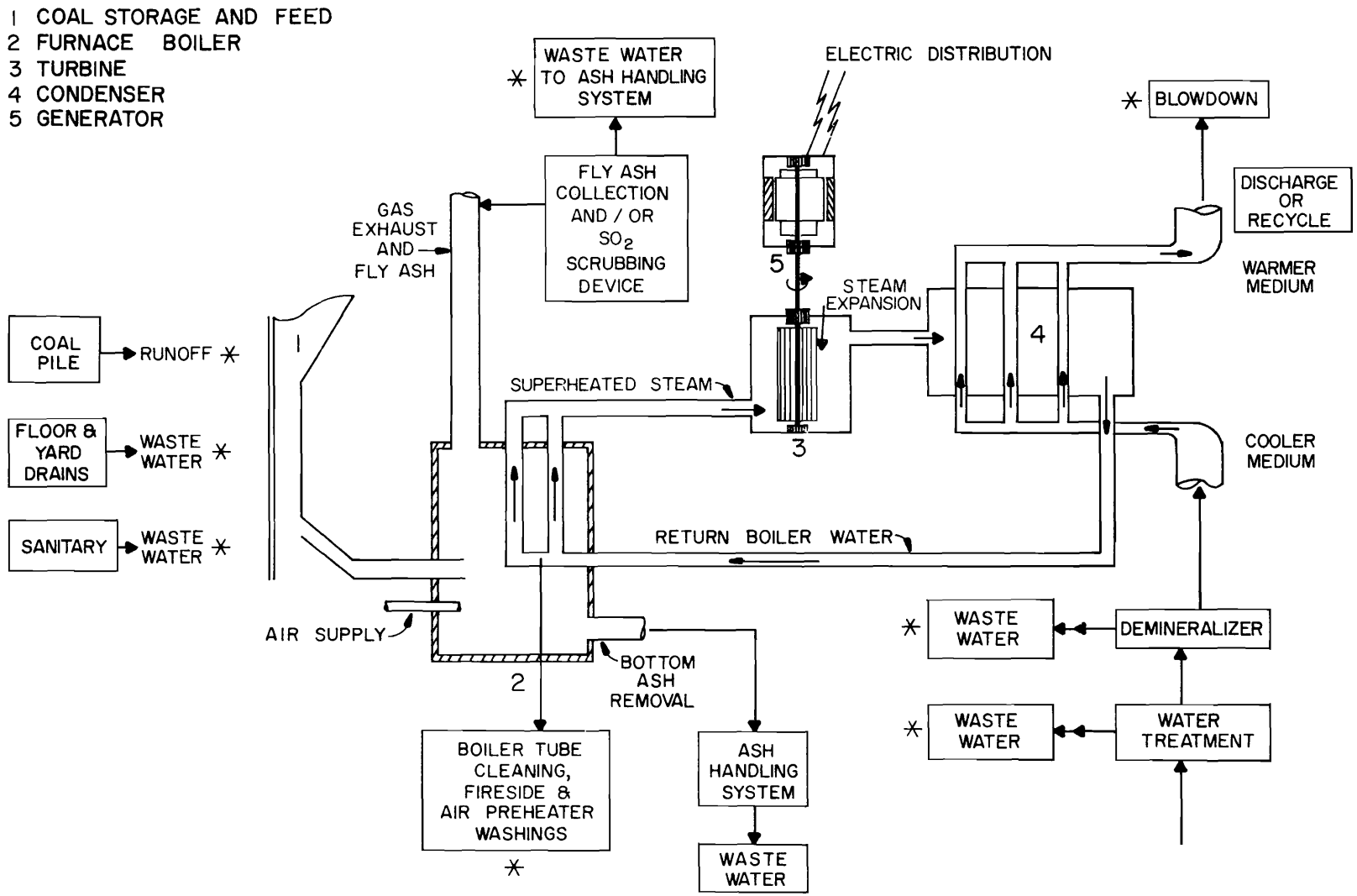

Figure 11. Coal fired powerplant diagram.

Binary variables are assigned to the units that have more than one segment and/or to those units whose cost data require a definition of the intercept in the objective function. The binary variables are identified in the applied model by the letters Y or Z and are subscripted by one or two numbers.

Rows

At least one row, and often several rows, are needed to describe each production and treatment unit in the model. Each unit is abbreviated by three characters (usually letters), and a fourth character (always a letter) is used with the three character abbreviation distinguishing one unit segment from another. The fourth character of the row name is always the same as the third character of the variable subscript for the same unit. The fifth (and sometimes sixth) letter used in combination in row names is used to distinguish each row name of the same unit. For example, the row name CNDAX is used to describe the influent to the condenser unit and the row name CNDAQ is used to describe the effluent from the condenser unit.

Table 10 lists the production and treatment units that are defined in the model and includes the abbreviated unit name, the segment unit letter, the two characters associated with the unit, and the integer binary variables associated with the unit.

Costs

The total cost of each unit was calculated on the basis of defining the fractions of the total cost contributed by the capital cost and other input costs such as operation and maintenance (O&M) cost, water costs, and energy costs that are incurred on the basis of the capacity of the unit. The costs are calculated based on the quantity of influent treated in contrast to calculating the cost based on the product effluent from the technology. The flowrate of all variables are in terms of thousand tons per day and is referred to as KTONs/day.

The cost data were developed from data in the literature. When the data appeared in the literature with reference to the year in which the data were published, the month of January was assumed as the reference point in that year. All capital and operation and maintenance (O&M) costs of the technologies were updated to April 1977 costs using the "Construction Cost Index History 1913-1976" from Engineering News Record, March 24, 1977, p. 67. The updated costs are considered the base costs with the assumption that energy costs are $20 per megawatt hour and water costs are $20 per acre foot. The capital recovery factor was used to reduce the capital cost to an annual cost. The life of equipment was assumed to be 30 years and the cost of capital assumed to be 10 percent compounded annually. Finally, a total annual cost was reduced to a total daily cost by dividing the total annual cost by 365.

DATA DEVELOPMENT

The units listed in Table 10 are compatible with the streams produced by a coal fired power generating facility and are also found in coal conversion facilities. A review of the literature related to the energy conversion facilities and the alternative waste processes provided the data required for model application to the case study situation.

Production facility—a 750 megawatt coal fired steam electric power generating plant

Coal is used in steam electric power generation to raise the temperature of incoming boiler water and produce steam. The steam passes from the boiler, and condenses after turning turbines to do work and generate electricity.

> Where the water-steam cycle (the Rankine cycle) is used to convert work to heat, the maximum theoretical efficiency that can be obtained is limited by the temperatures at which the heat can be absorbed by the steam and discarded to the environment. The upper temperature is limited by the temperature of the fuel bed and the structural strength and other aspects of the boiler. The lower temperature is ideally the ambient temperature of the environment, although for practical purposes, the reject temperature must be set by design significantly above the highest anticipated ambient temperature. Within these temperatures, it can be shown that the conversion of heat into other forms of energy is limited to efficiencies of about 40 percent regardless of any improvements to the present day machines employed. For any steam electric power generation scheme, therefore, a minimum of about 60 percent of the energy contained in the fuel must be rejected to the cooling environment as waste heat. (U.S. Environmental Protection Agency (EPA), 1974, p. 24-25.)

In actual practice, power plants only approach the performance of the Rankine cycle. The steam produced in the boiler must be superheated (heat above the saturation equilibrium temperature) to prevent excess condensation in the turbines. After being released into the condenser, the steam cools to a liquid phase. Unfortunately, condensers cannot be designed to condense the steam at ideal efficiency and the condensate must be preheated before it is returned to the boiler. Divergences from optimum theoretical conditions cause conversion efficiencies to be lower than the Rankine cycle predictions.

Table 10. Model units and abbreviations.

Unit	Unit Abbreviation	Unit Segment	Unit Number	Unit Binary Variable (Respectively)
BOILER	BOL	A	OB	
CONDENSER	CND	A	OC	
SANITARY WASTES	SAN	A	OD	
CLEANING WASTES	CLN	A	OH	
WATER SOURCE	WAT	A	01	
WATER SINK	STM	A	02	
ATMOSPHERIC SINK	SKY	A	03	
EVAPORATION POND	EVP	A	04	
LAND DISPOSAL	LND	A	05	
MECHANICAL DRAFT WET 5 CYCLE COOLING	CL5	A	11	Z_2
20 CYCLE COOLING	CL2	A	14	Z_5
50 CYCLE COOLING	CL6	A	15	Z_6
100 CYCLE COOLING	CL1	A	16	Z_7
DRY COOLING	CLD	A	17	Z_8
SETTLING POND	STL	A	23	
LIME SOFTENING	FLC	A	24	Y_{28}
THICKENER I	TK1	A	25	
TRICKLING FILTER	TRL	A	26	Y_{29}
ACTIVATED SLUDGE	SLG	A	34	Y_{32}
AIR FLOTATION	OIL	A	35	
THICKENER II	TK2	A	38	
ION EXCHANGE	ION	A,B	40	Y_{10}, Y_{11}
EVAPORATOR-CRYSTALIZER	DST	A	41	
MULTI-STAGE FLASH DISTILLATOR	MSF	A,K,U	42	Z_{18}, Z_{20}, Z_{22}
ELECTRO-DIALYSIS	DLS	A,F,P,U	43	$Z_{23}, Z_{24}, Z_{26}, Z_{27}$
REVERSE OSMOSIS	OSM	A,B,K,L	44	$Z_{12}, Z_{13}, Z_{16}, Z_{17}$
LIMESTONE SCRUBBER	SCB	A	51	Y_{34}
ELECTROSTATIC PRECIPITATOR	EPR	A	52	Y_{33}
GAS STACK	STK	A	53	
PARTICULATE SCRUBBER	PRT	A	54	Y_{35}
COMBINATION ELECTROST-PPTOR, LIMESTONE SCRUBBER	CMB	A	55	Y_{36}
SLURRY DISPOSAL	SLR	A	60	
TRUCK DISPOSAL	TRK	A	61	

The individual coal fired steam electric power plants in the power plant networks are categorized into discrete segments for the purpose of establishing effluent limitation guidelines. (EPA, 1974). The factors which are used to categorize coal burning powerplants are: 1) processes employed, 2) raw materials utilized, 3) site characteristics, and 4) mode of operation.

Process employed. The steam electric power generation process can be described as a five unit system. The units are: 1) storage and handling of fuel-related materials before and after conversion; 2) production of high temperature, high pressure steam by burning the fuel and converting water into steam from the heat of combustion; 3) conversion of heat to work by passing steam across

turbines to move the turbines; 4) mechanical transfer of energy from the rotating turbines to the electric generators; 50 transfer of heat from steam to water in the condensers and returning the water to the boiler. Figure 11 is a schematic depection of the five unit coal fired steam electric power generating plant.

1) Fuels

Delivered coal must be stored until the coal is ready for use and spent material from burning the fuel is stored on site until the spent material can be removed from the plant site. Usually, the stored coal will amount to the quantity required for a 90 day operation. The fuel, after being transported to a furnace is burned by combusting oxygen with the fuel to produce heat, gaseous and solid (ash) residuals. Some of the ash, called fly ash, is carried along with the hot gasses while the remainder of the ash, called bottom ash, settles to the bottom of the furnace in the combustion zone. A sub-bituminous coal with a 7.5 percent ash content will form a fly ash and bottom ash fractions after combustion. A normal value for the bottom ash fraction is 30 percent of the total ash and the value of the fraction depends on the fuel type and boiler design. The bottom ash can be tapped from the furnace or removed hydraulically to a settling pond. Hydraulic sluicing of the ash requires a flowrate of between 11 and 43 liters per MWH (U.S. Enviornmental Protection Agency, 1976, p. 49). Fly ash is often removed from the gaseous combustion products in most modern power plants by means of an electrostatic precipitator. Scrubbers may also be required on powerplants if the sulfur content of the fuel is more than minimal. When fly ash has a commercial value, it is usually handled by air conveyor, and otherwise sluiced to a settling basin. Final ash disposal is usually by land burial or covering.

2) High pressure steam production

The high quality boiler water influent enters the boiler from the condenser and flows through the vertical boiler tubes located in the furnace. The heat of combustion is transferred from the hot furnace gases through the wall of the boiler tubes to the boiler water and converts the liquid water to gaseous steam. Maximum conversion efficiency can be obtained by superheating the steam and releasing the steam to the turbine unit at high pressure. Modern turbines operate at steam pressures of 3500 psi and temperatures of 1050°F.

3) Steam expansion

The steam passes through the turbine, forcing the resisting turbine blades to rotate the turbine. The steam expands while rotating the turbine and energy is extracted from the superheated steam. The turbine is highly sensitive to the pressure at which the steam is released (backpressure) and turbine design is based on one backpressure level. When ambient conditions change throughout the year, the heat sink conditions change and cause the optimal conversion conditions to deviate from the optimum.

4) Generation of Electricity

Electricity is generated when the electric generator, which is usually connected directly to the turbine, is rotated when the steam does work on the turbine. Energy transfer at this energy transfer stage of the conversion process is practically 100 percent efficient.

5) Steam Condensation

A condenser is a steam electric power plant is used to maintain a low turbine exhaust pressure. The steam leaves the turbine at a temperature corresponding to vacuum conditions, and provides a high cycle efficiency for recovering the condensate and for recycling to the high quality boiler water from the condenser. Either surface or direct contact condensers are used in power plants. Nearly all power plants use surface condensers of the shell and tube heat exchanger type. The condenser consists of a shell with a chamber at each end, connected by banks of tubes (EPA, 1974, p. 60). The cooling water passes through the tubes of the condenser and increases in temperatures as the steam is passed into the shell and condenses by cooling on the outer surface of the tubes. The heat of the steam, therefore, is transferred to the condenser cooling water.

The condenser cooling water is transferred from the condenser to a heat sink. When the condenser water is cooled in a tower and recirculated to the condenser, the system is considered closed. An alternative to the closed system is the once-through, or open system, where the condenser cooling water passes through the condenser and is discharged. In areas where water is limited, cooling devices such as cooling towers or cooling ponds are used and the cooling water is recirculated to the condenser. For reasons of economy, closed systems typically operate at higher temperature differentials across the

condenser than once-through systems, balancing the somewhat reduced efficiency of the turbine against the lower quantity of cooling water required. The spent steam could be exhausted directly to the atmosphere, to avoid the condenser and cooling water requirement. However, the cost of avoiding the condenser and cooling water requirements would include poor cycle efficiency and large quantities of high quality makeup condenser water.

Nearly all cooling devices currently being used obtain their cooling effect from evaporation (wet cooling). Consequently, the dissolved solids concentration of closed cooling systems tends to increase to a level where precipitation and scaling occurs unless some blowdown water is discharged from the cooling water recirculating system. The evaporation and blowdown waters are replenished with a high quality makeup water. Without the blowdown and makeup water scheme, the concentration of the recirculating cooling water would reach a point where scaling on the condenser wall would interfere with heat transfer efficiencies.

Coal-raw material used. The characteristics of coal are diverse and are dependent on many variables. Coal is normally classified in three categories according to the age of the coal, i.e. anthracites, bituminous, or lignites.

Vegetation that once lived in swamps has been transformed into coal through the geologic ages. In geologic terms the youngest coals are the lignites, which often contain remnants of the plants from which they were formed and have extremely high water content and very low heating value. Lignite coal contains less than 50 percent fixed carbon and average 6,700 Btu/lb. Deposits of lignite coal in the U.S. are abundant.

From the more remote past, sub-bituminous and bituminous coals were formed under heat and pressure. The bituminous coal is the older coal type. The water content decreases and the heating value increases over time with bituminous coal containing 50 to 92 percent fixed carbon and a fuel value of 8,300 to 14,000 Btu/lb. Much of the bituminous coal has a low sulfur content.

The oldest coals are called anthracite and have a very high heating value with a low water content. Anthracite coal has traditionally been used for home heating, but supplies of anthracite are limited and expensive to mine (Hawkins, 1973 and EPA, 1974).

Site characteristics. For cooling purposes, it has been advantageous to locate the plant site near an adequate supply of water. Traditionally plants have also been located near population centers so that power transmission costs could be minimized. However, the trend in recent years has been to locate powerplants closer to the mine site and incur the transmission cost to alleviate the environmental problems associated with locating in high population centers. The selection of the plant site is dependent on cooling water supply, fuel supply, fuel delivery, handling facilities, proximity of load centers and environmental quality considerations.

Mode of operation. The Federal Power Commission defines the modes of operation in respect to power plants as follows.

> Baseline units are designed to run more or less continuously near full capacity, except for periodic maintenance shutdowns. Peaking units are designed to supply electricity principally during times of maximum system demand and characteristically run only a few hours a day. Units used for intermediate service between the extremes of base-load and peaking service must be able to respond readily to swings in systems demand, or cycling and are called cycling units. (EPA, 1974, p. 88.)

Study case—Intermountain Power Project located in Southern Utah

The Intermountain Power Project, a 3000 MW coal fired steam electric power generating facility proposed for construction two miles west of Factory Butte in southern Utah, is an example of a powerplant located in an arid region. Studies of the proposed project have provided some important data that are incorporated into the mixed integer programming model. The powerplant, consisting of four 750 MW power generating units, will be supplied with a bituminous coal with the characteristics listed in Table 11.

Table 11. Coal characteristics.

Heating Value	8,930-12,970 Btu/lb, wet
Sulfur Content	0.3-1.0%
Ash Content	4.4-12.5%

The Intermountain Power Project feasibility report (1976a) has provided useful data listed in Table 12. That data, where indicated were supplemented data from the EPA guidelines report (EPA, 1974).

The water quality, assuming 0.4 of the water originates from underground sources and 0.6 comes from the Fremont River, is estimated to contain 1483 ppm of total dissolved solids. An upper supply limit of 50,000 acre feet per year is

Table 12. Power plant data.

Design	
Boiler Air	- 1.7 X 10^6 standard ft^3/min - 91.722 KTONS/day (density of air at standard conditions in 1.2 grams/l)
Stack Height	- 750 ft.
Operating	
Coal Requirements	- 6,850 tons/day
Ash Produced	- 856 tons/day @ 12.5% ash content
Bottom Ash	- 256.8 tons/day (assumed at 30%)
Fly Ash	- 599.2 tons/day (assumed at 70%)
Ash Haulage to Disposal Site	- 57 miles
Sulfur Content	- 1.0%
NO_x Emissions	- Controlled by combustion temperature adjustment
Sanitary Waste	- 8,280 gallons/day with 138 employees US-1, p. 110
Boiler Cleaning Waste	- (EPA, 1974, p. 138-140)
Volume/Cleaning	- 151 X 10^3 gal
Cleaning Frequency	- 12/year
Air Pre-heating Cleaning Waste	- (From EPA, 1974, p. 141)
Volume/Cleaning	- 354 X 10^3 gal
Cleaning Frequency	- 12/year
Boiler Fireside Cleaning Waste	- (From EPA, 1974, p. 141)
Volume/Cleaning	- 79 X 10^3 gal
Cleaning Frequency	- 8/year
Coal Pile Runoff	- Negligible
Combined Average Total Dissolved Solids Concentration	3,885 ppm

Table 13. Water quality discharge standards.

	30 Day Average
Low Volume Waste	
TSS	30 mg/l
Oil and Grease	15 mg/l
Bottom Ash Sluice	
TSS	1.5 mg/l
Oil and Grease	0.75 mg/l
Fly Ash Sluice	
TSS	None
Oil and Grease	None
Metal Cleaning Waste	
TSS	30 mg/l
Oil and Grease	15 mg/l
Total Iron	1.0 mg/l
Total Copper	1.0 mg/l
Boiler Blowdown	
TSS	30 mg/l
Oil and Grease	15 mg/l
Total Iron	1.0 mg/l
Total Copper	1.0 mg/l
Cooling Tower Blowdown	
Free Available Chlorine	0.2 mg/l
Zinc	0
Chromium	0
Phosphorus	0
Other Corrosion Inhibitors	0

All discharging streams must be in the pH range of 6.0-9.0.

assumed. The ash can be disposed of by truck hauling or by slurry pumping to the mine site with an average transfer distance of 57 miles.

The concentration of nitrogen oxides formed during coal combustion can be reduced by controlling the temperature at which combustion occurs. No data were found in the literature to indicate the costs that would be incurred by combustion temperature adjustment for nitrogen oxide control.

Environmental standards

Water quality discharge standards. On October 8, 1974, the EPA presented the Effluent Guidelines and Standards, summarized in Table 13, for chemical discharges from new coal fired steam electric generating facilities (Federal Register, Vol. 39; no. 196, part III, Oct. 8, 1974).

Air quality emission standards. In 1971, the national ambient air standards were promulgated, and the primary and secondary standards were adopted. The primary standards were established to protect public health while the secondary standards were established to protect aesthetic values that contribute to the enjoyment of life. On October 8, 1974, the EPA published the air emission guidelines (Table 14) in which new coal-fired steam electric power generating plants were constrained to operate.

On December 5, 1974, the EPA published its Significant Deterioration of Air Quality Regulations in the Federal Register (Vol. 39). In these regulations, the EPA defined the maximum concentrations of SO_2, NO_2 and particulate matter which would be allowable for specific lengths of

Table 14. Federal air quality emission standards.

	lb/10^6 Btu of Coal (in.)	Emission at lb/day of 750 MW Plant @ 40% Efficiency	KTON DAY
Particulate	0.1	15,369	0.00768
SO_2	1.2	184,426	0.0922
NO_x	0.7	107,582	0.0538

time. Three classes of areas were designated. Class I and Class II were defined by limiting the total suspended particulate and/or sulfur concentrations to the ambient air quality existing on 1 January 1975. In areas classified as Class I practically any change in air quality would be significant. In Class II areas, well-controlled growth would not cause significant air quality deterioration. In Class III areas, ambient air quality deterioration would be allowed.

By defining these classes of areas, criteria were set allowing for emissions limits in the ambient air at different locations. In effect, the criteria would set a maximum allowable development that could be estimated from the emissions expected from additional development. To hold to these ambient air quality standards, a new coal fired plant may be required to perform at a higher level of air emission control than the point source standards require.

Thermal pollution control—cooling systems

Traditionally, steam electric power plants were located close to large water supplies. The large water supply was required primarily for condenser cooling in a once-through process; e.g. water was taken from the body of water, passed through the condenser to cool the steam, then the cooling water was returned to its source.

Many coal fields are located in areas where the water supply is insufficient for once-through cooling, and pumping large quantities of water for long distances is uneconomical. Other water supplies may not be large enough to accept the heat rejected from the large conversion plants without harm to the biota in the stream or lake. Even when the water source is large enough to accept the discharge heat, current federal and state standards prohibit heat discharges to lakes and streams. Hence, once-through cooling is not an available alternative to many modern energy conversion facilities. Condenser cooling alternatives are available but are not as efficient for energy conversion as once-through cooling. When other cooling alternatives are used, the steam must expand at higher exhaust pressures and cannot do as much work as it could expanding at lower pressures. Two alternatives to once-through cooling are 1) dry cooling towers - natural and mechanical draft and 2) wet cooling towers - natural and mechanical draft.

The efficiency of a water cooling system is based on the system's ability to transfer heat from the circulating cooling water to the environment. Cooling tower and pond performance therefore, vary with changeable weather conditions which have immediate effects on the plant performance.

Once-through cooling. A once-through cooling system requires a water supply pumped from a water source and through the shell of the condenser where its heat content increases. The cooling water is then returned to a heat sink. The return location is situated such that the warmer water will not mix and interfere with the conditions of the intake cooling water.

Jimeson and Adkins (1971) described the water requirements for a once-through cooling system of a 1,000 MW coal fired steam generating plant operating at a 15°F temperature rise across the condenser. On the basis of the Jimeson-Adkins discussion, it can be determined that the condenser cooling water required for a 750 MW power plant would require 28×10^5 tons of water/day with a consumptive use of 24×10^3 tons of water/day under the same operating conditions. A power plant using once-through cooling can operate at a turbine back pressure of 1.5 inches Hg and an operating efficiency of 35.8 percent (Jedlicka, 1973).

If a pumping head of 5 feet were the only energy requirements to operate the cooling system, the energy requirement (assuming 85 percent pumping efficiency) can be calculated by:

$$\text{H.P.} = \frac{Q\delta h}{550}$$

$$= \frac{(1050)(62.4)(5)}{550(0.85)}$$

$$= 700$$

in which

H.P. = energy defined in horsepower
Q = flowrate in ft^3/s
δ = flowrate in $lb./ft^3$
h = height of the pumping head in ft.
e = efficiency of pump

The conversion from horsepower to megawatt-hours/day is

$$700 \text{ HP} \times \frac{7.457 \times 10^2 \text{ Watts}}{\text{HP}} \times \frac{24 \text{ Hour}}{\text{Day}}$$

$$= 12.528 \text{ MWH/day}$$

On the basis of $100 per horse power, the capital cost of the once-through cooling system would be $70,000.

Dry tower cooling. In dry cooling towers, water is circulated within cooling coils. Air passes over the surface of the coils and heat is transferred from the water through the coil surface to the air. Because the cooling water is contained, evaporation losses are eliminated. There are essentially two types of air cooled condenser systems, indirect and direct.

The principal units of the indirect (Heller system) dry type cooling tower are 1) direct contact steam condenser; 2) circulating water pumps; 3) water recovery turbine (optional); 4) cooling coils; 5) a means for moving air across the coils (natural or mechanical draft) (Rossie, 1971a). The cooled circulating water from the cooling coils is sprayed and mixed with the steam from the turbine in the condenser. Both the circulating water from the cooling tower and the condensed steam water fall to the bottom of the condenser and are removed by a circulating pump. Most of the water is returned to the cooling coils in the tower while an amount equal to the exhaust steam from the turbine is returned to the boiler as feed water. The cooling tower water, therefore, has the same quality as the boiler water.

The direct air cooled condensing system requires larger volumes of exhaust steam than the indirect system and its use is restricted to the 200 or 300 MW plant size (Rossie et al., 1971, p. 2). The principal units of the direct air-cooled condensing system are: 1) exhaust steam trunk, 2) cooling coils, 3) motor driven fans, and 4) condensate pumps. The turbine exhaust steam of the direct system is transferred through the exhaust trunk to the air-cooled coils where the steam is condensed in the coils and returned to the boiler.

The initial temperature difference (ITD) and the terminal temperature difference are used for dry tower design purposes. The ITD is the difference in temperature between the steam saturation temperature and the dry bulb temperature. The steam saturation temperature is the sum of the cold water temperature, the condenser temperature rise, and the terminal temperature difference. Figure 12 describes the relationship between the turbine backpressure and steam condensing temperature.

The terminal temperature difference (TTD) is the difference between the steam saturation temperature and the temperature of the hot water leaving the condenser. Under normal operations, the TTD varies between 5 to 10°F. The dry bulb temperature used for design methods is usually the dry bulb temperature not exceeded more than 5 percent of the time in the four warmest consecutive months at the design site.

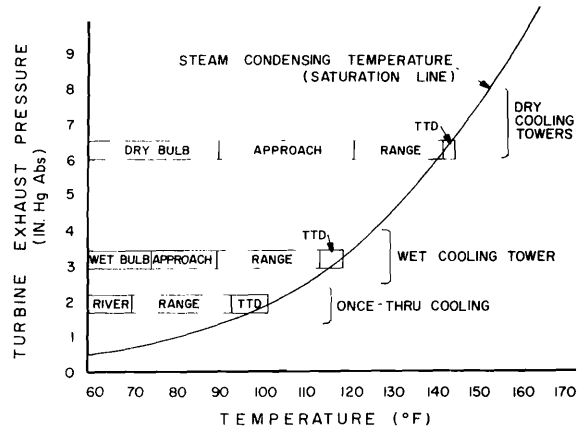

Figure 12. Cooling system temperature-exhaust pressure relationships.

Economic studies...indicate that the TTD of economically optimized dry-towers will be from 55° to 60°F...there are a number of possible savings available to a utility with dry-type cooling systems which would tend to reduce or possibly offset the increased production costs from a dry-type cooling system:

1. Possible fuel cost savings as a result of the greater flexibility of plant location.
2. Possible transmission cost savings as a result of greater flexibility at plant location.
3. Possible savings in cooling water make-up when compared to an evaporative-type cooling tower plant. For a cooling water make-up cost of $100/acre ft. (approximately 31 cents/1,000 gal.) the water savings for the dry tower installation would approximate 0.2 mil/k.w. hr.

The use of dry-type cooling systems with steam electric generating plants will eliminate the need for a large supply of water as a basic site requirement, and will result in greater freedom of plant setting than has been possible.

There are large deposits of coal and lignite in the U.S. which are not yet fully developed, notably in Arizona, Montana, North Dakota, Utah, and Wyoming, which lack sufficient water supplies for the makeup requirements of evaporative cooling means. Except for the use of dry-type cooling systems, the alternatives available for development of these coal and lignite supplies for large generating plants are to bring water to the mine mouth plant sites, or to transport the fuel to a plant site where water is available. The use of dry-type cooling systems with mine mouth generating plants in those areas opens up new possibilities for use of the important fuel reserves (Rossie, 1971a).

The disadvantages of dry tower systems is the large capital expense and the necessity for the plant to operate at high backpressure. Table 15 is a summary of the nomographs used by Jedlicka (1973) to estimate the cost of using a mechanical draft dry tower.

Table 15. Mechanical draft dry tower.

Net Generating Capacity (MW)		750
Type of Power Plant		Fossil
Plant Heat Rate (Btu/kw-hr)		9137
Dry Bulb Temperature (°F)		95
	Source Page	Value
Heat Rejection Rate (10^9 Btu/hr)	N-23	3.9
Turbine Back Pressure (inches Hg)	N-23	6.5
Saturation Temperature (°F)	N-24	144
Initial Temperature Difference (°F)	N-24	47
Capital Cot ($\$10^6$)	N-25(B)	18.5
Auxiliary Power Requirements (MW) (Fan and Pump Power)	N-26(B)	20.5
Plant Efficiency (%)	N-31	33.8
Additional Heat Capacity (MW)	N-29	3.9

Efficiency Loss Over Once-Through Cooling
= 35.8% - 33.8%
= 2.0%
= 360 MWH/day

Wet tower cooling. The circulating water in a wet tower system, after having condensed the steam while passing through the shell of the condenser and acquired the heat from the condensing steam, enters the top of the cooling tower. As the water falls to the bottom, the heat is transferred from the water to the air passing through the tower and eventually dissipated to the atmosphere.

In wet cooling towers, the water either forms a thin film or breaks into small droplets, resulting in a large water surface area and the promotion of heat transfer. During the heat transfer, water is cooled by evaporation, causing some water loss in the cooling process. A small amount of water is also lost when small droplets are carried by the drift of the air from the tower. The air can be circulated through the tower naturally or mechanically with fans by force or induction.

The cooling tower water eventually reaches the bottom of the tower where it is collected and recirculated to the shell of the condenser. (Woodson, 1971). The circulating cooling water contains some dissolved solids which become concentrated as water is lost through evaporation and drift. If a portion of the circulating water is not removed continuously and replenished with a higher quality water, the salts will reach a saturation concentration and precipitate from solution. The water removed from the cooling water circulating system is called blowdown water and the replenish water is called makeup water. Some of the salts in the blowdown are characterized by reverse solubility; e.g., the solubility of the salts decreases when the temperature of the water rises. The reverse solubility salt tends to precipitate when the temperature of the water, in which the salt is dissolved, increases. Unless the salt concentration is reduced before it reaches the saturation point, precipitation and scaling occurs when the saturated solution is heated in the condenser. The scaling effect reduces heat transfer across the condenser walls and hence, energy conversion efficiency is reduced.

The blowdown (B) required to maintain the circulating water quality below its saturation point is a function of the available makeup water quality. The relationship among blowdown, evaporation (Ev) and drift (D) is:

$$C = (B + Ev + D)/(B + D)$$

in which C is the number of concentration cycles; a dimensionless number which expresses the number of times the concentration of any constituent in the make-up water is allowed to increase from its original value. The parameters B, Ev, and D are expressed in consistent units (e.g. percent of circulating water flow rate or actual flow rate) (EPA, 1974, p. 115).

The saturation level of a solution at a specific temperature is a known constant, and a high quality water can be circulated through more concentrations than a lower quality water. Some of the advantages of circulating to a high C value are: 1) makeup requirements can be minimized, 2) blowdown requirements can be minimized, and 3) the size and costs of handling makeup and blowdown facilities can be minimized.

About 0.75 percent of the cooling water flow (circulating water) is lost through evaporation for every 10°F of condenser temperature change. New cooling towers usually have drift losses as low as 0.005 percent of the cooling circulating water for mechanical draft towers. Figures 13 and 14 indicate the amount of evaporative losses which can be expected from the cooling systems under varying conditions of the wet bulb temperature and relative humidity.

Crits and Glover (1975) and Gold et al. (1977) discussed the blowdown water quality of cooling towers in relation to the number of concentrating cycles. Table 16 indicates the upper concentration limits for various chemical parameters in blowdown water.

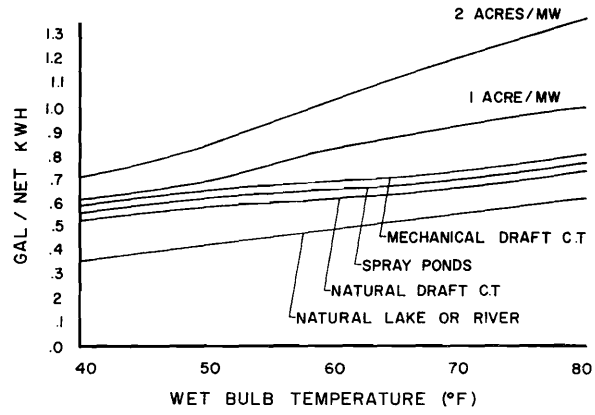

Figure 13. A comparison of evaporative losses for various types of cooling systems for varying wet bulb temperatures.

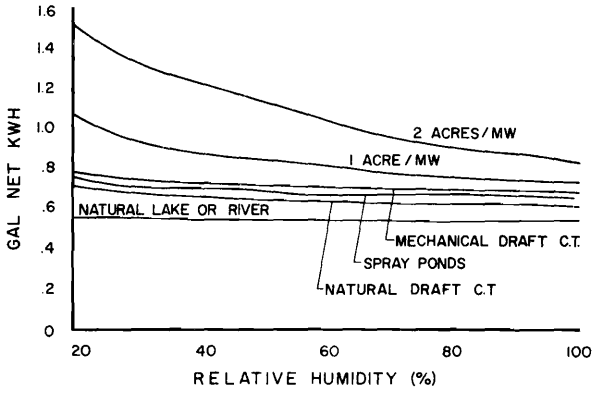

Figure 14. A comparison of evaporative losses for various types of cooling systems for varying relative humidities.

Table 16. Control limits for cooling tower circulating water composition.

pH	7.5 to 8.5
Suspended Solids (mg/l)	300
Ca x CO_3 (as $CaCO_3$)	6,000
Carbonates (mg/l)	5
Bicarbonates (mg/l)	300
Silica (mg/l)	150
Mg x SiO_2 (mg/l)	60,000
Ca x SO_4 (as $CaCO_3$)	2.5 x 10^6
Chlorides	3,000

Water conditioning is practiced to prevent reduction in plant efficiency from scale formation. Scale formers such as Mg, Ca, and SiO_2 ions can be substituted with a more water soluble ion such as Na^+. In other cases, the $SO_4^=$ ion has a greater solubility than the carbonates ($CO_3^=$) and bicarbonates (HCO_3^-) and can be used to reduce scale formation. The chemical conditioning reactions can be described as follows:

$$CaCO_3 + H_2SO_4 = CaSO_4 + H_2O + CO_2\ (g)$$

$$Mg(HCO_3)_2 + H_2SO_4 = MgSO_4 + 2H_2O + 2CO_2\ (g)$$

(from EPA, 1974, p. 119-120)

Organic compounds that act as sequestering agents can also be added to the cooling circulating water to react with and prevent the metallic ions from combining with the carbonates and bicarbonates to form scale compounds.

In addition to preventing scaling, water conditioning must inhibit the corrosive properties or water. Common corrosion inhibitors used in cooling recirculating systems have been inorganic polyphosphates, chromate, and zinc.

Biological growth in the cooling and water recirculating system is promoted by the moist and sometimes nutrient rich atmosphere of the recirculating water and must be controlled. Biological growth can foul and reduce the efficiency of the cooling system. Growth, however, can be controlled by adding chemicals such as chlorine to the system.

In summary, scale formation, corrosion, and biological growth in the cooling recirculating water must be controlled for efficient energy conversion. The problem, however, is that the chemical additives used to promote high cooling efficiencies become concentrated in the blowdown water. Their discharge into streams is prohibited by federal regulations.

The design of wet cooling towers is based on the wet-bulb temperature of the air, the approach range, and terminal temperature difference.

The wet-bulb temperature of the air is an important parameter in the design and performance of an evaporative-type cooling tower, since the wet-bulb temperature of the air is the lowest temperature to which the water circulating through the tower can be cooled. The term "approach" is used in evaporative tower terminology to designate the difference between the temperature of the cooled water leaving the cooling tower and the wet-bulb temperature of the ambient air. The design wet-bulb temperature of the air for a specific site is generally selected as that wet-bulb temperature which is exceeded for no more than a small percentage of time on the average.

A wet-type cooling tower with a 15°F approach will cool the circulating water to within 15°F of the ambient air wet-bulb temperature at design heat rejection load. Carrying the design heating rejection load from the condenser, such a tower would cool the water to 100°F when the wet-bulb temperature is 85°F (Rossie, 1971a).

The natural draft wet towers, usually constructed from reinforced concrete, have a hyperbolic design for aerodynamic and structural reasons. The tower and packing can be designed and operated with the air flowing upward through the packing (counterflow) or horizontally across the packing (crossflow). However, "the natural-draft tower has its best application in the power industry, where winter may exceed summer loads, total heat load is very large and payout is long. Low relative humidities in Southern California, Arizona, Utah and Nevada preclude its use for power plants in this section." (Elliot et al., 1973). One advantage of selecting wet cooling towers over dry towers is the higher efficiency derived by the energy conversion process because of the lower backpressures at which the wet towers can operate. A significant disadvantage of wet towers is that large quantities of water lost through evaporation must be replaced by makeup water.

Jedlicka (1973, p.5) compiled a set of nomographs designed to estimate "the heat rejection system performance, cooling tower costs and the perturbations to the powerplant efficiency and costs. Thus, the key factors and parameters from the various alternative systems can be qualified and analyzed at a given utility plant site following application of the nomographs." By using the nomographs with the particular design criteria of an area, the costs of different cooling systems can be found. Table 17 represents the data obtained from the Jedlicka nomographs which were used for estimating the cost of mechanical draft wet cooling towers.

Table 18 is a summary of the cost data for the different cooling processes.

Table 17. Mechanical draft wet tower costs.

Net Generating Capacity (MW)		750
Type of Plant		Fossil
Plant Heat Rate (Btu/kw-hr)		9137
Wet Bulb Temperature (°F)		66
Condenser Outlet Temperature (°F)		114
Range or Condenser Rise (°F)		30
Approach		18
	Source Page	Value
Tower Correction Factor	N-7	1.06
Condenser Inlet Temperature (°F)	N-8	84
Turbine Back Pressure (inches Hg)	N-27	3.5
Heat Rejection Rate (10^9 Btu/hr)	(from IPP study)	4
Water Flow Rate (10^6 GPM)	N-9	0.27
Number of Tower Units (10^6)	N-10	0.3
Capital Cost @ $4.7/Tower Unit ($10^6$)	N-10	1.4
Fan Power Requirements (MW)	N-11	2.5
Pump Power Requirements @ 60 feet of Total Pumping Head (MW)	N-12	3.7
Plant Efficiency (%)	N-31	35.35
% Evaporative Loss (% of Water Flow Rate)	N-35	2.305
Drift Loss (% of Water Flow Rate)		0.005

C	Blowdown (% of Water Flow Rate)	Make-Up (% of Water Flow Rate)	Return (% of Water Flow Rate)
5	0.570	2.875	97.125
10	0.2506	2.555	97.445
15	0.1592	2.4642	97.536
20	0.11605	2.4211	97.579
50	0.04194	2.3469	97.653
100	0.01823	2.3232	

Liquid phase pollution control

Several technologies are available for treating the liquid wastes from a coal conversion facility. A discussion of these technologies is provided as one step in developing useful data for the model being developed in this study.

Evaporation pond. Some small powerplants comply with waste discharge standards by water containment in evaporation ponds. Liquid residuals, generated during production, are transferred from the plant side to ponds where the water is evaporated. The pond would be lined with a water-proof substance to inhibit seepage and contamination of the groundwater. Davis (1975) discussed the costs incurred from using an evaporation pond for powerplant discharges. The costs were calculated for 214 x 10^6 gallons per year capacity. A summary of the costs are listed in Table 19.

Settling pond. Conventional water and ash disposal methods used by electric power generating plants include settling ponds. The water balance from one powerplant settling pond is summarized in Table 20.

The costs of a settling pond are summarized in Table 21. The characteristics of the pond are that its capacity is 55 KTONs of water covering an area of 8 acres with an average wall height of 5 feet.

Table 18. Cooling processes (Cost data-summary).

Cooling Type	Capital Energy		Conversion %	Difference With Once-Through %	Total Energy MWH/Day	Evaporation Loss Tons of Water/Day
	Total $	Pumping, Etc. MWH/Day				
Once-Through	70,000	12.528	35.8	0	0	24.27×10^3
Mechanical Draft–Wet	1.4×10^6	148.8	35.35	0.45	152.175	37.30×10^3
Mechanical Draft–Dry	18.5×10^6	492.0	33.8	360	852	0
Natural Draft-Dry	19.5×10^6	170.4	33.8	360	530.4	0

Table 19. Evaporation pond water balance.

	Total Cost	Daily Cost (1977)
Pipeline	$\$1.065 \times 10^6$	$ 370
Dam	$\$2.250 \times 10^6$	$ 781
Lining	$\$5.879 \times 10^6$	$2041.65
Land ($100/Acre)	$\$0.0475 \times 10^6$	$ 16.50
Pumps (10 ft. Head)	$\$0.00802 \times 10^6$	$ 2.78
Total	$\$9.25 \times 10^6$	$3211.93
Pump Energy	$\frac{8.857 \times 10^{-3} \text{ MWH}}{\text{KTON}}$	

Table 20. Settling pond water balance (from EPA, 1974, p. 306).

Evaporation	1.8% of Transport Water
Loss to Solids	20% Ash Moisture
Recycle	78.2% of Transport Water

Table 21. Settling pond costs.

	Total Costs (1975)
Pipeline	$\$17.9 \times 10^3$
Dam	37.9×10^3
Lining	99.0×10^3
Land	0.8×10^3
Pumps	1.01×10^3
Total	$\$156.61 \times 10^3$
Pump Energy	4.4285×10^{-3} MWH/KTON

Lime softening. Suspended solids can be removed by treating the solution with lime. When the lime is added to a solution containing suspended particles, the particles become destabilized and adsorb to each other in the presence of the dissolved lime. Subsequently, the particles are removed after increasing in size and density and settling.

Van Note et al. (1975) provided a description of a flocculator basin with the use of lime as the coagulating agent. The system removed 81 percent of the BOD, 86 percent of the suspended solids and 91 percent of the phosphorus in the influent. The brine stream was 1 percent of the influent and contained 10 percent solids.

The flow diagram for the flocculator clarifier, using lime, is described in Figure 15 (after Van Note et al., 1975, p. III-15). The costs were based on February 1973 indexes and approximated by the linear functions presented in Table 22.

Table 22. Lime softening costs.

	Cost Function	
	0-30 KTON/Day	30-70 KTON/Day
Capital	$y = 68 + 3.0\,(x)$	$y = 89 + 2.3\,(x)$
O & M	$y = 57.6 + 3.36\,(x)$	$y = 100.8 + 1.928\,(x)$

Mills and Tchobanoglous (1975) described the electrical energy consumption for an operating sedimentation basin. The energy consumption for a 2,300 ft^2 unit was 11.5 MWH/KTON of influent water.

$$\left[\frac{48 \text{ KWH}}{\text{Day}} \times \frac{\text{Day}}{10^6 \text{ gal}} \times \frac{10^6 \text{ gal}}{4.1685} \times 10^{-3} \text{ KTON}\right]$$

$$= 11.5 \text{ MWH/KTON}$$

Figure 16 is a description of the energy requirements for sedimentation tanks for a TDS concentration of product effluent at 1000 ppm.

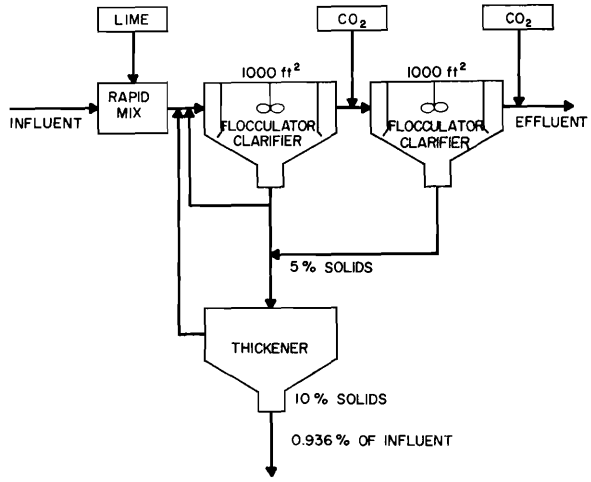

Figure 15. Flocculator-clarified flow diagram.

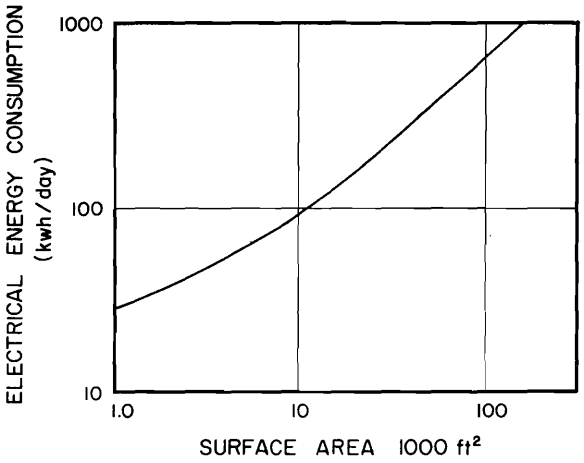

Figure 16. Electrical power requirements.

Sludge thickening—filtration. The water content of sludges can be reduced by filtering processes. One method of filtering allows sludge effluents to seep through the meshed material wrapped around a drum. As the drum rotates, some of the solids are filtered onto the meshed material and subsequently removed as the effluent seeps through the mesh.

Van Note et al. (1975) provided a description and cost data for a filtration unit. The influent quality was 10 percent solids with 67 percent of the influent passing through the filter and 95 percent of the solids collected on the filter. Van Note et al., 1975, provided a capital cost estimate of \$4.50/KTON and \$2.40/KTON for O & M costs, including power requirements of 8.59×10^{-3} MWH/KTON. Figure 17 is a description of the sludge thickening unit.

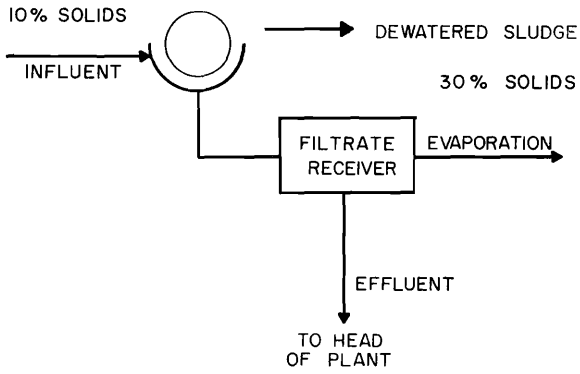

Figure 17. Sludge thickening flow diagram.

For lack of additional information, it will be assumed that the thickener used for air cleanup streams requires three times the capital, O & M, and energy that the above described thickener requires. Thickening performances are assumed the same.

Trickling filter. A trickling filter unit can be used to reduce high concentrations of BOD in wastewater. The unit requires a relatively small amount of land and consists of a tank containing a media with a high surface area. As the wastewater trickles over the surface area, microorganisms growing on the surface assimilate the nutrients from the water and convert the nutrients to biomass. Eventually, the biomass thickens over the media's surface and prevents a food transfer to the organisms attached to the media. Consequently, the microorganisms attached to the media are essentially starved and the entire biomass is hydraulically washed from the surface.

Van Note et al. (1975) provided a description of a trickling filter unit and its capital and operating costs. The treatment unit removed 80 percent of the BOD, 77 percent of the suspended solids and 18 percent of the phosphorous. The brine effluent stream contained 6 percent solids and consisted of .00432 percent of the influent flowrate. Figure 18 is a flow diagram of the tricling filter unit. Mills and Tchobanoglous (1975, p. 26) estimated the energy requirements for the trickling filter process (5 ft pumping head) at 0.01 MWH/KTON.

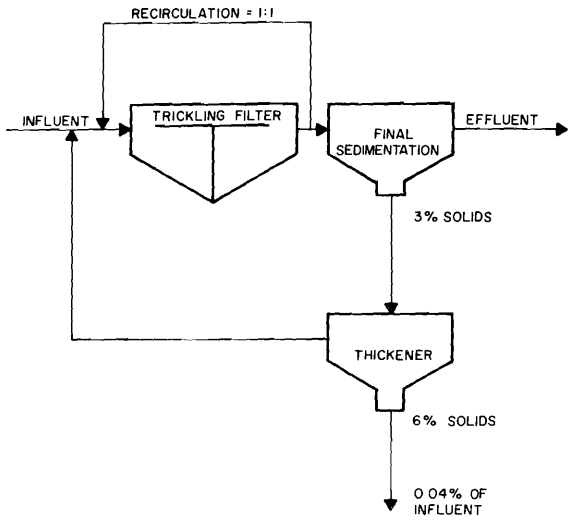

Figure 18. Trickling filter flow diagram.

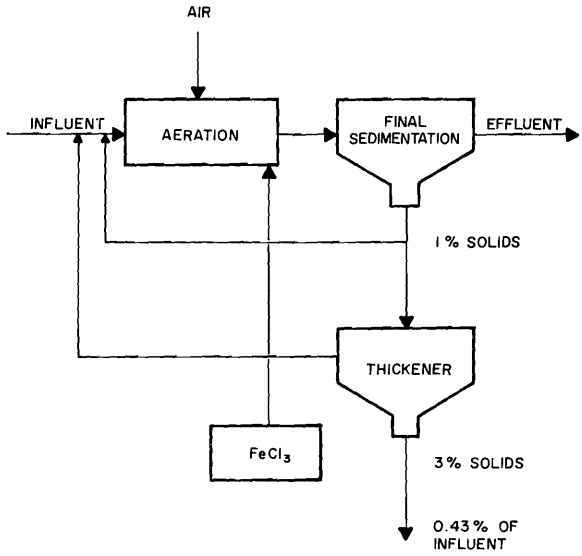

Figure 19. Activated sludge flow diagram.

Activated sludge. An activated sludge unit can be used to reduce the biological nutrients in a wastewater by promoting rapid metabolic activity among the microorganisms indigenous to the activated sludge process. The metabolic rate is increased by recycling the microorganisms from a sedimentation tank to the reactor and saturating the nutrient rich reactor wastewater with oxygen. The microorganisms, returning from the sedimentation tank where the nutrient content is relatively low, shift their metabolic rate from one of endogenous respiration to one of exogenous respiration where organic matter and nutrients are assimilated to the biomass.

Figure 19 is a flow diagram of an activated sludge treatment process. Van Note et al. (1975) presented the capital and O & M data for the activated sludge treatment process. Mills and Tchobanoglous (1975, p. 5) inventoried the energy consumed from an activated sludge treatment process at 0.034 MWH/KTON.

Ion exchange. Resins containing functional groups on their surfaces are useful for exchanging ions in solution for ions held by electrostatic forces to the functional groups. The ion exchange unit is used primarily for reducing water hardness, iron concentrations, and manganese concentrations. Ion exchange can also be used for treating a variety of industrial wastewaters and for recovering valuable waste materials. "Observed preferences of ion-exchange resins for certain ions within classes of similar charge characteristics is an important consideration in determining the feasibility of a given exchange reaction" (Weber, 1972, p. 274). Most resins are characteristically and relatively insensitive to heat and are stable at temperatures to 100°C and higher. "Complete demineralization operations generally involve a cation exchanger followed by a weekly basic anion exchanger" (Weber, 1972, p. 290). A schematic diagram of the process is presented in Figure 20.

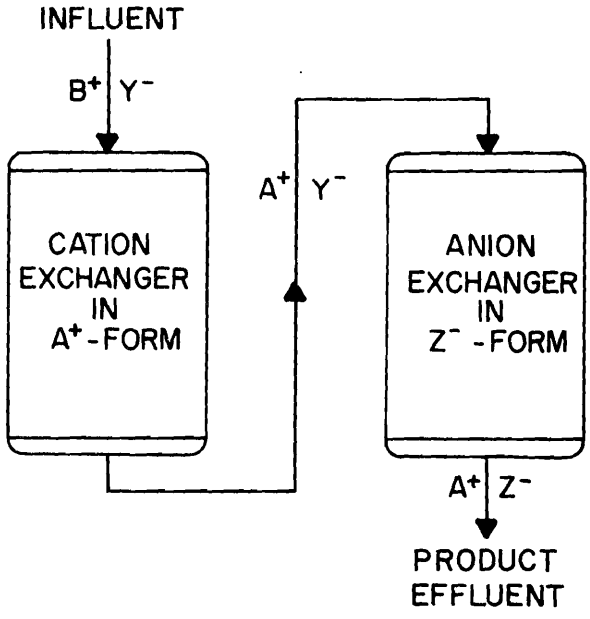

Figure 20. Ion exchange flow diagram.

The number of exchange sites in an ion-exchange unit are limited and are filled by ions in solution as the process proceeds. During the process, as the number of exchange sites becomes limited, the degree of removal is reduced. As a result, the resins must periodically be backwashed with strong chemical solutions to replenish the active sites by substituting the active sites with their original ions and removing the ions which were originally in solution. The backwash water becomes the waste stream from the process. Some resins, because of their nature, can remove many different kinds of ions, but require more of the original ions to replenish the active sites.

The cost of ion exchange units depends on the type of water being purified. "Exchangers employing highly basic resins, which are regenerated with sodium hydroxide, involve higher operating costs than those employing weakly basic resins. Additionally, regeneration of the form is a less efficient process than that for the weakly basic resins... It is estimated that for solids concentrations in the neighborhood of 1000 mg/liter the economics of treatment begin to favor other processes " (Weber, 1972, p. 297).

The costs of an ion-exchange unit for removing nitrogen from wastewater has been estimated by Van Note et al. (1975). The capital costs are estimated by: $Y = 163{,}270X^{0.88} - 0.17 + 0.021X$ and the operating costs were estimated by: $Y = 3{,}746.2X^{0.72} + 15{,}161.5X^{0.86}$ in which

X = MGD
Y = dollars per year

The electric power requirements can be estimated by assuming a pumping head of 4 feet and pumping efficiency of .85 and 33 percent of the influent flow is required for backwashing. Therefore, the power requirements are 0.01966 MWH/KTON.

If the average product effluent concentration from the ion exchange unit were 150 mg/l, then the brine effluent stream concentrations if the upper concentration limit on the influent were 1000 mg/l, would be 3,310 mg/l. The linear equations that describe the total cost of the ion exchange unit are: $Y = 264.5 + 94.708X$ for flowrates between 0 and 35 KTONs of water per day and: $Y = 596 + 85.5X$ for flowrates between 35 and 70 KTONs of water per day.

Oil and grease removal—flotation chamber. Flotation is a conventional method used for removing oil and grease from a liquid stream. When large quantities of small gas bubbles are released from the bottom of a holding tank, oil and grease are adsorbed to the bubbles and are floated to the top. Skimming can then be used for final oil and grease removal.

Blecker and Nichols (1973) estimated 1972 capital cost at \$550/ft^3 capacity. When a retention time of 30 minutes is assumed, the capacity of a 10 ft^3 flotation unit would be 480 ft^3 per day. The capital cost of a flotation unit in 1977 prices would be \$243/KTON. Operation and maintenance costs are estimated at \$4.86/KTON, and energy costs are 0.017 MHW/KTON. Other assumptions are: 99.99 percent oil and grease removal, a waste stream of .01 percent of influent streams, and oil and grease influent concentration is 20 ppm.

Evaporator crystallizer. An evaporator crystallizer has been used successfully to control the blowdown from a coal fired steam electric powerplant in Utah. Davis (1975) presented a description of the unit depicted in Figure 21. Wastewater enters the feed tank for acid treatment to control the pH. The influent is subsequently pumped through the head exchanger to increase the influent temperature to near atmospheric boiling, then deaerated to eliminate dissolved gases such as carbon dioxide, nitrogen, and oxygen. After deaeration, the wastewater enters the evaporator sump where it is mixed with the treated brine slurry and then recirculated to the top of the evaporator. The slurry flows down on the inside wall of the tubes and about 0.5 percent of the recirculated brine slurry is evaporated when heat transfer occurs across the tube wall.

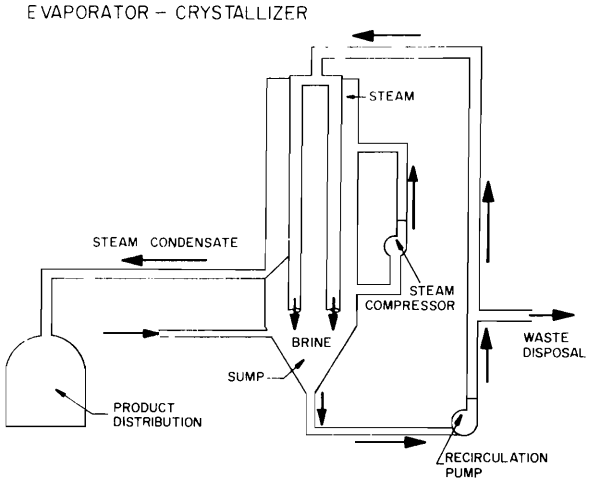

Figure 21. Evaporator-crystallized flow diagram.

The steam is compressed at about 2 psi, and the steam condensation temperature is raised about 6 degrees above the boiling point of the circulating brine. The steam condenses on the shell side as the steam heat is transferred across the tube surface. The condensed product water is subsequently collected for re-distribution. According to Lacey (1977a) who described the performance of the evaporator-crystallizer, the influent concentration is 2,500 ppm total dissolved solids and the product water consists of less than 10 ppm TDS, and is about 98 percent of the influent. The process required about 13.866 MWH/KTON of liquid influent and required a capital investment of $2 x 10^6 in 1974 for the 175 gallon per minute unit process. Operation and maintenance costs average about $13.04/KTON. The brine stream concentration would be 124,510 mg/l.

Multi-stage flash evaporation. In the multi-staged flash evaporation process, saline water is pumped through the evaporation feed tubes. The feed tubes pass from the last stage of the evaporation unit to the first and serve as a condenser. The temperature of the feed water is heated as vapor from the evaporator stages condenses on the feed tube surface. After additional heating, the feed water is introduced into the first stage where some rapid boiling and evaporation (flashing) occurs. The additional heat is usually supplied from steam. The water vapor released in the flashing process is condensed on the cooler feed tubes, collected in a condensate trough, and becomes the first part of the condensate stream. That portion of the saline water which was not evaporated is passed into the following stage for additional flashing. As the quantity of product water increases, the concentration of solids in the feed water increases until the brine solution is discharged from the evaporation unit in the last stage. The water vapor which was condensed in the first stage also passes into the second and succeeding stages where flashing and condensing occurs and the product water is accumulated in the trough.

The saline water is flashed at about 220°F in the first stage of the evaporator unit then passed into succeeding stages and flashed at progressively lower pressures. Both the condensate or product water and the brine streams leave the final stage of the evaporator at pressure below atmospheric and the streams must be pumped from the last stage (MacLeod, Gendel, and El Sahrigi, 1963).

Figure 22 is a schematic diagram of the multi-stage flash evaporator and a schematic diagram of a cross section of one of the evaporator stages.

Childer's (1966) estimated the capital cost of the multi-stage flash distillation process in terms of plant capacity according to source capital cost in 1966 prices as:

$$Y = (\$1.4 \times 10^6) \times MGD^{0.82}$$

where MGD = 10^6 gallon per day.

The amount of product water in relation to the amount of brine water generated in a MSF plant is a function of the feedwater TDS concentration. The ratio can be found by:

$$\frac{Q_i}{Q_p} = 1.2 + 0.92 \frac{Q_b}{Q_p}$$

in which

Q_i = influent rate (in MGD) into the MSF unit
Q_b = brine effluent rate (in MGD) from the MSF unit
Q_p = product rate (in MGD) from the MSF unit

The Q_b/Q_p ratio should be: 0.2 when the feedwater TDS concentration is less than 10,000 mg/l; 0.5 for TDS concentrations of 10,000 - 20,000 mg/l; 1.0 for TDS concentrations of 20,000 to 30,000 mg/l; 1.7 for TDS concentrations of 30,000 to 40,000 mg/l; and 3.4 for TDS concentrations of 40,000 to 40,000 mg/l (Childers, 1966, p. 28). Figure 23 is a graph of the above equation. In the equation, the final concentration of the TDS in the product water is held constant at 10 mg/l.

Energy costs are incurred by the MSF process from steam requirements and pumping requirements. The steam cost has been reported by Childers (1966) as 62.374 MWH/KTON of product water. Table 22 describes the portion of influent which results as product when the concentration of the influent is varied. Table 23 also describes the equivalent steam energy required to produce an effluent product concentration of 10 ppm TDS. The steam requirements are found by dividing the energy requirement by the percent product factor.

Childers (1966) presented the MSF energy requirements for pumping described by Figure 24. The operating and maintenance costs other than energy requirements were defined by Childers (1966) as .5 percent of capital expense + $85,000/year.

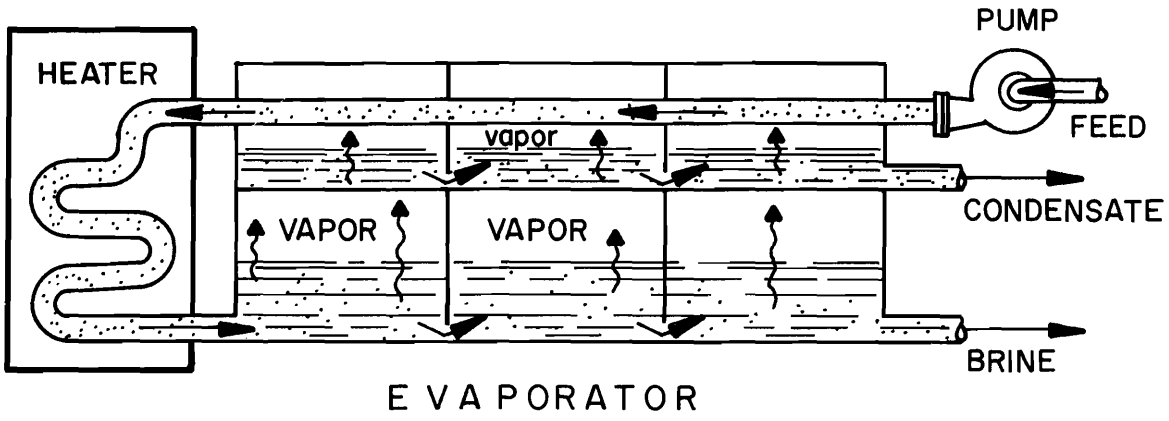

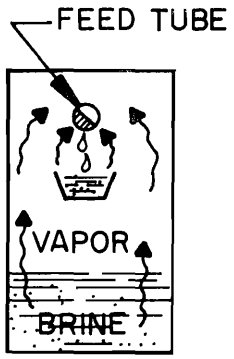

Figure 22. Multi-stage flash distillator.

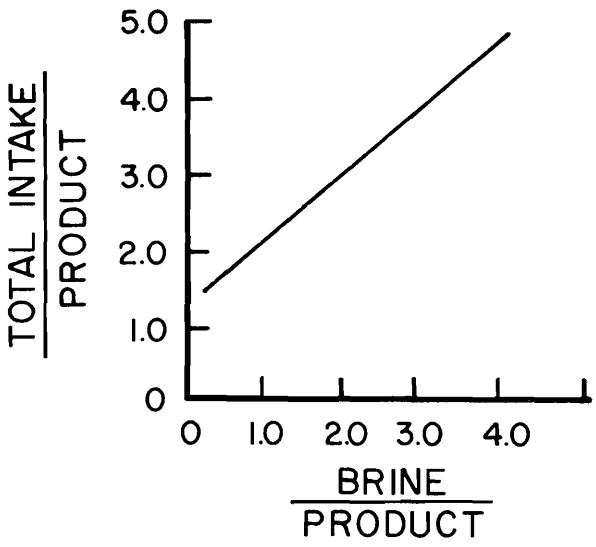

Figure 23. Brine-product ratio.

Table 24 is a summary of the total cost data for a multi-stage flash unit when different influent concentrations are treated.

Electrodialysis. The electrodialysis process uses anion and cation specific membranes which are located next to each other in alternating sequence. Several single anion-cation membrane pairs, referred to as a membrane stack, can be contained in a single stage and several stages can be located in series to promote additional dissolved solids removal at each stage. As the influent is pumped into the first stage, the stream is divided to form the product and brine streams. Figure 25 is a schematic diagram of a membrane stack. When an electric current is applied to the anode and cathode of the stack, cations of the product stream pass through the cation exchanger membrane while the anions pass through the anion exchanger membrane. The result of the process is a demineralized product stream and two mineral concentrated brine streams in a stack.

Table 23. Power requirements and water characteristics.

TDS (ppm)	% of Influent as Product	Steam Energy Required Per Influent Flow (MWH/KTON)	Concentration (mg/l)	
			Brine	Product
< 10,000	70.25	86.33		
10,000 - 20,000	60.24	103.54	50,287	10
20,000 - 30,000	42.17	132.23		
30,000 - 40,000	30.18	206.67	57,286	10
40,000 - 50,000	23.05	270.60	64,974	10

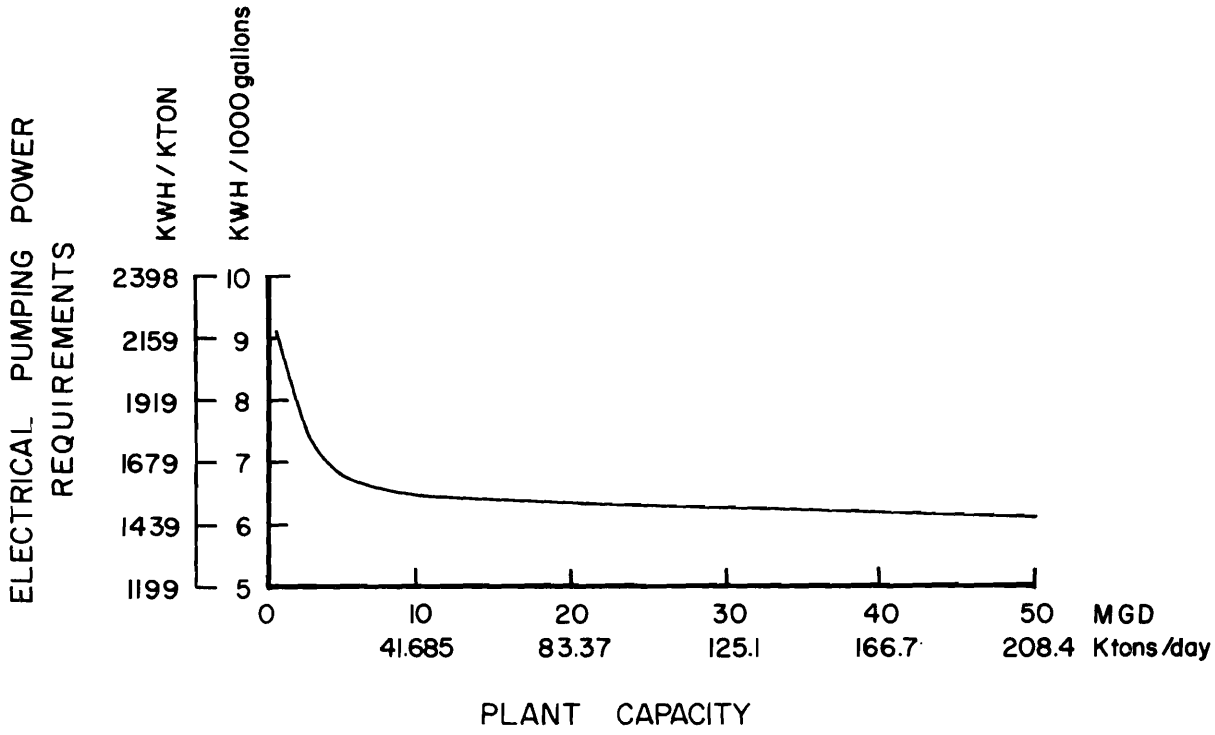

Figure 24. Multi-stage flash pumping power requirements vs. plant capacity.

Table 24. Multi-stage flash unit total costs.

Influent Concentration (ppm)	Linear Total Cost Equation
0 - 10,000	y = 780 + 2499 (x)
10,000 - 30,000	y = 778 + 3417 (x)
30,000 - 50,000	y = 778 + 6184.5 (x)

A stack is characterized by its removal efficiency and its hydraulic loading rate. A single stack usually removes from 30 to 60 percent of the TDS entering the stack and removal efficiency depends on the electric current applied in the stack and on the temperature of the water. Usually, less electric current is required for a warmer water than with a cooler water with the same TDS concentrations. Desalinization of water with a TDS of less

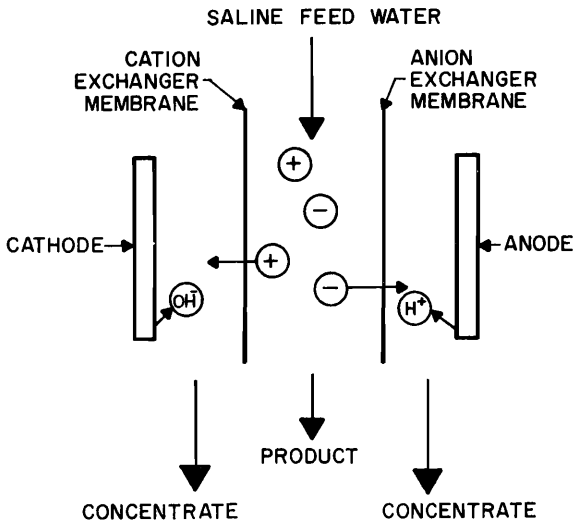

Figure 25. Electrodialysis stack.

than 10,000 ppm has been the principal use of electrodialysis.

Childers (1966) discussed the capabilities and costs of operating an electrodialysis unit. The influent water temperature of an electrodialysis unit used in a steam electric power would tend to be relatively warm based on information from Childers (1966). A 50 percent removal rate per stack appears appropriate for cost estimate purposes. Electrodialysis stacks can be designed with a hydraulic loading rate per stack of

$$\frac{1.042 \text{ KTON of Water/Stack}}{\text{Day}}.$$

The capital and energy costs of an electrodialysis unit were discussed by Weber (1972), Childers (1966), and Allegrezza et al. (1975) who indicated that the costs were directly proportional to the concentration of minerals in the influent water.

The capital costs of an electrodialysis plant can be estimated, according to Childers (1966), by either of the following equations:

$Y = [1.58 \times 10^5 + 4.0187 \times 10^4 (x)]$ for 1-10 Stacks or 0-10.4 KTONS/Day

$Y = [2.7 \times 10^5 + 2.854 \times 10^4 (x)]$ for 10-100 Stacks or 10.4-1042 KTONS/Day

in which

Y = capital cost in dollars/day
x = KTONs/day

The energy costs of an electrodialysis plant are incurred as a result of pumping and applying an electric current in the membrane process. Childers (1966) estimated the pumping costs at 479.8 KWH/KTON. The electric power required for solids removal was estimated by Childers (1966) at 5 KWH per thousand gallons of product water per thousand ppm of dissolved solids removed. Other operating costs, in addition to energy costs, have been estimated as $1.47/KTON. The amount of brine product can be calculated by assuming a brine stream dissolved solids concentration of 40,000 ppm. A dissolved solids concentration of 50,000 ppm is usually the maximum concentration attainable. Iron, manganese, silica, organic compounds and high calcium concentrations tend to foul membranes if introduced into an operating electrodialysis unit.

The fractions of product brine produced from the electrodialysis unit can be calculated by:

$$\frac{C_b}{C_p} = \frac{TDS_i - TDS_p}{TDS_b - TDS_i}$$

in which

$\frac{C_b}{C_p}$ = brine to product ratio

TDS_p = total dissolved solids concentration of the product effluent

TDS_i = total dissolved solids concentration of the influent

TDS_b = total dissolved solids concentration of the brine effluent

The fraction of product effluent and brine effluent can be found respectively by:

$$\text{percent product} = \frac{C_p}{C_p + C_b}$$

$$\text{percent brine} = \frac{C_b}{C_p + C_b}$$

The number of stages required in the electrodialysis unit can be calculated by the relationship:

$$(1 - f)^n = \frac{TDS_p}{TDS_i}$$

$$\text{or } n[\ln (1-f)] = \ln TDS_p - \ln TDS_i$$

in which

n = the number of stages required
f = the fraction of dissolved solids removed per stage

For a product effluent of 10 ppm of TDS, the number of stages required for different influents is shown in Table 25.

Table 25. Electrodialysis stages.

TDS_i (ppm)	n
10,000	10
5,000	9
2,500	8
1,250	7
78	3

The linearized total cost equations that describe the electrodialysis unit are presented in Table 26 for different quality influents.

Table 26. Electrodialysis unit total costs.

Influent Quality (ppm)	Cost Function
0 - 78	y = 598 + 22.3 (x)
78 - 1,250	y = 1,398 + 80.2 (x)
1,250 - 5,000	y = 1,797 + 201.9 (x)
5,000 - 10,000	y = 1,996 + 365.8 (x)

Reverse osmosis. When two solutions of different dissolved solids concentrations are separated in two cells by a semi-permeable membrane, the more dilute solution will move across the membrane to dilute the more concentrated solution. The movement is called osmosis.

When an increasingly higher pressure is applied to the concentrated solution, an equilibrium pressure will finally be reached where the net flow across the membranes will be zero. The pressure at which the flow is in equilibrium is called the osmotic pressure of the solution. An additional pressure increase on the more concentrated solution beyond the osmotic pressure will cause a reverse movement of flow; e.g. the water will flow from the more concentrated cell to the more dilute cell while the solids movement across the membrane is selectively prevented by the nature of the membrane. The reverse flow across the membrane is called reverse osmosis. As a result of reverse osmosis, the concentrated solution will become increasingly more concentrated. In practical reverse osmosis, a pressure of 600 to 1000 psi is commonly used.

The membranes used in the reverse osmosis process are not completely selective or semi-permeable. Because of the membrane imperfection, researchers continue to develop better membranes which will approach a more semi-permeable nature, withstand higher water temperatures, and have a longer life expectancy (Weber. 1972, and Clark, 1969). For design purposes, "the most important performance parameter of a reverse osmosis membrane is the product water flux, usually expressed as gallons of fresh water produced per day through one square foot of membrane. Another important membrane property is the salt rejection characteristics of the membrane, which in turn determine the quality of the product water " (Clark, 1969, p. 66).

Weber (1972, p. 315-316) discussed the percent water recovery in relation to water quality and water flux. Weber noted that the quality of the product water decreases as the feedwater dissolved solids concentration increases at a constant pressure. An increase in temperature will allow a higher water flux while the salt rejection remains constant. Current research has produced a membrane with a water flux of 28 gal/ft^2/day with removal as high as 99.9 percent for heavy metals (Peterson and Cobian, 1976).

The reverse osmosis system is sensitive to some components of a wastewater stream and thus, the water should be pretreated for turbidity and suspended solids, pH and temperature control, biological growth control, organics, and compounds which can form and plug or coat the membranes. Turbidity and suspended solids can be controlled with coagulation, flocculation and sedimentation and/or filtration. Calcium compounds of carbonates and sulfates can be controlled at pH 5 to prevent membrane interference. Organic compounds can be controlled by activated carbon treatment or by allowing the compounds to deposit, and maintaining a frequent filter cleaning program. Biological growth can be retarded by chlorinating the influent to produce 1-2 mg/l free residual chlorine.

Reverse osmosis units operate at pressures much higher than the total head loss through the unit. For this reason, some of the pump energy required to maintain the high pressure can be recovered by passing the effluent from the unit through a turbine system. Oak Ridge National Laboratory (1970) reported that power recovery equipment becomes economically feasible to install at the 5 mgd capacity, and total dissolved solids influent concentrations in the 8,000 to 10,000 ppm range can be treated by reverse osmosis.

The Oak Ridge National Laboratories (1970) published the capital, operating, and energy costs for treating two different concentrations of influents by reverse osmosis. From the information that was provided in the publication, the costs can be computed in terms of amount of water treated and amount of total dissolved solids removed. Data from the publication is displayed in Table 27. The percent product effluent is assumed at 60 percent influent.

Table 27. Reverse osmosis costs.

Flow Rate	Costs		
	Capital	O & M	Energy
KTONS/Day	$/KTON (1000 ppm Removed)	$/KTON (1000 ppm Removed)	MWH/KTON (1000 ppm Removed)
12	17.73	6.51	0.46
24	16.69	5.34	0.365
36	15.91	4.56	0.362
48	15.12	4.17	0.360
60	14.60	3.91	0.357

Gas phase pollution control

Limestone slurry scrubber. McGlamery et al. (1975) evaluated the cost estimates for five desulfurization processes including the limestone slurry process. The cost estimates were provided for 200, 500, and 1000 MW powerplants whose coals contained 2, 3.5, and 5 percent sulfur.

Among the conclusions from the study were:

1. For new coal fired systems, the lime scrubbing process has the lowest investment even when the sulfur content of coal varies.

2. The cost to remove 80 percent of the SO_2 derived from 3.5 percent S coal to meet emission standards is 3 to 5 percent less than the cost required to remove 90 percent of the SO_2.

3. The limestone process has the lowest annual operating cost for a 3.5 percent S coal fired power unit.

4. Energy costs are significant for all sulfur control systems.

5. About 5 percent to 6 percent of the total operating cost is saved when 80 percent SO_2 is removed instead of 90 percent SO_2 removal.

The limestone slurry unit required the lowest investment and was found to be as reliable as the other desulfurization processes. In the limestone slurry process, the SO_2 contained in the stack gas is passed through an aqueous phase of limestone ($CaCO_3$) to produce a solid phase precipitate of calcium sulfate. The chemical reactions believed to describe the limestone process are:

$$SO_2 + H_2O \leftrightharpoons H_2SO_3 \leftrightharpoons HSO_3^- + H^+$$
$$HSO_3^- \leftrightharpoons H^+ + SO_3^-$$
$$CaCO_3 \rightleftharpoons Ca^{++} + CO_3^{--}$$
$$Ca^{++} + SO_3^- + \tfrac{1}{2}H_2O \rightleftharpoons CaSO_3 \cdot \tfrac{1}{2}H_2O$$

The resulting precipitate from the limestone slurry process is transferred from the scrubber as the cleaned gas advances to the gas stack where the gas in emitted to the atmosphere. A portion of the slurry is wasted as a spent slurry while the remaining slurry stream is reconstituted with fresh slurry.

A schematic diagram of the system is provided in Figure 26. Although the concept of gas scrubbing is relatively simple, to actually operate scrubbers is difficult because of difficulties with corrosion, erosion, and solids deposition (mud and scaling).

The costs of a limestone slurry scrubbing unit designed to remove 90 percent of the SO_2 and 99.5 percent particulate removal generated from a 750 MW powerplant burning 1 percent sulfur coal are presented in Table 28 based on the assumptions: 1) Off-site disposal requires 81.7 percent of normal capital cost; 2) Energy requirements for operations require 9.42 percent of O&M costs or 324.33 MWH/day; and 3) Water requirements are 1.5 KTONs/day (consumed in disposal).

Table 28. Limestone slurry process costs.

Capital	$Y = [11.0 \times 10^6 + 0.13072\ (X)]\ (0.817)$ $
O&M	$Y = [2.74 \times 10^6 + 0.0549\ (X)]\ (0.9037)$ $/Year
Water	Makeup at 1.5 KTON/Day
Energy	324.33 MWH/Day = 3.5368 MWH/KTON of air
	in which X = KTONS/Day of air

Electrostatic precipitator. According to Bump (1977, p. 129-130) electrostatic precipitation can be defined as "a physical process by which a particulate suspended in a gas stream is charged and, under the electrical field, separated from the gas stream." The electrostatic precipitator system "consists of a positively charged (grounded)

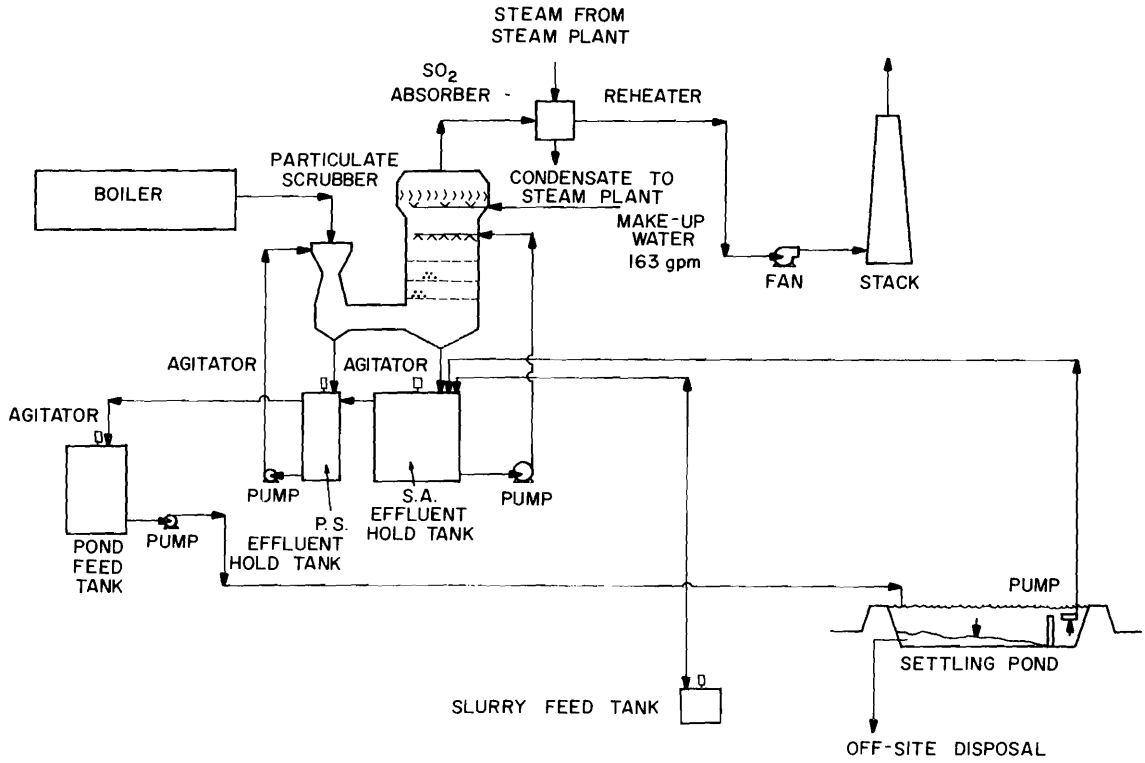

Figure 26. Limestone slurry process flow diagram.

collecting surface in juxtaposition to a negative charge-emitting electrode. A high-voltage DC charge is imposed on the emitting electrode, setting up an electrical field between the emitter and the grounded surface. As the dust particles pass between the electrodes, the particles are charged with a dense negative field and attracted to the oppositely charged collecting surface.

"Periodically, the collected particles must be removed from the collecting surface. This is done by vibrating or rapping the surface to dislodge the dust. The dislodged dust drops below the electrical treatment zone and is collected for ultimate disposal " (Bump, 1977, p. 129).

Many design variables are required to optimize the design of an electrostatic precipitator. Among the variables are: gas volume, temperature, particulate size range, and resistivity. The removal efficiency of an electrostatic precipitator is a direct function of electrical power. For 98.7 percent removal efficiency of a hot-side precipitator, about 760 watts/1000 cfm are required.

In addition to being a function of electrical power, removal efficiency also depends on fuel type. Bump (1977) found that a change from a 2 percent sulfur bituminous coal to a 0.5 percent sulfur, sub-bituminous coal decreased efficiency from 99.5 percent to 90 percent. The low sulfur fuels usually have a higher ash content than high sulfur fuels, and the ash has an electrical resistivity several orders of magnitude greater than that from higher-sulfuric coals. Because of the high resistivity of low sulfur coals, small quantities of SO_3 are injected into the flue gas to reduce the ash resistivity. This process can be used when the gas stream has a temperature of 250 to 350°F. The process is called ash conditioning and is usually accomplished by either direct injection or evaporation of liquid SO_3; catalytic conversion of SO_3; vaporization of sulfuric acid, sulfur burning followed by the catalytic conversion of SO_2 to SO_3. Utah coals have a low resistivity of about 1×10^{10} ohm-cm (de Nevers, 1975). Other chemical constituents in the fly ash such as sodium oxide can also affect the electrostatic precipitate removal performance and the units design should, therefore, be based on the worst expected fuel to be used at the plant.

A hot electrostatic precipitator can be installed ahead of the air preheater and operate effectively at gas temperatures ranging from 650 to 850°F. "At these temperatures, fly ash resistivity decreases; correspondingly, adhesive characteristics are reduced thus enhancing plate cleaning

with lighter rapping. Furthermore, the sulfur content of the flue gas makes little difference at these temperatures. The sensitivity of the precipitator to normal fluctuations in operating conditions is greatly reduced; making it more reliable." (Intermountain Power Project, 1976b.)

The electrostatic precipitator units are most useful for removing particles in the one to ten micron range. The precipitator units are generally preceded in the gas flow stream by mechanical collectors to remove the large particles that can cause damage to the discharge electrodes in the precipitator (Doyle et al., 1974, p. 362).

The capital cost of an electrostatic precipitator can be estimated in the range of $15 to $16 per KW ($35.655/KTON) (Lacey, 1977b). Edmisten and Bunyard (1970, p. 449) provided some capital cost data in 1968 but when updated to present value, costs were considerably less than 1977 estimates by Lacey (1977b). The particulate removal efficiency was 99.9 percent.

The maintenance costs are approximately $1.19/KTON of air in 1977 prices. The corona power (the power required to overcome the resistivity of stack gas particles) for 99.9 percent removal efficiency is about 1,100 watts per 1000 cfm 0.4893 MWH/KTON air.

Gas stacks. The ventilation stacks can be considered air pollution control equipment because their purpose is to reduce temperatures of exhaust gases while increasing the dispersion of contaminants, and hence, reducing sulfur dioxide concentrations. The stack's height is dependent on both the temperature of the gas and prevalent atmospheric conditions. According to Doyle et al. (1974), the capital cost of stacks has been estimated at $1,295 per foot for the first 600 feet and $3,240 for each additional foot in 1977 prices. For a 48-inch diameter stack operation and maintenance is in the range of 0.2 to 1 percent of capital cost. When stacks are not capable of delivering the gases to required elevations for gas dispersion, gas temperatures can be raised to cause the gases to reach higher elevations. For lack of contrary evidence the model assumes the stack height is sufficient without additional gas heating requirements.

Particulate wet scrubber. Fly ash can be removed from the stack gas without noticeably affecting the corrosive SO_x and NO_x concentrations. Edmisten and Bunyard (1970, p. 448-449) provided an estimate of the capital and O & M costs for a wet scrubber operating at 90 percent particulate removal.

The capital investment can be estimated by:

$$Y = \$5{,}263\ 3609.3\ (X)$$

in which

Y = capital investments
X = flowrate in KTONs air/day

The O & M costs can be estimated as 60 percent of annual capital charges. The energy costs can be estimated at 1.36 MWH/KTON or 60 percent of the energy requirements for a limestone scrubber (McGlamery et al., 1975). The water requirements for the wet scrubber are about two thirds the limestone scrubber requirements or 0.0109 KTONs of water per KTON of air. The quality of the effluent would be 539,000 ppm of total solids.

Solid phase pollution control

The solids phase residuals of a coal fired steam electric powerplant are produced from 1) solid phase streams such as bottom ash removal, 2) gas phase streams such as fly ash removal from an electrostatic precipitator, 3) liquid phase such as the precipitate from a settling pond containing brine waste streams.

Several methods are available for removing solid residuals from the power generating site. Stone and Smallwood (1973) described the costs of using a pipeline for slurry disposal and a tank truck for slurry and/or dry solid disposal. Table 29 is a description of the updated costs for the two disposal processes with variations in the distance to the disposal site.

Flow diagram

Figure 27 was developed after studying the literature on coal conversion facility and treatment alternatives to use as a flow pattern for the applied model application. The flows are defined by arrows representing the direction of flow. Whenever streams combine, the arrow tips of each flow are connected by a common dot. If two lines intersect on the diagram and no dot or arrow is present at the point of intersection, the junction does not exist and the streams do not join.

Any flow arrows pointing to a treatment or process unit and connected by other flow arrows with the same direction are considered the possible influents. Likewise, an arrow represented in the diagram as leaving a unit is considered as an effluent from that unit. Each unit is labeled with the number appearing in the model as subscripts to the liquid, gas and solid phase variables.

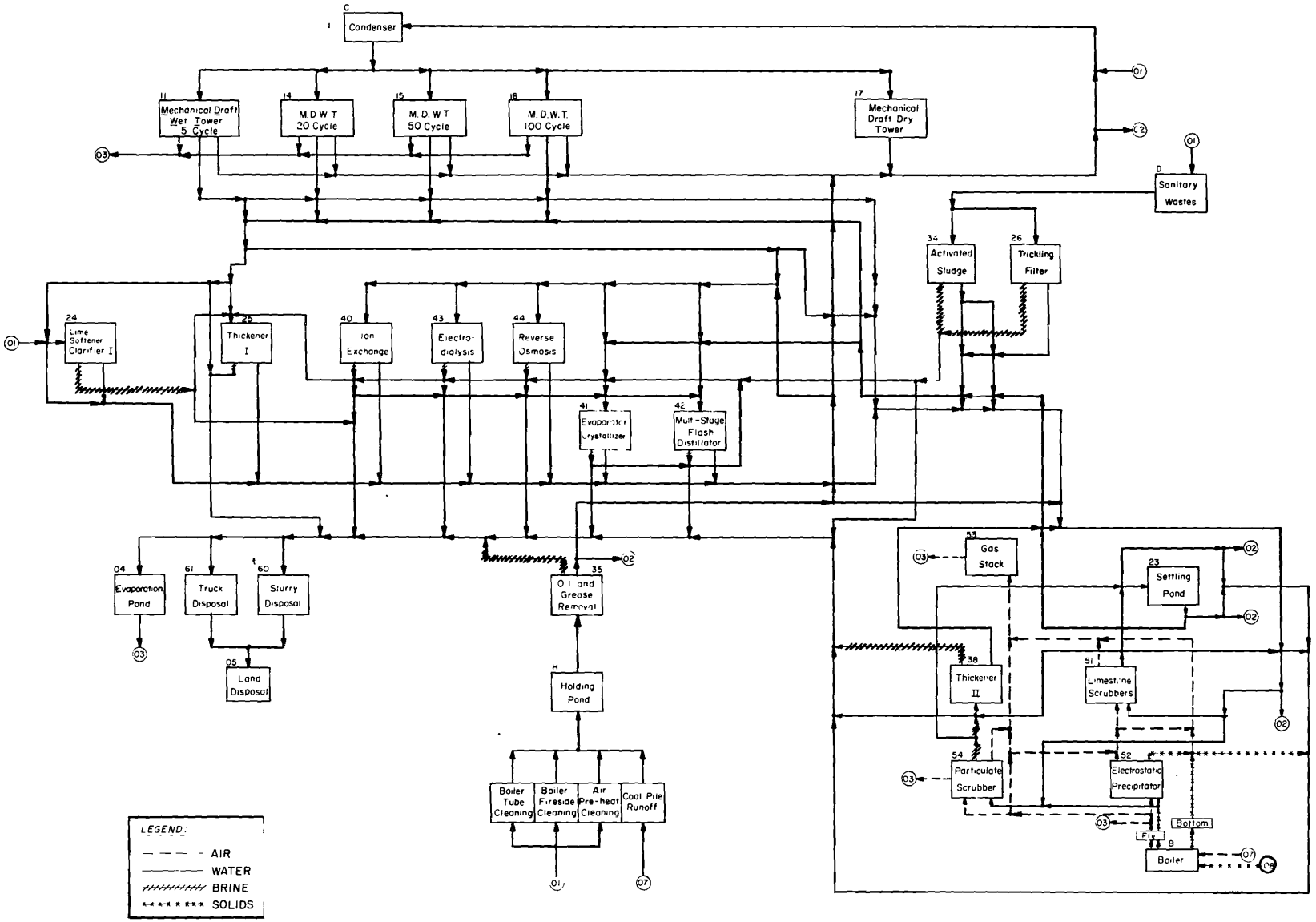

Figure 27. Treatment, recycle, and discharge alternatives for coal fired steam electric power generating facility.

Table 29. Residue disposal costs/ton vs. distance to disposal site (costs in $/ton).

	Distance to Disposal Site (Miles)				
	25	100	200	350	57
Pipeline					
Capital	$47.86	89.96	310.50	484.20	51.57
O & M	0.54	1.00	3.45	5.38	0.57
Energy	4.80	9.00	31.05	48.42	5.16
Tank Truck					
Capital	69.30	224.10	379.80	674.10	128.48
O & M	0.77	2.49	4.22	7.49	1.43
Energy	6.93	22.41	37.98	67.41	12.85

Assumptions:
energy 0.09 of total cost
O & M 0.01 of total cost
capital 0.90 of total cost

The model was restricted to the use of only one cooling tower unit and the use of only one emission treatment technology.

SUMMARY OF MODEL

Base case

Appendix A summarizes the data developed from the literature which constitute the base case for the model. Capital costs and O & M costs are evaluated at 1977 prices, water costs are $20/ac ft, energy costs are $20/MWH. For environmental quality constraints, a discharge standard of 500 ppm of TDS, a particulate emission standard of 7.68 tons/day and a SO_x emission standard of 92.2 tons/day are imposed. In Appendix A, flow diagrams are used to describe the liquid, solid, and gas influent and effluent streams of each unit. Figure 28 is a general description of the flow diagrams of Appendix A. The numbers at the top of the arrows pointing to the unit diagram box represents the influents that can enter the unit. The numbers at the tip of the arrows pointing from the unit diagram box represent the destinations where the effluent stream may be transferred for recycle, disposal, discharge, or additional treatment. Usually, the diagram box of a treatment unit has two effluent vectors sets. The top sets of effluent are the product streams and the bottom sets are the concentrated, or brine streams.

Below the table are other specifications for the unit that appear in the model. Table 30 is a description of the information found in Figure 28 and in Appendix A.

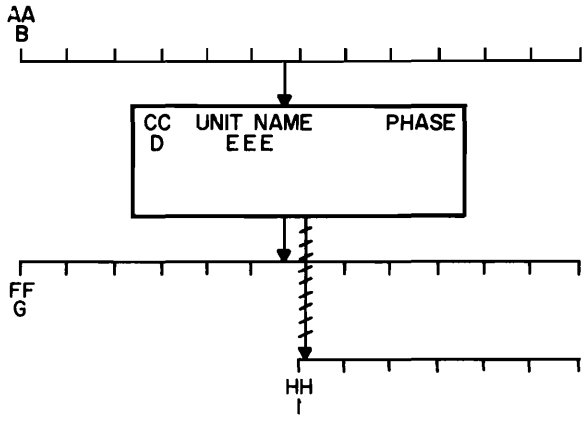

Figure 28. General appendix flow diagram.

Table 30. General flow diagram explanation.

AA	–	Number of subscripted influent variable of unit AA
B	–	Segment of unit AA
CC	–	Number of unit for which the flow diagram is intended
D	–	Segment of unit CC
EEE	–	Abbreviation of unit CC
FF	–	Number of subscripted product effluent variable to unit FF
G	–	Segment of unit FF
HH	–	Number of subscripted brine effluent variable to unit HH
I	–	Segment of unit HH
Phase	–	An identification defining the influent and effluent vectors as either liquid, solid, or gas

Model solution and sensitivity analysis

The applied mixed integer programming model was evaluated on the basis of updated costs, then subjected to sensitivity analysis for the following conditions:

Capital case	- an increase in all capital costs by 0.6 and 1.0 (multiplied by a factor of 1.6 and 2.0)
O & M case	- an increase in all operation and maintenance costs by 0.6 and 1.0 (multiplied by a factor of 1.6 and 2.0)
Energy case	- an increase in all energy costs from \$20/MWH in the base case to \$68/MWH and \$100/MWH
Water case	- an increase in all water costs from \$20/acft in the base case to \$500/acft and \$1,000/acft.

Table 31 is a summary of the costs that are entered in the objective function of the model for the various conditions. The value appearing under a continuous variable is the coefficient appearing in the objective function with the respective variable for each case. The coefficients of the continuous variables have the units of dollars per KTON and the continuous variables have units of KTONs per day. Likewise, values appearing under binary variables are coefficients to the respective binary variables and have the units of dollars per day. The binary variables are unitless. When the objective function is evaluated, the total cost for each unit in the optimal solution is in units of dollars per day.

In addition to the cost change sensitivity, the model was also used to evaluate the sensitivity to changes in discharge and emission standards for the following conditions:

Particulate case	- particulate emissions of 7.68 tons/day as the base case, to 21 tons/day and 60 tons/day
SO_x case	- sulfur oxide emissions of 92.2 tons/day as the base case, to 10 tons/day and 7 tons/day.
Discharge case	- total solids discharge of 500 ppm as the base case, to 5,500 ppm.

The discharge and emission standards were varied to provide an estimate of cost changes and resource input changes when standards are changed. The evaluation could provide useful information to society when new environmental standards are considered.

Table 31. Cost data summary.

	Variable	Influent Water	Evaporation Pond	5 Cycle	20 Cycle	50 Cycle	100 Cycle	Dry Cooling	Settling Pond	Lime Softening		Thickener I	Trickling Filter	
		XX_{01A}	X_{04A}	Z_2	Z_5	Z_6	Z_7	Z_8	X_{23A}	Y_{28}	X_{24A}	X_{25A}	Y_{29}	X_{26A}
	Increase by:													
Base		14.72	1,317.27	3,694	3,694	3,694	3,694	25,649	14.86	82.5	69.34	8.43	189	7.656
Capital	0.6	14.72	2,107.5	4,085	4,085	4,085	4,085	30,815	23.72	85.5	69.44	11.66	251	11.098
	1.0	14.72	2,634.4	4,346	4,346	4,346	4,346	34,259	29.63	87.4	69.51	13.82	292	13.392
O & M	0.6	14.72	1,317.27	3,694	3,694	3,694	3,694	25,649	14.86	129.	71.2	10.16	240	8.69
	1.0	14.72	1,317.27	3,694	3,694	3,694	3,694	25,649	14.86	160.	72.5	11.31	275	9.4
Energy	$68/MWH	14.72	1,317.7	10,998	10,998	10,998	10,998	66,545	15.1	82.5	227.7	8.84	189	8.1
	$100/MWH	14.72	1,318.0	15,868	15,868	15,868	15,868	93,809	15.2	82.5	330.3	9.10	189	8.4
Water	$500/AcFt	367.95												
	$1000/AcFt	735.89												

Note: - Coefficients to binary variables are in units of dollars per day.
- Coefficients to continuous variables are in units of dollars per KTON.
- Z and Y variables are binary and all other variables are continuous.

Table 31. Continued

	Variable	Activated Sludge		Air Flotation	Thickener II	Ion Exchange A		Ion Exchange B		Evapor. Crystal	MSF A		MSF K	
		Y_{32}	X_{34A}	X_{35A}	X_{38A}	Y_{10}	X_{40A}	Y_{11}	X_{40B}	X_{41A}	Z_{18}	X_{42A}	Z_{20}	X_{42K}
	Increase by													
Base		330	21.035	248.2	24.95	264.5	94.708	596	85.5	1,011.3	780	2,499	778	3,417.04
Capital	0.6	434	24.5	394.0	34.65	416	150.0	936	135.5	1,411.6	1,243	2,583.5	1,243	3,501.5
	1.0	504	26.7	491.2	41.12	516	186.9	1,166	168.9	1,728.4	1,553	2,639.8	1,553	3,557.8
O & M	0.6	422	29.8	251.1	30.13	272	96.0	612	86.6	1,021.4	781	2,855	781	3,773.0
	1.0	485	35.7	253.1	33.57	278	96.8	622	87.3	1,028.2	782	3,092.3	782	4,010.4
Energy	$68/MWH	330	22.7	249.0	25.37	265	95.7	596	86.5	1,676.9	778	6,735	778	9,856.2
	$100/MWH	330	23.8	249.6	25.64	265	96.3	596	87	2,120.6	778	9,558	778	14,149.0

Table 31. Continued.

	Variable	MSF U		Dialysis A		Dialysis F		Dialysis P		Dialysis U		Reverse Osmosis A		Reverse Osmosis B	
		Z_{22}	X_{42U}	Z_{23}	X_{43A}	Z_{24}	X_{43F}	Z_{26}	X_{43P}	Z_{27}	X_{43U}	Z_{12}	X_{44A}	Z_{13}	X_{448}
	Increase by:														
Base		778	6,184.46	598	22.306	1,398	80.2	1,797	201.92	1,996	365.8	1,076	291.45	2,716	245.92
Capital	0.6	1,243	6,268.9	958	33.7	2,236	106.8	2,875	236.0	3,243	402.7	1,378	430.0	3,801	362.3
	1.0	1,553	6,325.2	1,198	41.2	2,795	124.4	3,594	258.8	3,994	428.9	1,579	521.6	4,525	439.8
O & M	0.6	781	6,540.4	599	23.2	781	3,199.2	781	5,261.8	781	6,540.4	1,400	324.5	3,255	272.9
	1.0	782	6,777.8	599	23.8	782	3,436.5	782	5,499.2	782	6,777.8	1,615	346.5	3,614	291.1
Energy	$68/MWH	778	19,265.4	599	26.8	778	7,905.3	778	14,918.1	778	19,265.4	1,161	306.5	2,737	262.7
	$100/MWH	778	27,986.0	599	29.8	778	11,280.0	778	21,593.0	778	27,986.0	1,218	316.5	2,752	273.9

Table 31. Continued.

	Variable	Reverse Osmosis K		Reverse Osmosis L		Limestone Scrubber		Electro. Precip.	Stack	Particulate Scrubber		Combination pptor-Scrub		Slurry Disposal	Truck Disposal
		Z_{16}	X_{44K}	Z_{17}	X_{44L}	Y_{34}	O_{51A}	O_{52A}	H_{53A}	Y_{35}	O_{54A}	Y_{36}	O_{55A}	XT_{60A}	XT_{61A}
	Increase by:														
Base		381.6	101.1	909	86.43	11,852	70.736	46.63	0.489	5.6	31.012	11,852	117.37	57.3	142.7
Capital	0.6	482	147	1,270	125.1	13,829	70.736	68.024	0.782	7.6	32.4	13,829	138.8	88.2	219.8
	1.0	846	152.9	1,511	150.9	15,147	70.736	82.286	0.978	9.0	33.4	15.147	153.0	108.9	271.2
O & M	0.6	489	112.1	1,088	95.4	16,987	70.736	47.345	0.489	6.0	31.9	16,987	118.1	57.6	143.6
	1.0	561	119.4	1,208	101.4	20,410	70.736	47.821	0.489	7.6	32.4	20,410	118.6	57.9	144.1
Energy	$68/MWH	923	97.6	931	103.2	11,853	240.5	70.117	0.489	6.0	96.3	11,853	310.6	60.4	150.4
	$100/MWH	938	108.8	945	114.4	11,853	353.68	85.775	0.489	6.0	139.8	11,853	439.4	62.5	155.5

DISCUSSION OF RESULTS

BASE CASE

The mixed integer programming model was run on the Burrough's 6700/7700 Tempo version 28,6000,000. The model consisted of 213 rows and 573 variables. Of the variables, 25 were integer zero-one variables. Appendix B contains a summary of the data which was entered into the model for the base case evaluation. A user will find Appendix B contains the data in the order required for the Tempo program.

Table 32 is a summary of the base case optimal solution. The table presents the optimal

Table 32. Summary of optimal base solution.

Control Technology	Optimal Capacity (mgd)	Cost Segment ($/Day)	($/Day)	Total Costs ($/Day)	Percent of Total	Energy (MWH/Day)	Water (mgd)
Cooling Tower 5 Cycle		Capital	650.14				
		Energy	3043.86		22.51	152.19	
		Total		3694.00			
Lime Softener	12.125	Capital	16.72				
		O & M	264.38		16.22	119.04	
		Energy	2380.85				
		Total		2662.19			
Electrodialysis	12.811	Capital	3176.40				
		O & M	54.61		27.73	65.99	
		Energy	1319.71				
		Total		4550.72			
Thickener	3.291	Capital	54.40				
		O & M	28.94		0.52	0.09	
		Energy	1.79				
		Total		85.13			
Air Flotation	0.0003	Capital	0.03				
		O&M			0.03		
		Energy					
		Total		0.03			
Trickling Filter	0.011	Capital	54.40				
		O & M	28.94		1.15	0.10	
		Energy	1.79				
		Total		189.26			
Pipeline Slurry Disposal	1.364	Capital	215.86				
		O & M	2.40		1.46	1.08	
		Energy	21.59				
		Total		239.84			
Influent Water	8.723	Water	394.00		2.40		8.723
		Total		394.00			
Electrostatic (ACFM) Precipitator	4226.46	Capital	3236.40				
		O & M	105.66		25.75	44.38	
		Energy	887.54				
		Total		4226.36			
	(ft.)						
Gas Stack	750	Capital	366.75		2.25		
		Total		366.75			
Total				16,408.28	100.00	382.87	8.723

control and recycle strategy including the optimal capacity of treatment unit, the total cost per day, and the capital, O & M, and other resource requirements for each treatment unit. The influent streams to the production and treatment units in the optimal solution are summarized in Table 33. The total energy in the base case was 383 MWH/day. Of this amount, the cooling tower would require 152 MWH/day or 40 percent of the total energy consumed. Other high energy consumers include the lime softening unit with a consumption rate of 119 MWH/day or 31 percent of the total energy required in the base case, the electrodialysis unit with an energy consumption rate of 6.6 MWH/day and the electrostatic precipitator with a consumption rate of 44 MWH/day.

SENSITIVITY ANALYSIS CASES

The model was subjected to increases in capital, energy, water and other O & M costs in addition to changes in air emission and water discharge standards to compare the effects of the cases with the base case. The results of the cases are summarized in Table 34 and depicted in Figures 29-38. Table 34 also includes a summary of the optimized and the normal costs for each of the cases. Table 40 summarizes the optimal treatment unit sizes for the different cases.

Table 33. Treatment unit and process unit influent sources.

Optimal Treatment Unit	Influent Source	Stream Size (mgd)
Trickling Filter	Sanitary Waste	8.156×10^{-3}
Air Flotation	Cleaning Waste	2.4×10^{-5}
Lime Softening	Stream	7.298
	Cooling Tower	1.627
Electrodialysis	Cooling Tower	0.589
	Lime Softening	8.841
	Air Flotation	2.4×10^{-5}
Thickener	Lime Softening	0.084
	Trickling Filter	2.4×10^{-6}
	Electrodialysis	2.339
Truck Disposal	Thickener	0.799
	Boiler	0.064
	Elect-PPTOR	0.1418
Electrostatic Precipitator	Boiler	
Condenser	Stream	2.455
	Cooling Tower	377.623
	Thickener	1.623
	Activated Sludge	8.15×10^{-3}
	Electrodialysis	7.09
		(ACFM)[a]
Stack	Boiler	1.08589
	Elect-PPTOR	90.63611

[a]ACFS = actual cubic feet per minute.

The optimized cost refers to the actual cost identified in the total cost summary when the objective function of the model was calculated in the optimal solution. The optimized cost data were normalized against the base case to provide a method of comparing resource input requirements with the base case and with the other cases.

The normalized cost is explained with the example of the capital case. After the capital costs of all the units were increased by 60 percent from the base case (multiplied by a factor of 1.6) and the optimal solution identified, the optimized capital cost factor for each unit is identified. The optimized capital cost for each unit is subsequently reduced to a normal capital cost by dividing the optimized capital cost by a factor of 1.6. The resulting normal capital cost is considered the actual amount of capital used and is described in units of dollars per day. In the example of the capital case the optimized O & M, energy, and water costs do not require normalizing because the cost of those input factors are not changed and are, therefore, also considered normal costs. Likewise, the water case requires a comparison of water requirements. However, rather than reducing the water costs to units of dollars per day, a convenient unit of comparison of water requirements. However, rather than reducing the water costs to units of dollars per day, a convenient unit of comparison for water resource requirements is KTONs of influent water per day. The method of normalizing the data for comparison purposes is the same for both cases.

The normal total cost for any case is identified by subtracting the difference between the optimal and normal factor costs from the optimized total cost. Table 34 summarizes the total cost requirements including the water and energy requirements for the sensitivity cases. Tables 35 through 39 are summaries of the normalized and optimal capital, O & M, energy, and water costs requirements, respectively, for each of the units in the optimal solution for the sensitivity cases. Table 40 summarizes the optimal size of each treatment unit for each evaluated sensitivity case.

Capital cost case

The model's response to the capital cost changes are summarized in Figures 29 and 32.

Table 36. O & M costs optimal and normalized for sensitivity cases.

	Case: Base	Capital		O & M		Energy		Water		Particulate		SOX		TDS
		0.6	1.0	0.6	1.0	$68/MWH	$100/MWH	$500/AcFt	$1000/AcFt	60 TPD	21 TPD	7 TPD	10 TPD	5500 PPM
							($/Day)							
Mechanical Draft Wet Cooling														
Influent Water														
Lime Softener	264.38	261.84	278.26	268.86 430.18	267.45 534.90	262.07	262.34	262.32	278.49	262.32	264.38	259.21	259.36	264.38
Electrodialysis	54.61	64.34	48.95					54.61	49.25	54.61	54.61	53.55	53.60	54.61
Ion Exchange				101.99 163.18	101.94 203.87	86.99	87.14							
Reverse Osmosis						451.96	464.40							
Trickling Filter	69.13	66.66	65.39	72.27 115.63	77.68 155.37	67.42	66.36	69.13	69.13	69.13	69.13	69.13	69.13	69.13
Thickener I	28.94	28.97	25.34	38.48 61.56	38.51 77.02	48.40	48.19	28.94	25.26	28.94	28.94	28.13	28.17	28.94
Thickener II												12.28	11.61	
Slurry Disposal	2.40	2.58	2.05	3.04 4.86	3.06 6.11	0.39	0.40	2.40	2.15	2.36	2.39	2.28	2.27	2.40
Air Flotation														
Electrostatic Precipitator	105.66	104.81	104.41	107.28 171.65	108.36 216.72	108.04	108.84	105.66	105.66	96.33	105.43			105.66
Stack														
Limestone Scrubber												8569.07	8583.43	

Table 35. Capital costs optimal and normalized for sensitivity cases.

	Case: Base	Capital		O & M		Energy		Water		Particulate		SOX		TDS
		0.6	1.0	0.6	1.0	$68/MWH	$100/MWH	$500/AcFt	$1000/AcFt	60 TPD	21 TPD	7 TPD	10 TPD	5500 PPM
							($/Day)							
Mechanical Draft Wet Cooling	650.14	651.68 1041.68	651.3 1302.6	650.14	650.14	648.88	650.59	650.14	650.14	650.14	650.14	650.14	650.14	650.14
Influent Water														
Lime Softener	16.72	16.09 25.75	8.25 17.05	17.92	16.50	16.12	17.50	16.72	17.49	16.72	16.72	16.36	16.37	16.72
Electrodialysis	3176.40	3164.91 5063.86	2874.10 5748.21					3179.40	2864.87	3176.40	3176.39	3114.69	3117.76	3176.40
Ion Exchange				4182.80	4182.26	3461.04	3459.91							
Reverse Osmosis						1231.08	1264.96							
Trickling Filter	118.14	114.57 183.31	112.62 225.25	120.82	118.14	115.57	113.76	118.14	118.14	118.14	118.14	118.14	118.14	118.14
Thickener I	54.40	54.39 87.02	47.50 95.01	72.19	72.32	90.30	90.40	54.40	47.48	54.40	54.40	52.87	52.95	54.40
Thickener II												23.08	21.83	
Slurry Disposal	215.86	215.74 345.19	193.98 387.95	272.34	271.92	332.22	329.80	215.86	194.00	213.16	215.17	205.20	204.10	215.86
Air Flotation	0.02	0.02 0.04	0.02 0.05	0.02	0.02	0.02	0.02	0.02	0.02	0.02	0.02	0.02	0.02	0.02
Electrostatic Precipitator	3236.40	3233.0 5172.8	3233.08 6466.16	3231.25	3233.40	3234.76	3234.11	3333.16	3233.16	2947.65	3158.74			3236.40
Stack	366.75	366.56	366.56	366.75	366.75	366.75	366.75	366.75	366.75	366.75	366.75	366.75	366.75	366.75
Limestone Scrubber		586.50	733.5									3303.22	3310.62	

Table 34. Total costs and resource input requirements for sensitivity cases.

	Case: Base	Capital		O & M		$/MWH Energy		$/Ac.Ft. Water		Part		SOX		TDS
		0.6	1.0	0.6	1.0	68	100	500	1000	60 TPD	21 TPD	7 TPD	10 TPD	5500 PPM
Influent Water (Ac. ft/d)	19.7	19.7	19.39	20.50	20.50	21.32	21.32	19.70	19.38	19.70	19.70	19.97	20.00	19.7
Total Energy (MWH/d)	382.94	382.16	411.69	338.82	337.77	315.02	314.33	382.98	410.76	379.05	381.83	652.84	634.66	382.94
								$/Day						
Total Cost														
Normal	16,408.28	16,382.76	16,902.67	16,692.50	16,673.98	17,248.65	17,277.57	16,408.21	16,624.84	16,032.06	16,312.30	30,300.57	29,958.47	16,408.28
Optimized		21,072.57	24,121.71	17,047.65	17,270.98	32,369.73	42,420.22	25,862.43	35,621.74					
Capital Cost														
Normal	7,831.58	7,816.34	7,219.04	8,914.23	8,911.45	9,496.74	9,527.80	7,831.59	7,492.05	7,543.38	7,756.47	7,850.45	7,858.58	7,831.58
% of Total	47.73	47.71	45.02	53.40	53.44	55.06	55.14	47.73	45.06	47.05	47.55	25.91	26.23	47.73
Optimized		12,506.15	14,438.08											
O & M Cost														
Normal	525.13	529.30	667.07	591.91	597.00	1,025.47	1,037.67	523.06	529.93	513.69	524.88	8,993.65	9,007.47	525.13
% of Total	3.20	3.23	3.15	3.55	3.58	5.94	6.00	3.19	3.19	3.20	3.22	29.68	30.07	3.20
Optimized				947.06	1,193.99									
Energy Cost														
Normal	7,657.32	7,643.20	8,628.80	6,776.32	6,755.47	6,300.45	6,285.66	7,659.63	8,215.13	7,580.98	7,636.69	13,056.78	12,693.11	7,657.32
% of Total	46.66	46.65	49.50	40.59	40.52	36.53	36.38	46.68	49.41	47.29	46.82	43.09	42.37	46.66
Optimized						21.421.53	31.428.31							
Water Cost														
Normal	394.00	394.00	387.75	410.05	410.05	426.41	426.41	393.93	387.69	393.99	393.99	399.65	399.33	394.00
% of Total	2.40	2.40	2.33	2.46	2.46	2.47	2.47	2.40	2.33	2.46	2.42	1.32	1.33	2.40
Optimized								9,848.15	19,384.59					

Ac. ft/d - acre feet per day
MWH/d - megawatt hours per day
$/day - dollars per day
TPD - tons per day
PPM - parts per million

Table 37. Energy costs optimal and normalized for sensitivity cases.

	Case: Base	Capital		O & M		Energy		Water		Particulate		SOX		TDS
		0.6	1.0	0.6	1.0	$68/MWH	$100/MWH	$500/AcFt	$1000/AcFt	60 TPD	21 TPD	7 TPD	10 TPD	5500 PPM
							($/Day)							
Mechanical Draft Wet Cooling	3043.00	3043.32	3043.86	3043.86	3043.40	3043.86 10349.12	3043.48 15217.41	3043.86	3043.86	3043.86	3043.86	3043.86	3043.86	3043.00
Influent Water														
Lime Softener	2380.85	2381.29	3084.14	2794.12	2778.66	2294.79 7802.30	2280.90 11404.48	2383.15	3070.50	2383.15	2380.85	2314.28	2318.07	2380.85
Electrodialysis	1319.71	1306.18	1195.80					1319.71	1190.28	1319.71	1319.70	1294.07	1295.35	1319.71
Ion Exchange				17.03	17.17	13.74 46.73	13.74 68.70							
Reverse Osmosis						41.64 141.59	42.75 213.74							
Trickling Filter	1.98	1.41	1.81	3.84	1.81	1.85 6.28	1.83 9.16	1.99	1.99	1.99	1.99	1.99	1.99	1.98
Thickener I	1.79	1.77	1.46	2.45	2.27	2.92 9.93	2.88 14.38	1.79	1.56	1.79	1.79	1.79	1.74	1.79
Thickener II												0.72	0.72	
Slurry Disposal	21.59	21.41	19.66	26.75	27.50	15.66 53.25	13.82 69.08	21.59	19.40	21.32	21.52	20.52	20.41	21.59
Air Flotation														
Electrostatic Precipitator	887.54	887.82	887.51	888.27	884.20	885.98 3012.33	886.27 4431.36	887.54	887.54	809.16	866.98			
Stack														
Limestone Scrubber													6379.56	6011.07

Table 38. Energy requirements for sensitivity cases.

	Case: Base	Capital		O & M		Energy		Water		Particulate		SOX		TDS
		0.6	1.0	0.6	1.0	$68/MWH	$100/MWH	$500/AcFt	$1000/AcFt	60 TPD	21 TPD	7 TPD	10 TPD	5500 PPM
							(MWH/Day)							
Mechanical Draft Wet Cooling	152.19	152.17	152.17	152.17	152.17	152.19	152.17	152.19	152.19	152.19	152.19	152.19	152.19	152.19
Influent Water														
Lime Softener	119.04	119.06	154.21	139.71	138.93	114.74	114.04	119.16	153.54	119.16	119.04	115.71	115.90	119.04
Electrodialysis	65.99	65.31	59.79					65.99	59.51	65.99	65.98	64.70		65.99
Ion Exchange				0.85	0.86	0.69	0.69							
Reverse Osmosis						2.08	2.14							
Trickling Filter	0.10	0.07	0.09	0.07	0.09	0.09	0.09	0.10	0.10	0.10	0.10	0.10	0.10	0.10
Thickener I	0.09	0.08	0.07	0.12	0.11	0.15	0.14	0.09	0.97	0.09	0.09	0.09	0.09	0.09
Thickener II												0.04	0.04	
Slurry Disposal	1.08	1.07	0.98	1.34	1.37	0.78	0.69	1.08		1.07	1.08	1.03	1.02	1.08
Air Flotation														
Electrostatic Precipitator	44.38	44.39	44.38	44.41	44.21	44.30	44.36	44.38	44.35	40.46	43.35			44.38
Stack														
Limestone Scrubber												318.98	300.55	

Table 39. Water costs—normal and optimized for sensitivity cases ($/day).

	Case: Base	Capital		O & M		Energy		Water		Particulate		SOX		TDS
		0.6	1.0	0.6	1.0	$68/MWH	$100/MWH	$500/AcFt	$1000/AcFt	60 TPD	21 TPD	7 TPD	10 TPD	5500 PPM
Influent Water	394.00	394.00	387.75	410.05	410.05	426.41	426.41	394.00 9848.15	387.69 19,384.59	393.99	393.99	399.65	399.33	394.00

Table 40. Optimal design capacity for sensitivity cases.

	Case: Base	Capital		O & M		Energy		Water		Particulate		SOX		TDS
		0.6	1.0	0.6	1.0	$68/MWH	$100/MWH	$500/AcFt	$1000/AcFt	60 TPD	21 TPD	7 TPD	10 TPD	5500 PPM
Mechanical Draft Wet Cooling	5 Cycle	5 Cycle	5 Cycle	5 Cycle	5 Cycle	5 Cycle	5 Cycle	5 Cycle	5 Cycle	5 Cycle	5 Cycle	5 Cycle	5 Cycle	5 Cycle
							MGD							
Influent Water	6.421	6.421	6.32	6.683	6.682	6.949	6.949	6.421	4.630	6.421	6.421	6.513	6.508	6.421
Lime Softener	8.925	8.925	11.36	10.490	10.489	8.426	8.426	8.925	11.36	8.925	8.925	8.675	8.687	8.925
Electrodialysis	9.430	9.430	8.095					9.430	8.095	9.430	9.430	9.166	9.179	9.430
Ion Exchange				10.391	10.391	8.347	4.02							
Reverse Osmosis						2.216	2.216							
Trickling Filter	0.008	0.008	0.008	0.008	0.008	0.008	0.008	0.008	0.008	0.008	0.008	0.008	0.008	0.008
Thickener I	2.423	2.423	2.114	3.216	3.216	4.024	4.024	4.024	2.114	2.423	2.423	2.355	2.358	2.423
Thickener II												0.347	0.328	
Slurry Disposal	1.004	1.004	0.902	1.266	1.266	1.532	1.532	1.004	0.902	0.992	1.00	0.955	0.9495	1.004
							ACFM							
Air Flotation (2.3×10^{-5} MGD)	X	X	X	X	X	X	X	X	X	X	X	X	X	X
Electrostatic Precipitator	1.68×10^6	1.68×10^6	1.68×10^6	1.68×10^6	1.68×10^6	1.68×10^6	1.68×10^6	1.68×10^6	1.68×10^6	1.53×10^6	1.642×10^6			1.68×10^6
Stack	1.7×10^6	1.7×10^6	1.7×10^6	1.7×10^6	1.7×10^6	1.7×10^6	1.7×10^6	1.7×10^6	1.7×10^6	1.7×10^6	1.7×10^6	1.7×10^6	1.7×10^6	1.7×10^6
Limestone Scrubber												1.677×10^6	1.586×10^6	

Figure 29 indicates that as the cost of capital increases, the amount of capital used by the optimal control unit alternatives decreases. The model, according to the results summarized in Table 40, was able to identify treatment alternatives that require less capital to minimize the total cost. The optimal treatment units were the same as the base case but with different capacities. The changes that result from capital cost increases are increases in the capacity of the O & M and energy intense lime softener and decreases in the optimal capacity of the capital intense electrodialysis unit. As a result of capacity differences in the capital case, less water was used (see Table 40 and Figure 32). The model identified alternative treatment strategies that could be used to compensate for the decrease in capital requirements and simultaneously meet environmental and production requirements. The capital requirements would be replaced by increases in O & M (see Figure 30) and energy requirements when the cost of capital increases.

O & M cost case

Unlike the normal capital which decreased its use of capital with an increase in the cost of capital, an increase in the cost in the O & M case elicited a slight increase in the normalized cost of the O & M used (see Figure 31). However, the ion exchange replaced the electrodialysis unit from the base case

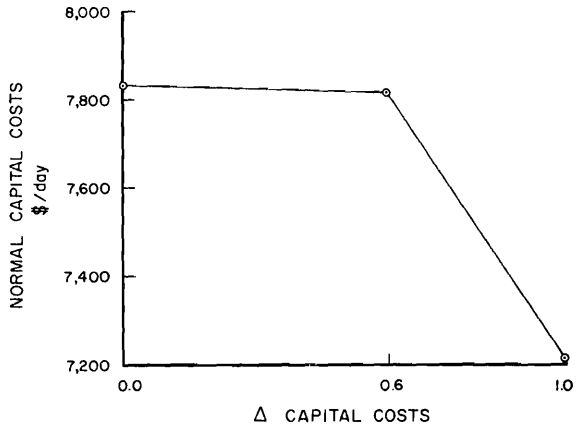

Figure 29. Capital cost change vs. capital requirements.

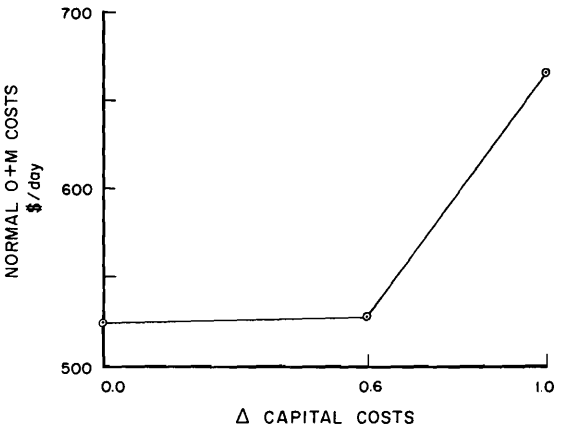

Figure 30. Capital cost change vs. O & M requirements.

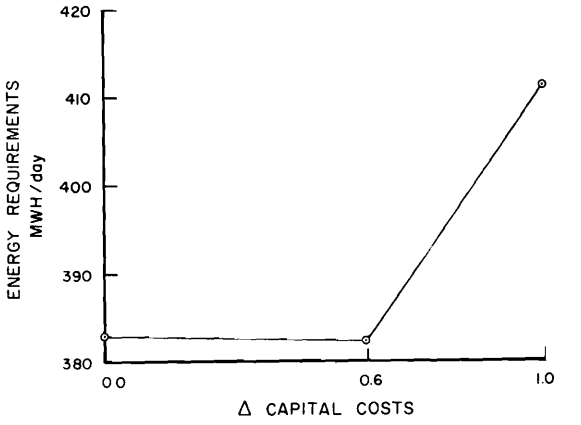

Figure 31. Capital cost change vs. energy requirements.

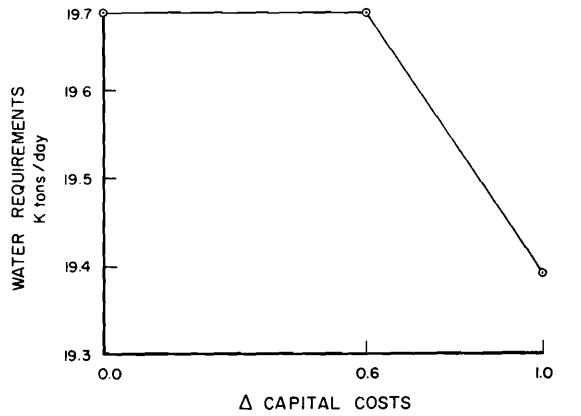

Figure 32. Capital cost change vs. water requirements.

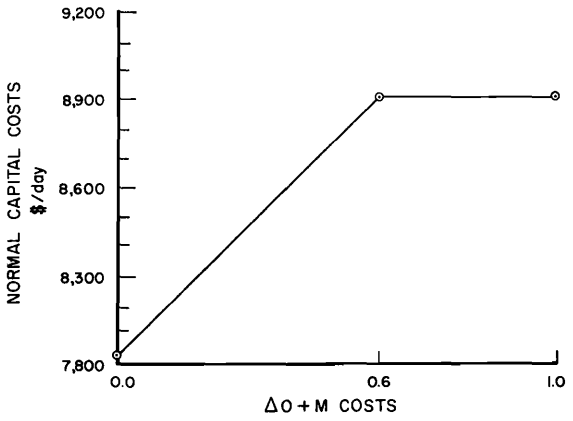

Figure 33. O & M cost change vs. capital requirements.

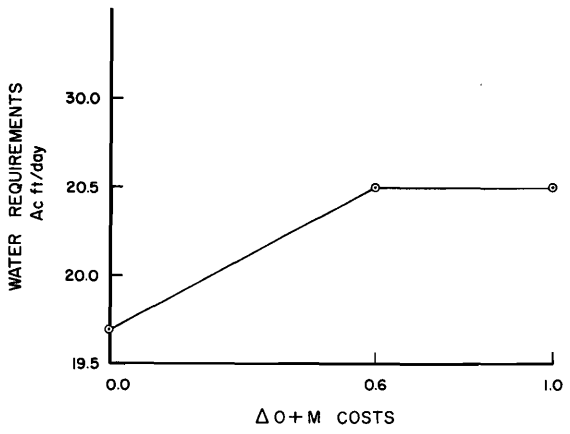

Figure 36. O & M cost change vs. water requirements.

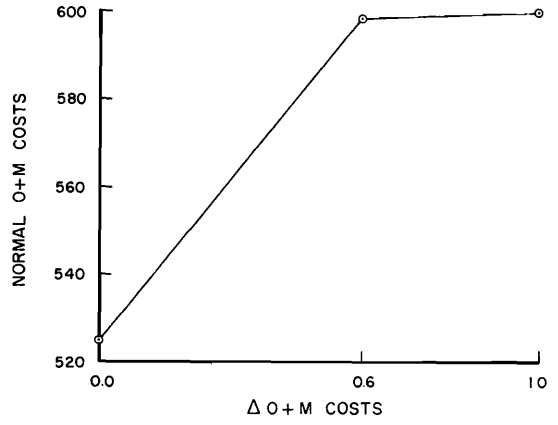

Figure 34. O & M cost changes vs. O & M requirements.

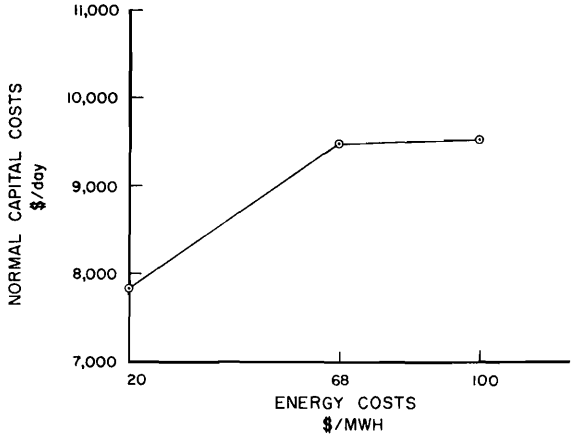

Figure 37. Energy cost change vs. capital requirements.

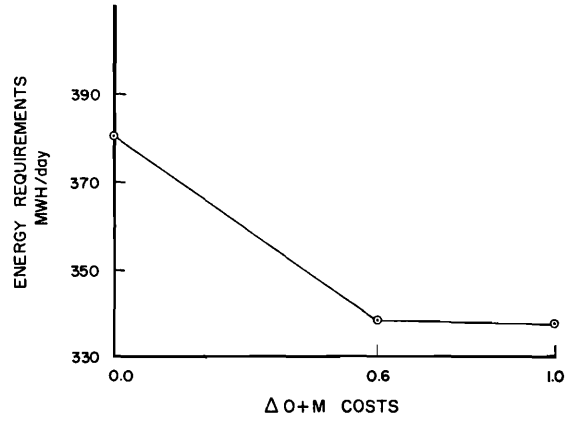

Figure 35. O & M cost change vs. energy requirements.

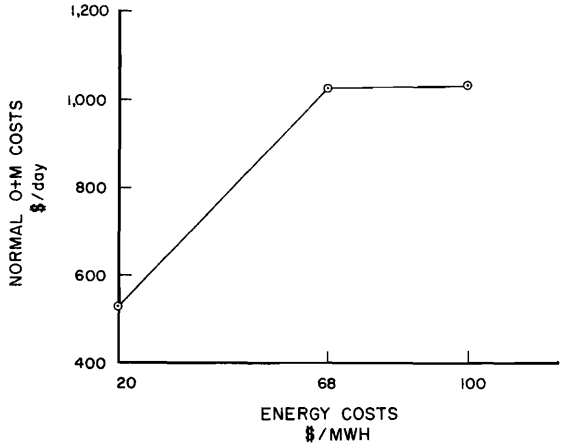

Figure 38. Energy cost change vs. O & M requirements.

and the capacity of the lime softener was increased to avoid even higher O & M requirements (see Table 36). By using the ion exchange unit in the optimal solution to minimize the O & M requirements, the total energy requirements were also reduced (see Figure 35) while capital and water requirements were increased. The capital, O & M, and other resource requirements were relatively insensitive to change when the O & M costs were increased more than 60 percent (see Figures 33, 34, 35, and 36 respectively).

Energy cost case

Figure 39 describes the response of the model's energy requirements to changes in the cost of energy. With an increase in energy costs from \$20/MWH in the base case to \$68/MWH, ion exchange and reverse osmosis units entered in the optimal solution to replace the electrodialysis unit from the base solution (see Table 40). Because of changes in energy cost and in the optimal treatment units, the amount of O & M, energy, and water requirements increases from the base case. Changes in energy costs from \$68/MWH to \$100/MWH require significantly smaller changes in the amount of capital, O & M, energy and water in comparison to the energy cost changes from \$20/KWH to \$68/KWH (see Figures 37 through 40).

Water cost case

Figure 44 shows that the water requirements in the model are relatively insensitive to changes in water costs. However, the cost of water has a significant effect on the amount of capital and energy used and only small effects on the amount of O & M required (see Figures 41, 42, and 43 respectively).

When the cost of water was increased, the optimal sizes of the lime softener and the electrodialysis unit were changed with reduced energy requirements (see Figure 43) and capital requirements (see Figure 41), and increased O & M requirements (see Figure 42).

Particulate emission standard case

As illustrated in Figures 45, 46, 47, and 48, imposing stricter emission standards increase the over all capital, O & M, and energy costs respectively. There is, however, no effect on water requirements. The differences in the volume of the boiler gas stream treated by the electrostatic precipitator influences the size of the optimal slurry disposal unit (see Table 40). Therefore, the cost of the electrostatic precipitator and the slurry disposal

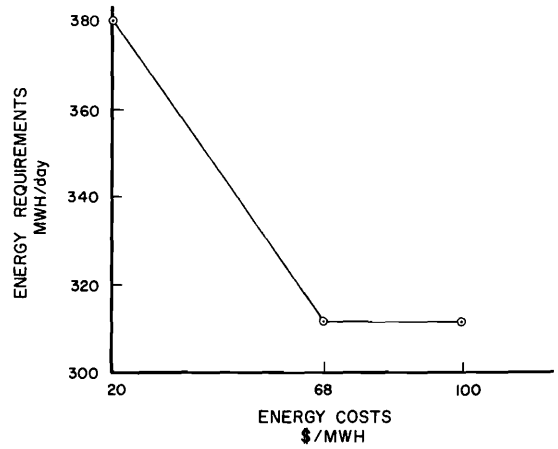

Figure 39. Energy cost change vs. energy requirements.

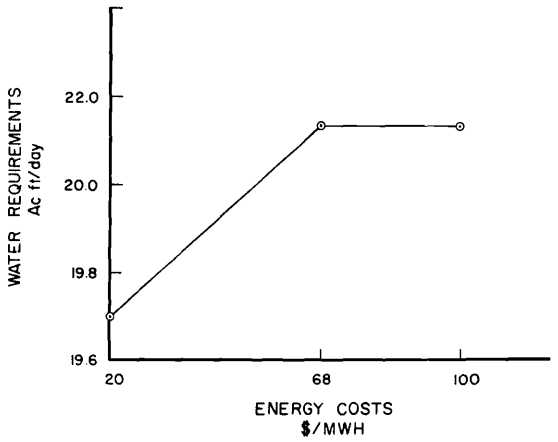

Figure 40. Energy cost change vs. water requirements.

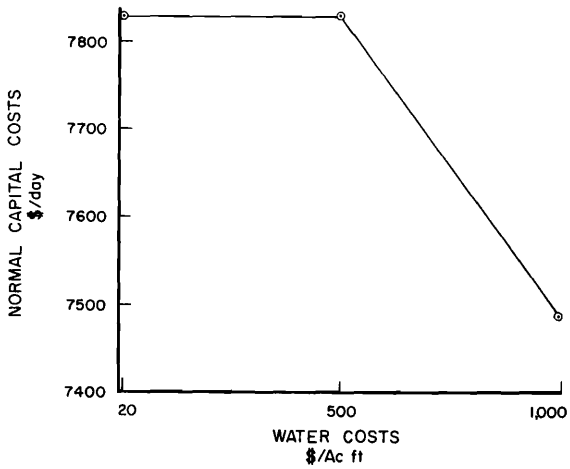

Figure 41. Water cost change vs. capital requirement.

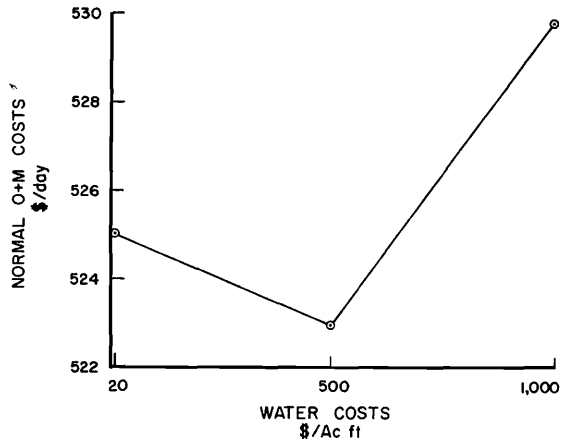

Figure 42. Water cost change vs. O & M requirement.

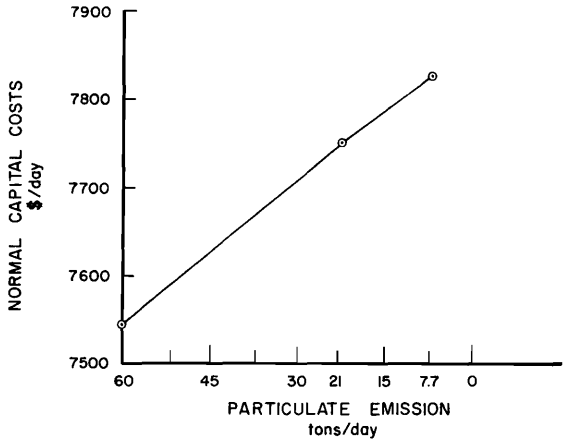

Figure 45. Particulate emission standard change vs. capital requirement.

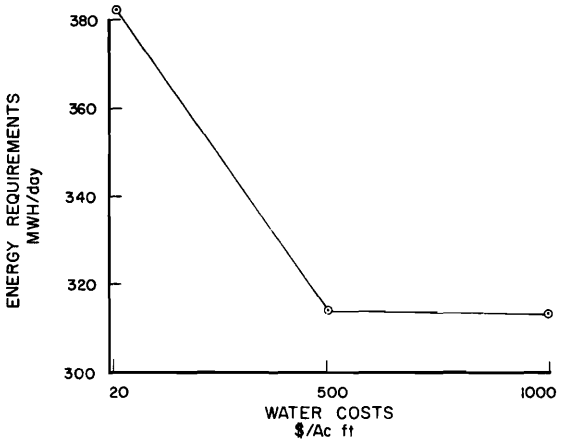

Figure 43. Water cost change vs. energy requirement.

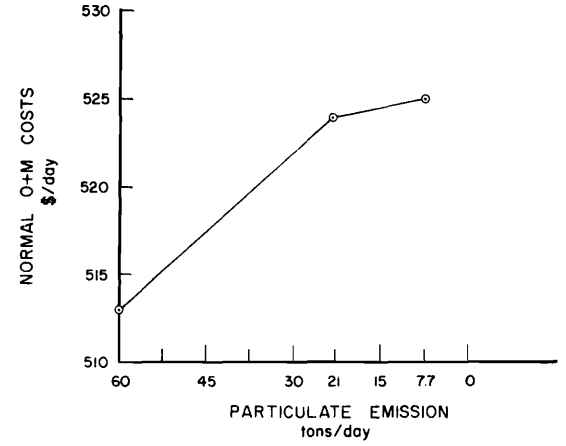

Figure 46. Particulate emission standard change vs. O & M requirement.

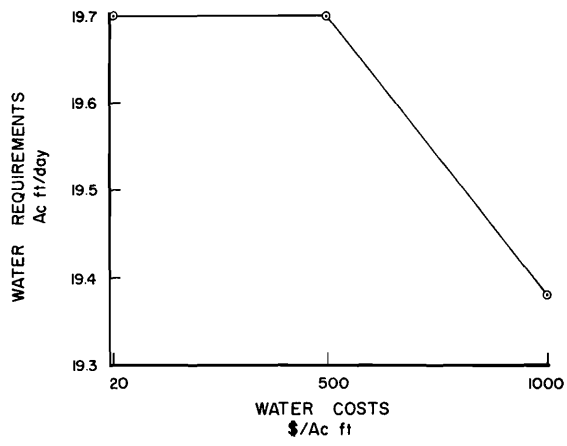

Figure 44. Water cost change vs. water requirement.

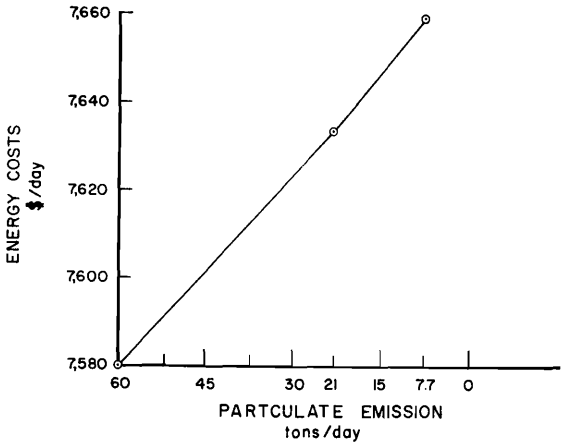

Figure 47. Particulate emission standard change vs. energy requirement.

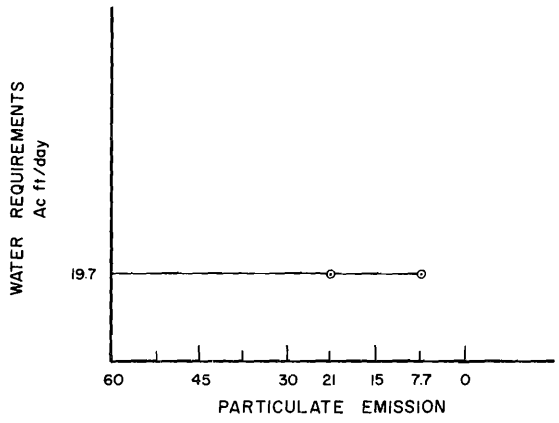

Figure 48. Particulate emission standard change vs. water requirement.

units contribute to changes in the total and the individual cost segments.

Sulfur dioxide emission standard case

For the base case, the particulate emission standard of 7.68 tons per day is the controlling environmental constraint as in the sulfur oxide emission standard of 92.2 tons per day does not affect the solution. To test the sensitivity to the sulfur oxide emission standard, the particulate emission standard was relaxed to a level where it was no longer binding, and the sulfur oxide emission standards were restricted to 10 tons per day and 7 tons per day. When the sulfur oxide standard becomes a binding constraint, the electrostatic precipitator unit is replaced in the optimal solution by the limestone slurry scrubber unit. As the result of using the limestone slurry scrubber unit, the thickener unit (provided in the model for air derived slurry stream thickening) was introduced into the optimal solution. Other changes that occur in the optimal solution with the sulfur oxide emission standard case are shown in Table 40. Although the units in the sulfur oxide emission standard case are the same as those in the base case, the optimal size of the units all change.

While the energy and water requirements increase with tighter restrictions on sulfur oxide emissions, the capital and O & M requirements decrease significantly at sulfur oxide emissions standards less than 10 tons per day (see Figures 51, 52, 49, and 50 respectively). The peaking effect seen in Figures 49 and 50 can be explained by the fact that in the base case solution (represented on the abscissa by 92.2 tons per day), an electrostatic precipitator is required. This is replaced by a limestone slurry scrubber process, in the two cases, when sulfur oxide emissions are restricted. The secondary effects are economies of scale with larger sizes of other units at the 7 tons/day SO_x emission standard and account for the drop in capital and O & M requirements seen in Figures 49 and 50. If the limestone slurry scrubber had been in the optimal base case solution instead of the electrostatic precipitator, the capital and O & M curves in Figures 49 and 50 would probably be represented by more uniform decreasing cost curves.

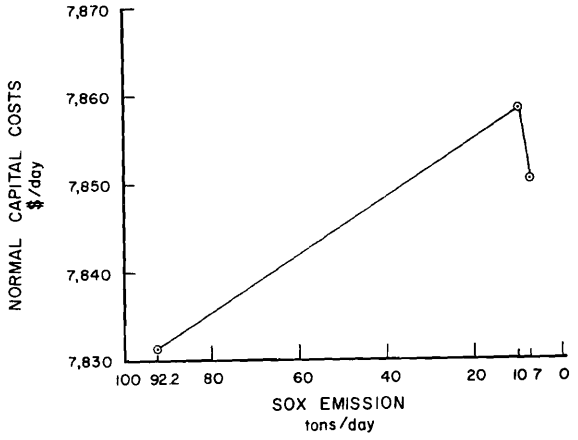

Figure 49. Sulfur oxides emission standard change vs. capital requirement.

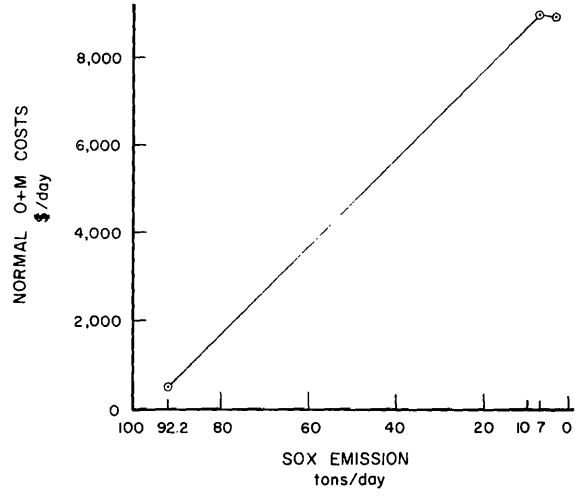

Figure 50. Sulfur oxides emission standard change vs. O & M requirement.

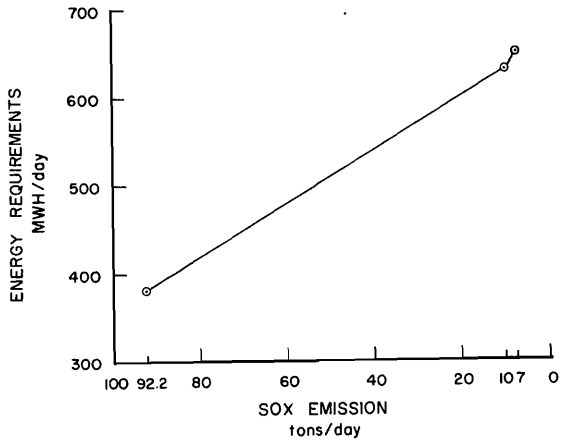

Figure 51. Sulfur oxides emission standard change vs. energy requirement.

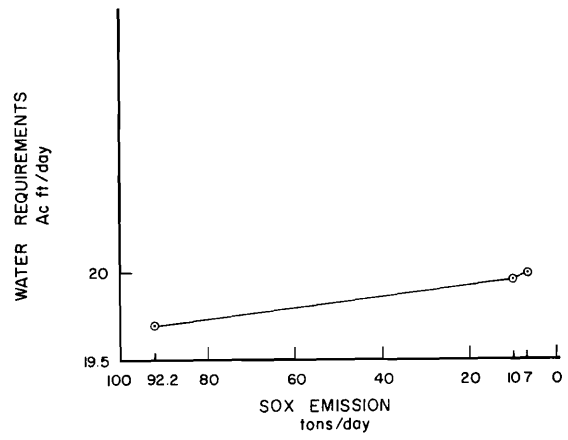

Figure 52. Sulfur oxides emission standard change vs. water requirement.

Water quality discharge standard case

The effluent discharge standard was relaxed from 500 ppm to 5,500 ppm with no resulting changes from the base case (see Tables 33 through 39). The model indicates, therefore, that it is more economical to recycle after treatment than to discharge the water to the stream.

Sensitivity analysis summary—total costs

As a result of changes in resource factor costs, and of changing environmental standards, the optimized total costs requirements for controlling the residuals from the 750 MW powerplant also change. Figures 53-58 summarize the response optimized total costs to the sensitivity cases.

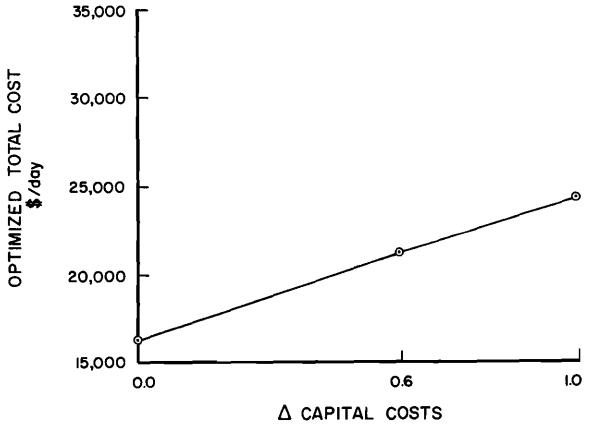

Figure 53. Capital cost change vs. total cost.

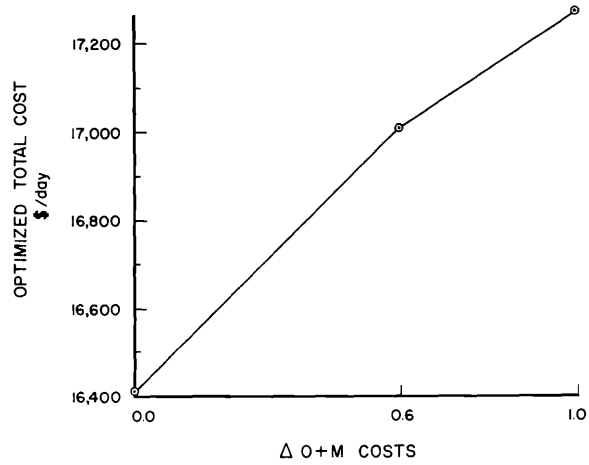

Figure 54. O & M cost change vs. total cost.

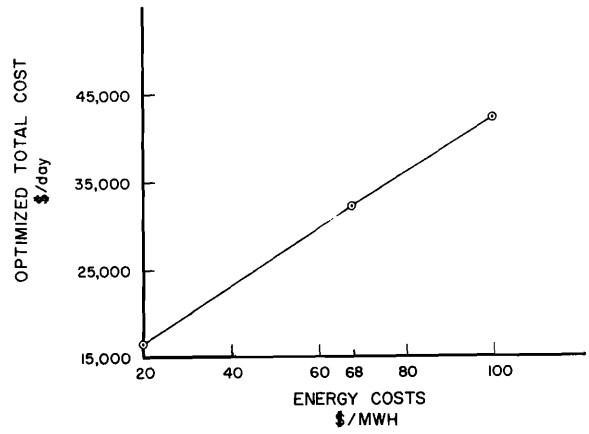

Figure 55. Energy cost change vs. total cost.

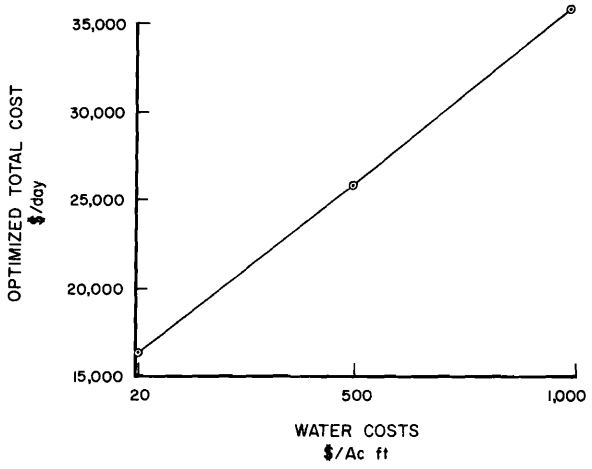

Figure 56. Water cost change vs. total cost.

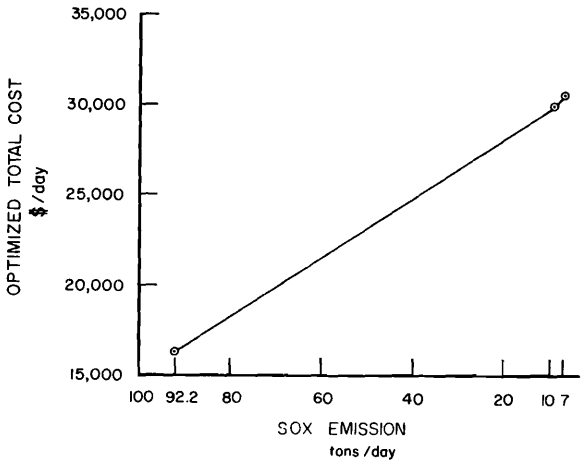

Figure 58. SO_x standard vs. total cost.

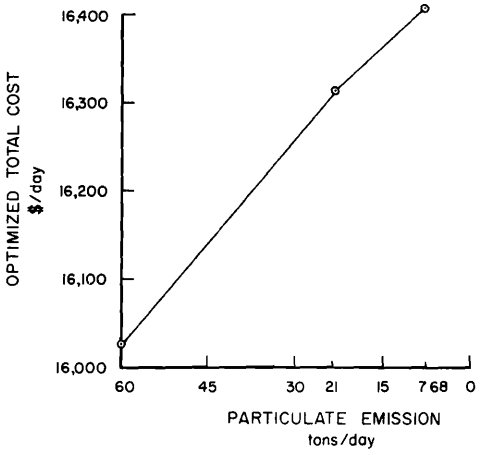

Figure 57. Particulate emission standard change vs. total cost.

SUMMARY

CONCLUSIONS AND DISCUSSION

The mixed integer programming model can provide a method of analyzing optimal treatment and recycle strategies when the cost of capital and other input factors change, and when environmental standards change. In addition, the model is useful for defining the optimal treatment unit sizes.

The model may provide a method for production-oriented managers to evaluate the least cost of pollution control under different circumstances. The method may also be important to those who are interested in evaluating the effect of tightening environmental standards on society. The analysis would be done on the basis of calculating the increased cost to the production facility when environmental standards are changed.

A basic weakness in the model is that, to optimize with more than one chemical parameter per phase stream would tremendously increase the cost of operating the model. Using the model for planning purposes would require an evaluation of other important chemical parameters when the optimal solution is identified.

Future studies with the model might include an application of the model to other production facilities which have several production unit effluents. Sensitivity was based on one design, and when other alternatives are provided in the model, the results could be significantly different.

SUMMARY

A mixed integer programming model has been presented which was designed with several pollution control alternatives and used to:

1. Identify the least cost solution for controlling pollution emissions and discharges for a 750 MW coal fired steam electric powerplant located in a region similar to the climate of Southern Utah. The costs were calculated on the basis of identifying the costs that would be incurred by the powerplant in excess of once through cooling costs and with no discharge or emissions standards. Within the optimal solution was an identification of: a) optimal treatment units; b) the optimal size of the treatment units; and c) the individual total cost of each treatment unit. From a previous definition of the total cost of each unit appearing in the model's cost function, the contribution of capital operation and maintenance, energy, and water required could be identified.

2. Evaluate the least cost treatment control scheme for the powerplant when: a) The cost of capital was increased; b) the cost of O & M was increased; c) the cost of energy was increased; d) the cost of water was increased; e) the particulate emission standards were changed; f) the sulfur oxide emission standards were changed; and g) the stream discharge standards were changed. When the model was subjected to sensitivity analysis, the model was able to identify new minimum cost solutions and minimize the increasing costs of the individual cost segments. Generally, when an individual cost factor such as capital cost was increased, the total amount of the individual cost factor in the optimal solution was reduced and the other cost factors such as O & M, energy, and water, were increased.

The cost function of each treatment unit, consisting of either a continuous variable or a binary integer and continuous variable, can be used to approximate nonlinear total cost functions of the treatment units. The binary integer variables are always of the zero-one type. The binary integer variable, in addition to being associated with the continuous variable in the total cost function, can be used in the row constraints to define upper flow limits and upper concentration limits of the treatment and production units.

The mixed integer linear programming model was designed with interfacing between the liquid, gas, and solid phases and included methods of discharge to the environment and/or recycle when stream quality constraints were satisfied. The model was also provided with alternatives for solid and liquid waste disposal.

Increases in the cost of water indicated that the optimum treatment and production strategy was insensitive to water costs. Discharge to a stream was never identified in an optimum solution and water recycle within the production facility was identified in all the sensitivity cases evaluated.

SELECTED BIBLIOGRAPHY

Adams, B.J. and D. Panagiotakopoulos. 1977. Network approach to optimal wastewater treatment system design. Water Pollution Control Federation Journal 49(4):623-632.

Allegrezza, A.E., J.M. Charpentier, R.B. Davis, and M.J. Coplan. 1975. Hollow fiber reverse osmosis membranes, Paper 86b at the 68 Annual Meeting of American Institute of Chemical Engineering, Los Angeles, California.

Blecker, H.G. and T.M. Nichols. 1973. Capital and operating costs of pollution control equipment modules. Vol. II, Data Manual. Office of Research and Monitoring, EPA. 183 p.

Bump, R.L. 1977. Electrostatic precipitators in industry. Chemical Engineering 84(2):129-136.

Calloway, J.A., A.K. Schwartz and R.G. Thompson. 1974. An integrated power process model of water use and wastewater treatment in ammonia production. (NTIS publication number PB-237 219) 88 p.

Childers, R.E. 1966. Manual of procedures and methods for calculating comparative costs of municipal water supply from saline and conventional water sources in Texas. Office of Saline Water; Research and Development. Report no. 257.

Clark, C.F. 1969. Cost analysis of six water desalting processes. Research and Development Progress report number 495. Office of Saline Water, U.S. Department of Interior (I 1.88: (#495). 100 p.

Crits, G.J. and G. Glover. 1975. Cooling blowdown in cooling towers. Water and Wastes Engineering. April, p. 45-52.

Davis, F.N. 1975. Utah Power and Light Company brine concentration in a closed cycle. Prepared for the National Conference on Management and Disposal of Residues from the Treatment of Industrial Wastewaters. Utah Power and Light Company, Salt Lake City, Utah. 29 p.

de Nevers, Noel. 1975. The application of cost-benefit analysis to air pollution control regulation: A general discussion with application to the example of sulfur dioxide control at the Huntington and Emery powerplants. Utah Power and Light Light Company, Salt Lake City, Utah. 157 p.

Doyle, F.J., H.G. Bhatt, and J.R. Rapp. 1974. Cost estimates for air pollution control equipment. In—Analysis of Pollution Control Costs. Appalachian Regional Commission, Washington D.C., and U.S. Environmental Protection Agency, Washington D.C. (EPA-670/2-74-009, Feb. 1975):361-384.

Ecker, J.G. and J.R. McNamera. 1971. Geometric programming and the preliminary design of industrial waste treatment plants. Water Rersources Research 7(1). p. 18-22.

Edmisten, N.G. and F.L. Bunyard. 1970. A systematic procedure for determining the cost of controlling particulate emissions from industrial sources. Journal of the Air Pollution Control Association 20(7):446-452.

Elliot, T.C., (ed). 1973. Cooling towers. Power (March):24.

Evenson, D.E., G.T. Orlob, and J.R. Monser. 1969. Preliminary selection of waste treatment systems. Water Pollution Control Federation Journal 41(11)-1. 1845-1858 p.

Gold, H., D.J. Goldstein, R.F. Probstein, J.S. Shen, and D. Yung. 1977. Water requirements for steam-electric power generation and synthetic fuel plants in the western United States. U.S. EPA (EPA 600/7-77-037). 259 p.

Hawkins, A.E. 1973. The electricity supply industry; in Fuel and the Environment: conference proceedings. Published by Ann Arbor Science Publishers Inc., P.O. Box 1452, Ann Arbor, Michigan. p. 51-78.

Inoue, K., E.J. Henley, G.H. Otto, and R.G. Thompson. 1974. Water use policies and power plant economies. (NTIS PB 239 822)102 p.

Intermountain Power Project. 1976a. Preliminary engineering and feasibility study: Project overview (Vol I). Intermountain Power Project, Salt Lake City, Utah.

Intermountain Power Project. 1976b. Preliminary engineering and feasibility study: Generating station (Vol 2, part 1) Intermountain Power Project, Salt Lake City, Utah.

Jedlicka, C.L. 1973. Nomographs for thermal pollution control system. Office of Research and Development (US EPA. EPA-660/2-73-004). 171 p.

Jimeson, R.M. and G.G. Adkins. 1971. Waste heat disposal in power plants. Chemical Engineering Progress 67(7):64-69.

Kohn, R. 1969. A linear programming model for air pollution control in the St. Louis airshed. PhD dissertation, Washington University, St. Louis, Missouri.

Lacey, J. 1977a. Private telephone communication on June 27, 1977. Utah Power and Light in Salt Lake City, Utah.

Lacey J. 1977b. Personal telephone conversation of September 13, 1977. Utah Power and Light in Salt Lake City, Utah.

MacLeod, L.H., A. Gendel, and A.F. El Sahrigi. 1963. The optimal temperature for the operation of a non-scaling multi-stage flash evaporator plant. Sea Water Conversion Laboratory Report No. 63-1. University of California, Berkeley Sea Water Conversion Laboratory, Berkeley, California.

McGlamery, G.G., R.L. Torstrick, W.J. Broadfoot, J.P. Simpson, L.J. Henson, S.V. Tomlinson, and J.F. Young. 1975. Detailed cost estimates for advanced effluent desulfurization processes. Office of Research and Development, U.S. EPA, (EPA-600/2-75-006).

Mills, R.A. and G. Tchobanoglous. 1975. Energy consumption in wastewater treatment. Presented at the Seventh National Agricultural Waste Management Conference, Syracuse, New York. Richard A. Mills (ed) State Water Resources Control Board, Sacramento, California. 46 p.

Oak Ridge National Laboratory and Office of Saline Water. 1970. Special report on status of desalting. United States Department of the Interior (I 1.2:045/9). 111 p.

Oleson, K.A. and R.R. Boyle. 1971. How to cool steam electric power plants. Chemical Engineering Progress 67(7):70-76.

Peterson, R.J. and K.E. Cobian. 1976. Reverse osmosis recycle of electroplating chemicals at pH extremes. Plating and Surface Finishing 63(6):51-63.

Rossie, J.P. 1971a. Dry-type cooling systems. Chemical Engineering Progress 67(7):58-63.

Rossie, J.P., E.A. Cecil, P.R. Cunningham, and C.J. Steiert. 1971b. Electric power generation with dry type cooling systems; presented at the American Power Conference, Chicago, Illinois. R.W. Beck and Associates, Denver, Colorado. 16 p.

Shih, C.S. and P. Krishnan. 1969. Dynamic optimization for industrial waste treatment design. Water Pollution Control Federation Journal 41(10):1787-1802.

Singleton, F.D. Jr., J.A. Calloway, and R.G. Thompson. 1975. An integrated power process model of water use and waste water treatment in chlor-alkali production. Water Resources Research, Vol. 11(4):515-525 and NTIS (PB-242 159).

Stone, R. and H. Smallwood. 1973. Intermedia aspects of air and water pollution control. Office of Research and Development, U.S. EPA (EPA 1.23/3:EPA 600/5-73-003 Aug. 73).

Stone, J.C., A.K. Schwartz, Jr., R.A. Klein, F.D. Singleton, Jr., J.A. Calloway, and R.G. Thompson. 1975a. An integrated power process model for ethylene production. Water Resources Research 11(6):810-814.

Stone, J.C., A.K. Schwartz, Jr., R.A. Klein, F.D. Singleton, Jr., J.A. Calloway, and R.G. Thompson. 1975b. An integrated power process for water use and wastewater treatment in olefins production. U.S. NTIS, PB-244 269.

Teller, A., and J.R. Norsworthy. 1970. The evaluation of the cost of alternative strategies for air pollution control: in Natural Resource Systems Models in Decision Making, Purdue University Water Resources Research Center, West Lafayette, Indiana. p. 87-99.

United States Environmental Protection Agency. 1974. Development document for effluent limitations guidelines and new source performance standards for the steam electric power generating point source category. EPA, Washington D.C. (EPA 440/1-74 029-a Group I).

United States Environmental Protection Agency. 1976. Supplement for pretreatment to the development document for the steam electric power generating point source category. Office of Water and Hazardous Materials, U.S. EPA, (EPA 440/1-76/084).

Van Note, R.H., P.V. Herbert, R.M. Patel, C. Chupek, and L. Feldman. 1975. A guide to the selection of cost-effective wastewater treatment systems. Becktel, Inc., prepared for the Environmental Protection Agency (EPA 440/9-75-002) Distributed by: National Technical Information Service, U.S. Department of Commerce: (PB-244-417).

Weber, W.J. 1972. Physiochemical processes for water quality control. Wiley Interscience. 640 p.

Woodson, R.D. 1971. Cooling towers. Scientific American. May: 70-78.

APPENDIX A
APPLIED MODEL UNIT FLOW DIAGRAMS

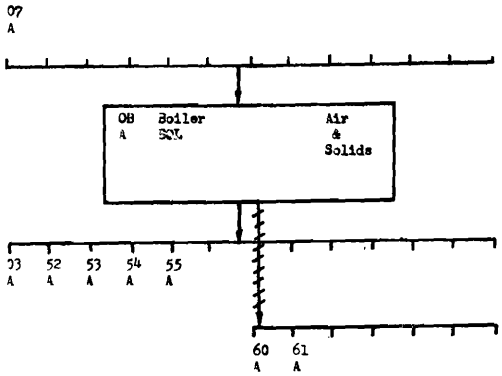

INFLUENT AIR KTON/DAY	PARTICULATE KTON/DAY	PARTICULATE %	SO_x KTON/DAY	SO_x %
21.722	0.356	0.333(0)	.06349	.075

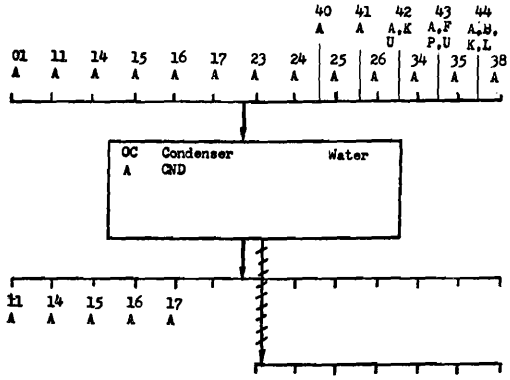

FLOW
= 1620.7

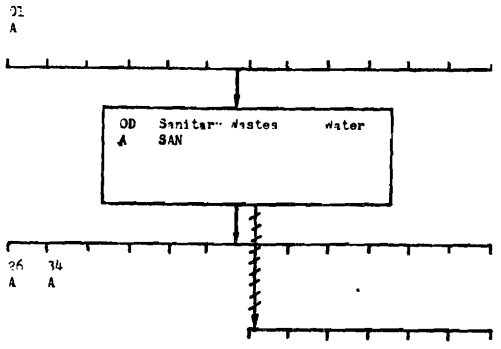

FLOW
KTON/DAY
0.034

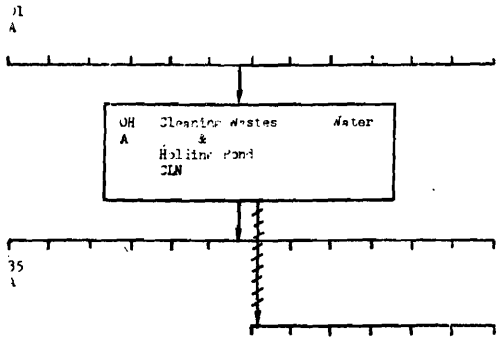

FLOW
KTON/DAY
.2021

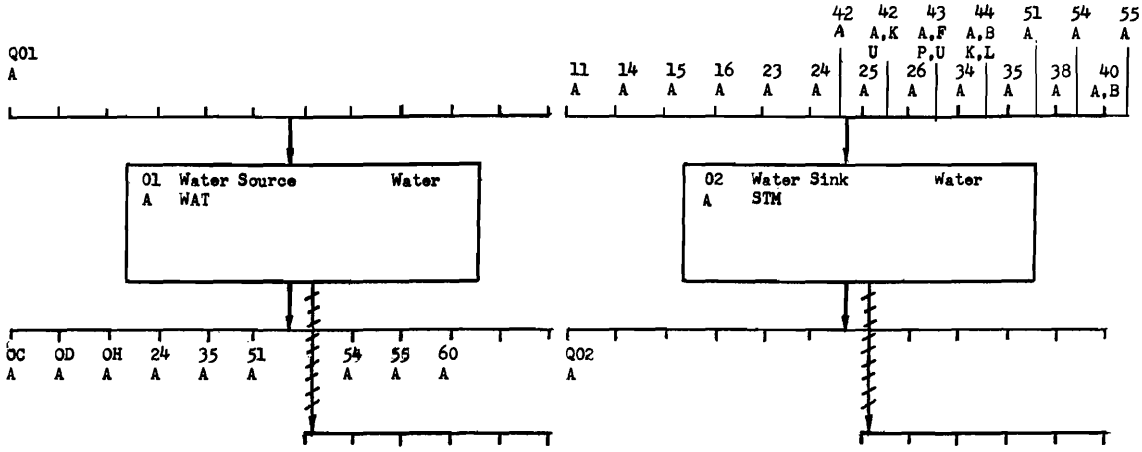

FLOW KTON/DAY	QUALITY PPM	BASE COST $/KTON
≤ 186.2	1,483	14.72

BASE DISCHARGE STANDARD

500 ppm

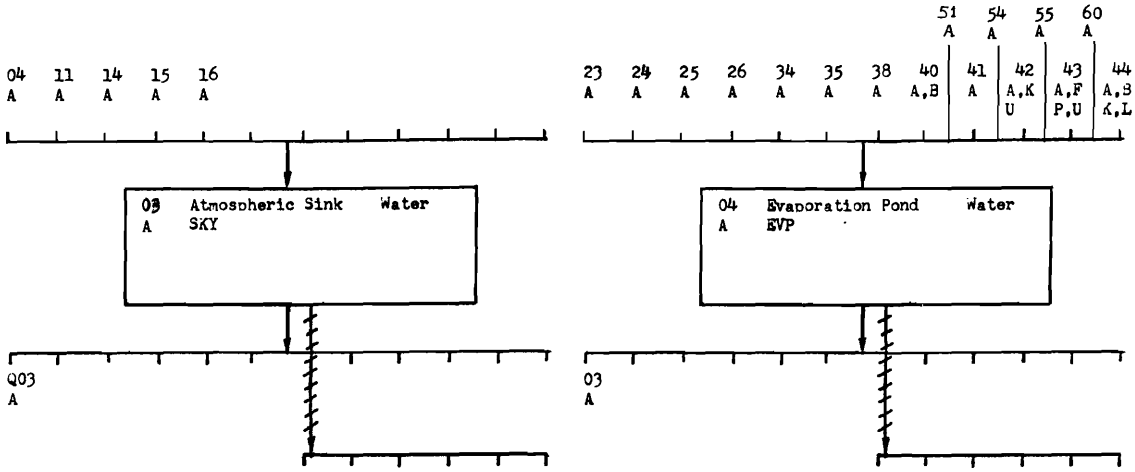

BASE EMISSION STANDARD

Particulates	≤ 7.68 Tons/day
SOx	≤ 92.2 Tons/day

BASE COST $/KTON

$1317.27

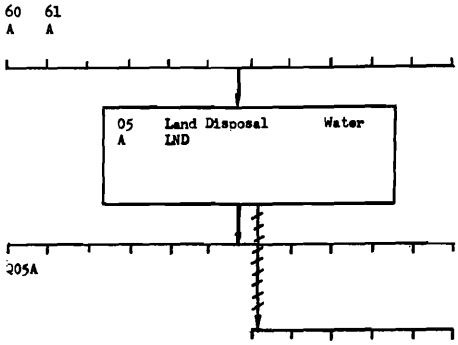

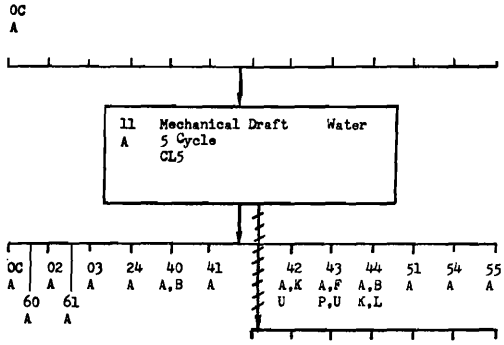

BASE COST $/DAY	ASSOC. Z	EVAPORATION (%)	MAKEUP QUANTITY %	QUALITY PPM	BLOWDOWN QUALITY (ppm)
$3694	Z2	2.305	2.375	346.	5,000

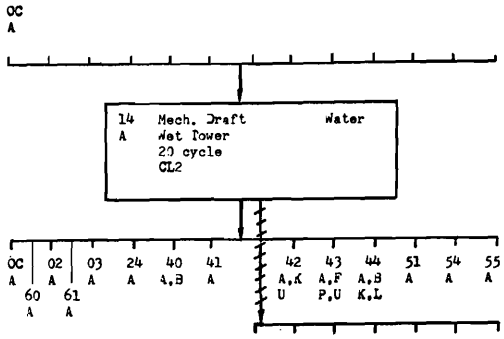

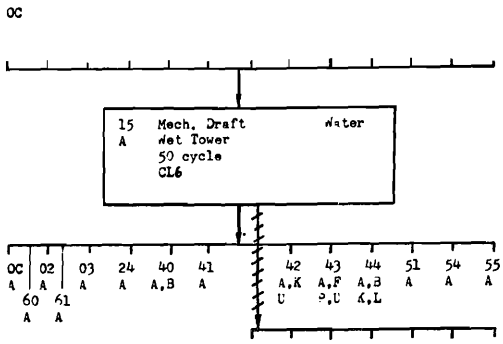

BASE COST $/DAY	ASSOC. Z	EVAP. %	MAKEUP QUANTITY %	QUALITY PPM	BLOWDOWN QUALITY PPM
$3694	Z5	2.305	2.416	86	5,000

BASE COST $/DAY	ASSOC. Z	EVAP. %	MAKEUP QUANTITY %	QUALITY PPM	BLOWDOWN QUALITY PPM
$3694	Z6	2.305	2.3469	34.6	5,000

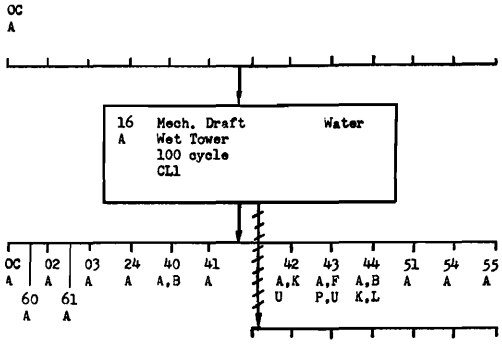

BASE COST $/DAY	ASSOC. Z	EVAP. %	MAKEUP QUANTITY %	QUALITY PPM	BLOWDOWN QUALITY PPM
$3694	27	2.305	2.323	17.3	5,000

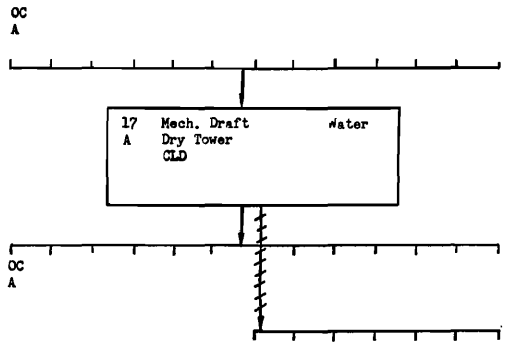

BASE COST $/DAY	ASSOC. Z
$25,649	28

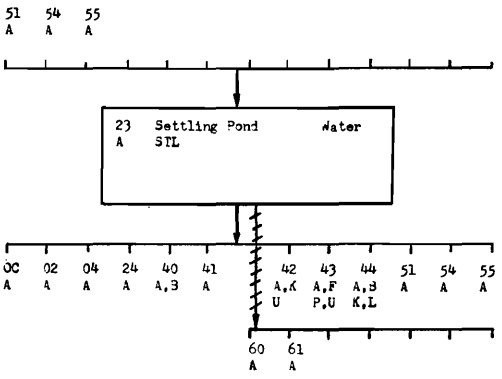

BASE COST $/DAY	BRINE FRACTION %	PRODUCT CONCENTRATION PPM
14,86(	20	3,328

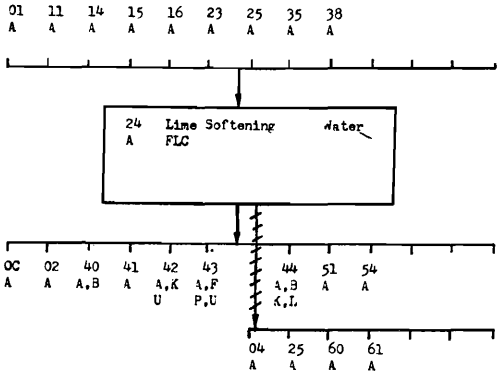

BASE COST $/DAY	ASSOC. Y	BRINE %	PRODUCT CONCENTRATION PPM
82.5+69,34(	29	0.946	1,000

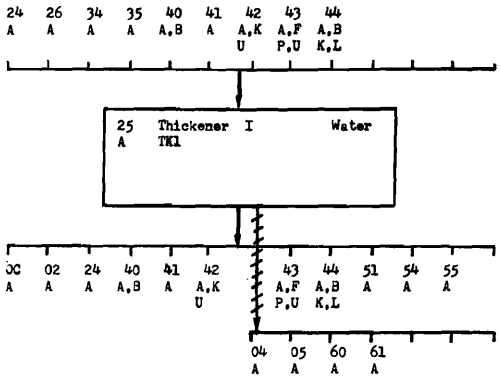

BASE COST $/DAY	BRINE %	BRINE CONCENTRATION	PRODUCT CONCENTRATION PPM
8.43 X	33.	300,000	71

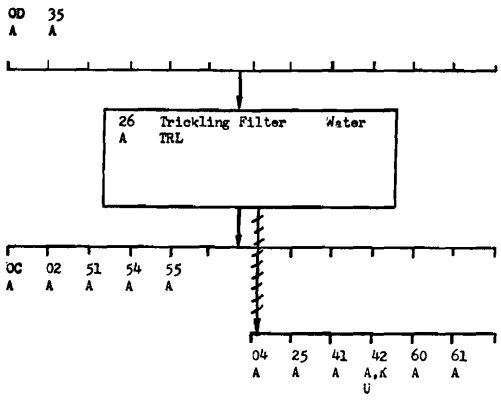

BASE COST $/DAY	ASSOC. Y	BRINE %	BRINE CONCENTRATION	PRODUCT CONCENTRATION
19947.65X	Y29	.0432	60,000	5,000

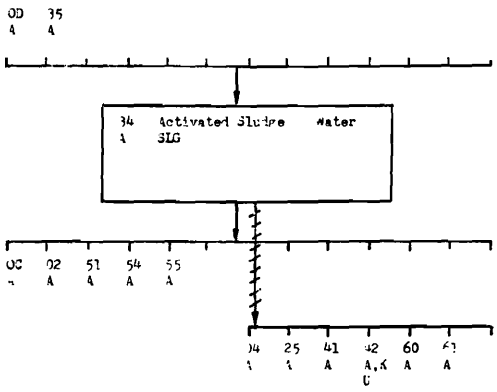

BASE COST $/DAY	ASSOC. COST	BRINE %	BRINE CONCENTRATION	PRODUCT CONCENTRATION
330+21.035X	Y32	0.432	30,000	5,000

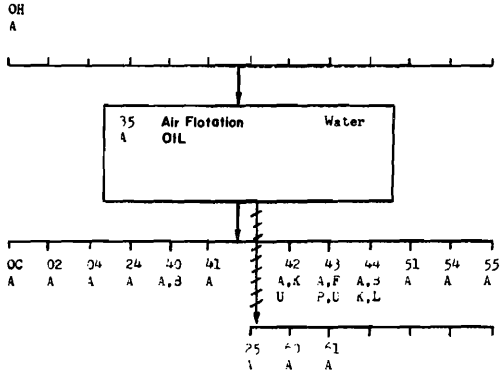

BASE COST $/DAY	BRINE %	BRINE CONCENTRATION PPM	PRODUCT CONCENTRATION PPM
248.2(	0.11	10,000	3,385

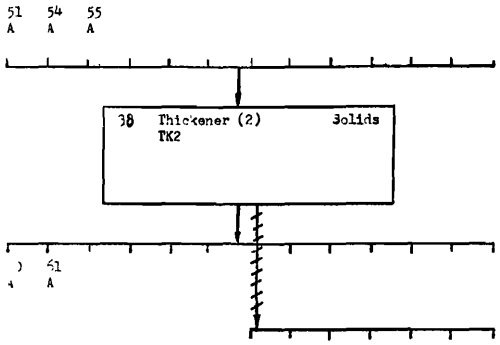

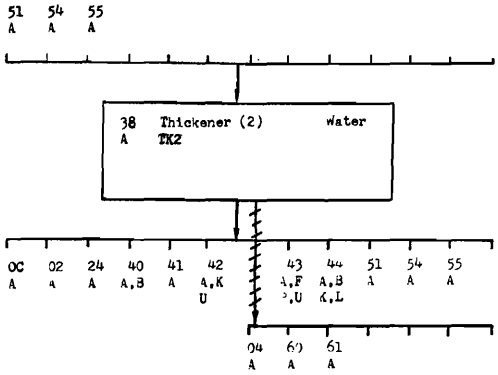

BASE COST $/DAY	BRINE $	BRINE CONCENTRATION PPM	PRODUCT CONCENTRATION PPM
24.95X	33.0	600,000	71

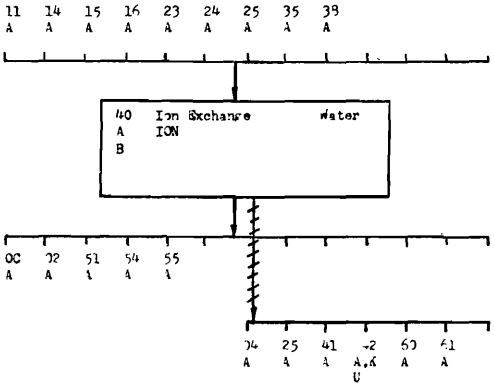

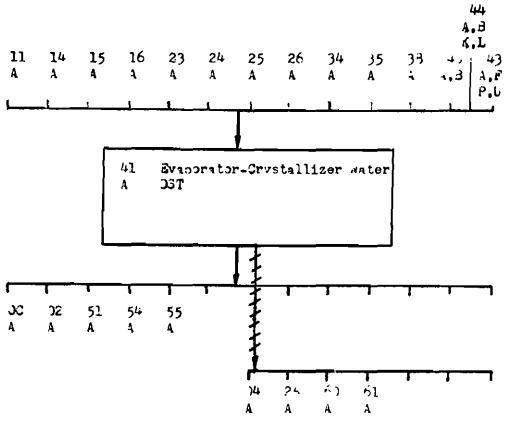

BASE COST $/DAY	ASSOC.	INFLUENT FLOW KTON/DAY	INFLUENT CONC. CAPACITY PPM	CONCENTRATION BRINE $	CONCENTRATION BRINE	CONCENTRATION PRODUCT
A 264.5+34.208X	Y10	25(536	1,000	33.0	3,310	10
B 57+35.5(	Y11	36*(.72	1,000	33.0	3,310	10

BASE COST $/DAY	INFLUENT CONCENTRATION CAPACITY PPM	BRINE $	BRINE CONCENTRATION PPM	PRODUCT CONCENTRATION PPM
1062.2(	2,500	2.0	124,510	10

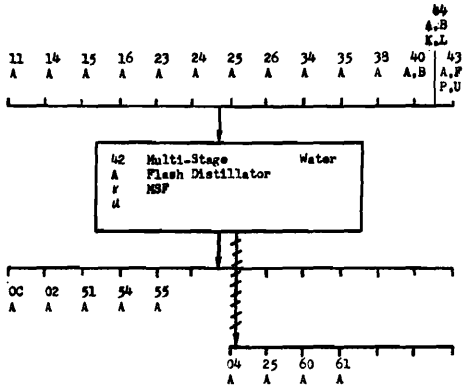

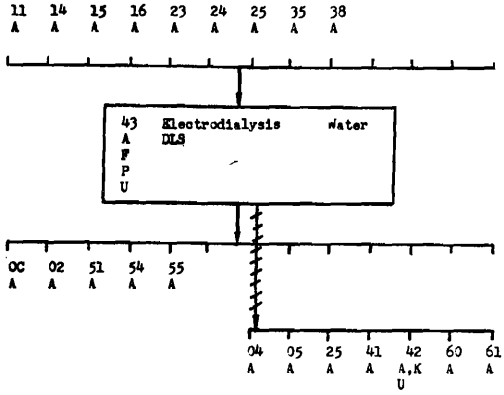

BASE COST $/DAY	ASSOC. Z	INFLUENT FLOW KTON/DAY	INFLUENT CONC. CAPACITY	BRINE %	BRINE CONC.	PRODUCT CONC.
A 7904+2,499X	Z18	0≤X≤100	10,000	27.3	50,297	10
K 7794+3,417.94X	Z20	0≤X≤100	30,000	61.3	57,236	10
U 7796+6,134.46X	Z22	0≤X≤100	50,000	76.9	64,974	10

BASE COST $/DAY	ASSOC. Z	INFLUENT FLOW KTON/DAY	INFLUENT CONC. CAPACITY PPM	BRINE %	CONCENTRATION BRINE PPM	PRODUCT PPM
A 593+2.306X	Z23	72	78	22.6	310	10
F 1399+30.2X	Z24	72	1,250	24.8	4,506	10
P 1737+231.92X	Z26	72	5,000	25.0	14,470	10
U 1996+365.8X	Z27	72	10,000	25.0	30,470	10

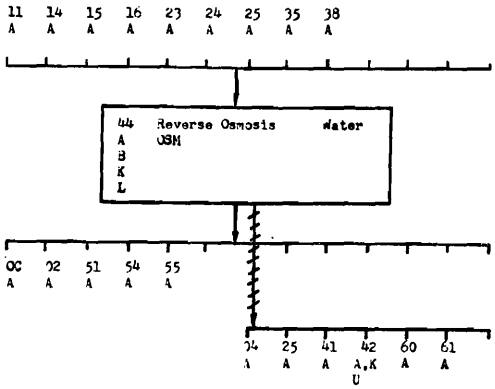

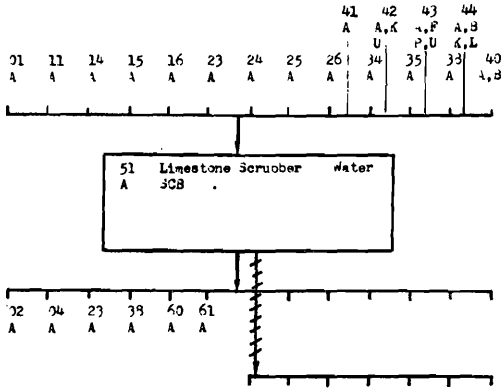

BASE COST $/DAY	ASSOC. Z	INFLUENT FLOW KTON/DAY	INFLUENT CONC. CAPACITY PPM	CONCENTRATION BRINE %	BRINE PPM	PRODUCT PPM
A 1076+231.45X	Z12	0≤(≤36	2,666	30.0	17,717	10
B 2716+245.917X	Z13	36≤X≤72	2,666	30.0	17,717	10
K 381.6+101.1X	Z16	0≤X≤36	8,000	65.0	12,302	10
L 393+3[illegible].43X	Z17	36≤X≤72	8,000	65.0	12,302	10

INFLUENT FLOW %	INFLUENT QUALITY PPM	EFFLUENT PRODUCT PPM
1.6(0)	≤ 5,000	433,800

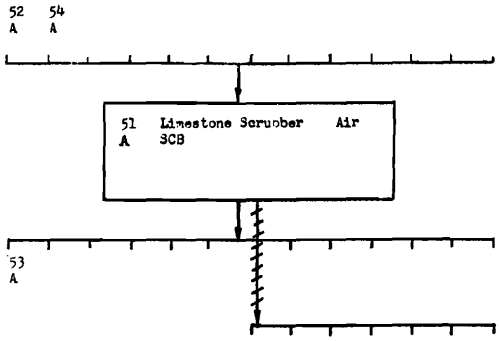

BASE COST $/DAY	ASSOC. Y	PARTICULATES REMOVED %	SOX REMOVED %
11,352+72.736(Q)	Y34	99.5	90.0

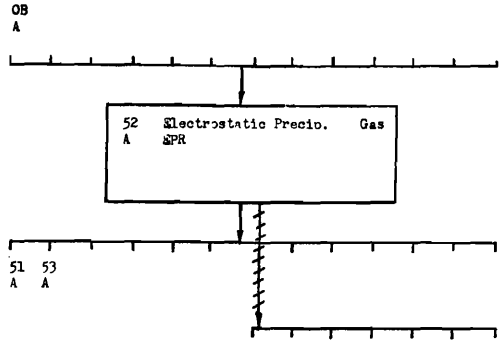

BASE COST $/DAY	ASSOC. Y	PARTICULATES REMOVED %
46.63(Q)	Y33	99.9

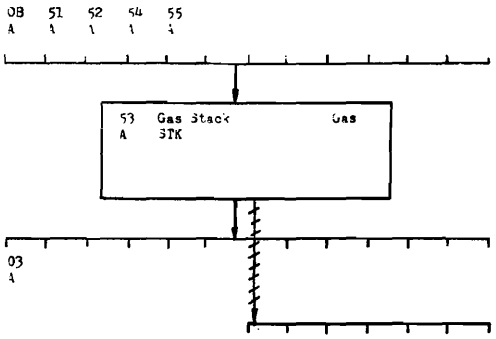

BASE COST $/DAY	HEIGHT FT.	EMISSIONS PARTICULATES TON/DAY	EMISSIONS SO TON/DAY
9.489(+4)	750	.00768	.0922

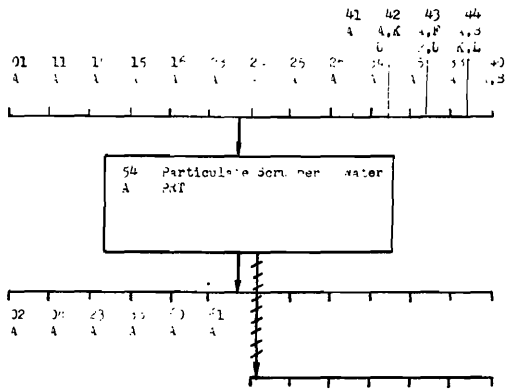

WATER FLOW #	WATER QUALITY PPM	PRODUCT PPM
1.00(Q)	≤5,000	500,000

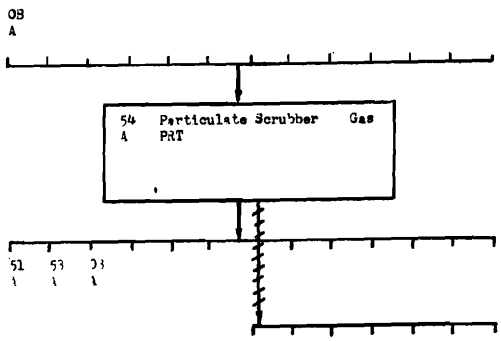

BASE COST $/DAY	ASSOC. Y	PARTICULATE REMOVAL %
5. +31.J12(J)	Y35	99.9

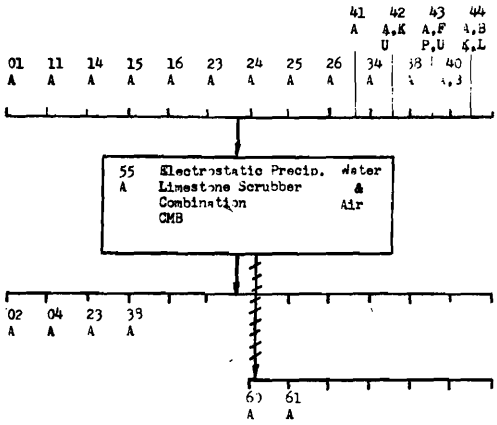

BASE COST $/DAY	ASSOC. Y	REMOVAL PARTICULATES %	REMOVAL SO_x %	WATER FLOW %	WATER QUALITY PPM
11,952+117.37(J)	Y36	99.9995	99.8357	1.6(J)	≤5,000

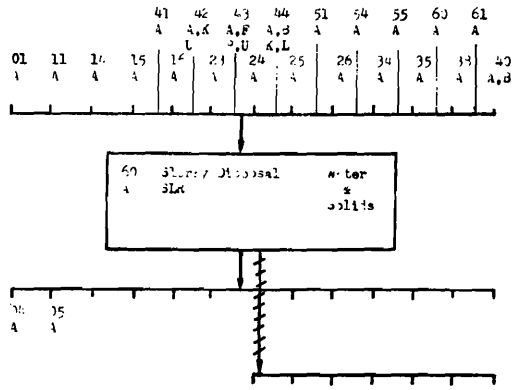

BASE
COST
$/DAY

57.3(XT)

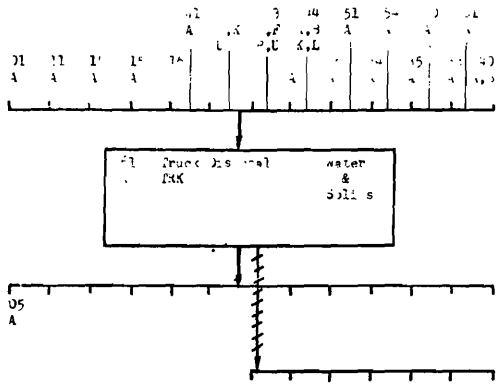

BASE
COST
$/DAY

142.7(XT)

APPENDIX B
COMPUTER OUTPUT OF APPLIED MODEL

ROW LIST and RIGHT HAND

SIDE SIGN

```
N  COST
L  WATAX
E  WATAQ
E  WATRCHRG
E  CNDAX
E  CNDAQ
E  CNDA
L  CL5AZU
L  CL2AZU
L  CL6AZU
L  CL1AZU
L  CLDAZU
E  Z1=8EX
L  CNDAXIU
E  STMAX
E  STMAQ
L  STMXIU
E  SKYAX
E  SKYAQ
E  SKYU
E  SKYA
E  EVPAX
E  EVPAQ
E  LNDAX
E  LNDAQ
E  CL5AX
E  CL5AQ
E  EVP5Q
E  CL50CA
E  CL5MQ
E  CL2AX
E  CL2AQ
E  EVP2Q
E  CL20CA
E  CL2MQ
E  CL6AX
E  CL6AQ
E  EVP6Q
E  COR6Q
E  CL60CA
E  CL6MQ
E  CL1AQ
E  CL1AX
E  EVP1Q
E  CND1Q
E  CL1MQ
E  CLDAX
E  CLDAQ
E  STLAX
E  STLAQ
E  STLADQ
E  FLCAX
E  FLCAQ
E  FLCADQ
L  FLCAYU
E  TK1AX
E  TK1AQ
E  TK1ADQ
E  TRLAX
E  TRLAQ
E  TRLADQ
L  TRLAYU
E  SLGAX
E  SLGAQ
E  SLGADQ
L  SLGAYU
E  OILAX
E  OILAQ
E  OILADQ
E  TK2AX
E  TK2AQ
E  TK2ADQ
E  IONAX
E  IONBX
L  IONAYU
G  IONBYL
L  IONBYU
L  Y10Y11EX
E  IONAQ
E  IONBQ
E  IONADQ
E  IONBDQ
L  IONAXIU
L  IONBXIU
E  DSTAX
E  DSTAQ
E  DSTADQ
L  DSTAXIU
E  MSFAX
E  MSFKX
E  MSFUX
E  MSFAQ
E  MSFKQ
E  MSFUQ
E  MSFADQ
E  MSFKDQ
E  MSFUDQ
L  MSFAZU
L  MSFKZU
L  MSFUZU
L  Z18=22EX
L  MSFAXIU
L  MSFKXIU
L  MSFUXIU
E  DLSAX
E  DLSFX
E  DLSPX
E  DLSUX
E  DLSAQ
E  DLSFQ
E  DLSPQ
E  DLSUQ
E  DLSADQ
E  DLSFDQ
E  DLSPDQ
E  DLSUDQ
L  DLSAZU
L  DLSFZU
L  DLSPZU
L  DLSUZU
L  Z23=27EX
L  DLSAXIU
L  DLSFXIU
L  DLSPXIU
L  DLSUXIU
E  OSMAX
E  OSMBX
E  OSMKX
E  OSMLX
E  OSMAQ
E  OSMBQ
E  OSMKQ
E  OSMLQ
E  OSMADQ
E  OSMBDQ
E  OSMKDQ
E  OSMLDQ
L  OSMAZU
G  OSMBZL
L  OSMBZU
L  Z12Z13EX
L  OSMKZU
G  OSMLZL
L  OSMLZU
L  Z16Z17EX
L  Z12=17EX
L  OSMAXIU
L  OSMBXIU
L  OSMKXIU
L  OSMLXIU
L  Y33=Y36E
E  SCBAA
E  SCBAO
L  SCBAY34
E  SCBAPA
E  SCBASA
E  SCBAX
E  SCBAQ
E  SCBNQ
L  SCBAXIU
E  EPRAA
E  EPRAO
L  EPRAY33
E  EPRAPA
E  STKAA
E  STKAO
E  HEIGHT
E  STKAPA
L  STKAPO
E  STKASA
L  STKASO
E  PRTAA
E  PRTAO
L  PRTAY35
E  PRTAPA
E  PRTAX
E  PRTAQ
E  PRTAXO
L  PRTAXIU
E  SLRAX
E  SLRAQ
E  SLRAXT
E  TRKAX
E  TRKAQ
E  TRKAXT
E  CMBAA
E  CMBAO
L  CMBAY36
E  CMBAPA
E  CMBASA
E  CMBAX
E  CMBAQ
E  CMBANQ
L  CMBAXIU
E  BOLAA
E  BOLAO
E  BOLAN
E  BOLAPT
E  BOLAPBT
E  BOLASO
E  BOLASBT
E  SANAX
E  SANAQ
E  SANA
E  CLNAX
E  CLNAQ
E  CLNA
E  SLRAT
E  TRKAT
E  TK2AP
E  TK2AT
E  STLAP
E  STLAT
```

COLUMN LIST and VALUES

START1	'MARKER'		'BIVORG'	
Y10	COST	264.50000	IONAYU	-36.00000
Y10	Y10Y11EX	1.00000		
Y11	COST	596.00000	IONBYL	-36.00000
Y11	IONBYU	-100.00000	Y10Y11EX	1.00000
Y28	COST	82.50000	FLCAYU	-1000.00000
Y29	COST	189.00000	TRLAYU	-1.00000
Y32	COST	330.00000	SLGAYU	-1.00000
Y33	EPRAY33	-100.00000	Y33-Y36E	1.00000
Y34	COST	11852.00000	SCBAY34	-100.00000
Y34	Y33-Y36E	1.00000		
Y35	COST	5.60000	PRTAY35	-100.00000
Y35	Y33-Y36E	1.00000		
Y36	CMBAY36	-100.00000	COST	11852.50000
Y36	Y33-Y36E	1.00000		
Z12	COST	1076.00000	OSMAZU	-36.00000
Z12	Z12-17FX	1.00000		
Z13	COST	2716.00000	OSMBZL	-36.00000
Z13	OSMBZU	-72.00000	Z12-17EX	1.00000
Z16	COST	381.60000	OSMKZU	-36.00000
Z16	Z12-17EX	1.00000		
Z17	COST	909.00000	OSMLZL	-36.00000
Z17	OSMLZU	-72.00000	Z12-17EX	1.00000
Z18	COST	780.00000	MSFAZU	-1000.00000
Z18	Z18-22EX	1.00000		
Z2	CL5AZU	-2000.00000	COST	3694.00000
Z2	Z1-8EX	1.00000		
Z20	COST	778.00000	MSFKZU	-1000.00000
Z20	Z18-22EX	1.00000		
Z22	COST	778.00000	MSFUZU	-1000.00000
Z22	Z18-22EX	1.00000		
Z23	COST	598.00000	DLSAZU	-72.00000
Z23	Z23-27EX	1.00000		
Z24	COST	1398.00000	DLSFZU	-72.00000
Z24	Z23-27EX	1.00000		
Z26	COST	1797.00000	DLSPZU	-72.00000
Z26	Z23-27EX	1.00000		
Z27	COST	1996.00000	DLSUZU	-72.00000
Z27	Z23-27EX	1.00000		
Z5	CL2AZU	-2000.00000	COST	3694.00000
Z5	Z1-8EX	1.00000		
Z6	CL6AZU	-2000.00000	COST	3694.00000
Z6	Z1-8EX	1.00000		
Z7	CL1AZU	-2000.00000	COST	3694.00000
Z7	Z1-8EX	1.00000		
Z8	CLDAZU	-2000.00000	COST	25649.00000
Z8	Z1-8EX	1.00000		

END1	'MARKER'		'BIVEND'	
A08A03A	SKYO	-1.00000		
A08A51A	BOLAO	-1.00000	SCBAA	1.00000
A08A51A	STKASA	-0.00068		
A08A52A	BOLAO	-1.00000	EPRAA	1.00000
A08A53A	BOLAO	-1.00000	STKAA	1.00000
A08A53A	STKAPA	-0.00653		
A08A54A	BOLAO	-1.00000	PRTAA	1.00000
A08A55A	BOLAO	-1.00000	CMBAA	1.00000
A03A	SKYA	1.00000		
A08A03A	BOLAA	1.00000		
A51A53A	SCBAO	-1.00000	STKAA	1.00000
A51A53A	STKAPA	-0.00003	STKASA	-0.00007
A52A53A	EPRAO	-1.00000	STKAPA	-6.50000E-06
A52A53A	STKASA	-0.00068	STKAA	1.00000
A53A03A	SKYO	-1.00000	STKAO	-1.00000
A54A03A	SKYO	-1.00000		
A54A53A	PRTAO	-1.00000	STKAA	1.00000
A54A53A	STKAPA	-0.00065	STKASA	-0.00068
A55A53A	CMBAO	-1.00000	STKAA	1.00000
A55A53A	STKASA	-0.00007		
H53A	COST	0.48900	HEIGHT	1.00000
O08A	BOLAA	-1.00000	BOLAN	1.00000
O08A	BOLAO	1.00000	BOLAPT	-0.00933
O08A	BOLASO	-0.00075		
O03A	SKYA	-1.00000	SKYO	1.00000
O51A	COST	70.73600	SCBAA	-1.00000
O51A	SCBAO	1.00000	SCBAPA	-0.00650
O51A	SCBASA	-0.00164	SCBAY34	1.00000
O51A	SCBNQ	-0.01600		
O52A	COST	46.63000	EPRAA	-1.00000
O52A	EPRAO	1.00000	EPRAPA	-0.00652
O52A	EPRAY33	1.00000		
O53A	STKAA	-1.00000	STKAO	1.00000
O54A	COST	31.01200	PRTAA	-1.00000
O54A	PRTAO	1.00000	PRTAPA	-0.00588
O54A	PRTAXO	-0.01090	PRTAY35	1.00000
O55A	CMBAA	-1.00000	CMBAO	1.00000
O55A	CMBAPA	-0.00653	CMBASA	-0.00164
O55A	CMBAY36	1.00000	CMBANQ	-0.01600
O55A	COST	117.37000		
P08A60A	BOLAPBT	1.00000	SLRAT	-1.00000
P08A61A	BOLAPBT	1.00000	TRKAT	-1.00000
P51A23A	SCBAPA	1.00000		
P51A38A	SCBAPA	1.00000		
P51A60A	SCBAPA	1.00000	SLRAT	-1.00000
P51A61A	SCBAPA	1.00000	TRKAT	-1.00000
P52A60A	EPRAPA	1.00000	SLRAT	-1.00000
P52A61A	EPRAPA	1.00000	TRKAT	-1.00000
P53A	STKAPA	1.00000	STKAPO	1.00000

P54A23A	PRTAPA	1.00000		
P54A38A	PRTAPA	1.00000		
P54A60A	PRTAPA	1.00000	SLRAT	-1.00000
P54A61A	PRTAPA	1.00000	TRKAT	-1.00000
P55A23A	CMBAPA	1.00000		
P55A38A	CMBAPA	1.00000		
P55A60A	CMBAPA	1.00000	SLRAT	-1.00000
P55A61A	CMBAPA	1.00000	TRKAT	-1.00000
Q0CA11A	CL5AX	-1.00000	CL5AZU	1.00000
Q0CA11A	CNDAQ	1.00000		
Q0CA14A	CL2AX	-1.00000	CL2AZU	1.00000
Q0CA14A	CNDAQ	1.00000		
Q0CA15A	CL6AX	-1.00000	CL6AZU	1.00000
Q0CA15A	CNDAQ	1.00000		
Q0CA16A	CL1AX	-1.00000	CL1AZU	1.00000
Q0CA16A	CNDAQ	1.00000		
Q0CA17A	CLDAX	-1.00000	CLDAZU	1.00000
Q0CA17A	CNDAQ	1.00000		
Q0DA26A	SANAQ	1.00000	TRLAX	-1.00000
Q0DA34A	SANAQ	1.00000	SLGAX	-1.00000
Q0MA35A	CLNAQ	1.00000	OILAX	-1.00000
Q01A0CA	CNDAX	-1.00000	CNDAXIU	1483.00000
Q01A0CA	WATAQ	1.00000		
Q01A0DA	SANAX	-1.00000	WATAQ	1.00000
Q01A0MA	CLNAX	-1.00000	WATAQ	1.00000
Q01A21A	FLCAX	-1.00000	WATAQ	1.00000
Q01A35A	WATAQ	1.00000		
Q01A51A	SCRAXIU	1483.00000	SCRAX	-1.00000
Q01A51A	WATAQ	1.00000		
Q01A54A	PRTAX	-1.00000	PRTAXIU	1483.00000
Q01A54A	WATAQ	1.00000		
Q01A55A	CMRAX	-1.00000	CMRAXIU	1483.00000
Q01A55A	WATAQ	1.00000		
Q01A60A	SLRAX	-1.00000	WATAQ	1.00000
Q02A	STMAQ	1.00000		
Q03A	SKYAQ	1.00000		
Q04A03A	FVP2Q	1.00000	SKYAX	-1.00000
Q05A	[illegible]AQ	1.00000		
Q10M	CL6AQ	1.00000	CNDAXIU	-34.00000
Q11A0CA	CL5AQ	1.00000	CL5OCA	1.00000
Q11A0CA	CNDAX	-1.00000		
Q11A02A	CL5AQ	1.00000	STMAX	-1.00000
Q11A02A	STMXIU	5000.00000		
Q11A03A	CL5AQ	1.00000	FVP5Q	1.00000
Q11A03A	SKYAX	-1.00000		
Q11A21A	CL5AQ	1.00000	FLCAX	-1.00000
Q11A[illegible]A	CL5AQ	1.00000	IONAX	-1.00000
Q11A[illegible]A	IONAXIU	5000.00000		
Q11A[illegible]M	CL5AQ	1.00000	IONMX	-1.00000
Q11A[illegible]M	IONMXIU	5000.00000		

Q11A41A	CL5AQ	1.00000	DSTAX	-1.00000
Q11A41A	DSTAXIU	5000.00000		
Q11A42A	CL5AQ	1.00000	MSFAX	-1.00000
Q11A42A	MSFAXIU	5000.00000		
Q11A42K	CL5AQ	1.00000	MSFKX	-1.00000
Q11A42K	MSFKXIU	5000.00000		
Q11A42U	CL5AQ	1.00000	MSFUX	-1.00000
Q11A42U	MSFUXIU	5000.00000		
Q11A43A	CL5AQ	1.00000	DLSAX	-1.00000
Q11A43A	DLSAXIU	5000.00000		
Q11A43F	CL5AQ	1.00000	DLSFX	-1.00000
Q11A43F	DLSFXIU	5000.00000		
Q11A43P	CL5AQ	1.00000	DLSPX	-1.00000
Q11A43P	DLSPXIU	5000.00000		
Q11A43U	CL5AQ	1.00000	DLSUX	-1.00000
Q11A43U	DLSUXIU	5000.00000		
Q11A44A	CL5AQ	1.00000	DS4AX	-1.00000
Q11A44A	DS4AXIU	5000.00000		
Q11A44M	CL5AQ	1.00000	DSMAX	-1.00000
Q11A44M	DSMMXIU	5000.00000		
Q11A44K	CL5AQ	1.00000	DSMKX	-1.00000
Q11A44K	DSMKXIU	5000.00000		
Q11A44L	CL5AQ	1.00000	DSMLX	-1.00000
Q11A44L	DSMLXIU	5000.00000		
Q11A51A	CL5AQ	1.00000	SCRAX	-1.00000
Q11A51A	SCRAXIU	5000.00000		
Q11A54A	CL5AQ	1.00000	PRTAX	-1.00000
Q11A54A	PRTAXIU	5000.00000		
Q11A55A	CL5AQ	1.00000	CMRAX	-1.00000
Q11A55A	CMRAXIU	5000.00000		
Q11A60A	CL5AQ	1.00000	SLRAX	-1.00000
Q11A61A	CL5AQ	1.00000	TRKAX	-1.00000
Q11M	CL5MQ	1.00000	CNDAXIU	-346.00000
Q14A0CA	CL2AQ	1.00000	CL2OCA	1.00000
Q14A0CA	CNDAX	-1.00000		
Q14A02A	CL2AQ	1.00000	STMAX	-1.00000
Q14A02A	STMXIU	5000.00000		
Q14A03A	CL2AQ	1.00000	FVP2Q	1.00000
Q14A03A	SKYAX	-1.00000		
Q14A24A	CL2AQ	1.00000	FLCAX	-1.00000
Q14A40A	CL2AQ	1.00000	IONAX	-1.00000
Q14A40A	IONAXIU	5000.00000		
Q14A40M	CL2AQ	1.00000	IONMX	-1.00000
Q14A40M	IONMXIU	5000.00000		
Q14A41A	CL2AQ	1.00000	DSTAX	-1.00000
Q14A41A	USTAXIU	5000.00000		
Q14A42A	CL2AQ	1.00000	MSFAX	-1.00000
Q14A42A	MSFAXIU	5000.00000		
Q14A42K	CL2AQ	1.00000	MSFKX	-1.00000
Q14A42K	MSFKXIU	5000.00000		

Q14A42U	CL2AQ	1.00000	MSFUX	-1.00000
Q14A42U	MSFUXIU	5000.00000		
Q14A43A	CL2AQ	1.00000	DLSAX	-1.00000
Q14A43A	DLSAXIU	5000.00000		
Q14A43F	CL2AQ	1.00000	DLSFX	-1.00000
Q14A43F	DLSFXIU	5000.00000		
Q14A43P	CL2AQ	1.00000	DLSPX	-1.00000
Q14A43P	DLSPXIU	5000.00000		
Q14A43U	CL2AQ	1.00000	DLSUX	-1.00000
Q14A43U	DLSUXIU	5000.00000		
Q14A44A	CL2AQ	1.00000	OSMAX	-1.00000
Q14A44A	OSMAXIU	5000.00000		
Q14A44B	CL2AQ	1.00000	OSMBX	-1.00000
Q14A44B	OSMBXIU	5000.00000		
Q14A44K	CL2AQ	1.00000	OSMKX	-1.00000
Q14A44K	OSMKXIU	5000.00000		
Q0CA16A	CL1AX	-1.00000	CL1AZU	1.00000
Q0CA16A	CNDAQ	1.00000		
Q0CA17A	CLDAX	-1.00000	CLDAZU	1.00000
Q0CA17A	CNDAQ	1.00000		
Q0DA26A	SANAQ	1.00000	TRLAX	-1.00000
Q0DA34A	SANAQ	1.00000	SLGAX	-1.00000
Q0HA35A	CLNAQ	1.00000	OILAX	-1.00000
Q01A0CA	CNDAX	-1.00000	CNDAXIU	1483.00000
Q01A0CA	WATAQ	1.00000		
Q01A0DA	SANAX	-1.00000	WATAQ	1.00000
Q01A0HA	CLNAX	-1.00000	WATAQ	1.00000
Q01A24A	FLCAX	-1.00000	WATAQ	1.00000
Q01A35A	WATAQ	1.00000		
Q01A51A	SCBAXIU	1483.00000	SCBAX	-1.00000
Q01A51A	WATAQ	1.00000		
Q01A54A	PRTAX	-1.00000	PRTAXIU	1483.00000
Q01A54A	WATAQ	1.00000		
Q01A55A	CMBAX	-1.00000	CMBAXIU	1483.00000
Q01A55A	WATAQ	1.00000		
Q01A60A	SLRAX	-1.00000	WATAQ	1.00000
Q02A	STMAQ	1.00000		
Q03A	SKYAQ	1.00000		
Q04A03A	EVPAQ	1.00000	SKYAX	-1.00000
Q05A	LNDAQ	1.00000		
Q10B	CL6MQ	1.00000	CNDAXIU	-34.60000
Q11A0CA	CL5AQ	1.00000	CL50CA	1.00000
Q11A0CA	CNDAX	-1.00000		
Q11A02A	CL5AQ	1.00000	STMAX	-1.00000
Q11A02A	STMXIU	5000.00000		
Q11A03A	CL5AQ	1.00000	EVP5Q	1.00000
Q11A03A	SKYAX	-1.00000		
Q11A24A	CL5AQ	1.00000	FLCAX	-1.00000
Q11A40A	CL5AQ	1.00000	IONAX	-1.00000
Q11A40A	IONAXIU	5000.00000		
Q11A40B	CL5AQ	1.00000	IONBX	-1.00000
Q11A40B	IONBXIU	5000.00000		
Q11A41A	CL5AQ	1.00000	DSTAX	-1.00000
Q11A41A	DSTAXIU	5000.00000		
Q11A42A	CL5AQ	1.00000	MSFAX	-1.00000
Q11A42A	MSFAXIU	5000.00000		
Q11A42K	CL5AQ	1.00000	MSFKX	-1.00000
Q11A42K	MSFKXIU	5000.00000		
Q11A42U	CL5AQ	1.00000	MSFUX	-1.00000
Q11A42U	MSFUXIU	5000.00000		
Q11A43A	CL5AQ	1.00000	DLSAX	-1.00000
Q11A43A	DLSAXIU	5000.00000		
Q11A43F	CL5AQ	1.00000	DLSFX	-1.00000
Q11A43F	DLSFXIU	5000.00000		
Q11A43P	CL5AQ	1.00000	DLSPX	-1.00000
Q11A43P	DLSPXIU	5000.00000		
Q11A43U	CL5AQ	1.00000	DLSUX	-1.00000
Q11A43U	DLSUXIU	5000.00000		
Q11A44A	CL5AQ	1.00000	OSMAX	-1.00000
Q11A44A	OSMAXIU	5000.00000		
Q11A44B	CL5AQ	1.00000	OSMBX	-1.00000
Q11A44B	OSMBXIU	5000.00000		
Q11A44K	CL5AQ	1.00000	OSMKX	-1.00000
Q11A44K	OSMKXIU	5000.00000		
Q11A44L	CL5AQ	1.00000	OSMLX	-1.00000
Q11A44L	OSMLXIU	5000.00000		
Q11A51A	CL5AQ	1.00000	SCBAX	-1.00000
Q11A51A	SCBAXIU	5000.00000		
Q11A54A	CL5AQ	1.00000	PRTAX	-1.00000
Q11A54A	PRTAXIU	5000.00000		
Q11A55A	CL5AQ	1.00000	CMBAX	-1.00000
Q11A55A	CMBAXIU	5000.00000		
Q11A60A	CL5AQ	1.00000	SLRAX	-1.00000
Q11A61A	CL5AQ	1.00000	TRKAX	-1.00000
Q11B	CL5MQ	1.00000	CNDAXIU	-346.00000
Q14A0CA	CL2AQ	1.00000	CL20CA	1.00000
Q14A0CA	CNDAX	-1.00000		
Q14A02A	CL2AQ	1.00000	STMAX	-1.00000
Q14A02A	STMXIU	5000.00000		
Q14A03A	CL2AQ	1.00000	EVP2Q	1.00000
Q14A03A	SKYAX	-1.00000		
Q14A24A	CL2AQ	1.00000	FLCAX	-1.00000
Q14A40A	CL2AQ	1.00000	IONAX	-1.00000
Q14A40A	IONAXIU	5000.00000		
Q14A40B	CL2AQ	1.00000	IONBX	-1.00000
Q14A40B	IONBXIU	5000.00000		
Q14A41A	CL2AQ	1.00000	DSTAX	-1.00000
Q14A41A	DSTAXIU	5000.00000		
Q14A42A	CL2AQ	1.00000	MSFAX	-1.00000
Q14A42A	MSFAXIU	5000.00000		
Q14A42K	CL2AQ	1.00000	MSFKX	-1.00000
Q14A42K	MSFKXIU	5000.00000		

Q14A42U	CL2AQ	1.00000	MSFUX	-1.00000
Q14A42U	MSFUXIU	5000.00000		
Q14A43A	CL2AQ	1.00000	DLSAX	-1.00000
Q14A43A	DLSAXIU	5000.00000		
Q14A43F	CL2AQ	1.00000	DLSFX	-1.00000
Q14A43F	DLSFXIU	5000.00000		
Q14A43P	CL2AQ	1.00000	DLSPX	-1.00000
Q14A43P	DLSPXIU	5000.00000		
Q14A43U	CL2AQ	1.00000	DLSUX	-1.00000
Q14A43U	DLSUXIU	5000.00000		
Q14A44A	CL2AQ	1.00000	OSMAX	-1.00000
Q14A44A	OSMAXIU	5000.00000		
Q14A44B	CL2AQ	1.00000	OSMBX	-1.00000
Q14A44B	OSMBXIU	5000.00000		
Q14A44K	CL2AQ	1.00000	OSMKX	-1.00000
Q14A44K	OSMKXIU	5000.00000		
Q14A44L	CL2AQ	1.00000	OSMLX	-1.00000
Q14A44L	OSMLXIU	5000.00000		
Q14A51A	CL2AQ	1.00000	SCBAX	-1.00000
Q14A51A	SCBAXIU	5000.00000		
Q14A54A	CL2AQ	1.00000	PRTAX	-1.00000
Q14A54A	PRTAXIU	5000.00000		
Q14A55A	CL2AQ	1.00000	CMBAX	-1.00000
Q14A55A	CMBAXIU	5000.00000		
Q14A60A	CL2AQ	1.00000	SLRAX	-1.00000
Q14A61A	CL2AQ	1.00000	TRKAX	-1.00000
Q14B	CL2MQ	1.00000	CNDAXIU	-86.00000
Q15A0CA	CL6AQ	1.00000	CL60CA	1.00000
Q15A0CA	CNDAX	-1.00000		
Q15A02A	CL6AQ	1.00000	STMAX	-1.00000
Q15A02A	STMXIU	5000.00000		
Q15A03A	CL6AQ	1.00000	EVP6Q	1.00000
Q15A03A	SKYAX	-1.00000		
Q15A24A	CL6AQ	1.00000	FLCAX	-1.00000
Q15A40A	CL6AQ	1.00000	IONAX	-1.00000
Q15A40A	IONAXIU	5000.00000		
Q15A40B	CL6AQ	1.00000	IONBX	-1.00000
Q15A40B	IONBXIU	5000.00000		
Q15A41A	CL6AQ	1.00000	DSTAX	-1.00000
Q15A41A	DSTAXIU	5000.00000		
Q15A42A	CL6AQ	1.00000	MSFAX	-1.00000
Q15A42A	MSFAXIU	5000.00000		
Q15A42K	CL6AQ	1.00000	MSFKX	-1.00000
Q15A42K	MSFKXIU	5000.00000		
Q15A42U	CL6AQ	1.00000	MSFUX	-1.00000
Q15A42U	MSFUXIU	5000.00000		
Q15A43A	CL6AQ	1.00000	DLSAX	-1.00000
Q15A43A	DLSAXIU	5000.00000		
Q15A43F	CL6AQ	1.00000	DLSFX	-1.00000
Q15A43F	DLSFXIU	5000.00000		
Q15A43P	CL6AQ	1.00000	DLSPX	-1.00000
Q15A43P	DLSPXIU	5000.00000		
Q15A43U	CL6AQ	1.00000	DLSUX	-1.00000
Q15A43U	DLSUXIU	5000.00000		
Q15A44A	CL6AQ	1.00000	OSMAX	-1.00000
Q15A44A	OSMAXIU	5000.00000		
Q15A44B	CL6AQ	1.00000	OSMBX	-1.00000
Q15A44B	OSMBXIU	5000.00000		
Q15A44K	CL6AQ	1.00000	OSMKX	-1.00000
Q15A44K	OSMKXIU	5000.00000		
Q15A44L	CL6AQ	1.00000	OSMLX	-1.00000
Q15A44L	OSMLXIU	5000.00000		
Q15A51A	CL6AQ	1.00000	SCBAX	-1.00000
Q15A51A	SCBAXIU	5000.00000		
Q15A54A	CL6AQ	1.00000	PRTAX	-1.00000
Q15A54A	PRTAXIU	5000.00000		
Q15A55A	CL6AQ	1.00000	CMBAX	-1.00000
Q15A55A	CMBAXIU	5000.00000		
Q15A60A	CL6AQ	1.00000	SLRAX	-1.00000
Q15A61A	CL6AQ	1.00000	TRKAX	-1.00000
Q16A0CA	CL1AQ	1.00000	CNDAX	-1.00000
Q16A0CA	CND1Q	1.00000		
Q16A02A	CL1AQ	1.00000	STMAX	-1.00000
Q16A02A	STMXIU	5000.00000		
Q16A03A	CL1AQ	1.00000	EVP1Q	1.00000
Q16A03A	SKYAX	-1.00000		
Q16A24A	CL1AQ	1.00000	FLCAX	-1.00000
Q16A40A	CL1AQ	1.00000	IONAX	-1.00000
Q16A40A	IONAXIU	5000.00000		
Q16A40B	CL1AQ	1.00000	IONBX	-1.00000
Q16A40B	IONBXIU	5000.00000		
Q16A41A	CL1AQ	1.00000	DSTAX	-1.00000
Q16A41A	DSTAXIU	5000.00000		
Q16A42A	CL1AQ	1.00000	MSFAX	-1.00000
Q16A42A	MSFAXIU	5000.00000		
Q16A42K	CL1AQ	1.00000	MSFKX	-1.00000
Q16A42K	MSFKXIU	5000.00000		
Q16A42U	CL1AQ	1.00000	MSFUX	-1.00000
Q16A42U	MSFUXIU	5000.00000		
Q16A43A	CL1AQ	1.00000	DLSAX	-1.00000
Q16A43A	DLSAXIU	5000.00000		
Q16A43F	CL1AQ	1.00000	DLSFX	-1.00000
Q16A43F	DLSFXIU	5000.00000		
Q16A43P	CL1AQ	1.00000	DLSPX	-1.00000
Q16A43P	DLSPXIU	5000.00000		
Q16A43U	CL1AQ	1.00000	DLSUX	-1.00000
Q16A43U	DLSUXIU	5000.00000		
Q16A44A	CL1AQ	1.00000	OSMAX	-1.00000
Q16A44A	OSMAXIU	5000.00000		
Q16A44B	CL1AQ	1.00000	OSMBX	-1.00000
Q16A44B	OSMBXIU	5000.00000		

Q16A40K	CL1AQ	1.00000	OSMKX	-1.00000
Q16A40K	OSMKXIU	5000.00000		
Q16A40L	CL1AQ	1.00000	OSMLX	-1.00000
Q16A40L	OSMLXIU	5000.00000		
Q16A51A	CL1AQ	1.00000	SCRAX	-1.00000
Q16A51A	SCRAXIU	5000.00000		
Q16A52A	CL1AQ	1.00000	PRTAX	-1.00000
Q16A52A	PRTAXIU	5000.00000		
Q16A55A	CL1AQ	1.00000	CMBAX	-1.00000
Q16A55A	CMBAXIU	5000.00000		
Q16A60A	CL1AQ	1.00000	SLRAX	-1.00000
Q16A61A	CL1AQ	1.00000	TRKAX	-1.00000
Q16A	CL1AQ	1.00000	CNDAXIU	-17.30000
Q17A0CA	CL1AQ	1.00000	CNDAX	-1.00000
Q23A0CA	CNDAX	-1.00000	CNDAXIU	3328.00000
Q23A0CA	STLAQ	1.00000		
Q23A02A	STLAQ	1.00000	STMAX	-1.00000
Q23A02A	STMXIU	3328.00000		
Q23A04A	EVPAX	-1.00000	STLAQ	1.00000
Q23A25A	FLCAX	-1.00000	STLAQ	1.00000
Q23A40A	IONAX	-1.00000	IONAXIU	3328.00000
Q23A40A	STLAQ	1.00000		
Q23A40B	IONBX	-1.00000	IONBXIU	3328.00000
Q23A40B	STLAQ	1.00000		
Q23A41A	DSTAX	-1.00000	DSTAXIU	3328.00000
Q23A41A	STLAQ	1.00000		
Q23A42A	MSFAX	-1.00000	MSFAXIU	3328.00000
Q23A42A	STLAQ	1.00000		
Q23A42K	MSFKX	-1.00000	MSFKXIU	3326.00000
Q23A42K	STLAQ	1.00000		
Q23A42U	MSFUX	-1.00000	MSFUXIU	3328.00000
Q23A42U	STLAQ	1.00000		
Q23A43A	DLSAX	-1.00000	DLSAXIU	3328.00000
Q23A43A	STLAQ	1.00000		
Q23A43F	DLSFX	-1.00000	DLSFXIU	3328.00000
Q23A43F	STLAQ	1.00000		
Q23A43P	DLSPX	-1.00000	DLSPXIU	3328.00000
Q23A43P	STLAQ	1.00000		
Q23A43U	DLSUX	-1.00000	DLSUXIU	3328.00000
Q23A43U	STLAQ	1.00000		
Q23A44A	OSMAX	-1.00000	OSMAXIU	3328.00000
Q23A44A	STLAQ	1.00000		
Q23A44B	OSMBX	-1.00000	OSMBXIU	3328.00000
Q23A44B	STLAQ	1.00000		
Q23A44K	OSMKX	-1.00000	OSMKXIU	3328.00000
Q23A44K	STLAQ	1.00000		
Q23A44L	OSMLX	-1.00000	OSMLXIU	3328.00000
Q23A44L	STLAQ	1.00000		
Q23A51A	SCRAX	-1.00000	SCRAXIU	3328.00000
Q23A51A	STLAQ	1.00000		

Q23A52A	PRTAX	-1.00000	PRTAXIU	3328.00000
Q23A52A	STLAQ	1.00000		
Q23A55A	CMBAX	-1.00000	CMBAXIU	3328.00000
Q23A55A	STLAQ	1.00000		
Q23A60A	SLRAX	-1.00000	STLADQ	1.00000
Q23A60A	STLAQ	1.00000		
Q23A61A	STLADQ	1.00000	STLAQ	1.00000
Q23A61A	TRKAX	-1.00000		
Q24A0CA	CNDAX	-1.00000	CNDAXIU	1000.00000
Q24A0CA	FLCAQ	1.00000		
Q24A02A	FLCAQ	1.00000	STMAX	-1.00000
Q24A02A	STMXIU	1000.00000		
Q24A04A	EVPAX	-1.00000	FLCADQ	1.00000
Q24A04A	FLCAQ	1.00000		
Q24A25A	FLCADQ	1.00000	FLCAQ	1.00000
Q24A25A	TK1AX	-1.00000		
Q24A40A	FLCAQ	1.00000	IONAX	-1.00000
Q24A40A	IONAXIU	1000.00000		
Q24A40B	FLCAQ	1.00000	IONBX	-1.00000
Q24A40B	IONBXIU	1000.00000		
Q24A41A	DSTAX	-1.00000	DSTAXIU	71.00000
Q24A41A	FLCAQ	1.00000		
Q24A42A	FLCAQ	1.00000	MSFAX	-1.00000
Q24A42A	MSFAXIU	1000.00000		
Q24A42K	FLCAQ	1.00000	MSFKX	-1.00000
Q24A42K	MSFKXIU	1000.00000		
Q24A42U	FLCAQ	1.00000	MSFUX	-1.00000
Q24A42U	MSFUXIU	1000.00000		
Q24A43A	DLSAX	-1.00000	DLSAXIU	1000.00000
Q24A43A	FLCAQ	1.00000		
Q24A43F	DLSFX	-1.00000	DLSFXIU	1000.00000
Q24A43F	FLCAQ	1.00000		
Q24A43P	DLSPX	-1.00000	DLSPXIU	1000.00000
Q24A43P	FLCAQ	1.00000		
Q24A43U	DLSUX	-1.00000	DLSUXIU	1000.00000
Q24A43U	FLCAQ	1.00000		
Q24A44A	FLCAQ	1.00000	OSMAX	-1.00000
Q24A44A	OSMAXIU	1000.00000		
Q24A44B	FLCAQ	1.00000	OSMBX	-1.00000
Q24A44B	OSMBXIU	1000.00000		
Q24A44K	FLCAQ	1.00000	OSMKX	-1.00000
Q24A44K	OSMKXIU	1000.00000		
Q24A44L	FLCAQ	1.00000	OSMLX	-1.00000
Q24A44L	OSMLXIU	1000.00000		
Q24A51A	FLCAQ	1.00000	SCRAX	-1.00000
Q24A51A	SCRAXIU	1000.00000		
Q24A52A	FLCAQ	1.00000	PRTAX	-1.00000
Q24A52A	PRTAXIU	1000.00000		
Q24A55A	CMBAX	-1.00000	CMBAXIU	1000.00000
Q24A55A	FLCAQ	1.00000		

Q24A60A	FLCADQ	1.00000	FLCAQ	1.00000
Q24A60A	SLRAX	-1.00000		
Q24A61A	FLCADQ	1.00000	FLCAQ	1.00000
Q24A61A	TRKAX	-1.00000		
Q25A0CA	CNDAX	-1.00000	CNDAXIU	71.00000
Q25A0CA	TK1AQ	1.00000		
Q25A02A	STMAX	-1.00000	STMXIU	71.00000
Q25A02A	TK1AQ	1.00000		
Q25A04A	EVPAX	-1.00000	TK1ADQ	1.00000
Q25A04A	TK1AQ	1.00000		
Q25A25A	FLCAX	-1.00000	TK1AQ	1.00000
Q25A40A	IONAX	-1.00000	IONAXIU	71.00000
Q25A40A	TK1AQ	1.00000		
Q25A40B	IONBX	-1.00000	IONBXIU	71.00000
Q25A40B	TK1AQ	1.00000		
Q25A41A	DSTAX	-1.00000	DSTAXIU	71.00000
Q25A41A	TK1AQ	1.00000		
Q25A42A	MSFAX	-1.00000	MSFAXIU	5000.00000
Q25A42A	TK1AQ	1.00000		
Q25A42K	MSFKX	-1.00000	MSFKXIU	5000.00000
Q25A42K	TK1AQ	1.00000		
Q25A42U	MSFUX	-1.00000	MSFUXIU	5000.00000
Q25A42U	TK1AQ	1.00000		
Q25A43A	DLSAX	-1.00000	DLSAXIU	71.00000
Q25A43A	TK1AQ	1.00000		
Q25A43F	DLSFX	-1.00000	DLSFXIU	71.00000
Q25A43F	TK1AQ	1.00000		
Q25A43P	DLSPX	-1.00000	DLSPXIU	71.00000
Q25A43P	TK1AQ	1.00000		
Q25A43U	DLSUX	-1.00000	DLSUXIU	71.00000
Q25A43U	TK1AQ	1.00000		
Q25A44A	OSMAX	-1.00000	OSMAXIU	71.00000
Q25A44A	TK1AQ	1.00000		
Q25A44B	OSMBX	-1.00000	OSMBXIU	71.00000
Q25A44B	TK1AQ	1.00000		
Q25A44K	OSMKX	-1.00000	OSMKXIU	71.00000
Q25A44K	TK1AQ	1.00000		
Q25A44L	OSMLX	-1.00000	OSMLXIU	71.00000
Q25A44L	TK1AQ	1.00000		
Q25A51A	SCBAX	-1.00000	SCBAXIU	71.00000
Q25A51A	TK1AQ	1.00000		
Q25A54A	PRTAX	-1.00000	PRTAXIU	71.00000
Q25A54A	TK1AQ	1.00000		
Q25A55A	CMBAX	-1.00000	CMBAXIU	71.00000
Q25A55A	TK1AQ	1.00000		
Q25A60A	SLRAX	-1.00000	TK1ADQ	1.00000
Q25A60A	TK1AQ	1.00000		
Q25A61A	TK1ADQ	1.00000	TK1AQ	1.00000
Q25A61A	TRKAX	-1.00000		
Q26A0CA	CNDAX	-1.00000	CNDAXIU	5000.00000
Q26A0CA	TRLAQ	1.00000		
Q26A02A	STMAX	-1.00000	STMXIU	5000.00000
Q26A02A	TRLAQ	1.00000		
Q26A04A	EVPAX	-1.00000	TRLADQ	1.00000
Q26A04A	TRLAQ	1.00000		
Q26A25A	TK1AX	-1.00000	TRLADQ	1.00000
Q26A25A	TRLAQ	1.00000		
Q26A41A	DSTAX	-1.00000	DSTAXIU	60000.00000
Q26A41A	TRLADQ	1.00000	TRLAQ	1.00000
Q26A42A	MSFAX	-1.00000	MSFAXIU	60000.00000
Q26A42A	TRLADQ	1.00000	TRLAQ	1.00000
Q26A42K	MSFKX	-1.00000	MSFKXIU	60000.00000
Q26A42K	TRLADQ	1.00000	TRLAQ	1.00000
Q26A42U	MSFUX	-1.00000	MSFUXIU	60000.00000
Q26A42U	TRLADQ	1.00000	TRLAQ	1.00000
Q26A51A	SCBAX	-1.00000	SCBAXIU	5000.00000
Q26A51A	TRLAQ	1.00000		
Q26A54A	PRTAX	-1.00000	PRTAXIU	5000.00000
Q26A54A	TRLAQ	1.00000		
Q26A55A	CMBAX	-1.00000	CMBAXIU	5000.00000
Q26A55A	TRLAQ	1.00000		
Q26A60A	SLRAX	-1.00000	TRLADQ	1.00000
Q26A60A	TRLAQ	1.00000		
Q26A61A	TRKAX	-1.00000	TRLADQ	1.00000
Q26A61A	TRLAQ	1.00000		
Q34A0CA	CNDAX	-1.00000	CNDAXIU	5000.00000
Q34A0CA	SLGAQ	1.00000		
Q34A02A	SLGAQ	1.00000	STMAX	-1.00000
Q34A02A	STMXIU	5000.00000		
Q34A04A	EVPAX	-1.00000	SLGADQ	1.00000
Q34A04A	SLGAQ	1.00000		
Q34A25A	SLGADQ	1.00000	SLGAQ	1.00000
Q34A25A	TK1AX	-1.00000		
Q34A41A	DSTAX	-1.00000	DSTAXIU	30000.00000
Q34A41A	SLGADQ	1.00000	SLGAQ	1.00000
Q34A42A	MSFAX	-1.00000	MSFAXIU	30000.00000
Q34A42A	SLGADQ	1.00000	SLGAQ	1.00000
Q34A42K	MSFKX	-1.00000	MSFKXIU	30000.00000
Q34A42K	SLGADQ	1.00000	SLGAQ	1.00000
Q34A42U	MSFUX	-1.00000	MSFUXIU	30000.00000
Q34A42U	SLGADQ	1.00000	SLGAQ	1.00000
Q34A51A	SCBAX	-1.00000	SCBAXIU	5000.00000
Q34A51A	SLGAQ	1.00000		
Q34A54A	PRTAX	-1.00000	PRTAXIU	5000.00000
Q34A54A	SLGAQ	1.00000		
Q34A55A	CMBAX	-1.00000	CMBAXIU	5000.00000
Q34A55A	SLGAQ	1.00000		
Q34A60A	SLGADQ	1.00000	SLGAQ	1.00000
Q34A60A	SLRAX	-1.00000		
Q34A61A	SLGADQ	1.00000	SLGAQ	1.00000

Q35A01A	TRKAX	-1.00000		
Q35A0CA	CNDAX	-1.00000	CNDAXIU	3885.00000
Q35A0CA	OILAQ	1.00000		
Q35A02A	OILAQ	1.00000	STMAX	-1.00000
Q35A02A	STMXIU	3885.00000		
Q35A04A	EVPAX	-1.00000	OILADQ	1.00000
Q35A04A	OILAQ	1.00000		
Q35A24A	FLCAX	-1.00000	OILAQ	1.00000
Q35A25A	OILADQ	1.00000	OILAQ	1.00000
Q35A25A	TK1AX	-1.00000		
Q35A40A	IONAX	-1.00000	IONAXIU	3885.00000
Q35A40A	OILAQ	1.00000		
Q35A40B	IONBX	-1.00000	IONBXIU	3885.00000
Q35A40B	OILAQ	1.00000		
Q35A41A	DSTAX	-1.00000	DSTAXIU	3885.00000
Q35A41A	OILAQ	1.00000		
Q35A42A	MSFAX	-1.00000	MSFAXIU	3885.00000
Q35A42A	OILAQ	1.00000		
Q35A42K	MSFKX	-1.00000	MSFKXIU	3885.00000
Q35A42K	OILAQ	1.00000		
Q35A42U	MSFUX	-1.00000	MSFUXIU	3885.00000
Q35A42U	OILAQ	1.00000		
Q35A43A	DLSAX	-1.00000	DLSAXIU	3885.00000
Q35A43A	OILAQ	1.00000		
Q35A43F	DLSFX	-1.00000	DLSFXIU	3885.00000
Q35A43F	OILAQ	1.00000		
Q35A43P	DLSPX	-1.00000	DLSPXIU	3885.00000
Q35A43P	OILAQ	1.00000		
Q35A43U	DLSUX	-1.00000	DLSUXIU	3885.00000
Q35A43U	OILAQ	1.00000		
Q35A44A	OILAQ	1.00000	OSMAX	-1.00000
Q35A44A	OSMAXIU	3885.00000		
Q35A44B	OILAQ	1.00000	OSMBX	-1.00000
Q35A44B	OSMBXIU	3885.00000		
Q35A44K	OILAQ	1.00000	OSMKX	-1.00000
Q35A44K	OSMKXIU	3885.00000		
Q35A44L	OILAQ	1.00000	OSMLX	-1.00000
Q35A44L	OSMLXIU	3885.00000		
Q35A51A	OILAQ	1.00000	SCHAX	-1.00000
Q35A51A	SCHAXIU	3885.00000		
Q35A54A	OILAQ	1.00000	PRTAX	-1.00000
Q35A54A	PRTAXIU	3885.00000		
Q35A55A	CMBAX	-1.00000	CMBAXIU	3885.00000
Q35A55A	OILAQ	1.00000		
Q35A60A	OILADQ	1.00000	OILAQ	1.00000
Q35A60A	SLRAX	-1.00000		
Q35A61A	OILADQ	1.00000	OILAQ	1.00000
Q35A61A	TRKAX	-1.00000		
Q38A0CA	CNDAX	-1.00000	CNDAXIU	71.00000
Q38A0CA	TK2AQ	1.00000		

Q38A02A	STMAX	-1.00000	STMXIU	71.00000
Q38A02A	TK2AQ	1.00000		
Q38A04A	EVPAX	-1.00000	TK2ADQ	1.00000
Q38A04A	TK2AQ	1.00000		
Q38A24A	FLCAX	-1.00000	TK2AQ	1.00000
Q38A40A	IONAX	-1.00000	IONAXIU	71.00000
Q38A40A	TK2AQ	1.00000		
Q38A40B	IONBX	-1.00000	IONBXIU	71.00000
Q38A40B	TK2AQ	1.00000		
Q38A41A	DSTAX	-1.00000	DSTAXIU	71.00000
Q38A41A	TK2AQ	1.00000		
Q38A42A	MSFAX	-1.00000	MSFAXIU	71.00000
Q38A42A	TK2AQ	1.00000		
Q38A42K	MSFKX	-1.00000	MSFKXIU	71.00000
Q38A42K	TK2AQ	1.00000		
Q38A42U	MSFUX	-1.00000	MSFUXIU	71.00000
Q38A42U	TK2AQ	1.00000		
Q38A43A	DLSAX	-1.00000	DLSAXIU	71.00000
Q38A43A	TK2AQ	1.00000		
Q38A43F	DLSFX	-1.00000	DLSFXIU	71.00000
Q38A43F	TK2AQ	1.00000		
Q38A43P	DLSPX	-1.00000	DLSPXIU	71.00000
Q38A43P	TK2AQ	1.00000		
Q38A43U	DLSUX	-1.00000	DLSUXIU	71.00000
Q38A43U	TK2AQ	1.00000		
Q38A44A	OSMAX	-1.00000	OSMAXIU	71.00000
Q38A44A	TK2AQ	1.00000		
Q38A44B	OSMBX	-1.00000	OSMBXIU	71.00000
Q38A44B	TK2AQ	1.00000		
Q38A44K	OSMKX	-1.00000	OSMKXIU	71.00000
Q38A44K	TK2AQ	1.00000		
Q38A44L	OSMLX	-1.00000	OSMLXIU	71.00000
Q38A44L	TK2AQ	1.00000		
Q38A51A	SCHAX	-1.00000	SCHAXIU	71.00000
Q38A51A	TK2AQ	1.00000		
Q38A54A	PRTAX	-1.00000	PRTAXIU	71.00000
Q38A54A	TK2AQ	1.00000		
Q38A55A	CMBAX	-1.00000	CMBAXIU	71.00000
Q38A55A	TK2AQ	1.00000		
Q38A60A	SLRAX	-1.00000	TK2ADQ	1.00000
Q38A60A	TK2AQ	1.00000		
Q38A61A	SLRAX	-1.00000	TK2ADQ	1.00000
Q38A61A	TK2AQ	1.00000	TRKAX	-1.00000
Q40A0CA	CNDAX	-1.00000	CNDAXIU	150.00000
Q40A0CA	IONAQ	1.00000		
Q40A02A	IONAQ	1.00000	STMAX	-1.00000
Q40A02A	STMXIU	150.00000		
Q40A04A	EVPAX	-1.00000	IONADQ	1.00000
Q40A04A	IONAQ	1.00000		
Q40A05A	IONAQ	1.00000		

Q40A25A	IONADQ	1.00000	IONAQ	1.00000
Q40A25A	TK1AX	-1.00000		
Q40A41A	DSTAX	-1.00000	DSTAXIU	2983.00000
Q40A41A	IONADQ	1.00000	IONAQ	1.00000
Q40A42A	IONADQ	1.00000	IONAQ	1.00000
Q40A42A	MSFAX	-1.00000	MSFAXIU	2983.00000
Q40A42K	IONADQ	1.00000	IONAQ	1.00000
Q40A42K	MSFKX	-1.00000	MSFKXIU	2983.00000
Q40A42U	IONADQ	1.00000	IONAQ	1.00000
Q40A42U	MSFUX	-1.00000	MSFUXIU	2983.00000
Q40A51A	IONAQ	1.00000	SCBAX	-1.00000
Q40A51A	SCBAXIU	150.00000		
Q40A54A	IONAQ	1.00000	PRTAX	-1.00000
Q40A54A	PRTAXIU	150.00000		
Q40A55A	CMBAX	-1.00000	CMBAXIU	150.00000
Q40A55A	IONAQ	1.00000		
Q40A60A	IONADQ	1.00000	IONAQ	1.00000
Q40A60A	SLRAX	-1.00000		
Q40A61A	IONADQ	1.00000	IONAQ	1.00000
Q40A61A	TRKAX	-1.00000		
Q40B0CA	CNDAX	-1.00000	CNDAXIU	150.00000
Q40B0CA	IONAQ	1.00000		
Q40B02A	IONBQ	1.00000	STMAX	-1.00000
Q40B02A	STMXIU	150.00000		
Q40B04A	EVPAX	-1.00000	IONBDQ	1.00000
Q40B04A	IONBQ	1.00000		
Q40B25A	IONBDQ	1.00000	IONBQ	1.00000
Q40B25A	TK1AX	-1.00000		
Q40B41A	DSTAX	-1.00000	DSTAXIU	2983.00000
Q40B41A	IONBDQ	1.00000	IONBQ	1.00000
Q40B42A	IONBDQ	1.00000	IONBQ	1.00000
Q40B42A	MSFAX	-1.00000	MSFAXIU	2983.00000
Q40B42K	IONBDQ	1.00000	IONBQ	1.00000
Q40B42K	MSFKX	-1.00000	MSFKXIU	2983.00000
Q40B42U	IONBDQ	1.00000	IONBQ	1.00000
Q40B42U	MSFUX	-1.00000	MSFUXIU	2983.00000
Q40B51A	IONBQ	1.00000	SCBAX	-1.00000
Q40B51A	SCBAXIU	150.00000		
Q40B54A	IONBQ	1.00000	PRTAX	-1.00000
Q40B54A	PRTAXIU	150.00000		
Q40B55A	CMBAX	-1.00000	CMBAXIU	150.00000
Q40B55A	IONBQ	1.00000		
Q40B60A	IONBDQ	1.00000	IONBQ	1.00000
Q40B60A	SLRAX	-1.00000		
Q40B61A	IONBDQ	1.00000	IONBQ	1.00000
Q40B61A	TRKAX	-1.00000		
Q41A0CA	CNDAX	-1.00000	CNDAXIU	10.00000
Q41A0CA	DSTAQ	1.00000		
Q41A02A	DSTAQ	1.00000	STMAX	-1.00000
Q41A02A	STMXIU	10.00000		

Q41A04A	DSTADQ	1.00000	DSTAQ	1.00000
Q41A04A	EVPAX	-1.00000		
Q41A25A	DSTADQ	1.00000	DSTAQ	1.00000
Q41A25A	TK1AX	-1.00000		
Q41A51A	DSTAQ	1.00000	SCBAX	-1.00000
Q41A51A	SCBAXIU	10.00000		
Q41A54A	DSTAQ	1.00000	PRTAX	-1.00000
Q41A54A	PRTAXIU	10.00000		
Q41A55A	CMBAX	-1.00000	CMBAXIU	10.00000
Q41A55A	DSTAQ	1.00000		
Q41A60A	DSTADQ	1.00000	DSTAQ	1.00000
Q41A60A	SLRAX	-1.00000		
Q41A61A	DSTADQ	1.00000	DSTAQ	1.00000
Q41A61A	TRKAX	-1.00000		
Q42A0CA	CNDAX	-1.00000	CNDAXIU	10.00000
Q42A0CA	MSFAQ	1.00000		
Q42A02A	MSFAQ	1.00000	STMAX	-1.00000
Q42A02A	STMXIU	10.00000		
Q42A04A	EVPAX	-1.00000	MSFADQ	1.00000
Q42A04A	MSFAQ	1.00000		
Q42A25A	MSFADQ	1.00000	MSFAQ	1.00000
Q42A25A	TK1AX	-1.00000		
Q42A51A	MSFAQ	1.00000	SCBAX	-1.00000
Q42A51A	SCBAXIU	10.00000		
Q42A54A	MSFAQ	1.00000	PRTAX	-1.00000
Q42A54A	PRTAXIU	10.00000		
Q42A55A	CMBAX	-1.00000	CMBAXIU	10.00000
Q42A55A	MSFAQ	1.00000		
Q42A60A	MSFADQ	1.00000	MSFAQ	1.00000
Q42A60A	SLRAX	-1.00000		
Q42A61A	MSFADQ	1.00000	MSFAQ	1.00000
Q42A61A	TRKAX	-1.00000		
Q42K0CA	CNDAX	-1.00000	CNDAXIU	10.00000
Q42K0CA	MSFKQ	1.00000		
Q42K02A	MSFKQ	1.00000	STMAX	-1.00000
Q42K02A	STMXIU	10.00000		
Q42K04A	EVPAX	-1.00000	MSFKDQ	1.00000
Q42K04A	MSFKQ	1.00000		
Q42K25A	MSFKDQ	1.00000	MSFKQ	1.00000
Q42K25A	TK1AX	-1.00000		
Q42K51A	MSFKQ	1.00000	SCBAX	-1.00000
Q42K51A	SCBAXIU	10.00000		
Q42K54A	MSFKQ	1.00000	PRTAX	-1.00000
Q42K54A	PRTAXIU	10.00000		
Q42K55A	CMBAX	-1.00000	CMBAXIU	10.00000
Q42K55A	MSFKQ	1.00000		
Q42K60A	MSFKDQ	1.00000	MSFKQ	1.00000
Q42K60A	SLRAX	-1.00000		
Q42K61A	MSFKDQ	1.00000	MSFKQ	1.00000
Q42K61A	TRKAX	-1.00000		

Q42U0CA	CNDAX	-1.00000	CNDAXIU	10.00000
Q42U0CA	MSFUQ	1.00000		
Q42U02A	MSFUQ	1.00000	STMAX	-1.00000
Q42U02A	STMXIU	10.00000		
Q42U04A	EVPAX	-1.00000	MSFUDQ	1.00000
Q42U04A	MSFUQ	1.00000		
Q42U25A	MSFUDQ	1.00000	MSFUQ	1.00000
Q42U25A	TK1AX	-1.00000		
Q42U51A	MSFUQ	1.00000	SCBAX	-1.00000
Q42U51A	SCBAXIU	10.00000		
Q42U5AA	MSFUQ	1.00000	PRTAX	-1.00000
Q42U5AA	PRTAXIU	10.00000		
Q42U55A	CMBAX	-1.00000	CMBAXIU	10.00000
Q42U55A	MSFUQ	1.00000		
Q42U60A	MSFUDQ	1.00000	MSFUQ	1.00000
Q42U60A	SLRAX	-1.00000		
Q42U61A	MSFUDQ	1.00000	MSFUQ	1.00000
Q42U61A	TRKAX	-1.00000		
Q43A0CA	CNDAX	-1.00000	CNDAXIU	10.00000
Q43A0CA	DLSAQ	1.00000		
Q43A02A	DLSAQ	1.00000	STMAX	-1.00000
Q43A02A	STMXIU	10.00000		
Q43A04A	DLSADQ	1.00000	DLSAQ	1.00000
Q43A04A	EVPAX	-1.00000		
Q43A25A	DLSADQ	1.00000	DLSAQ	1.00000
Q43A25A	TK1AX	-1.00000		
Q43A41A	DLSADQ	1.00000	DLSAQ	1.00000
Q43A41A	DSTAX	-1.00000	DSTAXIU	310.00000
Q43A42A	DLSADQ	1.00000	DLSAQ	1.00000
Q43A42A	MSFAX	-1.00000	MSFAXIU	310.00000
Q43A42K	DLSADQ	1.00000	DLSAQ	1.00000
Q43A42K	MSFKX	-1.00000	MSFKXIU	310.00000
Q43A42U	DLSADQ	1.00000	DLSAQ	1.00000
Q43A42U	MSFUX	-1.00000	MSFUXIU	310.00000
Q43A51A	DLSAQ	1.00000	SCBAX	-1.00000
Q43A51A	SCBAXIU	10.00000		
Q43A54A	DLSAQ	1.00000	PRTAX	-1.00000
Q43A54A	PRTAXIU	10.00000		
Q43A55A	CMBAX	-1.00000	CMBAXIU	10.00000
Q43A55A	DLSAQ	1.00000		
Q43A60A	DLSADQ	1.00000	DLSAQ	1.00000
Q43A60A	SLRAX	-1.00000		
Q43A61A	DLSADQ	1.00000	DLSAQ	1.00000
Q43A61A	TRKAX	-1.00000		
Q43F0CA	CNDAX	-1.00000	CNDAXIU	10.00000
Q43F0CA	DLSFQ	1.00000		
Q43F02A	DLSFQ	1.00000	STMAX	-1.00000
Q43F02A	STMXIU	10.00000		
Q43F04A	DLSFDQ	1.00000	DLSFQ	1.00000
Q43F04A	EVPAX	-1.00000		
Q43F25A	DLSFDQ	1.00000	DLSFQ	1.00000
Q43F25A	TK1AX	-1.00000		
Q43F41A	DLSFDQ	1.00000	DLSFQ	1.00000
Q43F41A	DSTAX	-1.00000	DSTAXIU	4506.00000
Q43F42A	DLSFDQ	1.00000	DLSFQ	1.00000
Q43F42A	MSFAX	-1.00000	MSFAXIU	4506.00000
Q43F42K	DLSFDQ	1.00000	DLSFQ	1.00000
Q43F42K	MSFKX	-1.00000	MSFKXIU	4506.00000
Q43F42U	DLSFDQ	1.00000	DLSFQ	1.00000
Q43F42U	MSFUX	-1.00000	MSFUXIU	4506.00000
Q43F51A	DLSFQ	1.00000	SCBAX	-1.00000
Q43F51A	SCBAXIU	10.00000		
Q43F54A	DLSFQ	1.00000	PRTAX	-1.00000
Q43F54A	PRTAXIU	10.00000		
Q43F55A	CMBAX	-1.00000	CMBAXIU	10.00000
Q43F55A	DLSFQ	1.00000		
Q43F60A	DLSFDQ	1.00000	DLSFQ	1.00000
Q43F60A	SLRAX	-1.00000		
Q43F61A	DLSFDQ	1.00000	DLSFQ	1.00000
Q43F61A	TRKAX	-1.00000		
Q43P0CA	CNDAX	-1.00000	CNDAXIU	10.00000
Q43P0CA	DLSPQ	1.00000		
Q43P02A	DLSPQ	1.00000	STMAX	-1.00000
Q43P02A	STMXIU	10.00000		
Q43P04A	DLSPDQ	1.00000	DLSPQ	1.00000
Q43P04A	EVPAX	-1.00000		
Q43P25A	DLSPDQ	1.00000	DLSPQ	1.00000
Q43P25A	TK1AX	-1.00000		
Q43P41A	DLSPDQ	1.00000	DLSPQ	1.00000
Q43P41A	DSTAX	-1.00000	DSTAXIU	19970.00000
Q43P42A	DLSPDQ	1.00000	DLSPQ	1.00000
Q43P42A	MSFAX	-1.00000	MSFAXIU	19970.00000
Q43P42K	DLSPDQ	1.00000	DLSPQ	1.00000
Q43P42K	MSFKX	-1.00000	MSFKXIU	19970.00000
Q43P42U	DLSPDQ	1.00000	DLSPQ	1.00000
Q43P42U	MSFUX	-1.00000	MSFUXIU	19970.00000
Q43P51A	DLSPQ	1.00000	SCBAX	-1.00000
Q43P51A	SCBAXIU	10.00000		
Q43P54A	DLSPQ	1.00000	PRTAX	-1.00000
Q43P54A	PRTAXIU	10.00000		
Q43P55A	CMBAX	-1.00000	CMBAXIU	10.00000
Q43P55A	DLSPQ	1.00000		
Q43P60A	DLSPDQ	1.00000	DLSPQ	1.00000
Q43P60A	SLRAX	-1.00000		
Q43P61A	DLSPDQ	1.00000	DLSPQ	1.00000
Q43P61A	TRKAX	-1.00000		
Q43U0CA	CNDAX	-1.00000	CNDAXIU	10.00000
Q43U0CA	DLSUQ	1.00000		
Q43U02A	DLSUQ	1.00000	STMAX	-1.00000
Q43U02A	STMXIU	10.00000		

[illegible]	DLSUDQ	1.00000	DLSUQ	1.00000
Q430004A	EVPAX	-1.00000		
Q430025A	DLSUDQ	1.00000	DLSUQ	1.00000
Q430025A	TK1AX	-1.00000		
Q430041A	DLSUDQ	1.00000	DLSUQ	1.00000
Q430041A	DSTAX	-1.00000	DSTAXIU	39970.00000
Q430042A	DLSUDQ	1.00000	DLSUQ	1.00000
Q430042A	MSFAX	-1.00000	MSFAXIU	39970.00000
Q430042K	DLSUDQ	1.00000	DLSUQ	1.00000
Q430042K	MSFKX	-1.00000	MSFKXIU	39970.00000
Q430042U	DLSUDQ	1.00000	DLSUQ	1.00000
Q430042U	MSFUX	-1.00000	MSFUXIU	39970.00000
Q430051A	DLSUQ	1.00000	SCHAX	-1.00000
Q430051A	SCHAXIU	10.00000		
Q430054A	DLSUQ	1.00000	PRTAX	-1.00000
Q430054A	PRTAXIU	10.00000		
Q430055A	CMBAX	-1.00000	CMBAXIU	10.00000
Q430055A	DLSUQ	1.00000		
Q430060A	DLSUDQ	1.00000	DLSUQ	1.00000
Q430060A	SLRAX	-1.00000		
Q430061A	DLSUDQ	1.00000	DLSUQ	1.00000
Q430061A	TRKAX	-1.00000		
Q4400CA	CNDAX	-1.00000	CNDAXIU	10.00000
Q4400CA	OSMAQ	1.00000		
Q4402A	OSMAQ	1.00000	STMAX	-1.00000
Q4402A	STMXIU	10.00000		
Q4404A	EVPAX	-1.00000	OSMADQ	1.00000
Q4404A	OSMAQ	1.00000		
Q4425A	OSMADQ	1.00000	OSMAQ	1.00000
Q4425A	TK1AX	-1.00000		
Q4441A	DSTAX	-1.00000	DSTAXIU	17717.00000
Q4441A	OSMADQ	1.00000	OSMAQ	1.00000
Q4442A	MSFAX	-1.00000	MSFAXIU	17717.00000
Q4442A	OSMADQ	1.00000	OSMAQ	1.00000
Q4442K	MSFKX	-1.00000	MSFKXIU	17717.00000
Q4442K	OSMADQ	1.00000	OSMAQ	1.00000
Q4442U	MSFUX	-1.00000	MSFUXIU	17717.00000
Q4442U	OSMADQ	1.00000	OSMAQ	1.00000
Q4451A	OSMAQ	1.00000	SCHAX	-1.00000
Q4451A	SCHAXIU	10.00000		
Q4454A	OSMAQ	1.00000	PRTAX	-1.00000
Q4454A	PRTAXIU	10.00000		
Q4455A	CMBAX	-1.00000	CMBAXIU	10.00000
Q4455A	OSMAQ	1.00000		
Q4460A	OSMADQ	1.00000	OSMAQ	1.00000
Q4460A	SLRAX	-1.00000		
Q4461A	OSMADQ	1.00000	OSMAQ	1.00000
Q4461A	TRKAX	-1.00000		
Q44B0CA	CNDAX	-1.00000	CNDAXIU	10.00000
Q44B0CA	OSMBQ	1.00000		

Q44B02A	OSMBQ	1.00000	STMAX	-1.00000
Q44B02A	STMXIU	10.00000		
Q44B04A	EVPAX	-1.00000	OSMBDQ	1.00000
Q44B04A	OSMBQ	1.00000		
Q44B25A	OSMBDQ	1.00000	OSMBQ	1.00000
Q44B25A	TK1AX	-1.00000		
Q44B41A	DSTAX	-1.00000	DSTAXIU	17717.00000
Q44B41A	OSMBDQ	1.00000	OSMBQ	1.00000
Q44B42A	MSFAX	-1.00000	MSFAXIU	17717.00000
Q44B42A	OSMBDQ	1.00000	OSMBQ	1.00000
Q44B42K	MSFKX	-1.00000	MSFKXIU	17717.00000
Q44B42K	OSMBDQ	1.00000	OSMBQ	1.00000
Q44B42U	MSFUX	-1.00000	MSFUXIU	17717.00000
Q44B42U	OSMBDQ	1.00000	OSMBQ	1.00000
Q44B51A	OSMBQ	1.00000	SCHAX	-1.00000
Q44B51A	SCHAXIU	10.00000		
Q44B54A	OSMBQ	1.00000	PRTAX	-1.00000
Q44B54A	PRTAXIU	10.00000		
Q44B55A	CMBAX	-1.00000	CMBAXIU	10.00000
Q44B55A	OSMBQ	1.00000		
Q44B60A	OSMBDQ	1.00000	OSMBQ	1.00000
Q44B60A	SLRAX	-1.00000		
Q44B61A	OSMBDQ	1.00000	OSMBQ	1.00000
Q44B61A	TRKAX	-1.00000		
Q44K0CA	CNDAX	-1.00000	CNDAXIU	10.00000
Q44K0CA	OSMKQ	1.00000		
Q44K02A	OSMKQ	1.00000	STMAX	-1.00000
Q44K02A	STMXIU	10.00000		
Q44K04A	EVPAX	-1.00000	OSMKDQ	1.00000
Q44K04A	OSMKQ	1.00000		
Q44K25A	OSMKDQ	1.00000	OSMKQ	1.00000
Q44K25A	TK1AX	-1.00000		
Q44K41A	DSTAX	-1.00000	DSTAXIU	12302.00000
Q44K41A	OSMKDQ	1.00000	OSMKQ	1.00000
Q44K42A	MSFAX	-1.00000	MSFAXIU	12302.00000
Q44K42A	OSMKDQ	1.00000	OSMKQ	1.00000
Q44K42K	MSFKX	-1.00000	MSFKXIU	12302.00000
Q44K42K	OSMKDQ	1.00000	OSMKQ	1.00000
Q44K42U	MSFUX	-1.00000	MSFUXIU	12302.00000
Q44K42U	OSMKDQ	1.00000	OSMKQ	1.00000
Q44K51A	OSMKQ	1.00000	SCHAX	-1.00000
Q44K51A	SCHAXIU	10.00000		
Q44K54A	OSMKQ	1.00000	PRTAX	-1.00000
Q44K54A	PRTAXIU	10.00000		
Q44K55A	CMBAX	-1.00000	CMBAXIU	10.00000
Q44K55A	OSMKQ	1.00000		
Q44K60A	OSMKDQ	1.00000	OSMKQ	1.00000
Q44K60A	SLRAX	-1.00000		
Q44K61A	OSMKDQ	1.00000	OSMKQ	1.00000
Q44K61A	TRKAX	-1.00000		

Q44L07A	CNDAX	-1.00000	CNDAXIU	10.00000
Q44L [illegible]	OSMLQ	1.00000		
Q44L02A	OSMLQ	1.00000	STMAX	-1.00000
Q44L02A	STMXIU	10.00000		
Q44L04A	OSMLDQ	1.00000	EVPAX	-1.00000
Q44L04A	OSMLQ	1.00000		
Q44L25A	OSMLDQ	1.00000	OSMLQ	1.00000
Q44L25A	TKIAX	-1.00000		
Q44L11A	OSMLDQ	1.00000	OSTAX	-1.00000
Q44L11A	OSTAXIU	12302.00000	OSMLQ	1.00000
Q44L02A	OSMLDQ	1.00000	MSFAX	-1.00000
Q44L02A	MSFAXIU	12302.00000	OSMLQ	1.00000
Q44L02A	FSMLQ	1.00000	MSFKX	-1.00000
Q44L02A	MSFKXIU	12302.00000	OSMLQ	1.00000
Q44L02D	OSMLDQ	1.00000	MSFUX	-1.00000
Q44L02D	MSFUXIU	12302.00000	OSMLQ	1.00000
Q44L51A	OSMLQ	1.00000	SCRAX	-1.00000
Q44L51A	SCRAXIU	10.00000		
Q44L54A	OSMLQ	1.00000	PRTAX	-1.00000
Q44L54A	PRTAXIU	10.00000		
Q44L55A	CMBAX	-1.00000	CMBAXIU	10.00000
Q44L55A	OSMLQ	1.00000		
Q44L60A	OSMLDQ	1.00000	OSMLQ	1.00000
Q44L60A	SLRAX	-1.00000		
Q44L61A	OSMLDQ	1.00000	OSMLQ	1.00000
Q44L61A	TRKAX	-1.00000		
Q51A02A	SCBAQ	1.00000	STMAX	-1.00000
Q51A02A	STMXIU	4.83800E 05		
Q51A04A	EVPAX	-1.00000	SCBAQ	1.00000
Q51A23A	SCBAQ	1.00000	STLAX	-1.00000
Q51A38A	SCBAQ	1.00000	TK2AX	-1.00000
Q51A60A	SCBAQ	1.00000	SLRAX	-1.00000
Q51A61A	SCBAQ	1.00000	TRKAX	-1.00000
Q54A02A	PRTAQ	1.00000	STMAX	-1.00000
Q54A02A	STMXIU	5.39011E 05		
Q54A04A	EVPAX	-1.00000	PRTAQ	1.00000
Q54A23A	PRTAQ	1.00000	STLAX	-1.00000
Q54A38A	PRTAQ	1.00000	TK2AX	-1.00000
Q54A60A	PRTAQ	1.00000	SLRAX	-1.00000
Q54A61A	PRTAQ	1.00000	TRKAX	-1.00000
Q55A02A	CMBAQ	1.00000	STMAX	-1.00000
Q55A02A	STMXIU	4.83800E 05		
Q55A04A	CMBAQ	1.00000	EVPAX	-1.00000
Q55A23A	CMBAQ	1.00000	STLAX	-1.00000
Q55A38A	CMBAQ	1.00000	TK2AX	-1.00000
Q55A60A	CMBAQ	1.00000	SLRAX	-1.00000
Q55A61A	CMBAQ	1.00000	TRKAX	-1.00000
Q60A04A	EVPAX	-1.00000	SLRAQ	1.00000
Q60A05A	LNDAX	-1.00000	SLRAQ	1.00000
Q61A05A	LNDAX	-1.00000	TRKAQ	1.00000

SL08A08A	BOLAPRT	-0.30000	POLAPT	1.00000
S08A60A	BOLASRT	1.00000	SLRAT	-1.00000
S08A61A	BOLASRT	1.00000	TRKAT	-1.00000
S08A08A	BOLASRT	-0.08000	BOLASO	1.00000
S51A23A	SCBASA	1.00000		
S51A38A	SCBASA	1.00000		
S51A60A	SCBASA	1.00000	SLRAT	-1.00000
S51A61A	SCBASA	1.00000	TRKAT	-1.00000
S53A	STKASA	1.00000	STKASO	1.00000
S55A23A	CMBASA	1.00000		
S55A38A	CMBASA	1.00000		
S55A60A	CMBASA	1.00000	SLRAT	-1.00000
S55A61A	CMBASA	1.00000	TRKAT	-1.00000
T23A60A	SLRAT	-1.00000		
T23A61A	TRKAT	-1.00000		
T38A60A	SLRAT	-1.00000		
T38A61A	TRKAT	-1.00000		
T60A	SLRAT	1.00000	SLRAXT	-1.00000
T61A	TRKAT	1.00000	TRKAXT	-1.00000
XT60A	COST	57.30000	SLRAXT	1.00000
XT61A	COST	142.70000	TRKAXT	1.00000
XX01A	COST	14.72000	WATRCHRG	-1.00000
X0CA	CNDA	1.00000	CNDAQ	-1.00000
X0CA	CNDAX	1.00000		
X0DA	SANA	1.00000	SANAQ	-1.00000
X0DA	SANAX	1.00000	WATRCHRG	-1.00000
X0HA	CLNA	1.00000	CLNAQ	-1.00000
X0HA	CLNAX	1.00000	WATRCHRG	-1.00000
X01A	WATAQ	-1.00000	WATAX	-1.00000
X01A	WATRCHRG	1.00000		
X02A	STMAQ	-1.00000	STMAX	1.00000
X02A	STMXIU	-500.00000		
X03A	SKYAQ	-1.00000	SKYAX	1.00000
X04A	COST	1317.27000	EVPAQ	-1.00000
X04A	EVPAX	1.00000		
X05A	LNDAQ	-1.00000	LNDAX	1.00000
X11A	CL5AQ	-1.00000	CL5AX	1.00000
X11A	CL5MQ	-0.02875	CL50CA	-0.97125
X11A	EVP5Q	-0.02305		
X14A	CL2AQ	-1.00000	CL2AX	1.00000
X14A	CL2MQ	-0.02416	CL20CA	-0.97579
X14A	EVP2Q	-0.02305		
X15A	CL6AQ	-1.00000	CL6AX	1.00000
X15A	CL6MQ	-0.02347	CL60CA	-0.97653
X15A	EVP6Q	-0.02305		
X16A	CL1AQ	-1.00000	CL1AX	1.00000
X16A	CL1MQ	-0.02323	CN01Q	-0.97677
X16A	EVP1Q	-0.02305		
X17A	CLDAQ	-1.00000	CLDAX	1.00000
X23A	COST	14.86000	STLADQ	-0.20000

X23A	STLAQ	-1.00000	STLAX	1.00000
X24A	COST	69.34000	FLCADQ	-0.00900
X24A	FLCAQ	-1.00000	FLCAX	1.00000
X24A	FLCAXU	1.00000		
X25A	COST	8.43000	TK1ADQ	-0.33000
X25A	TK1AQ	-1.00000	TK1AX	1.00000
X26A	COST	7.65600	TRLADQ	-0.00040
X26A	TRLAQ	-1.00000	TRLAX	1.00000
X26A	TRLAXU	1.00000		
X34A	COST	21.05500	SLGADQ	-0.00400
X34A	SLGAQ	-1.00000	SLGAX	1.00000
X34A	SLGAXU	1.00000		
X35A	COST	248.20000	OILADQ	-0.00010
X35A	OILAQ	-1.00000	OILAX	1.00000
X38A	COST	24.95000	TK2ADQ	-0.33000
X38A	TK2AQ	-1.00000	TK2AX	1.00000
X40A	COST	94.70800	IONADQ	-0.30000
X40A	IONAQ	-1.00000	IONAX	1.00000
X40A	IONAXIU	-1000.00000	IONAYU	1.00000
X40B	COST	85.50000	IONBDQ	-0.30000
X40B	IONBQ	-1.00000	IONBX	1.00000
X40B	IONBXIU	-1000.00000	IONBYL	1.00000
X40B	IONBYU	1.00000		
X41A	COST	1062.20000	DSTADQ	-0.02000
X41A	DSTAQ	-1.00000	DSTAX	1.00000
X41A	DSTAXIU	-2500.00000		
X42A	COST	2499.00000	MSFADQ	-0.27800
X42A	MSFAQ	-1.00000	MSFAX	1.00000
X42A	MSFAXIU	-20000.00000	MSFAZU	1.00000
X42K	COST	3417.04000	MSFKDQ	-0.61300
X42K	MSFKQ	-1.00000	MSFKX	1.00000
X42K	MSFKXIU	-30000.00000	MSFKZU	1.00000
X42U	COST	6184.46000	MSFUDQ	-0.74900
X42U	MSFUQ	-1.00000	MSFUX	1.00000
X42U	MSFUXIU	-50000.00000	MSFUZU	1.00000
X43A	COST	22.30600	DLSADQ	-0.22600
X43A	DLSAQ	-1.00000	DLSAX	1.00000
X43A	DLSAXIU	-78.00000	DLSAZU	1.00000
X43F	COST	80.20000	DLSFDQ	-0.24800
X43F	DLSFQ	-1.00000	DLSFX	1.00000
X43F	DLSFXIU	-1250.00000	DLSFZU	1.00000
X43P	COST	201.92000	DLSPDQ	-0.25000
X43P	DLSPQ	-1.00000	DLSPX	1.00000
X43P	DLSPXIU	-5000.00000	DLSPZU	1.00000
X43U	COST	365.60000	DLSUDQ	-0.25000
X43U	DLSUQ	-1.00000	DLSUX	1.00000
X43U	DLSUXIU	-10000.00000	DLSUZU	1.00000
X44A	COST	291.45000	OSMADQ	-0.30000
X44A	OSMAQ	-1.00000	OSMAX	1.00000
X44A	OSMAXIU	-2666.00000	OSMAZU	1.00000
X44B	COST	245.91700	OSMBDQ	-0.30000
X44B	OSMBQ	-1.00000	OSMBX	1.00000
X44B	OSMBXIU	-2666.00000	OSMBZL	1.00000
X44B	OSMBZU	1.00000		
X44K	COST	101.10000	OSMKDQ	-0.65000
X44K	OSMKQ	-1.00000	OSMKX	1.00000
X44K	OSMKXIU	-8000.00000	OSMKZU	1.00000
X44L	COST	85.43000	OSMLQ	-1.00000
X44L	OSMLX	1.00000	OSMLDQ	-0.65000
X44L	OSMLXIU	-2665.00000	OSMLZL	1.00000
X44L	OSMLZU	1.00000		
X51A	SCBAQ	-1.00000	SCBAX	1.00000
X51A	SCBAXIU	-5000.00000	SCBNQ	1.00000
X54A	PRTAQ	-1.00000	PRTAXO	1.00000
X54A	PRTAX	1.00000	PRTAXIU	-5000.00000
X55A	CMBAQ	-1.00000	CMBAX	1.00000
X55A	CMBAXIU	-5000.00000	CMBANQ	1.00000
X60A	SLRAQ	-1.00000	SLRAX	1.00000
X60A	SLRAXT	-1.00000		
X61A	TRKAQ	-1.00000	TRKAX	1.00000
X61A	TRKAXT	-1.00000		

RIGHT HAND SIDE VALUES OTHER THAN ZERO

RHS				
RHS	WATAX	186.20000	WATPCHRG	13.89000
RHS	CNDA	1620.70000	Z1-8EX	1.00000
RHS	Y10Y11EX	1.00000	Z18-22FX	1.00000
RHS	Z23-27EX	1.00000	Z12-17EX	1.00000
RHS	Y33-Y36E	1.00000	HEIGHT	750.00000
RHS	STKAPQ	0.00768	STKASQ	0.09220
RHS	BOLAN	91.72200	SANA	0.03400
RHS	CLNA	0.00010		
ENDATA				